United States
Environmental Protection
Agency

Environmental Research
Laboratory
Duluth MN 55804

EPA-600/3-80-094
December 1980

C.2

Research and Development

EPA

Environmental Effects of Western Coal Combustion:

Part IV - Chemical and Physical Characteristics of Coal Fly Ash

RESEARCH REPORTING SERIES

Research reports of the Office of Research and Development, U.S. Environmental Protection Agency, have been grouped into nine series. These nine broad categories were established to facilitate further development and application of environmental technology. Elimination of traditional grouping was consciously planned to foster technology transfer and a maximum interface in related fields. The nine series are:

1. Environmental Health Effects Research
2. Environmental Protection Technology
3. Ecological Research
4. Environmental Monitoring
5. Socioeconomic Environmental Studies
6. Scientific and Technical Assessment Reports (STAR)
7. Interagency Energy-Environment Research and Development
8. "Special" Reports
9. Miscellaneous Reports

This report has been assigned to the ECOLOGICAL RESEARCH series. This series describes research on the effects of pollution on humans, plant and animal species, and materials. Problems are assessed for their long- and short-term influences. Investigations include formation, transport, and pathway studies to determine the fate of pollutants and their effects. This work provides the technical basis for setting standards to minimize undesirable changes in living organisms in the aquatic, terrestrial, and atmospheric environments.

This document is available to the public through the National Technical Information Service, Springfield, Virginia 22161.

EPA 600/3-80-094
November

ENVIRONMENTAL EFFECTS OF WESTERN COAL COMBUSTION: PART IV - CHEMICAL AND PHYSICAL CHARACTERISTICS OF COAL FLY ASH

by

David F. S. Natusch and David R. Taylor
Department of Chemistry
Colorado State University
Fort Collins, Colorado 80523

Grant No. R803950

Project Officer

Donald I. Mount
Environmental Research Laboratory
Duluth, Minnesota 55804

Environmental Research Laboratory
Office of Research and Development
U.S. Environmental Protection Agency
Duluth, Minnesota 55804

U.S. Environmental Protection Agency
Region V, Library
230 South Dearborn Street
Chicago, Illinois 60604

DISCLAIMER

This report has been reviewed by the Environmental Research Laboratory-Duluth, U.S. Environmental Protection Agency, and approved for publication. Approval does not signify that the contents necessarily reflect the views and policies of the U.S. Environmental Protection Agency, nor does mention of trade names or commercial products constitute endorsement or recommendation for use.

FOREWORD

This report, part IV of a series, provides considerable information on the physical and chemical properties of coal fly ash. National reliance on coal for more of our energy will result in large increases in fly ash production. To properly dispose of this material and more importantly to find effective ways to use it as a resource rather than as a waste requires such knowledge.

Norbert A. Jaworski, Ph.D.
Director
Environmental Research Laboratory-Duluth

ABSTRACT

Coal fly ashes from a number of different sources have been extensively studied. Morphologically, fly ashes can be classified in terms of as many as twelve different particle types, which include, primarily, solid, hollow, encapsulating, and agglomerated particles. Both non-magnetic particles, which consist maninly of silicon, aluminum, calcium, potassium, and sodium, and magnetic particles, which consist mainly of hematite and magnetite, are found in all the ashes studied. The relative proportion of non-magnetic to magnetic particles varied considerably among coal types. The electrical resistivity of the coal fly ash decreases with increasing alkali metal content.

Potentially volatile trace elements, namely, As, Se, Ga, In, Pb, and Cd, are almost alsys preferentially associated with the smaller, more respirable fly ash particles. Many other minor and trace elements may also show an inverse particle size dependence, depending on the coal fly ash. Elements that do not exhibit any dependence of concentration on particle size include Al, Ba, Ca, Co, Fe, K, Mg, Rb, Sc, Si, Sr, Ta, Ti, and the rare earths. Surface analytical techniques indicate that many of the more volatile and potentially environmentally hazardous trace elements are associated with the surface layer of coal fly ash. Thus, the concentration levels of Pb, Tl, Cr, and Mn on the surface were much higher than in the bulk material. These elements are readily soluble in aqueous solution in contrst to the bulk of coal fly ash, which is very insoluble. It is believed that enrichment of trace elements results from the volatilization of the elements in the combustion zone and subsequent condensation and/or adsorption as the temperature falls in power plant plumes.

Most potentially hazardous inorganic species associated with coal fly ash can be leached into aqueous solution but are unlikely to give rise to solution concentrations of great concern. On the other hand, localized concentrations of soluble inorganic species could cause damage to a few lung cells in the microregion of particle deposition following inhalation.

The physical and chemical characteristics and behavior of polycyclic organic matter (POM) associated with coal fly ash has also been studied. Theoretical models, which have been generally verified by experiment, show that POMs associated with coal fly ash by adsorption from the vapor phase. This is a highly temperature-dependent process, although such factors as the energetics of adsorption, particle surface area, and vapor phase POM concentrations all influence the vapor-to-particle adsorption process. The models show that the adsorption process will occur within fractions of a second under the conditions found in a typical power plant emission stream and within a few seconds in the emitted plume.

Surface-adsorbed polycyclic organic compounds (mainly pyrene and benzo[a]pyrene) exposed to different nitrogen and sulfur oxides are shown to be highly reactive. Surfaces studied included coal fly ash, alumina, and silica gel. Reactions with nitrogen dioxide and sulfur trioxide appear to proceed most completely, with both reactions yielding several oxidation and substitution products. It is concluded that reactions of particulate POM with plume gases can result in major changes in both the chemical and toxicological characteristices of this species. On the other hand, adsorption of POM onto coal fly ashes result in significant stabilization against photochemical decomposition, therefy preserving the integrity of the original compounds against photo-oxidation. A new non-photochemical oxidation sequence has, however, been discovered for those hydrocarbons containing a benzylic carbon atom.

Overall, it can be stated that coal fly ash collected by electrostatic precipitators or other high-temperature control devices have essentially no associated POM. Fly ash emitted to the atmosphere, however, has much more POM but not enough to make a discernible impact on any terrestrial aquatic system.

CONTENTS

	Page
Foreword	iii
Abstract	iv
Figures	vii
Tables	xi
Acknowledgment	xiii
1. Introduction	1
2. Conclusions	3
3. Recommendations	6
4. Physical Characteristics of Coal Fly Ash	7
Particle Morphology	7
Mass, Density, and Ferromagnetism Distributions	18
Electrical Resistivity Distribution	21
Surface Area Distribution	27
5. Chemical Characteristics of Coal Fly Ash	29
Matrix Element Composition and Distribution	29
Mineral Composition	39
Trace Element Composition and Distribution	43
Inorganic Chemical Speciation and Leaching Characteristics	66
Surface Characterization	77
Health Effects	90
Particulate Associated Organic Compounds	91
Summary	115
References	116

Appendices 129

A. Experimental Procedures and Instrumental Techniques Used to Analyze Coal Fly Ash 130
B. Matrix Element Distributions for a Size, Density, and Magnetically Fractionated Coal Fly Ash 141
C. Trace Element Distributions for a Size, Density, and Magnetically Fractionated Coal Fly Ash 150
D. Results of Different Coal Fly Ash Leaching Experiments 175
E. Glossary of Abbreviations 200

LIST OF FIGURES

Number		Page
1	Scanning electron micrographs of representative coal fly ash particles	9
2	Scanning electron micrographs of coal fly ash particles, showing representative encapsulated and encapsulated particles and cenosphere shells	13
3	Calculated surface tension at 1400°C as a function of the percentage of encapsulating particles	17
4	Particle size distributions resulting from coal combustion in different boiler types	20
5	Particle size distribution of emissions from similar production units at the same power plant equipped with either an electrostatic precipitator (ESP) or a Venturi wet scrubber	20
6	Mass distribution of non-magnetic and magnetic coal fly ash fractions as a function of particle size	22
7	Mass distribution of size- and density-classified coal fly ash with and without crushing	25
8	Resistivity as a function of reciprocal absolute temperature for two different coal fly ashes	26
9	Concentration of silicon in non-magnetic and magnetic coal fly ash fractions as a function of particle size and density	31
10	Concentration of aluminum in non-magnetic and magnetic coal fly ash fractions as a function of particle size and density	32
11	Concentration of iron in non-magnetic and magnetic coal fly ash fractions as a function of particle size and density	33

Number		Page
12	Concentration of sulfur in non-magnetic and magnetic coal fly ash fractions as a function of particle size and density	34
13	Concentration of potassium in non-magnetic and magnetic coal fly ash fractions as a function of particle size and density	36
14	Concentration of sodium in non-magnetic and magnetic coal fly ash fractions as a function of particle size and density	37
15	Concentration of calcium in non-magnetic and magnetic coal fly ash fractions as a function of particle size and density	38
16	X-ray powder diffraction patterns of non-magnetic and magnetic coal fly ash particles	41
17	X-ray powder diffraction patterns of density-separated coal fly ash particles	42
18	Concentration of manganese in non-magnetic and magnetic coal fly ash fractions as a function of particle size and density	45
19	Concentration of zinc in non-magnetic and magnetic coal fly ash fractions as a function of particle size and density	47
20	Concentration of europium in non-magnetic and magnetic coal fly ash fractions as a function of particle size and density	48
21	Concentration of gallium in non-magnetic and magnetic coal fly ash fractions as a function of particle size and density	49
22	Concentration of antimony in non-magnetic and magnetic coal fly ash fractions as a function of particle size and density	50
23	Concentration of thallium in coal fly ash fractions as a function of particle size	52
24	Concentration of antimony in coal fly ash fractions as a function of particle size	52

Number		Page

25 Concentration of beryllium in coal fly ash fractions as a function of particle size 53

26 Concentration of cobalt in coal fly ash fractions as a function of particle size 53

27 Concentration of arsenic in coal fly ash fractions as a function of particle size 54

28 Concentration of lead in coal fly ash fractions as a function of particle size 54

29 Concentration of nickel in coal fly ash fractions as a function of particle size 55

30 Concentration of chromium in coal fly ash fractions as a function of particle size 55

31 Concentration of manganese in coal fly ash fractions as a function of particle size 56

32 Concentration of vanadium in coal fly ash fractions as a function of particle size 56

33 Dependence of As, Ni, and Cd concentrations in coal fly ash on particle size 63

34 Apparatus for ambient temperature soxhelt leaching 76

35 Ion microprobe depth profiles for the Group A elements (Ti, Al, Si) in unleached and leached fly ash 79

36 Ion microprobe depth profiles for the Group B elements (Fe, S) in unleached and leached fly ash 80

37 Ion microprobe depth profiles for the Group B elements (K, Na, Li) in unleached and leached fly ash 81

38 Ion microprobe depth profiles for the Group C elements (Pb, Tl) in unleached and leached fly ash 82

39 Ion microprobe depth profiles for the Group C elements (Cr, Mn, V) in unleached and leached fly ash 83

40 Ion microprobe depth profiles for the Group D elements (Ca, Mg) in unleached and leached fly ash 84

41 Auger Electron Spectrometry (AES) elemental depth profiles for unleached fly ash 88

Number		Page
42	Dependence of mole fraction (x) of PAH adsorbed on temperature	95
43	Dependence of half-time of adsorption on temperature	97
44	Percent conversion of irradiated benzo[a]pyrenecompared with a non-irradiated sample as a function of time	102
45	Percent conversion of fluorene adsorbed on coal fly ash as a function of time	104
46	Chromatograms of extracts from pyrene adsorbed on coal fly ash before and after exposure to NO_2 and SO_3	108
47	Chromatograms of extract from benzo[a]pyrene adsorbed on coal fly ash before and after exposure to NO_2 and SO_3	109
48	Chromatograms of extracts from pyrene adsorbed on silica gel exposed to NO_2, showing changes with aging	110
49	Low-resolution ESCA spectra of a (A) coal fly ash surface following pyrene adsorption and (B) the same coal fly ash surface following adsorption of pyrene and exposure to NO_2	111
50	High-resolution ESCA spectrum of a coal fly ash surface following adsorption of pyrene and exposure to NO_2	112

LIST OF TABLES

Number		Page
1	Relative abundance (wt %) of morphologic particle types in four coal size-classified fly ash fractions	1
2	Encapsulating particle bulk mass contribution (wt %) for the non-magnetic fraction of coal fly ash	14
3	Encapsulating particle bulk mass contribution (wt %) for the magnetic fraction of coal fly ash	15
4	Mass distribution (wt %) of non-magnetic fractions of fly ashes from midwestern bituminous and western sub-bituminous coals	23
5	Mass distribution (wt %) of magnetic fractions of fly ashes from midwestern bituminous and western sub-bituminous coals	24
6	Specific surface areas (m^2/g) of coal fly ash fractions from a midwestern bituminous coal	28
7	Typical matrix element composition ranges of some American and British coal fly ashes	30
8	Summary of elemental concentration dependence on particle size	58
9	Boiling points of possible inorganic species evolved during coal combustion	60
10	Elemental surface concentrations and layer thicknesses calculated using the surface deposition model	62
11	Enrichment factors for in-stack total suspended particulate material	66
12	Upper-limit concentrations of carbonate compounds in coal fly ash	68
13	Carbonate species contribution to leachable elemental concentrations	69

Number		Page
14	Changes in measured pH resulting from column leaching of a bulk a western sub-bituminous coal fly ash with solutions of different pH	74
15	Elemental concentrations in coal fly ash leachates	86
16	Summary of analytical results-surface characterization of coal fly ash	89
17	Polycyclic aromatic compounds identified in emitted coal fly ash	91
18	Polycyclic aromatic hydrocarbon emission factors for coal-fired furnaces	92
19	Measurement of POM emitted from a coal-fired power plant stack	98
20	Decomposition of irradiated polycyclic aromatic hydrocarbons adsorbed on coal fly ash	103
21	Decomposition of non-irradiated polycyclic aromatic hydrocarbons adsorbed on coal fly ash	105

ACKNOWLEDGMENTS

We thank Dr. R. K. Skogerboe for his editorial advice and assistance in the preparation of this report.

This research was primarily funded by the U.S. Environmental Protection Agency, Environmental Research Laboratory-Duluth, Research Grant No. R803950, awarded to Natural Resource Ecology Laboratory, Colorado State University, and Fisheries Bioassay Laboratory, Montana State University. Additional support was provided by the U.S. Department of Energy under Reseach Grant Nos. EE-77-S-02-4347 and DE-AS 02-78 EV 04960 and by the National Science Foundation under Research Grant No. ERT-74-24276.

SECTION 1

INTRODUCTION

Production of electric power from the combustion and conversion of fossil fuels represents a ubiquitous and increasing means of obtaining energy in most countries throughout the world. It is now apparent that, for the next several decades at least, deficits in the energy budget of the world will be made up primarily from increased coal usage. As a result, considerable emphasis is currently being placed on assessing the environmental impact of coal combustion and conversion operations. It is to this end that the present work, dealing with the characterization and assessment of the potential environmental impact of coal fly ash, is directed.

Particulate matter in the form of airborne fly ash constitutes a major pollutant emission from both the combustion and conversion of coal. Indeed some estimates indicate that coal fly ash, consisting of material retained by collection devices within a coal fired power plant, may soon constitute one of the largest tonnages of solid waste materials produced in the United States. It is appropriate therefore to seek information about both the nature and potential environmental impact of this material as emitted to the atmosphere and as retained by control devices in a power plant. To this end, a number of samples of coal fly ash have been studied. These have been derived from a variety of power plants in which combustion of either midwestern bituminous coal or western sub-bituminous coal occurs. For the purposes of the present project, however, one fly ash of each type has been studied extensively. Thus, fly ash representative of the burning of a western sub-bituminous coal was obtained from the Corrette Plant located in Billings, Montana. That representative of a midwestern bituminous coal was obtained from the Iowa/Illinois Gas and Electric Plant in Davenport, Iowa. The coal burned in the first plant was obtained from the Rosebud Mine located at Colstrip, Montana; that burned in the second plant was obtained from the Captain mine in southern Indiana.

In all cases two distinct types of fly ash are considered. These are:

1. Fly ash collected in bulk from mechanical or electrostatic precipitating devices and representative of material retained in a power plant.

2. Fly ash collected from flue gas in the stack downstream from the precipitator and thus representative of the material emitted to the atmosphere.

In all the studies of the physical and chemical characteristics of coal fly ash, emphasis was placed on the dependence of fly ash properties on

particle size since this parameter, perhaps more than any other, is of primary importance in determining the behavioral characteristics of particulate material. Thus, it is the aerodynamic particle size which determines the ability of a control device to collect a particle; it is the aerodynamic particle size which determines the atmospheric lifetime; it is the physical particle size which determines the amount of potentially undesirable material which can be leached from the fly ash; it is the aerodynamic particle size which determines the potential inhalation toxicological impact of airborne fly ash, and it is both the physical and aerodynamic particle size which have a profound effect upon the methodology employed for sampling and analysis of coal fly ash.

The text of this report is devoted to a description of the studies which have been performed for the specific purpose of obtaining a better understanding of the nature and behavior of coal fly ash. However, in order to perform many of these studies, it has been necessary to develop and/or apply a large number of specific analytical techniques. These techniques have involved sample handling, sample characterization and the interpretation of the results from the analyses. A number of such methodology -- related studies are presented in appendix A of this report.

SECTION 2

CONCLUSIONS

The following conclusions can be drawn from the results presented herein.

1. Coal fly ash as obtained from a conventional coal fired power plant exhibits a number of morphological forms. For most fly ashes, the most predominant forms include small, solid, spherical particles; hollow particles or cenospheres; and hollow spheres containing small solid particles encapsulated inside of them (plerospheres). The occurrence of quite large numbers of small particles inside the pleres pheres is not thought to be of much significance from the standpoint of environmental impact.

2. The mass of material of a given aerodynamic size range of coal fly ash particles emitted to the atmosphere is a function of both the nature of the combustion system and the type of control device. Cyclone coal-fired systems generally emit the smallest particles.

3. The relative mass proportions of non-magnetic versus magnetic particles in coal fly ash are mainly dependent on the coal that is burned. Density is determined more by the morphology of the particles than by their composition.

4. The electrical resistivity of coal fly ash is a function of both the concentration of alkali metals in the particles and the temperature. High sodium and potassium concentrations and low temperatures lower the resistivity of the particles and promote collection by electrostatic precipitators.

5. The specific surface areas of size fractionated fly ash particles above 15 μm in physical diameter are generally less than 1 m^2/g. However, values of up to 5 m^2/g have been found for small (<5 μm diameter) respirable particles. Specific surface area appears to be highest in the smallest (<20 μm) and largest size (>74 μm) size fractions. The latter observation is believed due to the porous, irregular shapes and high internal surface areas of the larger particles.

6. Coal fly ash particles are largely, made up of an impure aluminosilicate glass. Major elements are Al, Fe, Si, Ca, K, Na and Ti. As such, the particles are essentially insoluble.

7. A considerable number of potentially toxic trace elements; As, Br, Cd, Cu, Ga, Mo, Pb, Sb, Se and Zn are preferentially associated with smaller fly ash particles. The implications of this behavior are that such trace elements may be preferentially emitted from a coal fired power plant even under conditions where highly efficient particle collection devices are being utilized. Since small particles have longer atmospheric residence times, these toxic trace elements will have corresponding longer residence times in the atmosphere. Finally, such particles are capable of penetrating to the innermost (pulmonary) regions of the human lung when inhaled.

8. It has been established that those trace elements which are preferentially associated with small particles are in fact highly enriched in a thin layer at or near the particle surface.

9. Material present in the particle surface layer has been shown to be easily capable of mobilization in aqueous solution and can be readily extracted into body fluids.

10. It is postulated that the enrichment of certain trace elements on fly ash particle surfaces results from their being volatilized at the temperatures encountered in the coal combustion process. As the temperature falls downstream from the combustion zone, these vapors condense onto the external surface of co-entrained fly ash particles moving toward the stack exit. Considerable evidence is available in support of this volatilization-condensation model although it is not considered to be either fully validated nor to be the only possible mechanism which can result in surface association of trace elements.

11. The distribution of elements in coal fly ash is considered to be due to three primary factors. These include the particle size, the matrix composition of the particle, and the geochemical nature of the element in question. Thus, elements belonging to the siderophile, chalcophile and lithophile classifications behave quite distinctly in terms of their partitioning behavior during and following combustion in a coal fired power plant. The principal minerals in coal fly ash are mullite, quartz, magnetite and hematite.

12. The chemical forms in which trace and minor elements exist in the surface layer of coal fly ash particles are primarily sulfates, carbonates, silicates and oxides with smaller amounts of several chlorides and possibly mixed or complex salts.

13. The composition of aqueous leachates of coal fly ash is determined by the extent to which equilibrium is achieved between the solid fly ash and the leaching solution. The four most important parameters which commonly influence this equilibrium are the composition of the fly ash, the ratio of fly ash to solution volume, the method by which the fly ash and solution are brought into contact, and the chemical characteristics of the leaching solution.

14. Leaching of coal fly ash generally proceeds quite slowly, but relatively high amounts of certain trace elements may dissolve during this time due to their presence on the particle surfaces. The use of leaching solutions of low pH results in greater dissolution of metals than does leaching at higher pH.

15. A number of polycyclic organic species (POM) have been shown to be associated with coal fly ash which is actually emitted from the stack of a coal fired power plant. On the other hand, fly ash collected and retained inside the power plant stack system rarely contains detectable amounts of polycyclic organic matter.

16. Polycyclic organic species are strongly associated with the smallest particles of fly ash emitted from a coal fired power plant.

17. Polycyclic organic matter associated with fly ash is predicted to be present in the surface layer of the fly ash.

18. Strong evidence exists to support the idea that polycyclic organic matter is initially formed in the gas phase at elevated temperatures within the power plant stack system. As the temperature falls, however, POM vapor rapidly adsorbs onto the surface of coentrained coal fly ash particles. This process apparently takes place at or close to the stack exit and is probably complete within a short distance of the stack exit in the power plant plume.

19. Particulate polycyclic organic matter emitted from a coal fired power plant is stabilized against photochemical decomposition as a direct result of being adsorbed onto the surface of the coal fly ash. A number of polycyclic organic species are shown to oxidize in the absence of light as a direct result of being adsorbed onto the surface of coal fly ash thereby significantly changing their potentially carcinogenic properties.

20. A number of potentially carcinogenic polycyclic organic species have been shown to react with stack gases such as nitrogen dioxide forming a number of derivatives the most prominent of which are nitration derivatives. This process happens fairly rapidly and is likely to have profound effects on the toxicological potential of coal fly ash particles.

SECTION 3

RECOMMENDATIONS

1. It is recommended that consideration be given to establishing particle emission standards in the future in terms of particle mass distribution as a function of size rather than simply in terms of total mass emitted as at present.

2. Emphasis in further research should be placed on identifying the actual chemical forms in which potentially toxic trace metals are present.

3. Considerable emphasis should be placed on elucidating the role(s) of coal fly ash in the conversion of sulfur dioxide and sulfur trioxide to sulfuric acid and metal sulfates both within a coal fired plant stack system and in the plume emitted therefrom.

4. One or more methods for conducting laboratory leaching studies of coal fly ash should be standardized and the present simple mathematical models describing the leaching process extended to have predictive capability for field situations.

5. Studies should be conducted to determine the extent(s) to which different soil types are capable of adsorbing or otherwise fixing trace metals present in leachates percolating through soil (e.g., in the vicinity of a coal fly ash pond).

6. More precise emission factors should be obtained for polycyclic organic matter emitted from various types of coal fired power plants.

7. Considerable study should be directed towards understanding the rate and extent of transformations of polycyclic organic matter which occur in the emitted plume of coal fired power plants.

8. Emphasis should be placed on determining how the toxicological characteristics (e.g., mutagenic and carcinogenic properties) of emitted coal fly ash varies as a function of time and distance from the point of emission.

SECTION 4

PHYSICAL CHARACTERISTICS OF COAL FLY ASH

PARTICLE MORPHOLOGY

Two general classification schemes have been reported describing different morphological classes of coal fly ash. The first, (Natusch et al., 1978a) based mainly on optical and scanning electron microscopy studies, indicates five classes of fly ash can be distinguished:

1. Large irregular particles often exhibiting extensive spherical pitting (Figure 1A). These particles predominate in the physical size fraction greater than 74 micrometers (μm) and are frequently found in fly ashes derived from coal burned in power plants utilizing a chain grate stoker and in industrial boilers.

2. Solid spherical particles (Figure 1B) whose solidity is confirmed by etching deep into the particles with a stream of positive argon ions derived from an ion milling apparatus. These solid particles predominate in the physical size range below about 10 μm.

3. Hollow spherical particles (Figure 1C) whose interior voids are confirmed by breaking the particles or etching through their shells prior to examination by scanning electron microscopy (SEM). These hollow spheres, which are referred to as cenospheres (Raask, 1968), predominate in the 20-74 μm physical size range of fly ash. Their densities are generally less than 1 g/cm^3 so that they float on effluent settling ponds. They commonly comprise about 5 percent of the mass of fly ash retained in power plant precipitators.

4. Hollow spherical particles containing a number (5-100) of small solid particles encapsulated inside them (Figures 1D and 1E). The encapsulated particles called plerospheres (Raask, 1968) are observed by breaking the outer shell of the host particle, or etching through it with argon ion bombardment, prior to SEM examination. In some cases the encapsulated particles can also be observed by optical microscopy by utilizing an objective immersion oil whose refractive index is close to that of the shell material of the host particle.

5. Agglomerates of many small (<10 μm) spherical particles forming large nonspherical particles which predominate in the physical size range greater than 74 μm (Figure 1F).

Optical microscopic observation of fly ash shows that most of the particles are colored, semi-transparent spheres suggesting an impure glass. Magnetic particles are, however, opaque. In most cases the particles have a slightly roughened surface (Figure 1) to which adhere numerous, apparently crystalline particles of submicrometer size. This adhering material is readily removed by washing with either aqueous or organic solutions (Bolton et al., 1973).

In the second scheme, described by Fisher et al. (1978), a total of eleven particle types were differentiated. These particle types differ from those of Natusch et al. (1975) principally in that optical microscopy has been incorporated into the classification scheme. In addition, Fisher et al. (1978) collected and fractionated an ash to determine the mass distributions of the various particle types. Table 1 gives the results of Fisher et al. (1978) and contains both a general description of the particle types and their mass size distributions. The fly ash was collected downstream from the electrostatic precipitator in the stack breeching of a large western U.S. power plant burning a low sulfur (0.5%), high ash (23%) coal. Although the mass distribution by class cannot be considered necessarily indicative of the distributions resulting from the combustion of other coals in other power plants; it is probably representative of a typical plant system. The relative abundance of all particle types, except non-opaque, solid spheres was found to increase with the increasing particle sizes of the fly ash fractions. Non-opaque solid spheres were found to be inversely dependent on particle size. Particle density was found to be inversely related to particle size indicating that the smaller particles contained fewer hollow or encapsulating particles.

The different particle shapes appear to be primarily a function of three factors, the chemical composition, combustion zone temperature and the particles residence time in the combustion zone. The irregular particles or those with only slightly rounded edges were the result of limited high temperature exposure. The bulk of fly ash, especially the smallest size fractions, consist almost exclusively of smooth spherical particles. This suggests that they had been exposed to higher temperatures or longer residence times, although their appearance is partly attributable to the lower melting point expected because of their size. Fly ash particles, especially the spherical ones, tend to consist of magnetic and non-magnetic fractions. While the latter reflect a diversity of particle types such as the cenospheres, solid spheres, and plerospheres previously described, the former consist of mainly black solid spherical particles, the particle colors being caused mainly by the presence of magnetite, Fe_3O_4.

Figure 1. Scanning electron micrographs of representative coal fly ash particles. Approximate diameters are in parenthesis. A. clinker (85 μm), B. solid (20 μm), C. hollow (40 μm), D. encapsulating (70 μm), E. encapsulating (60 μm), F. agglomerate (250 μm). (Reprinted by permission of D.F.S. Natusch from Natusch et al., 1975 and by A. Loh from Loh, 1975.)

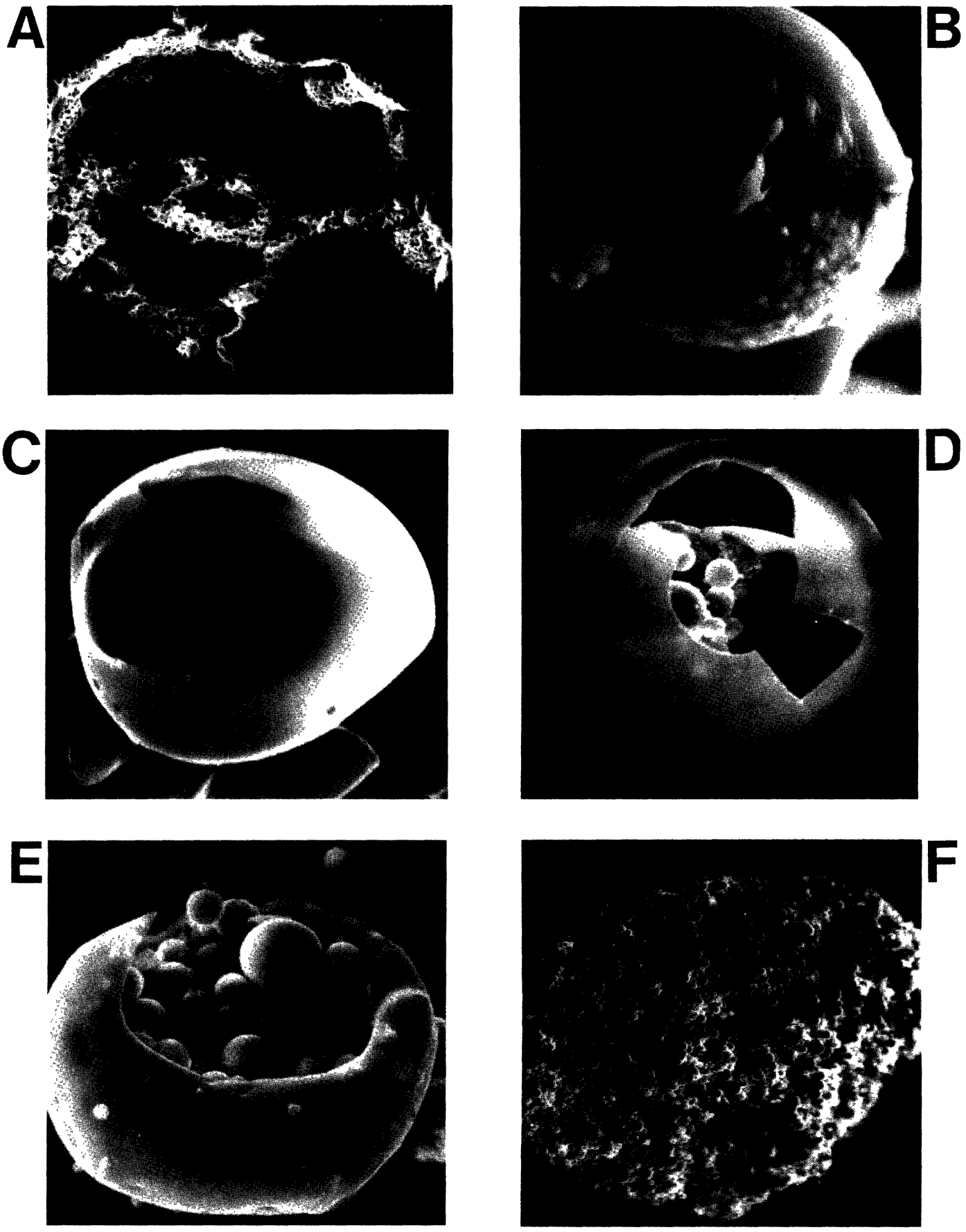
A
B
C
D
E
F

TABLE 1. RELATIVE ABUNDANCE (WT %) OF MORPHOLOGIC PARTICLE TYPES IN FOUR SIZE CLASSIFIED FLY ASH FRACTIONS* (FISHER ET AL., 1978)

	Particle type	Volume mean diameter (VMD) (μm)†			
		20	6.3	3.2	2.2
1.	Amorphous, non-opaque	7.25	2.13	0.79	0.33
2.	Amorphous, opaque	0.42	0.18	--	--
3.	Amorphous, mixed opaque and non-opaque	0.77	0.09	--	--
4.	Rounded, vesicular, non-opaque	12.39	6.67	2.91	2.99
5.	Rounded, vesicular, mixed opaque and non-opaque	2.27	0.24	--	0.03
6.	Angular, lacy, opaque	1.34	0.57	0.27	0.33
7.	Non-opaque, cenosphere	41.11	26.22	13.20	7.91
8.	Non-opaque, plerosphere	0.51	0.21	--	--
9.	Non-opaque, solid sphere	25.58	56.01	79.16	86.99
10.	Opaque sphere	1.56	0.90	0.33	0.24
11.	Non-opaque sphere with crystals	6.80	6.79	3.18	0.95
12.	Combined¶ particle types 2 and 6	--	--	0.15	0.24
	VMD (μm)	20	6.3	3.2	2.2
	Density§ (g/cm^3)	1.85	2.19	2.36	2.45

* A total of approximately 3000 particles for each size fraction were classified from random fields using three microscope slides per fraction.

† Samples aerodynamically sized by collection with an in-stack fractionator (McFarland et al., 1977).

¶ Combined due to inability to distinguish between these classes for the finer particles.

§ Apparent density determined by gravimetric displacement of 1-propanol.

Probably the most interesting aspect of fly ash morphology is the phenomenon of particle encapsulation; a phenomenon that has hereto been regarded mainly as a scientific curiosity (Matthews and Kemp, 1971; Fisher et al., 1976). However, the occurence of encapsulation in a substantial fraction of fly ash particles could have a significant influence on the overall environmental impacts of fly ash. This is because the encapsulated particles are almost always smaller than 5 micrometers (μm) in physical diameter (Figure 2). Such particles, if released from their encapsulating hosts, are difficult to control (Jones, 1972), have long atmospheric lifetimes (Butcher and Charlson, 1972; Heindrycdx and Dams, 1974), provide substantial surface area for heterogeneous reactions (Urone and Schroeder, 1969), produce significant light scattering (Butcher and Charlson, 1972), and may penetrate the innermost regions of the human lung when inhaled (Natusch and Wallace, 1974). Thus, reduced environmental impacts may result from encapsulation of large numbers of small particles emitted by enclosing them within larger, easily collected, host particles; this should be recognized as a desirable "natural" control process.

In order to establish whether or not encapsulation does influence the environmental impact of fly ash, several ashes were studied to determine specifically:

1. The physical and chemical characteristics of the encapsulated and the encapsulating particles.

2. The extent of encapsulation.

3. The probable encapsulation mechanism.

Fly ashes derived from five representative midwestern bituminous and western sub-bituminous coals collected from electrostatic precipitators of modern coal fired power plants were chosen for study. All plants utilized pulverized fuel feeds.

Fly ash particles were studied either individually or in groups by means of scanning electron microscopy (SEM) using carbon or gold coatings to increase particle conductivity. In order to identify a hollow or encapsulating particle it was necessary to rupture the outer shell. This was achieved by etching with a stream of positive argon ions, by cutting the tops off particles embedded in a plastic matrix using a microtome, by crushing the particles between two microscope slides, or by rolling a cylindrical metal bar over them. The latter was found to be most suitable for rupturing particle shells with minimal loss of their contents.

Evidence indicating that encapsulated particles are actually contained inside a host particle, as shown in Figures 2A, C, D, and E, and do not simply move there during particle rupture or SEM observation was obtained in several ways. First, encapsulated particles could occasionally be observed through holes in the encapsulating shells which were too small to permit their entry (Figure 2C). Secondly, where shell rupturing took place after particles had been carbon or gold coated, encapsulated particles exhibited considerable electrostatic charging indicating that they were not exposed at the time of coating. This effect is illustrated by the relative brightness

of the encapsulated particles compared to the host shells in Figures 2A and 2E. Thirdly, within a given size fraction, the crushed portion contained a significant number of small spherical particles which would have been removed by the size separation had they not been encapsulated (Figures 2D and E). In addition, encapsulated particles could sometimes be observed by optical microscopy using an oil immersion objective to render the intact encapsulating shells transparent (Matthews and Kemp, 1971). It seems probable, therefore, that encapsulation is not an artifact of sample preparation and observation.

In order to study the dependence of the encapsulation phenomenon on particle size, density, and magnetic character; the fly ashes were subdivided sequentially with respect to these parameters and examined by Scanning Electron Microscopy. Bulk fly ash was first separated into physical size fractions by mechanical sieving. Each of these fractions was divided into magnetic and non-magnetic fractions using a bar magnet. It is recognized that this separation is highly technique dependent, but it does serve to differentiate crudely between particles containing high and low concentrations of magnetic (iron) compounds. These fractions were then separated into several density fractions by the float - sink method (Ruch et al., 1974) using appropriate mixtures of either chloroform and diiodomethane or water and thallium formate/malonate (Clerici's solution) (Natusch et al., 1975). The contributions of encapsulating particles to the bulk mass for non-magnetic and magnetic fractions are presented in Tables 2 and 3.

Both hollow and encapsulating particles were observed in all fly ashes studied. In all cases, encapsulating particles occurred primarily in the size range 20 - 90 μm and in the density ranges <1.6-2.7 g/cm^3 and 2.1 - 3.4 g/cm^3 for non-magnetic and magnetic fractions, respectively, so only these fractions were considered in the following numerical estimates of encapsulation. Cenospheres were found to occur exclusively in the lowest density fractions and exhibited no preference for either magnetic or non-magnetic particles although their incidence has been correlated with high iron content by others (Raask, 1968).

The number of particles encapsulated inside a single host varied from about ten to several hundred with 30-100 particles being commonly observed (Figures 2A, D, E). Almost all encapsulated particles were found to be solid and to have physical diameters in the range 0.1 to 5 μm. Encapsulating shell thicknesses were typically about 5-10 percent of the diameter of the host particle (Figure 2). Elemental analyses of associated encapsulated and host particles by energy dispersive X-ray emission spectrometry excited by the SEM beam showed that the matrices were closely similar, indicating that both types were derived from essentially the same local matrix.

Figure 2. Scanning electron micrographs of coal fly ash particles showing representative encapsulated and encapsulating particles (A, C, D, E) and cenosphere shells (B, F). (Reprinted by permission of D. F. S. Natusch.)

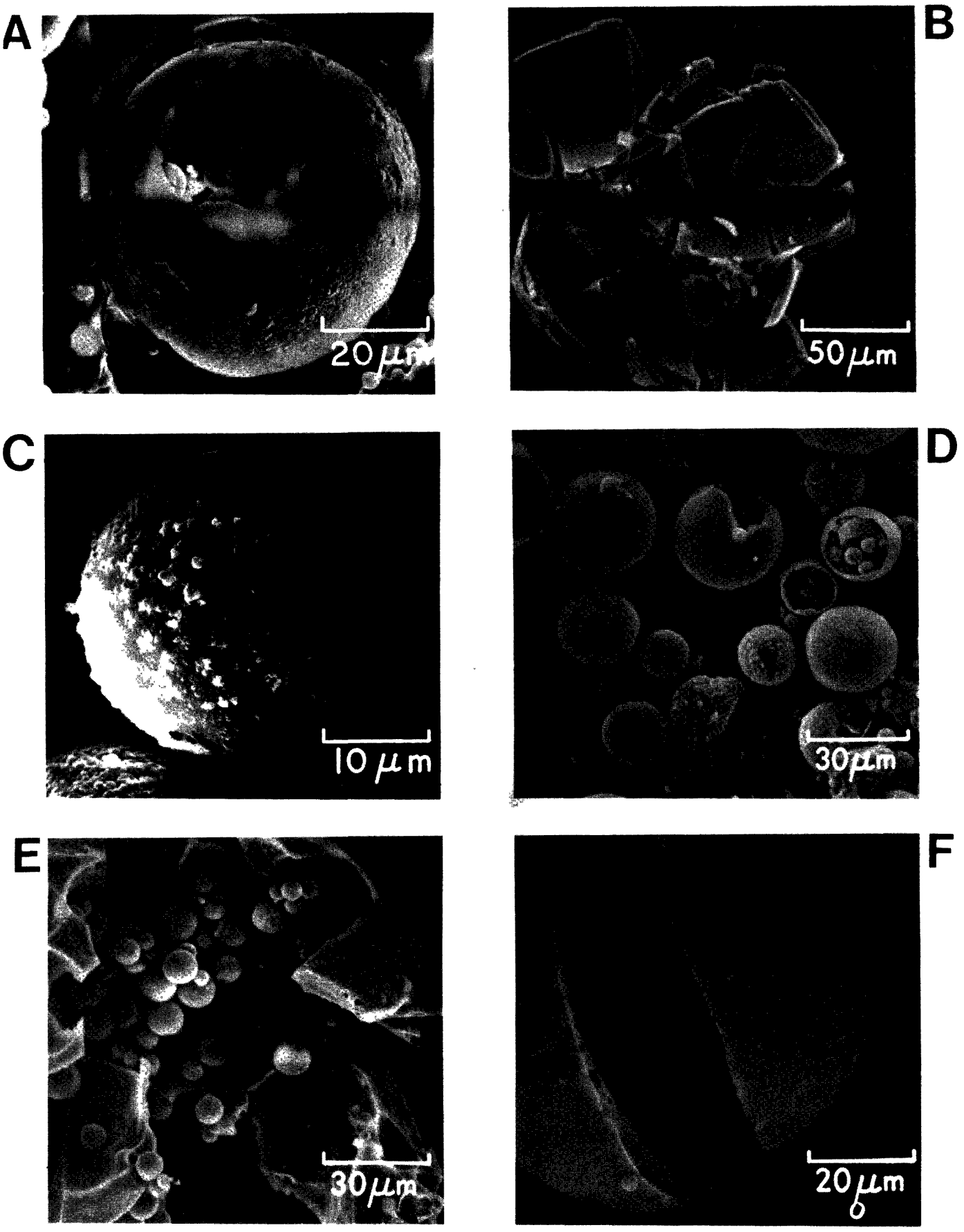
A
20 μm
B
50 μm
C
10 μm
D
30 μm
E
30 μm
F
20 μm

TABLE 2. ENCAPSULATING PARTICLE BULK MASS CONTRIBUTION (WT %) FOR THE NON-MAGNETIC FRACTION OF COAL FLY ASH*

Density (g/cm^3)	Particle size (μm)		
	20-45	45-60	60-90
<1.6	0.8-1.3	0.2-0.4	0.2-0.5
1.6-2.3	0.04-1.48	0.05-0.11	0.01-0.23
>2.3	ND†-7.01	0.04-0.97	0.03-0.55

* Data represent ranges for five different coal fly ashes.

† ND = Not detectable.

As expected, encapsulated particles have essentially no surface growths since it has been shown, both here and by other workers (Fisher et al., 1976), that microcrystal growth (Fig. 2C) usually occurs by exposure to moisture during collection and storage of fly ash. It has been suggested (Fisher et al. 1976) that SO_2 is hydrated and oxidized on the surface to H_2SO_4 which subsequently reacts with either CaO or NH_3 to form crystalline salts. It aslo has been suggested (Sarofim et al., 1977) that the crystalline material may result from deposition of fine silica particles. It has been reported (Raask, 1968; Fisher et al., 1976) that the gas contained inside cenospheres and encapsulating particles consists mainly of carbon dioxide with traces of nitrogen and water vapor. The internal pressure has been calculated to be in the range 0.3 to 0.5 atm. (Raask, 1968). On heating, all particles decrepitate (lose water) at about 300°C. The softening and slow collapsing of individual particles was observed when they were heated to 1150-1300°C on a high temperature optical or electron microscopic stage, but true melting does not take place until approximately 1350°C. Exact fusion temperatures were not determined.

The extent to which encapsulation occurs was estimated as follows. First, the relative number of encapsulating particles present in each sub-sample was determined by counting the number of spherical and non-spherical particles by optical microscopy and then counting the relative numbers of spherical particles shown to be encapsulating after each sub-fraction was crushed. This latter observation was made by means of scanning electron microscopy for which a typical field of view is shown in Figure 2D. Since encapsulating particles were always found to be spherical, this approach established the number fraction of encapsulating particles in each sub-sample. Secondly, number-fractions were generally equivalent to mass-fractions because of the narrow size and density of each sub-sample. The

TABLE 3. ENCAPSULATING PARTICLE BULK MASS CONTRIBUTION (WT %) FOR THE MAGNETIC FRACTION OF COAL FLY ASH*

Density (g/cm^3)	Particle size (μm)	
	20-60	60-90
<2.1	ND†	ND
2.1-2.9	ND-0.5	0.01-0.12
>2.9	0.39-1.4	0.05-1.00

* Data represent ranges for five different coal fly ashes.

† ND = Not detectable.

resulting percentages of the total sample mass shows that the mass percentages of the five different fly ashes involved in encapsulation were, 2.4%, 9.3%, 8.7%, 10.2%, and 1.8%.

Since a substantial fraction of the mass involved in encapsulation consists of respirable particles (Natusch and Wallace, 1974), it is appropriate to estimate just what mass percentage of all respirable particles produced are encapsulated. Based on the foregoing microscopic observations and X-ray analyses, it can be assumed that both encapsulated and host particles have the same density, that shell thicknesses are 5 to 10 percent of the host particle diameters, that host interiors are 30 to 70 percent occupied, and that all encapsulated particles are within the respirable range. These assumptions enable calculation of the percentage mass of each sample present as encapsulated, respirable particles. The ranges obtained were, 1 to 2%, 4 to 6%, 4 to 6%, 5 to 7%, and 0.8 to 1.2% for the five ashes studied. The mass percentage of free particles in the respirable range (≦5 μm) can be determined, for comparison, by plotting the cumulative fly ash mass percentage versus logarithmic physical diameter. This indicated that a closely Gaussian relationship existed and that the mass percentages of free respirable particles in each of the five fly ashes was 20%, 37%, 29%, 10%, and 25%.

Comparison of the mass percentages of both encapsulated and free particles of respirable size shows that, of all respirable particles produced by each power plant, the following mass percentages are encapsulated: 5 to 9%, 10 to 14%, 12 to 17%, 33 to 41%, and 3 to 5%. Thus, if quantitatively released to the atmosphere, encapsulated particles could significantly increase respirable particle emissions from a coal fired power plant.

Based on present information, it is not possible to state definitively whether the phenomenon should be regarded as being potentially beneficial or potentially hazardous. However, the evidence obtained in this study and by others (Raask, 1968; Matthews and Kemp, 1971; Fisher et al., 1976), suggests that encapsulated particles are actually formed inside their host particles in, or close to, the coal combustion zone. This further suggests that the mechanism of formation involves the following steps:

1. Molten spherical droplets of fly ash matrix material are formed at temperatures above 1350°C. The size distribution and viscosity of these droplets is determined by their matrix composition (and thus the original coal), the temperature, and the configuration of the combustion chamber.

2. Due to the production of gases within the molten droplets, they may expand like a balloon to an extent which is determined by their surface tension and the internal pressure. It has been suggested by Raask (1968) that the expanding gas is produced by reaction of iron oxides with residual carbon:

$$2\ Fe_2O_3 + C \rightleftarrows 4\ FeO + CO_2$$

Alternatively, decomposition of inorganic carbonates present in the coal could be involved. Either suggestion would account for the substantial amount of carbon dioxide found in particle voids and for the observation of small localized voids (Figure 2A, 2D, 2E). Expansion to equilibrium size in this way has been estimated to occur in less than a millisecond (Raask, 1968).

3. As the hollow spheres cool, their exterior surfaces solidify first leaving a molten interior whose viscosity and surface tension are sufficiently low to enable detachment of material from the concave inner surface. This, together with the reduction of internal pressure within the sphere on cooling, promotes "budding off" of molten droplets whose surface tension is now great enough to prevent extensive coalescence. Support for this process is provided by the fact that, for a given fly ash, the surface tension of molten matrix material, as calculated from the known composition of each sub-fraction (Morey, 1954), exhibits a significant correlation with the percentage of encapsulating particles (Figure 3). Further support comes from the close matrix identity observed for encapsulated and host particles.

In conclusion, it would appear that encapsulation does not result in the containment of small particles which might otherwise be emitted to the atmosphere. On the other hand, it is unlikely that it gives rise to additional particulate emission. If, however, encapsulated particles were subjected to sufficient mechanical shock to cause their rupture, a substantial increase in respirable particle emission should be anticipated.

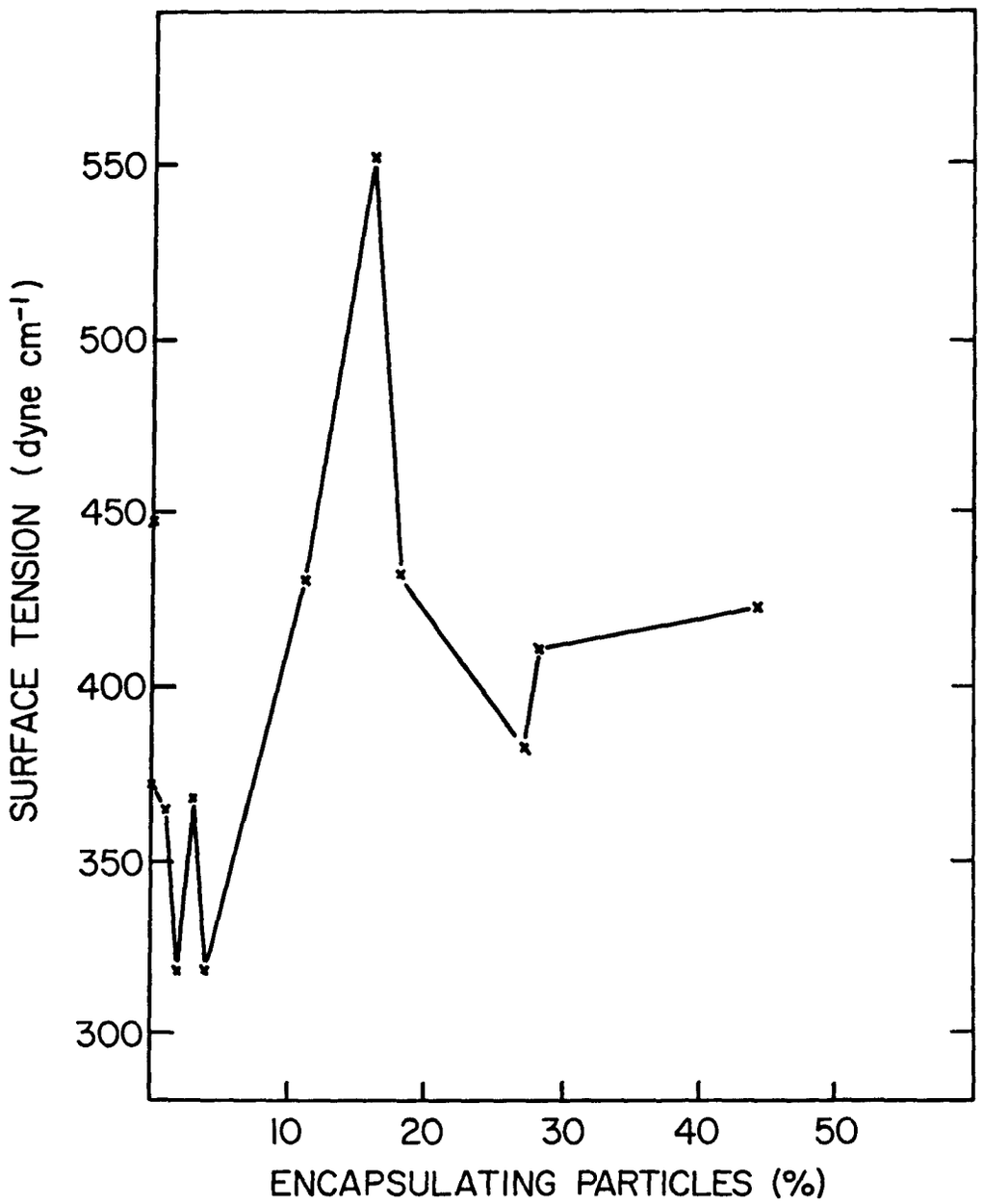

Figure 3. Calculated surface tension at 1400°C as a function of the percentage of encapsulating particles.

MASS, DENSITY, AND FERROMAGNETISM DISTRIBUTIONS

In addition to particle morphology, a number of other physical properties have been investigated in an attempt to elucidate the formation and behavioral characteristics of fly ash. Such properties include the mass distributions according to particle size, particle density, and ferromagnetic properties. The available data are incomplete and apply only to fly ash collected after a control device or from the device itself. Consequently, it is not presently possible to relate physical properties to parameters such as plant operating conditions or the type of coal from which the fly ash was derived. Nevertheless, it is qualitatively apparent that the physical properties of fly ash depend upon both of these parameters.

Measurements of the distribution of fly ash particle mass with size are of two distinct types. The first involves determination of the aerodynamic particle size distribution, which normally involves isokinetic collection of fly ash directly from a stack gas stream. Several sampling devices are available, but the most common involve the principle of inertial impaction and enable collection and size classification of fly ash in situ. Alternatively, bulk fly ash, such as might be collected from an electrostatic precipitator or bag house, can be differentiated into physical size fractions by mechanical sieving. In either case it is necessary to separate the various size fractions prior to weighing or microscopic counting for size estimation.

These two types of measurement are quite distinct. Aerodynamic size determination enables prediction of the atmospheric (air-stream) behavior of each size fraction, such as is important for establishing particulate collection efficiency, atmospheric residence, and inhalation characteristics (White, 1963; Butcher and Charlson, 1972; Natusch and Wallace, 1974; Yeh et al., 1976). On the other hand, physical size determination provides a straightforward measurement of the physical dimensions of the particles and can be directly related to particle number. Interconversion between aerodynamic and physical sizes can be accomplished using the relationship (Koltrappa and Light, 1972):

$$D_{ae}^2 = D_r^2 \frac{C(D_r)\rho_r}{C(D_{ae})\rho_{ae}} \qquad (1)$$

where D_{ae} is the aerodynamic particle diameter, D_r is the physical particle diameter, ρ_r is the particle density, ρ_{ae} is 1 g/cm^3 by definition, and $C(D_{ae})$ and $C(D_r)$ are the Cunningham slip correction factors for the diameters D_{ae} and D_r. Raabe (1976) has compared the commonly used conventions for description of the aerodynamic size of respirable aerosols including a detailed description of the slip correction and dynamic shape factors. Aerodynamic size distributions are often presented as lognormal probability functions of the grouped mass or number data derived from inertial impaction instrumentation.

Fisher et al. (1978) compared fly ash fractions collected isokinetically (Ondov et al., 1976, Ondov et al. 1979) with electrostatic precipitator samples from the same plant fractionated in the laboratory. The results show that, for the larger and generally less uniform particle sizes, the agreement between laboratory and field separations is not particularly good. However, for the smaller size fractions (physical diameter below about 2 μm) agreement was considerably better.

Despite the comparative simplicity of determining both the aerodynamic and physical size distributions of fly ash mass, the number of available measurements of fly ash prior to collection by control equipment is relatively sparse. It has been established, however, (Southern Research Institute, 1975) that the size and morphology of fly ash depend not only on the nature of the mineral inclusions in coal, as discussed in the previous section, but also on the manner in which the coal is burned. This latter dependence is illustrated in Figure 4 for fly ash derived from coal burned in a chain grate stoking unit, a pulverized coal fed unit, and a cyclone fired unit (Southern Research Institute, 1975). In each case the fly ash was sampled upstream from control equipment so it is representative of that generated by combustion.

It is apparent from Figure 4 that the fly ash mass approximates a log-normal distribution over the aerodynamic size range considered. Furthermore, although the geometric standard deviations of the three distributions are similar, their mass median diameters differ considerably (i.e., Cyclone ≅ 6 μm; Pulverized ≅ 18 μm; Stoker ≅ 42 μm).

From a practical standpoint, one is primarily interested in the aerodynamic size distribution of the fly ash which is actually emitted from a coal fired power plant. This is, of course, largely determined by the collection efficiency of the particle control equipment. Specifically, the size distribution of the emitted fly ash is determined by the product of the function describing the size dependence of fly ash mass entering a control device and that function describing the dependence of collection efficiency of this device on particle size. Examples of the physical size distributions of fly ash mass emitted from a coal fired power plant equipped with different control devices are presented in Figure 5 (Ondov et al., 1975). The results indicate that the size of the particles emitted by the two control devices were roughly comparable. However, the mass of material emitted in the respirable range was greater for the scrubber system than for the electrostatic precipitator (Ondov et al., 1979). Thus, determination of the densities of different fly ashes, and sub-fractions thereof, provides a means of interconverting aerodynamic and physical sizes according to Equation 1. In addition, some differentiation between distinct morphological and compositional characteristics can be achieved. For example, cenospheres can readily be distinguished from solid particles on the basis of density as can predominantly carbonaceous particles from aluminosilicates (Fisher et al., 1978).

Determination of fly ash particle density is achieved most simply by means of the traditional "float-sink" method which employs a series of liquids of different densities to separate the particles (Ruch et al., 1974; Olson and Skogerboe, 1975). Alternatively, separation can be achieved by

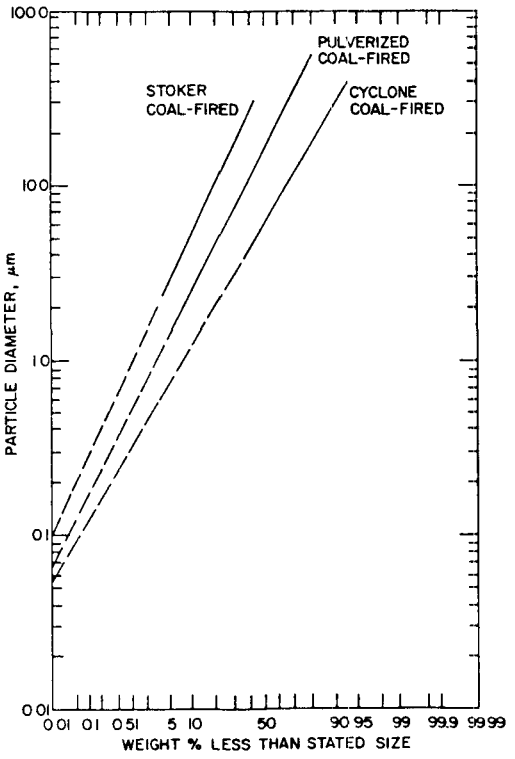

Figure 4. Particle size distributions resulting from coal combustion in different boiler types. (Reprinted by permission of A. E. Vandegrift and the Midwestern Research Institute from Vandegrift and Shannon, 1971.)

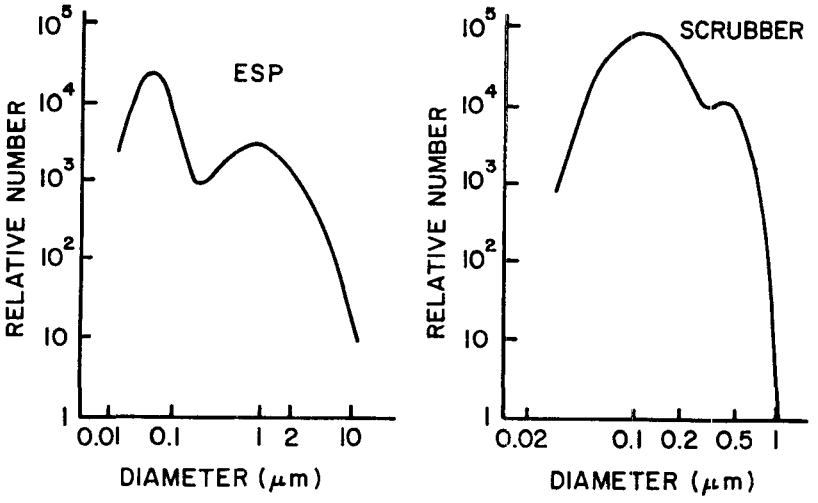

Figure 5. Particle size distribution of emissions from similar production units at the same power plant equipped with either an electrostatic precipitator (ESP) or a Venturi wet scrubber. (Reprinted by permission of J. Ondov from Ondov et al., 1976.)

placing the particles in a liquid in which a density gradient has been established (Loh, 1975).

While determination of particle density is of considerable interest in its own right, more definitive insights are obtained if density separations are carried out in conjunction with sequential size separations and with differentiation between ferromagnetic and non-ferromagnetic particles. This three dimensional fractionation scheme has been described in Section IV.

Typical mass distributions are presented in Figure 6 and Tables 4 and 5. Figure 6A shows the mass distribution in a typical midwestern U.S. bituminous coal fly ash while Figure 6B shows how the bulk ash is distributed between non-magnetic and magnetic fractions. Tables 4 and 5 enable comparisons to be made between mass distributions of midwestern bituminous and western sub-bituminous coal fly ashes for non-magnetic and magnetic fractions, respectively.

The data in Figure 6A and 6B illustrate two points. First, at least for electrostatic precipitator ash, the mass of fly ash in a given fraction varies inversely with the size of particles. Thus, the number of particles in the smallest (respirable) size fraction greatly exceeds those in the larger size fractions. Second, the distribution of mass between non-magnetic and magnetic fractions of the fly ash are reasonably constant as shown in Figure 6B. This suggests that no single fraction can be isolated solely by magnetic properties and also suggests that iron is fairly uniformly distributed in the fly ash.

A number of characteristics of coal fly ash can be distinguished from the data presented in Tables 4 and 5. It is apparent that both fly ashes are compositionally heterogeneous, since there are considerable differences between their mass distributions. As discussed above, much of the variation in densities observed is attributable to morphological rather than compositional characteristics. This is rather well illustrated by the data in Figure 7, where density distributions are presented as a function of particle size before and after crushing the fly ash. The observed shift to higher density on crushing indicates the presence of vesicular particles and cenospheres in the larger size fractions, as discussed previously. Interestingly, the X-ray powder diffraction patterns of each of the subfractions presented in Tables 4 and 5 reveal no convincing differences in matrix composition which depend upon either size or density (Natusch et al., 1975). This finding further supports the contention that the density distributions in fly ash are largely determined by morphology rather than by composition. There are, however, very distinct differences between the amount of magnetite (Fe_3O_4) present in the magnetic and nonmagnetic fractions. This suggests that magnetite is primarily responsible for the magnetic properties of coal fly ash.

ELECTRICAL RESISTIVITY DISTRIBUTION

The electrical resistivity of coal fly ash is an important physical property from the standpoint of control. Thus, it has been established (Bickelhaupt, 1974; 1975a, 1975b) that the collection efficiencies of

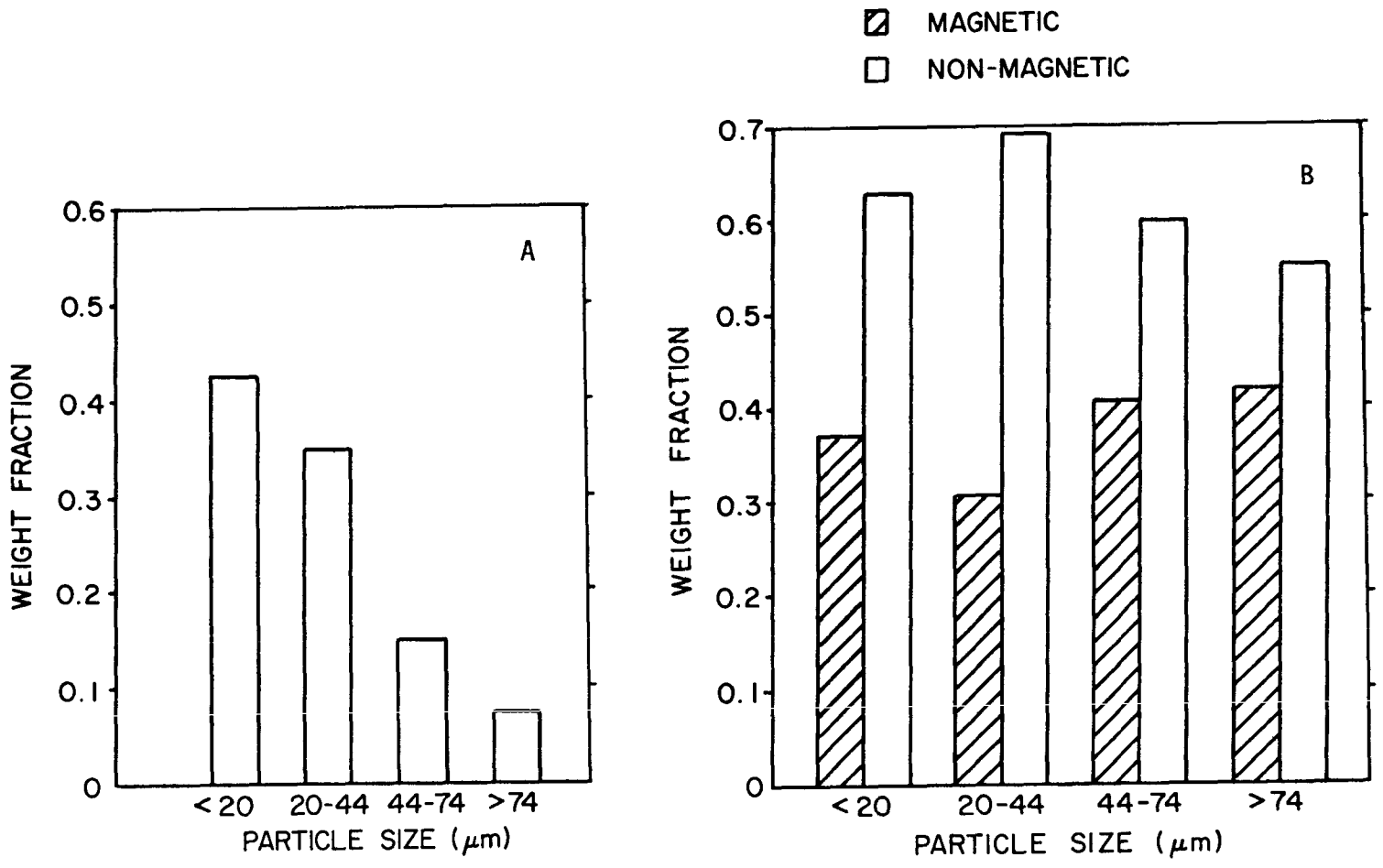

Figure 6. Mass distribution of non-magnetic and magnetic coal fly ash fractions as a function of particle size. A. Bulk ash distribution. B. non-magnetic and magnetic fraction distributions expressed as weight fractions of total weight (non-magnetic plus magnetic particles) of each size increment. (Reprinted by permission of A. Loh from Loh, 1975.)

TABLE 4. MASS DISTRIBUTION (WT %) OF NON-MAGNETIC FRACTIONS OF FLY ASHES FROM MIDWESTERN BITUMINOUS AND WESTERN SUB-BITUMINOUS COALS (D.F.S. NATUSCH, UNPUBLISHED RESULTS)

Type of coal	Particle size (μm)	Percent of total mass in density ranges indicated (g/cm³)					
		<1.6	1.6-2.0	2.0-2.3	2.3-2.7	2.7-3.0	>3.0
Midwestern coal	<20	*	*	0.2	28.0	*	*
	20-60	1.4	1.3	12.1	12.9	0.1	*
	60-90	0.7	1.0	0.6	1.1	0.6	0.1
	>90	0.1	0.1	0.1	0.6	0.5	0.2
Western coal	<20	*	*	*	0.7	*	*
	20-44	0.2	0.4	0.5	21.3	0.3	0.2
	44-74	0.5	0.8	1.0	45.6	0.6	0.5
	>74	0.2	0.3	0.4	16.1	0.2	0.2

* Less than 0.05%.

electrostatic precipitators increase with decreasing fly ash resistivity. Bickelhaupt (1974; 1975a, 1975b) has further shown that both the surface and volume resistivities of fly ash, at precipitator operating temperatures, are inversely proportional to the specific concentrations of alkali metals that are thought to act as charge carriers. These studies have shown that considerable differences in electrical resistivity occur between different fly ashes, and correlations are observed between fly ash resistivity and alkali metal content.

In addition, resistivity changes with temperature. This is illustrated in Figure 8 (Kropp et al., 1979) where a maximum is observed at about 180°C. It was found (Kropp et al., 1979) that the use of a wet scrubber, of either Venturi or centrifugal type, helped reduce resistivity. As a result, the collections efficiencies of in-line electrostatic precipitators was improved, probably due to reduction in flue gas temperatures.

No studies relating particle size to either surface resistivity (Bickelhaupt 1975a) or volume resistivity (Bickelhaupt, 1975b) have been reported.

TABLE 5. MASS DISTRIBUTION (WT %) OF MAGNETIC FRACTIONS OF FLY ASHES FROM MIDWESTERN BITUMINOUS AND WESTERN SUB-BITUMINOUS COALS (D.F.S. NATUSCH, UNPUBLISHED RESULTS)

Type of coal	Particle size (μm)	Percent of total mass in density ranges indicated (g/cm³)					
		<2.1	2.1-2.5	2.5-2.9	2.9-3.4	3.4-3.6	>3.6
Midwestern coal	<20	*	0.6	0.4	1.3	14.9	0.5
	20-60	0.2	0.6	1.8	11.5	3.1	0.1
	60-90	0.5	0.8	1.0	0.2	*	*
	>90	0.1	0.2	0.3	0.2	0.1	*
Western coal	<20	*	*	*	*	*	*
	20-60	*	*	*	1.0	*	*
	60-90	0.1	0.1	0.2	6.8	0.1	0.1
	>90	*	*	*	1.5	*	*

* Less than 0.05%.

However, a number of authors have reported changes in sodium and potassium concentrations as a function of particle size (Loh, 1975; Davison et al., 1974; Coles et al., 1979; Klein et al., 1975; Cambell et al., 1978; Block and Dams, 1976). These results indicate that some, but not all, coal fly ashes show increasing sodium and potassium concentrations in smaller particles. Sodium and potassium concentrations also have been reported to decrease with decreasing density (Loh, 1975). Similar, though less pronounced, density dependencies are observed in the magnetic fractions, but size dependencies, if any, are obscure (Loh, 1975). Since both decreasing density and decreasing physical size contribute to decreasing aerodynamic size, it is apparent that the efficiency of electrostatic precipitation per unit mass of size-classified fly ashes showing concentration trends increases with decreasing aerodynamic particle size. This is an extremely desirable characteristic. It should be pointed out, however, that since not all fly ashes show such concentration trends, improved collection efficiencies for small particles will not occur in all cases.

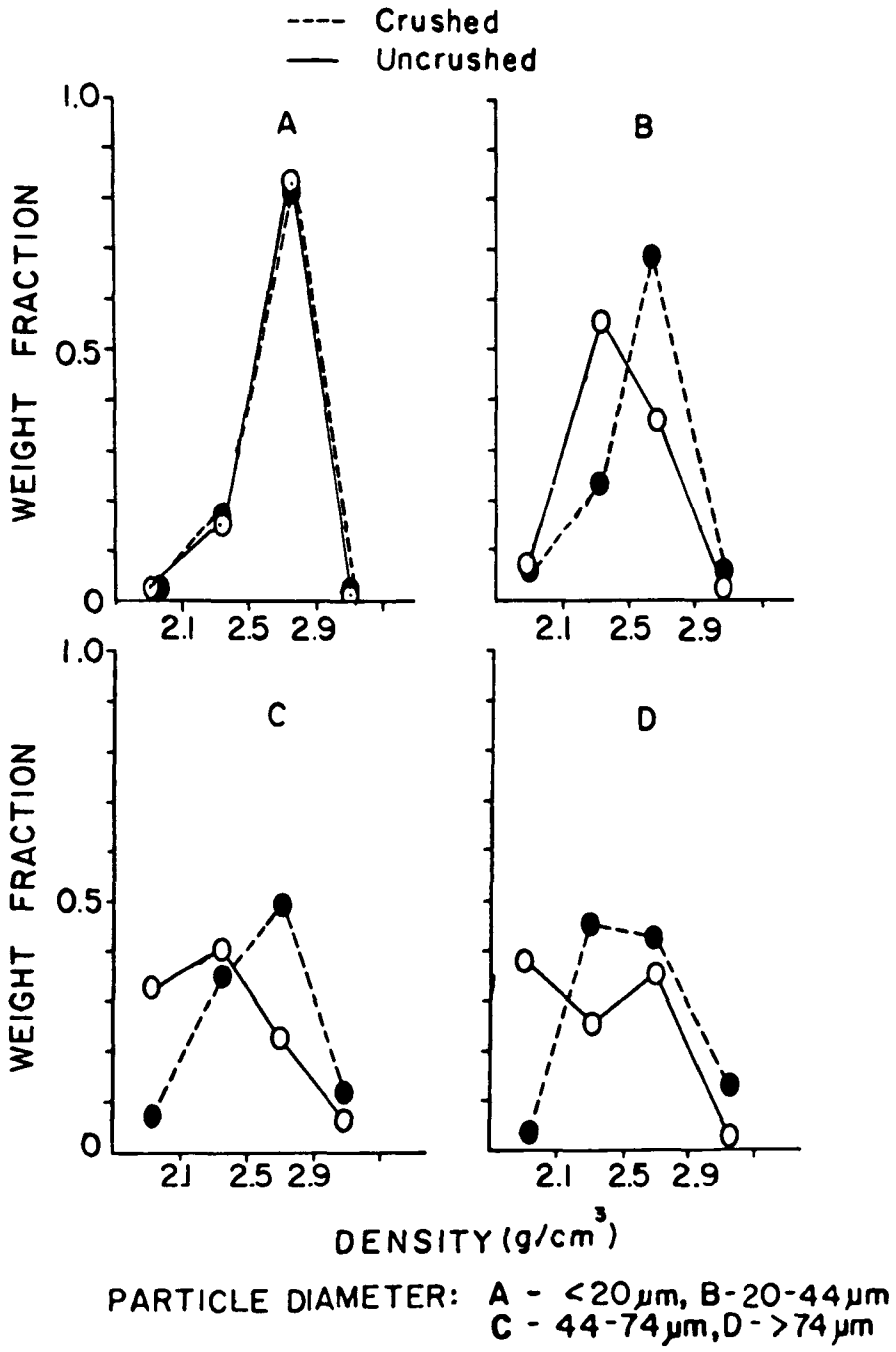

Figure 7. Mass distribution of size and density classified coal fly ash with and without crushing. The shift to higher densities after crushing is indicative of hollow or vesicular particles. (Reprinted by permission of A. Loh from Loh, 1975.)

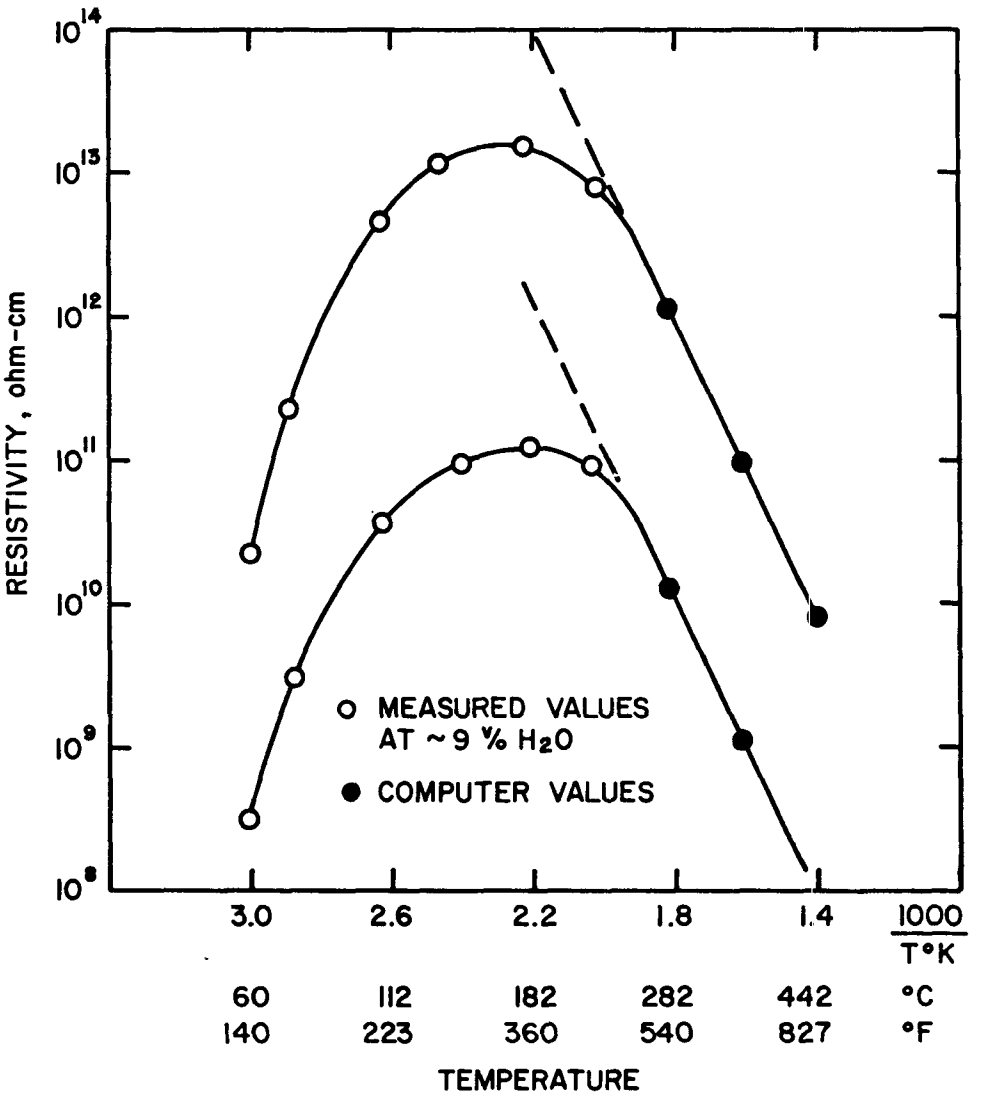

Figure 8. Resistivity as a function of reciprocal absolute temperature for two different coal fly ashes. Upper curve Na_2O 0.25 weight percent of ash. Lower curve Na_2O 2.31 weight percent of ash. (Reprinted by permission of the Air Pollution Control Association and R. E. Bickelhaupt from Bickelhaupt, 1975a.)

SURFACE AREA DISTRIBUTION

The specific surface area of fly ash particles is an important parameter in determining a number of behavioral characteristics. It is the surface area of a particle which determines the electrostatic charge which can be placed on that particle in an electrostatic precipitator (White, 1963; Bickelhaupt, 1974; 1975a, 1975b); it is the surface area of a particle which determines the extent of condensation or adsorption of species from the gas phase (Davison et al., 1974; Natusch and Tomkins, 1978); and it is the surface area of fly ash which significantly affects the rate and extent of its aqueous leaching (Natusch et al., 1975; Matusiewicz and Natusch, 1979).

To a reasonable approximation, one would expect the specific surface areas (m^2/g) of fly ash to increase linearly with decreasing particle diameter since the particles are predominantly spherical. Similar trends would also be expected for non-spherical particles having similar shape factors (Butcher and Charlson, 1972). In general, the specific surface area, S_w, is given (Exner and Hausner, 1974) by:

$$S_w = \frac{6\alpha}{D\rho} \qquad (2)$$

where α = shape factor, D = mean particle diameter (μm), and ρ = particle density (g/m^3).

The shape factor varies from 1 for spherical particles to 20 for irregular, elongated particles. The specific surface area is directly proportional to the shape factor and shows great variability of S_w with the morphology of the particles.

Specific surface areas of a size and density fractionated midwestern bituminous coal fly ash are given for illustrative purposes in Table 6. All measurements were made by adsorbing and desorbing the inert gases nitrogen and helium.

In general, the expected trend of increasing area with decreasing particle size was observed. However, there are exceptions, especially in the largest size fractions (>74 μm). It would be expected that these fractions would have a smaller number of particles per unit mass and consequently would have a lower specific surface area, but the opposite was true. The particles in these fractions are more irregular in shape and apparently exhibit a significant internal surface areas as well. Such behavior would result from a particularly porous surface, surface crystal formation or cracks that permitted the adsorbate gas to penetrate to the interior. The morphological studies reported in section IV support this. The possible influences of the small encapsulated and/or the hollow particles on surface area are unknown but could provide an explanation for the discrepency.

Several of the fractions show no significant dependence of surface area on particle diameter. These data suggest that the internal surface area is effectively proportional to particle volume rather than external surface area. In this regard, it has recently been suggested (Natusch, 1978b) that

collisionally efficient condensation processes may result in deposition of material from the gas phase predominantly onto the external particle surface, whereas much less efficient adsorption processes (Natusch and Tomkins, 1978) can deposit gases and vapors on both the internal and external surfaces of a particle.

In general, the specific surface areas can be seen to increase as the densities of the particles decrease. This is attributed to the fact that there are more particles per unit weight of sample and more hollow particles in the less dense fractions.

The magnetic and non-magnetic fly ash fractions, although not identical, show similar trends. However, the large specific surface areas of the larger, heavier magnetic fraction compared to their non-magnetic counterparts do stand out as an exception. Possibly these particles have a more porous structure or a greater internal surface area.

The results in Table 6 appear to be lower than those reported by some authors (Kaakinen et al., 1975; Miguel, 1976) but about the same as those of Watt and Thorne (1965). It should be noted, however, that only Miguel (1976) reports data for fractionated fly ash, so direct comparison between the data of these authors is not possible. It does appear that an upper specific surface area limit of about 4-5 m^2/g is reasonable for some bulk fly ashes, especially ashes having a high proportion of non-spherical particles.

TABLE 6. SPECIFIC SURFACE AREAS (m^2/g) OF COAL FLY ASH FRACTIONS FROM A MIDWESTERN BITUMINOUS COAL

	Particle size (μm)	S_w density ranges (g/cm^3) indicated			
		<2.1	2.1-2.5	2.5-2.9	>2.9
Non-magnetic	<20	0.35	0.35	0.33	0.30
	20-44	0.31	0.29	0.27	0.26
	44-74	0.22	0.26	0.24	0.24
	>74	0.96	0.25	0.13	0.29
Magnetic	<20	--*	--	0.30	0.24
	20-44	--	0.31	0.28	0.14
	44-74	--	0.37	0.22	0.15
	>74	--	1.16	0.68	0.18

* No meaningful data.

SECTION 5

CHEMICAL CHARACTERISTICS OF COAL FLY ASH

MATRIX ELEMENT COMPOSITION AND DISTRIBUTION

Elemental analyses of fly ash shows that the major (matrix) elements are Al, Fe and Si together with up to a few percent of Ca, K, Na, S, and Ti. These elements are generally present as oxides, carbonates, sulfates, or silicates. Fly ashes from western sub-bituminous coals usually exhibit higher levels of calcium than do midwestern bituminous coals. Numerous authors (Klein et al., 1975; Ondov et al., 1975; Coles et al., 1979; Cambell et al., 1978; Bickelhaupt, 1975a) have reported analyses for the matrix elements in different fly ashes. The reported compositions vary over considerable ranges. The range of values, as well as the values for the National Bureau of Standards (NBS) Standard Reference Material, SRM 1633, are reported in Table 7.

To further characterize the distributions of fly ash matrix elements, a midwestern sub-bituminous coal was analysed with respect to particle size, density, and ferromagnetism. The results of these analyses are given in the tables in Appendix B. However the dependence of concentration on these variables can be found by examination of Figures 9 to 16. Reference should be made to Figure 6 for the mass distribution of the fractions.

Silicon and Aluminum

The highest concentrations of aluminum and silicon were found in the low density, non-magnetic fractions as shown in Figures 9 and 10. This is because of the abundance of alumino-silicates (from optical microscopy data) and increasing amounts of mullite (SiO_2) in the low density fractions (from X-ray diffraction data). It is noteworthy that both silicon and aluminum are still present at significant concentrations in the high density, magnetic fractions. This is probably because of the presence of encapsulating particles (see Section IV) or particles which contain mixed phases. It can also be seen that aluminum and silicon concentrations do not vary greatly with particle size, confirming data from optical and electron microscopy.

Iron

The iron concentrations in the separated fly ash samples are presented in Figure 11. The highest concentrations of iron are found in the most dense, magnetic particles. Data from optical microscopy and X-ray diffraction have shown the presence of magnetite and hematite in the magnetic

TABLE 7. TYPICAL MATRIX ELEMENT COMPOSITION RANGES OF SOME AMERICAN AND BRITISH COAL FLY ASHES (WT % OF ASH)

Element	American*	British†	NBS-SRM 1633¶
Al	7-16	12-18	12.7
Ca	0.4-22	1.2-5.5	4.7
Fe	2-15	4-10	6.2
K	0.2-2.9	1.5-3.5	1.6
Na	0.2-1.7	0.2-1.4	0.3
S	0.2-1§	0.3-0.8ϕ	NRξ
Si	10-28	1.9-24	21
Ti	0.4-1.6	0.4-0.7	0.7

* Data adapted from Bickelhaupt (1975a) for several American ashes.

† Data adapted from Watt and Thorne (1965) for 14 British ashes.

¶ Data of Ondov et al. (1975) for the NBS standard reference material (SRM) 1633.

§ Soluble SO_4^{2-}.

ϕ Reported as SO_3.

ξ NR = Not reported.

fractions which explains the high concentrations of iron that are present. The iron concentrations in this fly ash sample are high because of the high pyrite content of Illinois coals used in the power plant (Rao and Gluskoter, 1973). The iron is still present at relatively high concentrations in the least dense, non-magnetic fractions.

Sulfur

Sulfur concentrations can be seen to be higher in the non-magnetic fraction but do not show any significant dependence on particle size or density (Figure 12). Sulfur was not found to be associated with iron, indicating that most of the pyrite in the coal had decomposed during coal combustion.

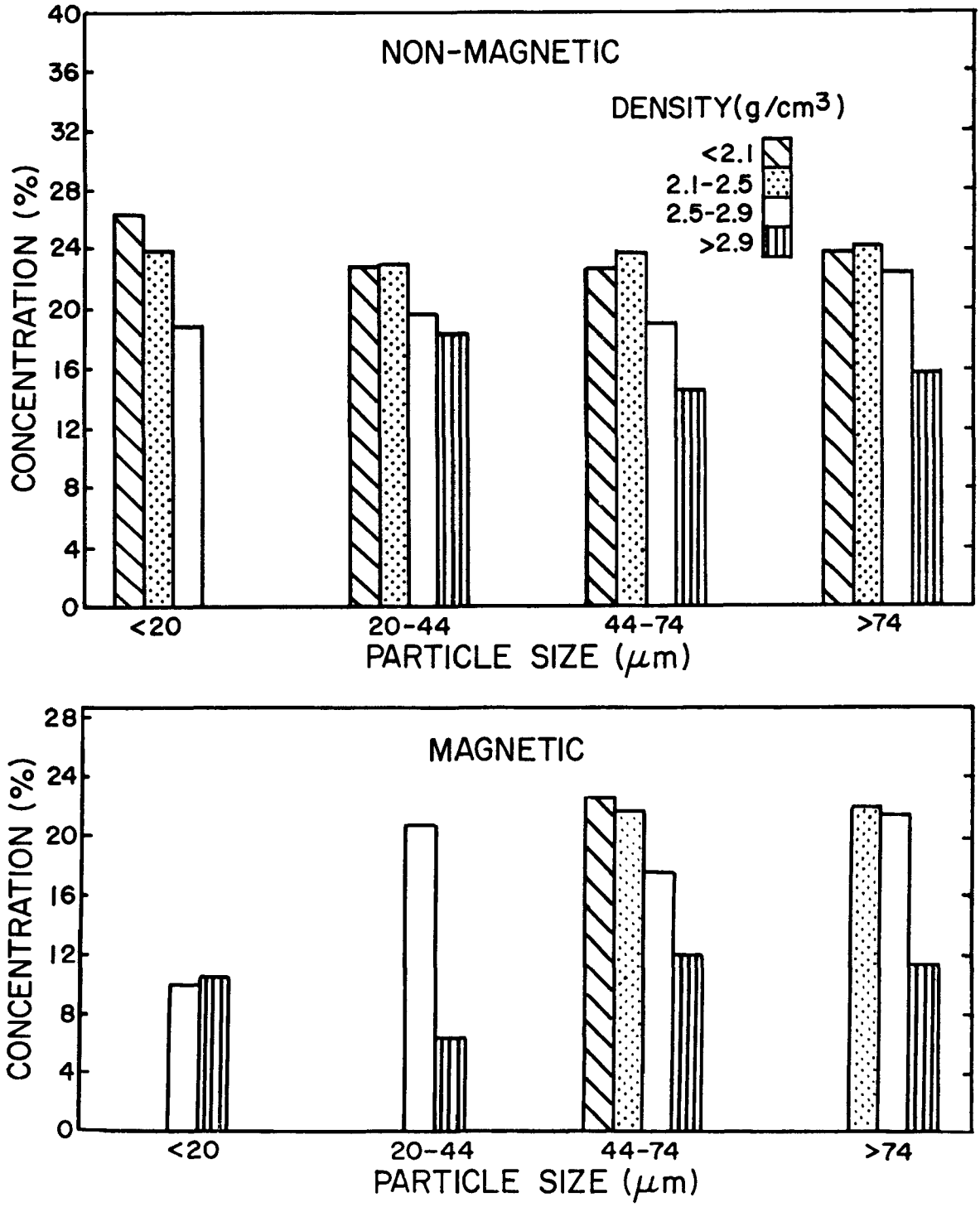

Figure 9. Concentration of silicon in non-magnetic and magnetic coal fly ash fractions as a function of particle size and density. (Data of Loh, 1975.)

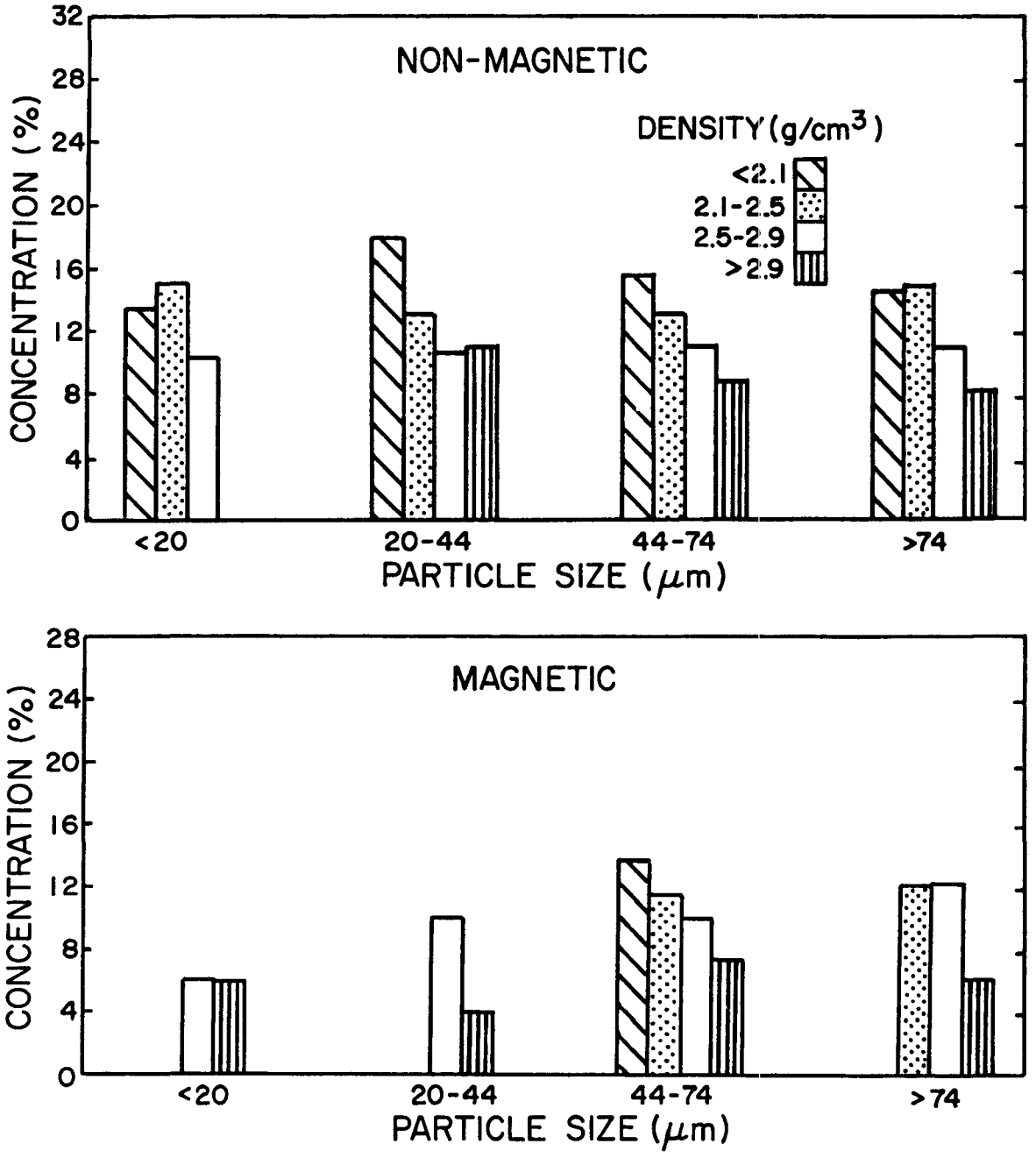

Figure 10. Concentration of aluminum in non-magnetic and magnetic coal fly ash fractions as a function of particle size and density (Data of Loh, 1975.)

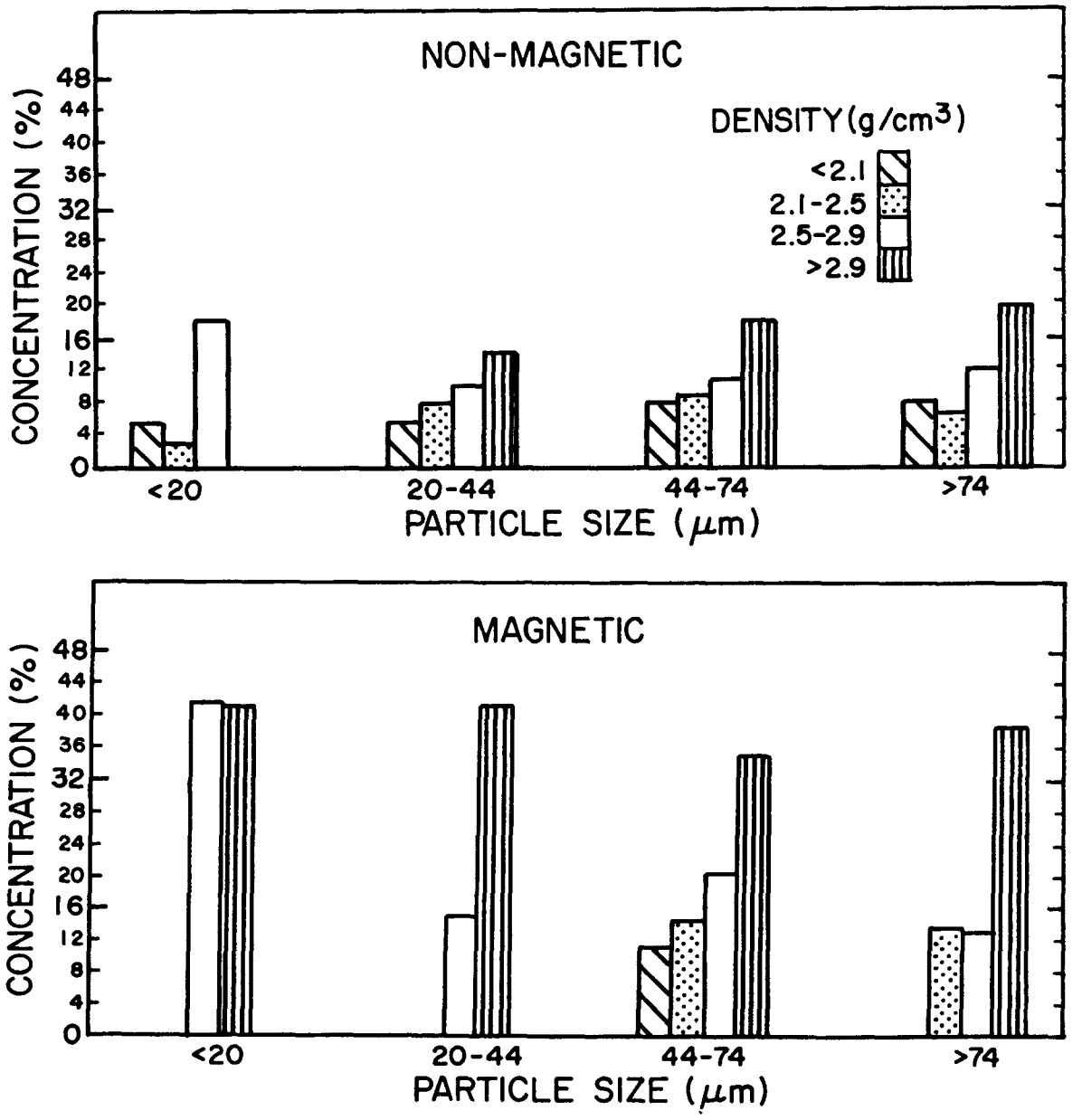

Figure 11. Concentration of iron in non-magnetic and magnetic coal fly ash fractions as a function of particle size and density. (Data of Loh, 1975.)

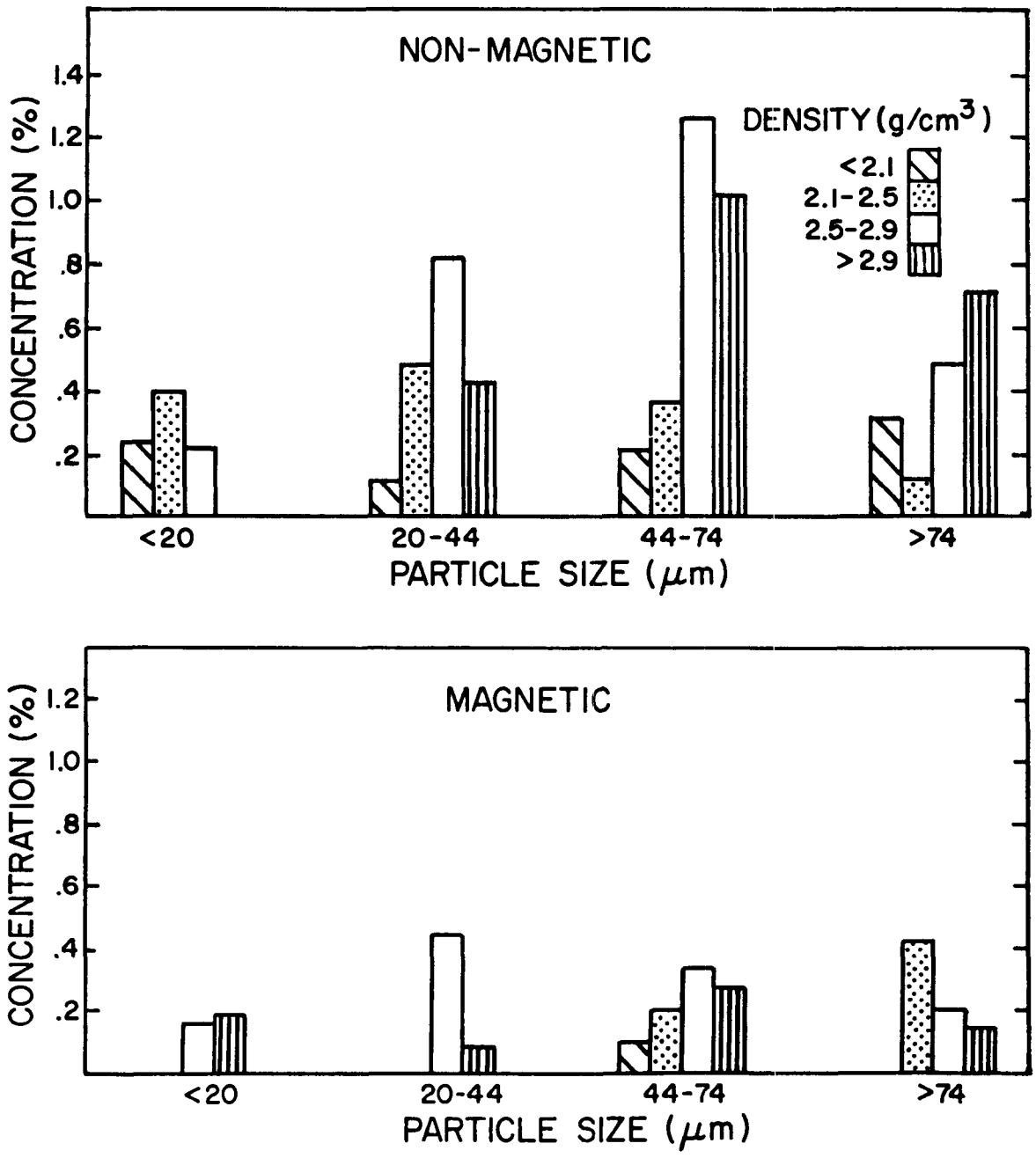

Figure 12. Concentration of sulfur in non-magnetic and magnetic coal fly ash fractions as a function of particle size and density. (Data of Loh, 1975.)

Potassium

Figure 13 shows the concentration of potassium in coal fly ash fractions separated by size, density and magnetic properties.

Potassium concentrates in the low density particles in both the magnetic and non-magnetic fractions. Potassium may be associated with the glassy, alumino-silicates which predominate in the less dense fractions. The presence of encapsulating particles or particles with different phases could explain the significant quantities of potassium found in the magnetic fractions. Potassium also appears to be more concentrated in the smaller particles indicating that the element may exhibit vaporization-condensation partitioning behavior.

Sodium

Figure 14 shows that sodium concentrations are also higher in the small size, low density fractions, following trends similar to those for potassium. The non-magnetic fractions show higher concentrations than the magnetic fractions as for potassium, but the differences between the two appear to be more pronounced. It is uncertain whether this difference is significant.

Calcium

Figure 15 shows that calcium concentrations increase with increasing density and particle size for the non-magnetic particles but appear to be fairly evenly distributed in the magnetic particles. The reasons for this are not clear but could be due to the presence of amorphous calcium compounds since X-ray powder diffraction did not show any calcium containing crystals. It should be noted that, even though the high density, non-magnetic fractions contain a high concentration of calcium, the total mass of these fractions is small. Consequently, the high density, non-magnetic fractions contribute only a small percentage of the total bulk sample calcium.

Titanium

Titanium appears to be quite homogeneously distributed in the separated fly ash fractions. The data were not plotted but are presented in Appendix B. Titanium would not be expected to volatilize in appreciable quantities during coal combustion and would tend to remain with the same elements with which it was associated in the original coal.

The elements discussed above comprise the major and minor constituents of the fly ash matrix. They are also the elements which tend to be present at higher concentrations (~0.05 to 3% by weight) in the coals burned; their presence as minor to major constituents in the ash is not surprising. Their combined presence in the glassy composite of the ash, primarily as mixed oxides, carbonates, and ferro- or alumino-silicates strongly influences the physical, chemical, and solubility properties of the ash (see discussion below).

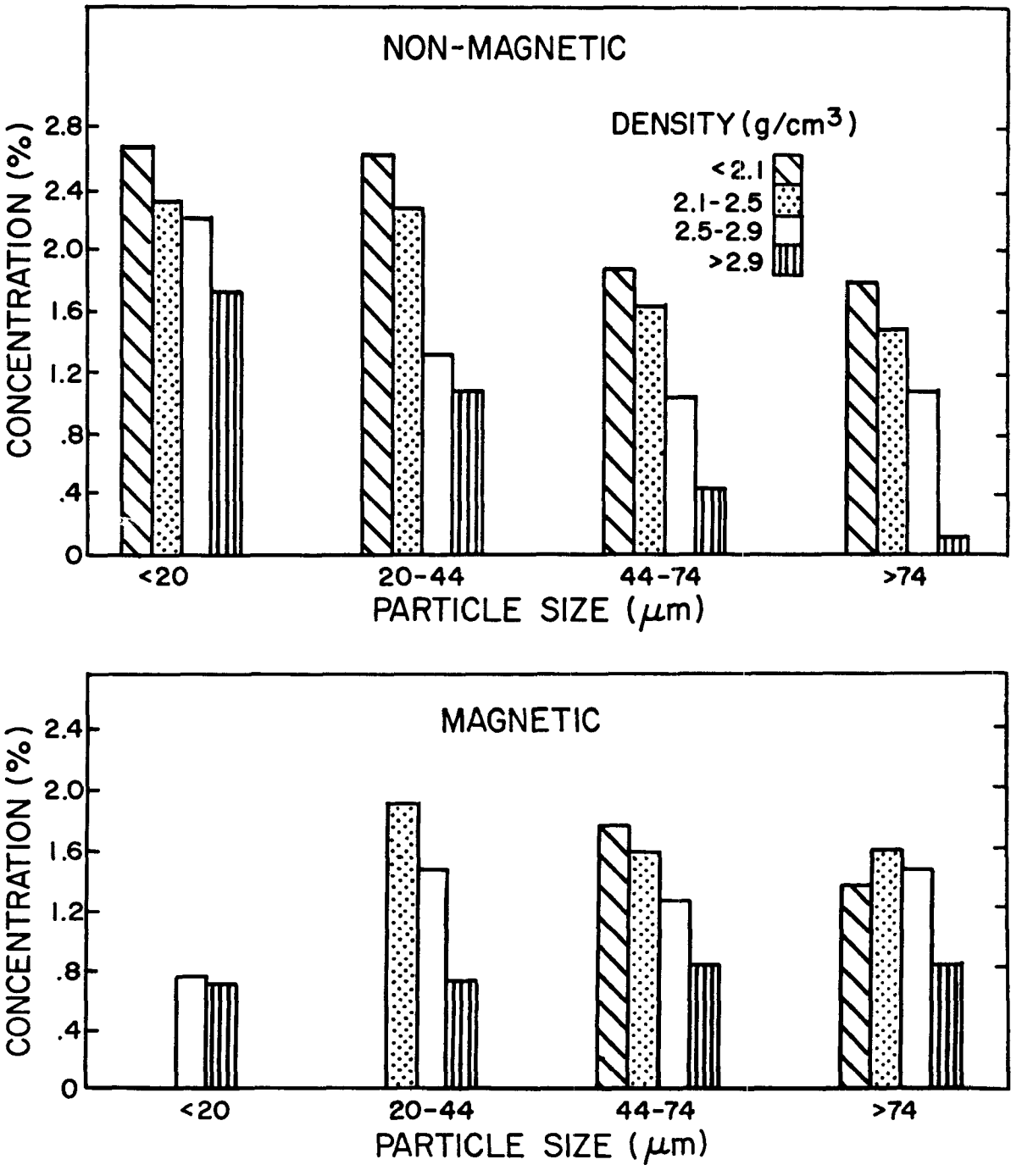

Figure 13. Concentration of potassium in non-magnetic and magnetic coal fly ash fractions as a function of particle size and density. (Data of Loh, 1975.)

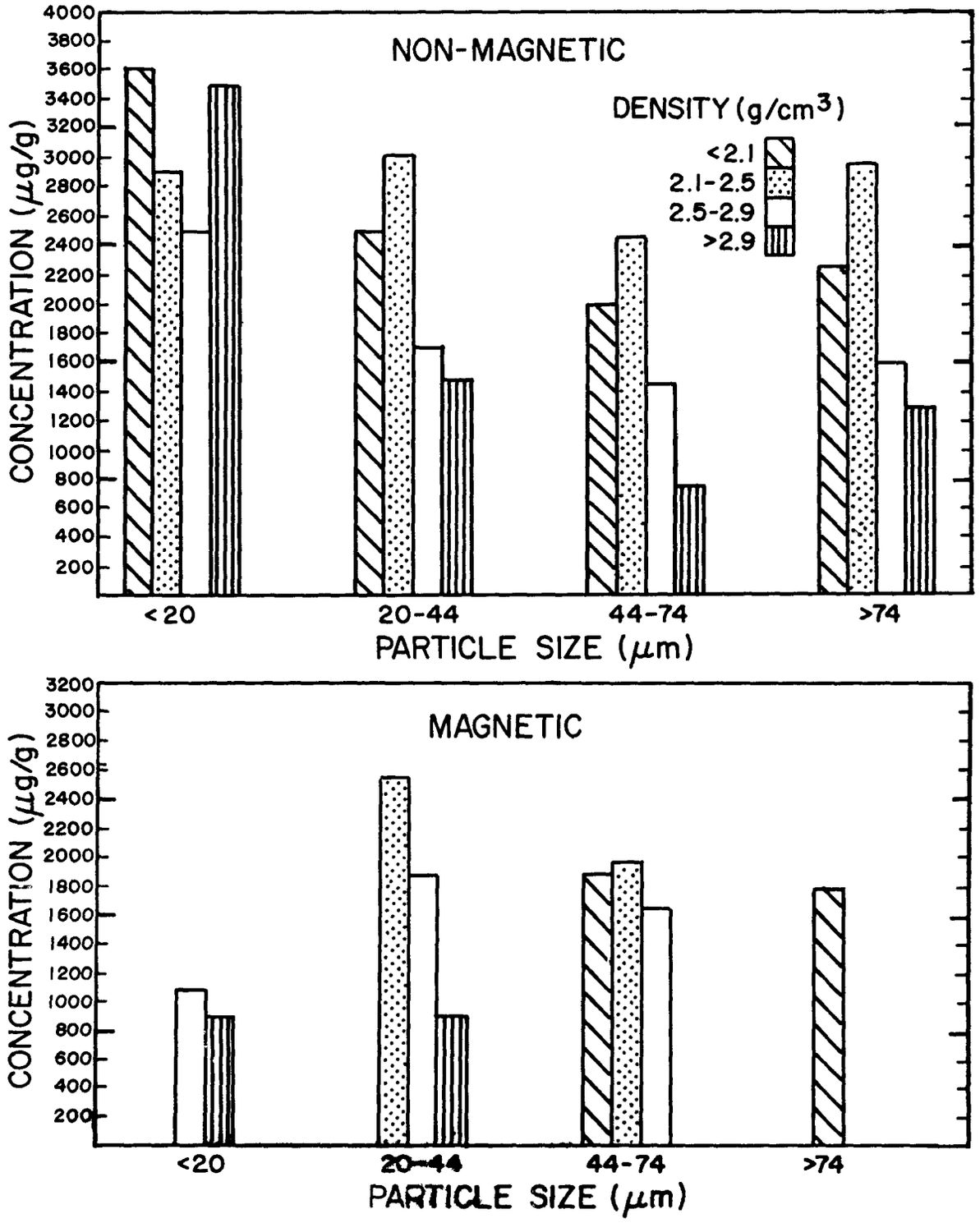

Figure 14. Concentration of sodium in non-magnetic and magnetic coal fly ash fractions as a function of particle size and density. (Data of Loh, 1975.)

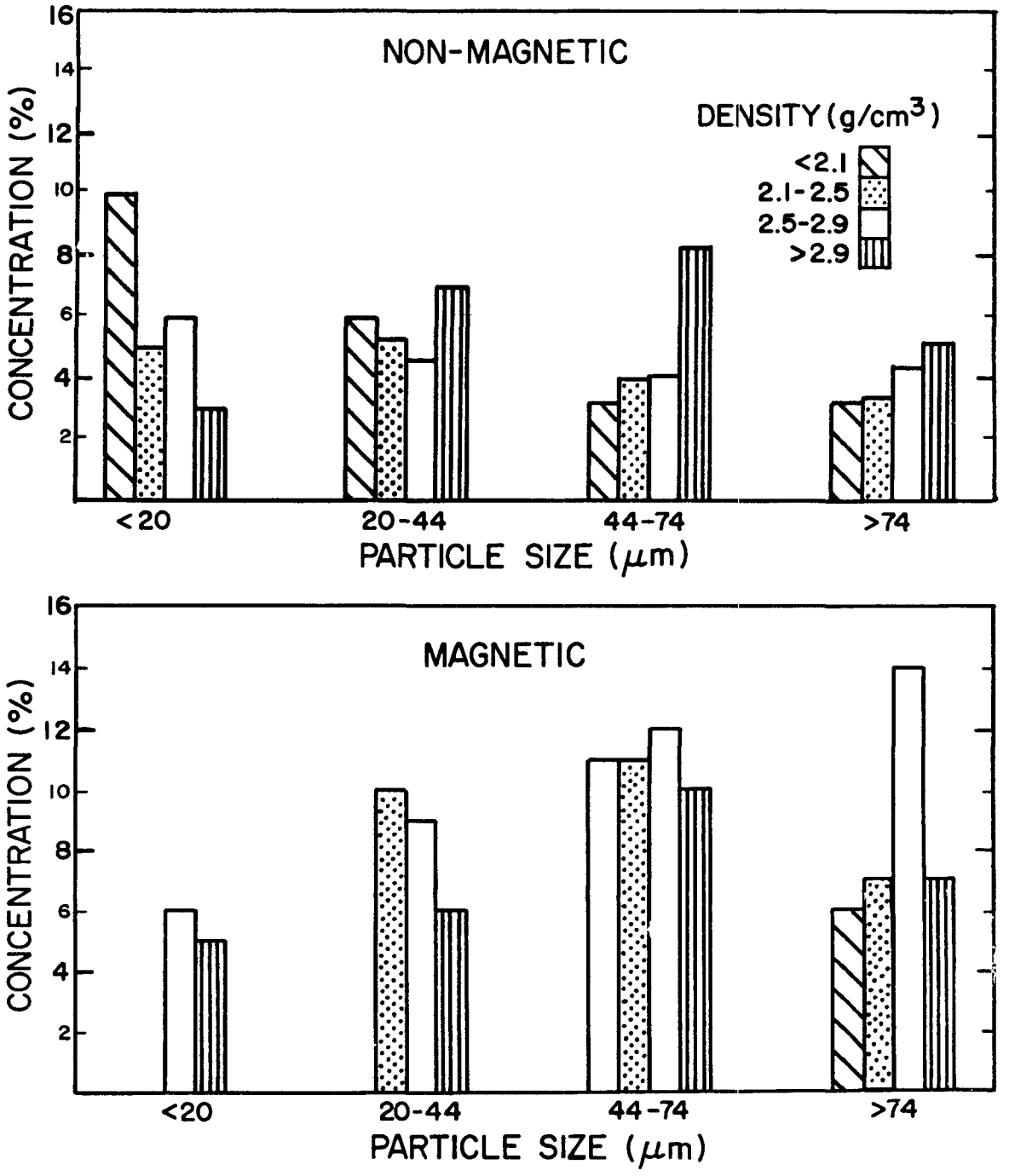

Figure 15. Concentration of calcium in non-magnetic and magnetic coal fly ash fractions as a function of particle size and density. (Data of Loh, 1975.)

MINERAL COMPOSITION

Mineral Composition of Coal

Identification of the chemical compounds present in fly ash can be made more readily with a knowledge of the inorganic minerals present in coal. The mineral composition of coal varies widely with the origin of the coal but a summary of the most common types of minerals which occur in coal is presented below (Rao and Gluskoter, 1973; Pringle and Bradburn, 1958; O'Gorman and Walker, 1971; Gluskoter, 1967; Littlejohn and Watt, 1963; Reid, 1971).

Clay Minerals--

These are the most commonly occurring inorganic minerals in coal and consist primarily of kaolinite [$Al_2O_3 \cdot 2SiO_2 \cdot 2H_2O$], and montmorillonite [$(Mg,Ca) \cdot Al_2O_3 \cdot 5SiO_2 \cdot 4H_2O$]. The general formula for these minerals is $MAl_2(Si_2O_5)(OH)_4$.

Sulfide Minerals--

These consist of pyrite [FeS_2, cubic], marcasite [FeS_2, rhombic], and sphalerite [Zn, Fe S]. General formula MS or MS_2.

Carbonate Minerals--

These consist of calcite [$CaCO_3$], dolomite [$Ca(Mg,Fe), (CO_3)_3$] and siderite [$FeCO_3$]. General formula (Ca, Mg, Mn, Fe) CO_3.

Halide Minerals--

These consist mainly of sylvite (KCl) and halite (NaCl). General formula MX (X = F, Cl, Br, I).

Silicate Minerals--

These consist mainly of quartz [SiO_2].

Iron Minerals--

Among the most common in this group are magnetite [Fe_3O_4], hematite [Fe_2O_3] and lepidocrocite [$Fe_2O_3 \cdot H_2O$].

Shale Minerals--

These minerals, closely related to the clay minerals, consist of illite [$(K,H_2O)(Al_2[AlSi]Si_3O_{10})(OH)_2$], muscovite [$K_2O \cdot 3Al_2O_3 \cdot 6SiO_2 \cdot 2H_2O$] and biotite [$k(MgFe)_3(AlSi_3O_{10}(OH)_2$].

Accessory Minerals--

There are a large number of minerals whose concentrations are heavily dependent on the particular coal source. Among these minerals are feldspars [$K,Na)_2O \cdot Al_2O_3 \cdot 6SiO_2$], garnet [$3CaO \cdot Al_2O_3 \cdot 3SiO_2$], hornblende [$CaO \cdot 3FeO \cdot 4SiO_2$], gypsum [$CaSO_4 \cdot 2H_2O$], apatite [$9CaO \cdot 3P_2O_5 \cdot CaF_2$], kyanite [$Al_2O_3 \cdot SiO_2$], tourmaline [$HgAl_3(BOH)_2Si_4O_{19}$], aluminum phosphate $Al_2(PO_4)_3$, and zircon [$ZrSiO_4$]. Many more minerals may be present in even smaller quantities.

Mineral Composition of Coal Fly Ash

X-ray powder diffraction was used to identify those minerals present in coal fly ash. Samples of a separated midwestern bituminous coal derived fly ash were first ground to a particle size of less than 44 μm then a thin film of particles was placed in the diffractometer.

Figure 16 shows X-ray diffraction patterns for magnetic and non-magnetic fly ash particles. The magnetic particles in the < 20 μm size fraction exhibited diffraction peaks which can be identified to originate from magnetite (Fe_3O_4) and hematite (Fe_2O_3). The bluish-black, opaque spheres (as observed by optical microscopy) are thus definitively classified as magnetite and the reddish-brown spheres as hematite. The non-magnetic particles showed diffraction peaks from two minerals; quartz (SiO_2) and mullite ($3Al_2O_3 \cdot 2SiO_2$).

Since only crystalline material with regularly repetitive atomic planes result in sharp diffraction peaks, it is this material which is easiest to identify. The broad bands observed in the diffraction patterns indicate the presence of amorphous compounds. These bands are attributed to the glassy aluminosilicates observed by optical microscopy. The presence of quartz and amorphous materials in the magnetic fraction show the overlap of the ferromagnetic separation of fly ash particles. No magnetite diffraction peaks are observed in the diffraction pattern of the non-magnetic particles, indicating that ferromagnetic separation is not only efficient in removing most of the magnetic particles, but also removes some non-magnetic particles that are agglomerated with the magnetic particles.

Figure 17 shows X-ray diffraction patterns for the density fractions of non-magnetic fly ash particles in the 20-44 μm size fraction. Small quantities of hematite are present in the density fraction between 2.5 g/cm^3 and 2.9 g/cm^3. This is because hematite is only weakly magnetic and is not efficiently separated by the magnet. Both quartz and mullite are present in significant quantities in the least dense fraction even though their densities are greater than 2.1 g/cm^3. This may be attributed to encapsulating particles (see Section IV) or particles which contain mixed phases (a single particle containing two or more compounds of varying density). The ratio of the areas under the broad band to the quartz peak ($2\theta = 2.67°$) indicates that the glassy, aluminosilicate particles also tended to be more concentrated in the least dense fraction.

The four main minerals in fly ash were found to be magnetite, hematite, quartz and mullite. Magnetite and hematite are probably formed from the oxidation of iron containing minerals (such as pyrite, marcasite and sphalerite) present in the coal. Quartz particles can be from the original quartz in the coal or formed from the breakdown of clay minerals in the coal. On heating, clay minerals (such as kaolinite) first dehydrate and then break down to form mullite at 1200-1400°C (Brindley and Nakahira, 1957).

These results are consistent with other work (Simons and Jeffrey, 1960; Watt and Thorne, 1965; Hulett and Weinberger, 1979) where it also was found that the principal mineralogical components of fly ash were quartz, mullite,

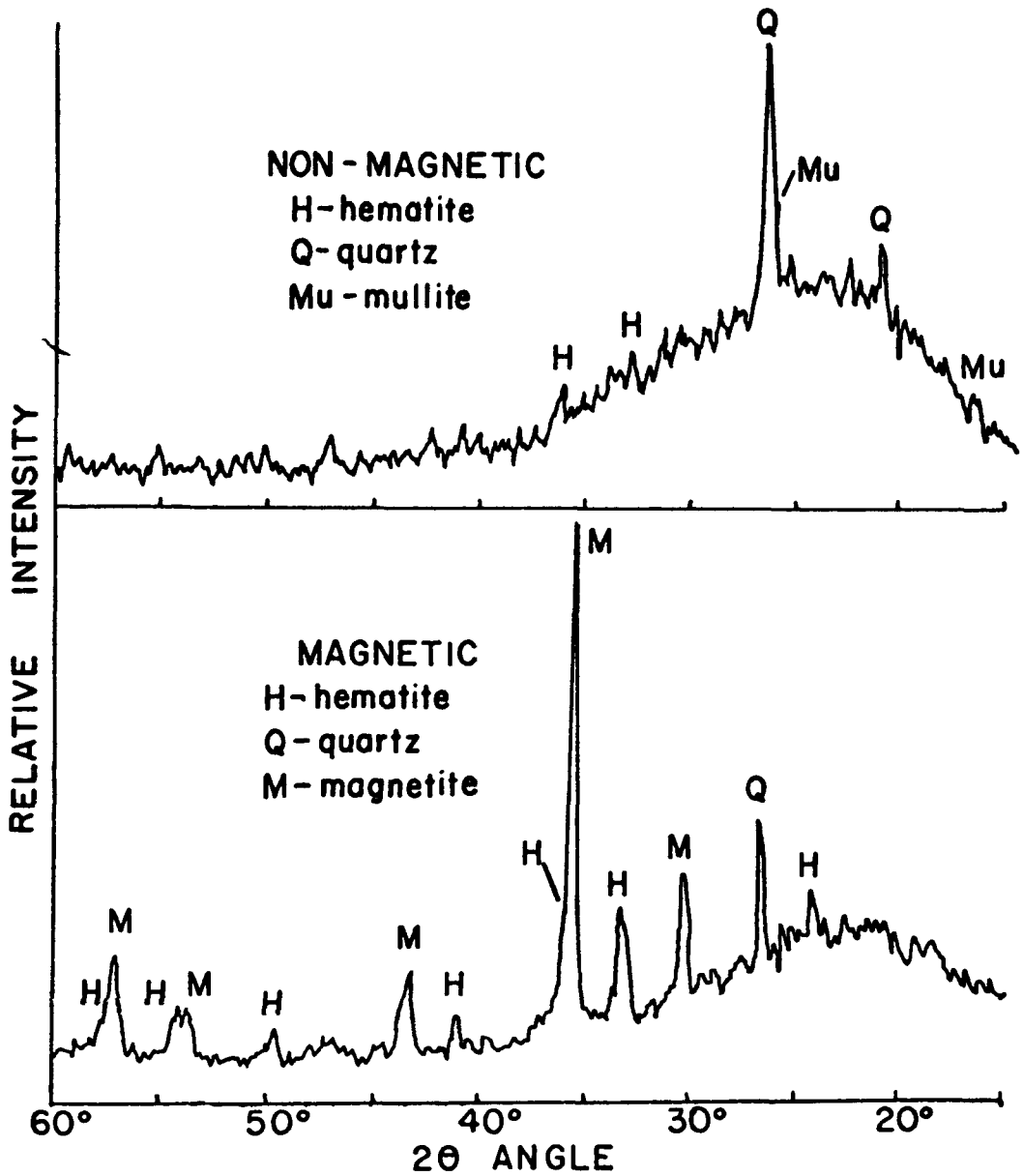

Figure 16. X-ray powder diffraction patterns of non-magnetic and magnetic fly ash particles. (Reprinted by permission of A. Loh from Loh, 1975.)

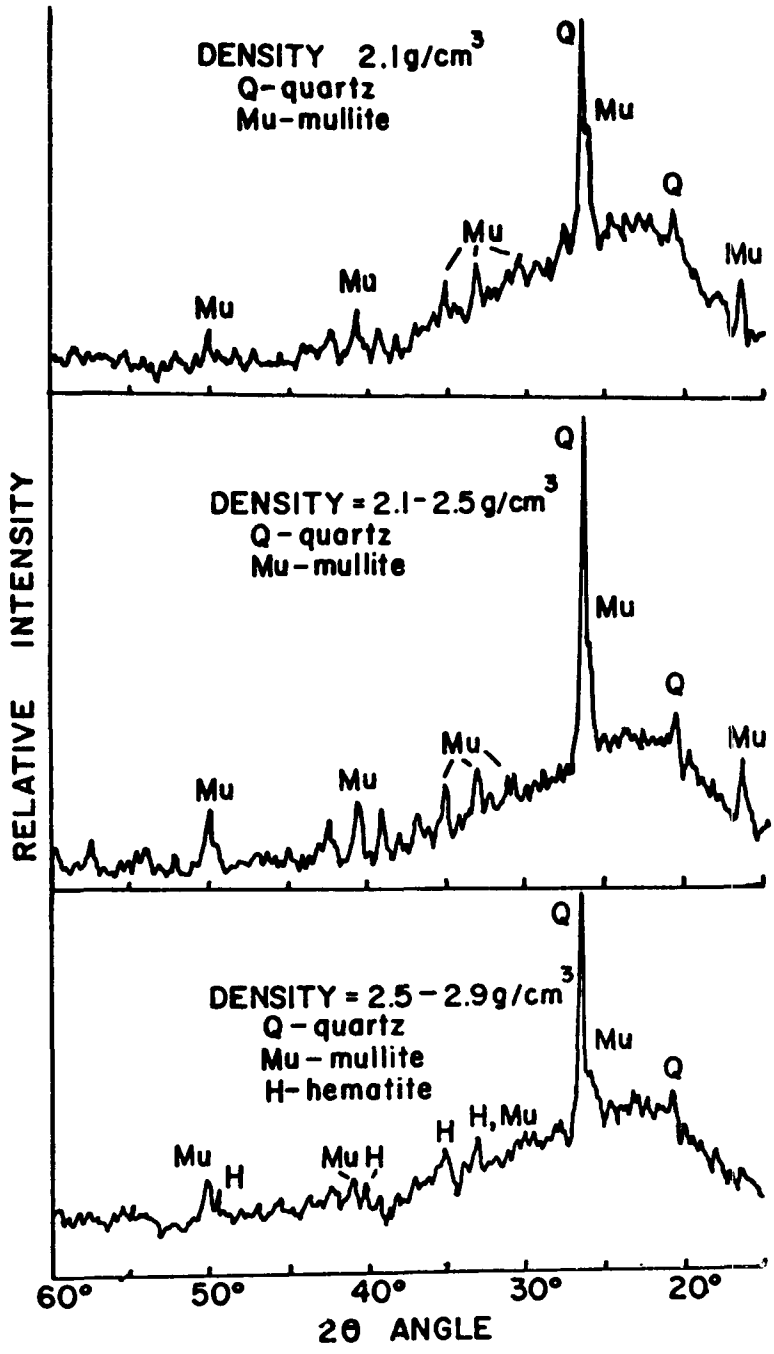

Figure 17. X-ray powder diffraction patterns of density separated coal fly ash particles. (Reprinted by permission of A. Loh from Loh, 1975.)

magnetite and hematite and a large amorphous glass fraction. The non-crystalline fraction ranged between 52 and 87% for a number of British fly ashes (Simons and Jeffrey, 1960; Watt and Thorne 1965) and between 28 and 80% for the American fly ashes that were studied (Simons and Jeffrey, 1960; Hulett and Weinberger, 1979).

TRACE ELEMENT COMPOSITION AND DISTRIBUTION

Dependence of elemental concentration on particle size, density and ferromagnetism

It is now well established that many high temperature combustion and smelting operations emit particles containing toxic elements such as Be, Cd, As, Se, Pb, Sb, Hg, Tl and V into the atmosphere (Schroeder, 1971). Many of these elements are enriched in ambient urban aerosols by as much as 100-1000 fold over their natural crustal abundance (Gordon and Zoller, 1973). In addition, it has been reported that a number of toxic elements (e.g., Sb, Cd, Ni, V, Sn and Zn) in urban areas have mass median equivalent diameters (MMED) of the order of one micrometer or less. This diameter is considerably smaller than those reported for such common matrix elements as Al, Fe and Si having MMED values in the range of 2.5-7.0 μm (Rahn et al., 1971; Lee et al., 1972; Colovos et al., 1974; Gladney et al., 1974). It is therefore meaningful to determine whether certain toxic trace elements predominate in the smallest particles emitted from particulate sources or whether the mass median diameter differences in urban aerosols are simply due to mixing of particles characteristic of individual source emissions.

The work reported in this section was conducted in two parts. In the first section, the midwestern fly ash that had been previously fractionated was examined to establish what trends in trace element composition might occur as a function of particle size, density and ferromagnetism. The results are given in Appendix C. Representative figures based on the tables in Appendix C are given in the discussion that follows.

The second section involved a much more detailed study in which the concentrations of a large number of elements were determined strictly as a function of particle size. In this study the fly ash was highly fractionated and samples from both within the plant as well as airborne material were examined. A large number of analytical techniques were employed in order to examine the relative merits of each for fly ash analyses and to establish the data firmly.

Both studies were designed to establish whether elements present in fly ash particles emitted from coal fired power plants exhibit a dependence of element concentration on particle size. A summary follows.

Magnesium--

Magnesium appears to be homogeneously distributed in the separated fly ash fractions. Since magnesium is not expected to volatilize in appreciable quantities during coal combustion, it would be expected to remain with the same elements with which it was associated in the original coal.

Manganese--

This element is more concentrated in the high density, large particle size, non-magnetic fractions as shown in Figure 18. Manganese is expected to be only partially volatilized during coal combustion. The trends in manganese are similar to those of several other elements, especially barium and arsenic and, to some extent, those of the matrix element, calcium (see Figure 15).

Arsenic--

This element shows trends very similar to those of manganese (see Figure 18), with the highest concentrations generally found in high density, large particle size, non-magnetic fractions. Arsenic and its compounds can be volatilized in the combustion of coal and deposit on the surface of fly ash particles. This condensation or adsorption process may be more favorable for non-magnetic particles. The higher concentrations in the larger particle fractions may be due to associations with refractory minerals in coal. These minerals are often not completely volatilized and tend to form larger irregular particles rather than small, spherical particles. The results are somewhat analogous to those of Lamb (1975) who found arsenic to be more concentrated in the low density, large particle size, non-magnetic fractions of roadside dust. He attributed this to selective adsorption of As by a soil component. A similar type of adsorption mechanism may be occurring in fly ash. However, it has been pointed out (Kaakinen et al., 1975) that As is mostly retained as arsenate/arsenite in high-calcium coals. In fact, comparison with the results for calcium (Figure 15) indicates that As correlates well with calcium revealing the probable existence of Ca-As compounds.

Barium--

The data show that barium is concentrated in the high density, non-magnetic fractions. This distribution is similar to that of manganese and arsenic (see Figure 18) indicative of a similar partitioning mechanism. In contrast to calcium, the element does not concentrate in the magnetic particles.

Strontium--

Strontium may be slightly more concentrated in the non-magnetic fractions, but otherwise it is relatively evenly distributed.

Cesium--

Cesium is only present in trace quantities in fly ash. Being an alkali element, cesium would be expected to follow the concentration trends of potassium and sodium. However, the data show that cesium is more concentrated in the magnetic particles. Cesium and its compounds are expected to volatilize in the combustion of coal thus the predominance of cesium in association with the magnetic particles may be due to selective deposition.

Rubidium--

Rubidium appears to behave as an alkali metal but no definitive conclusions can be deduced from the data.

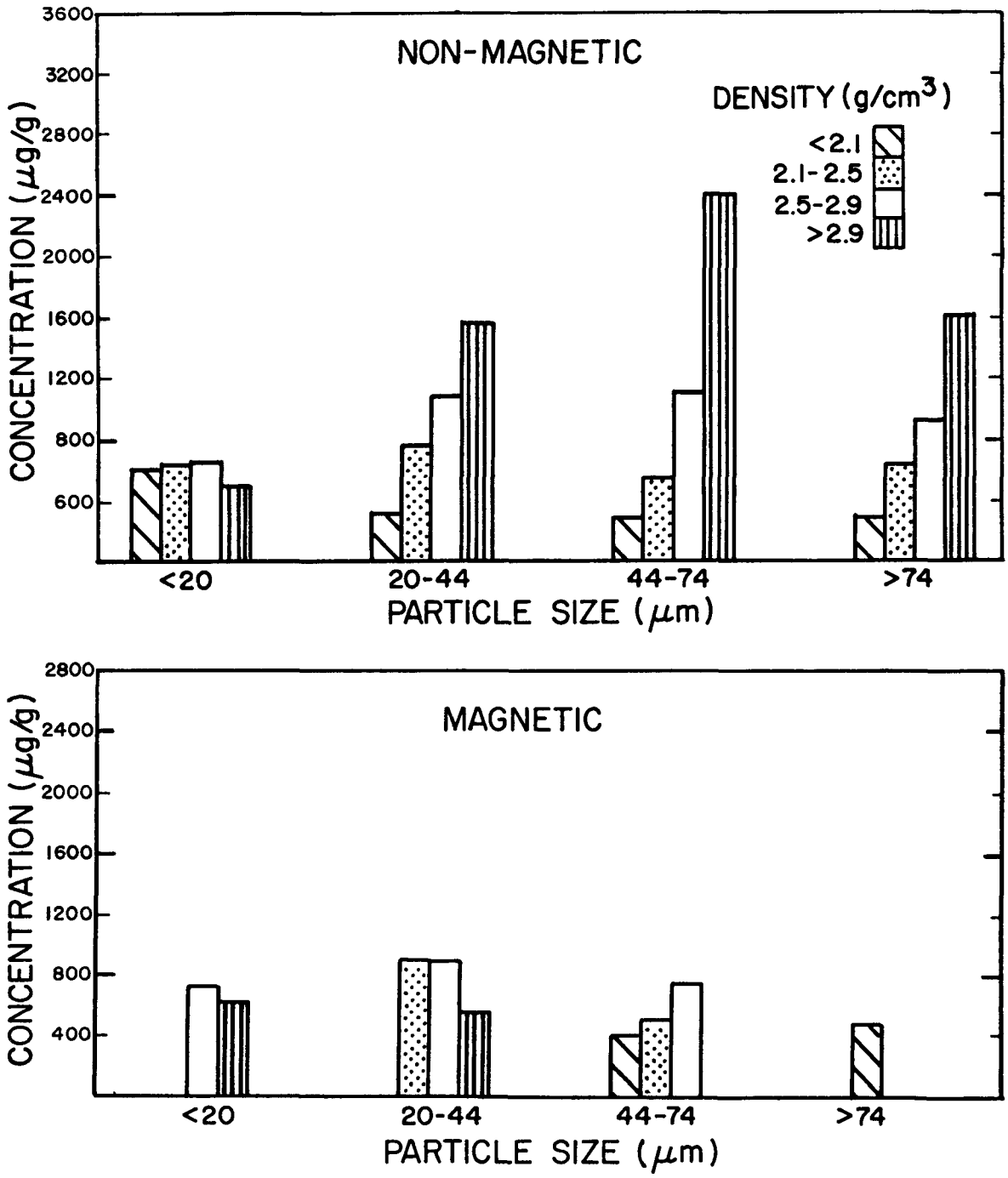

Figure 18. Concentration of manganese in non-magnetic and magnetic coal fly ash fractions as a function of particle size and density. (Data of Loh, 1975.)

Zinc--

Zinc is concentrated in the small particle size, high density, magnetic fractions as shown in Figure 19. Zinc has been postulated to undergo volatilization-condensation partitioning, hence its concentration in small particles. Zinc also occurs with iron as a sulfide mineral (sphalerite) present in coal and this could explain its preference for magnetic particles.

Chromium--

Chromium is much more concentrated in the magnetic fractions and shows trends similar to those of zinc (see Figure 19).

Cobalt--

Cobalt is also more concentrated in the magnetic particles, with concentrations increasing as the density increases. The distribution of this element also resembles that of zinc (see Figure 19).

Dysprosium, Europium, Hafnium, Lanthanum, Scandium, Samarium, Tantalum, Thorium, and Uranium--

These elements do not generally show any significant size/density trends. The data for Eu, which is fairly typical, is shown in Figure 20. In general, there were some slight non-magnetic/magnetic differences. Thus, the elements La, Hf, U, Dy and Sm are more concentrated in the nonmagnetic fractions, the elements Sc and Th are more concentrated in the magnetic fractions and the elements Eu and Ta do not show any significant variation in concentration. The reason why these elements are concentrated in certain fractions is not known but is attributed to their presence as constituents of the minerals in coal. All of these elements have high boiling points and are not expected to volatilize to significant extents in the high temperature combustion of coal. Thus, after coal combustion, these elements would be associated with the same mineral elements found in fly ash particles.

Gallium--

Figure 21 shows that gallium is definitely more concentrated in the small particle fractions. Gallium and its compounds can volatilize in the high temperature combustion of coal and deposit on the surface of particles.

Antimony--

Figure 22 shows that antimony is more concentrated in the smaller size fractions and, to some extent, in the magnetic fractions. Antimony has been shown to exhibit volatilization-condensation partitioning, hence its high concentration in small particles. Antimony also appears to be more concentrated in the higher density fractions as is arsenic but this trend is not definitive.

The concentration data for the different elements was also compared with the specific surface area data given earlier in Table 6. The comparison indicates that even the volatilizable elements (Sb, Ga, As), which are expected to be surface deposited, do not show simple linear relations with the specific surface area as would be expected if these elements condensed on the particles with the greatest specific surface area. The largest particles have high surface areas (by virtue of their porous structures), but this is

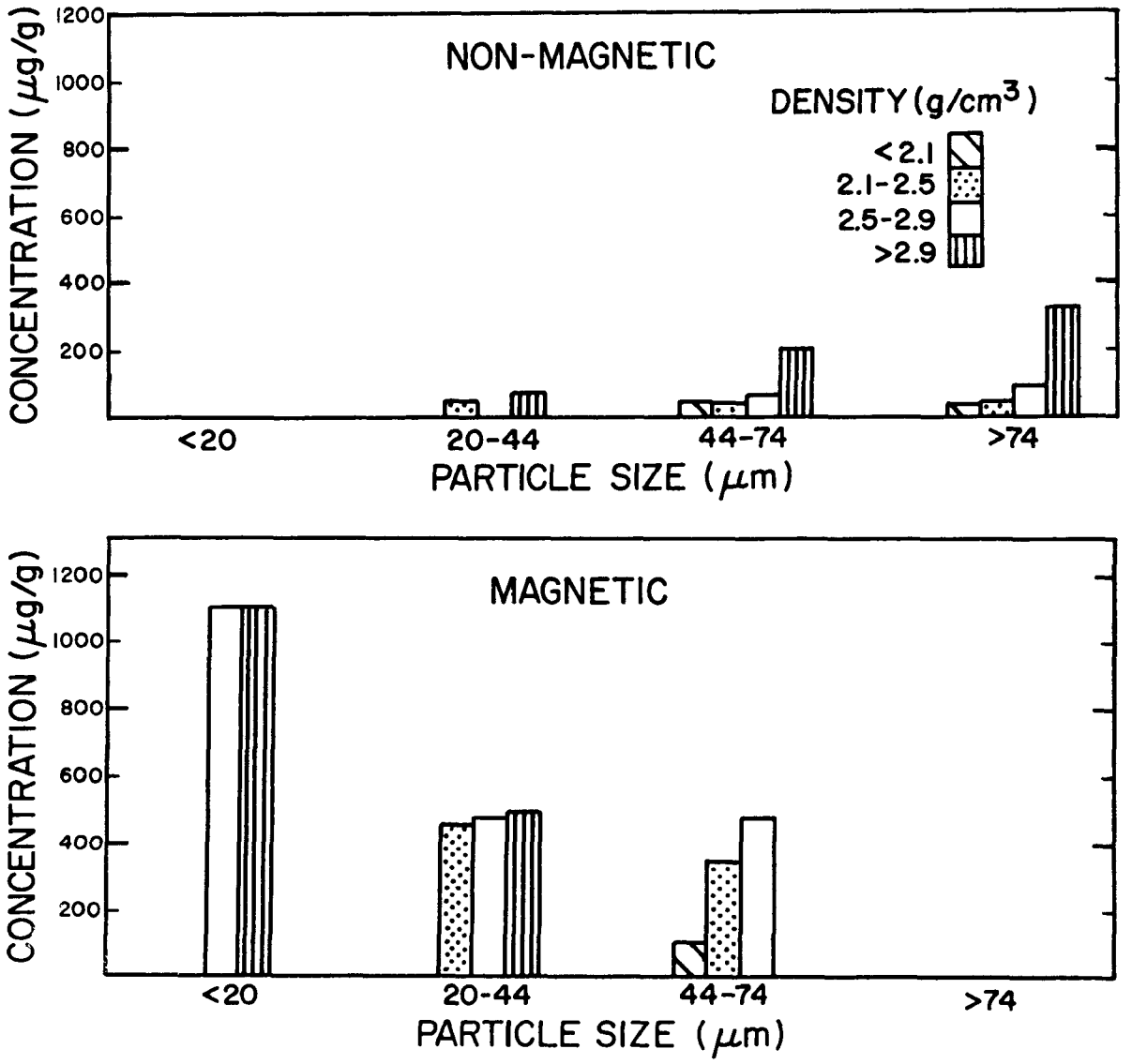

Figure 19. Concentration of zinc in non-magnetic and magnetic coal fly ash fractions as a function of particle size and density. (Data of Loh, 1975.)

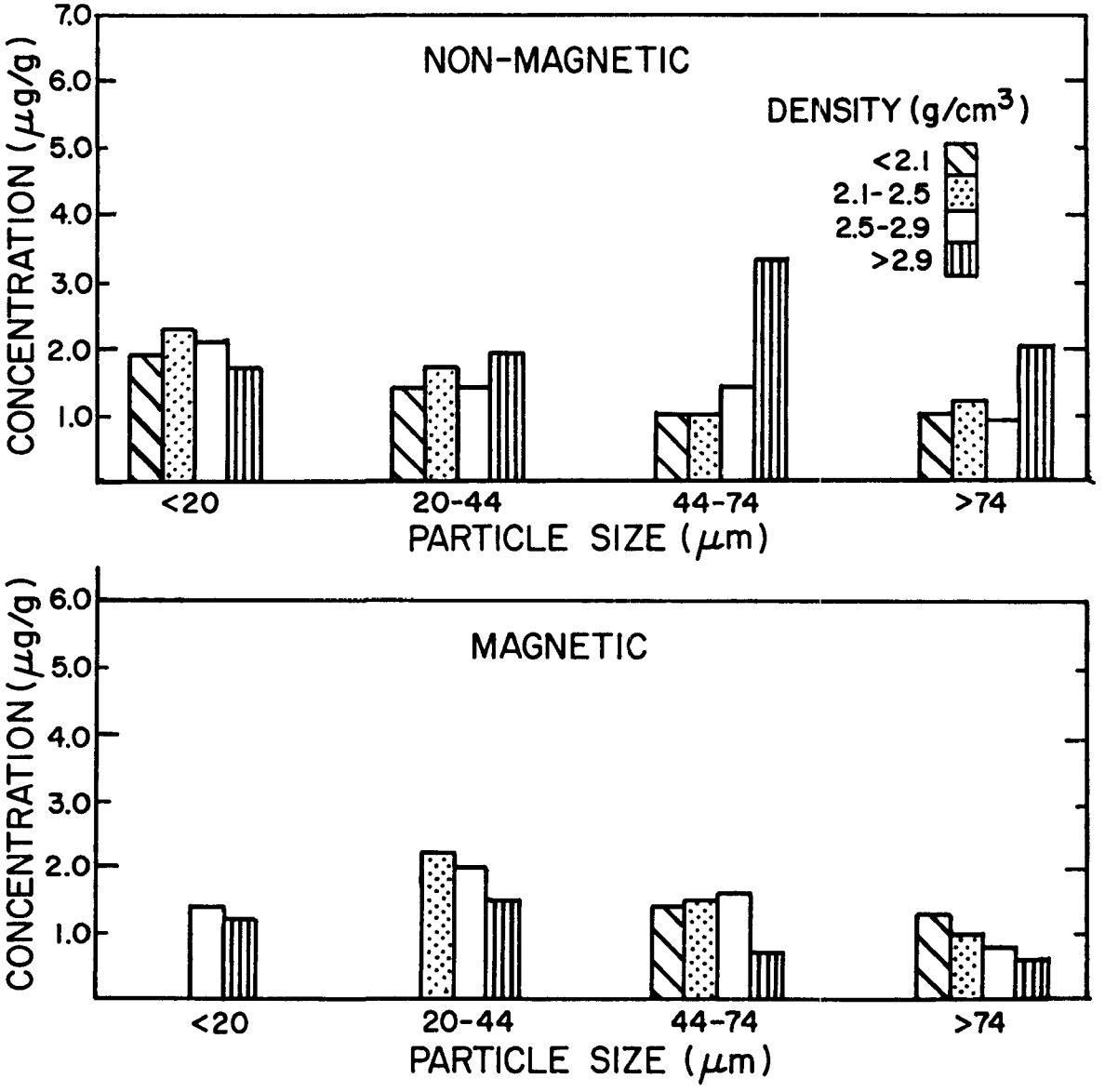

Figure 20. Concentration of europium in non-magnetic and magnetic coal fly ash fractions as a function of particle size and density. (Data of Loh, 1975.)

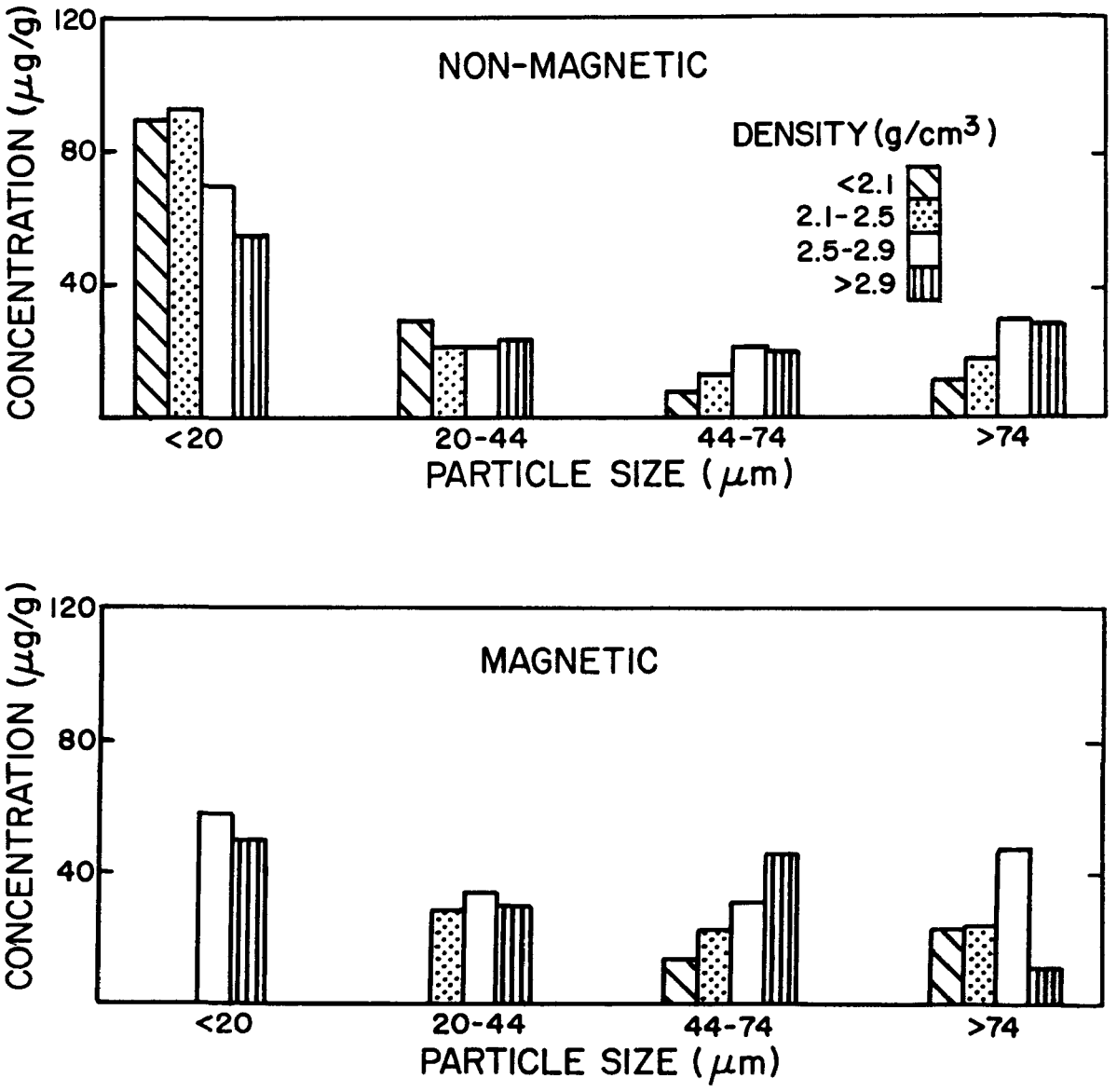

Figure 21. Concentration of gallium in non-magnetic and magnetic coal fly ash fractions as a function of particle size and density. (Data of Loh, 1975.)

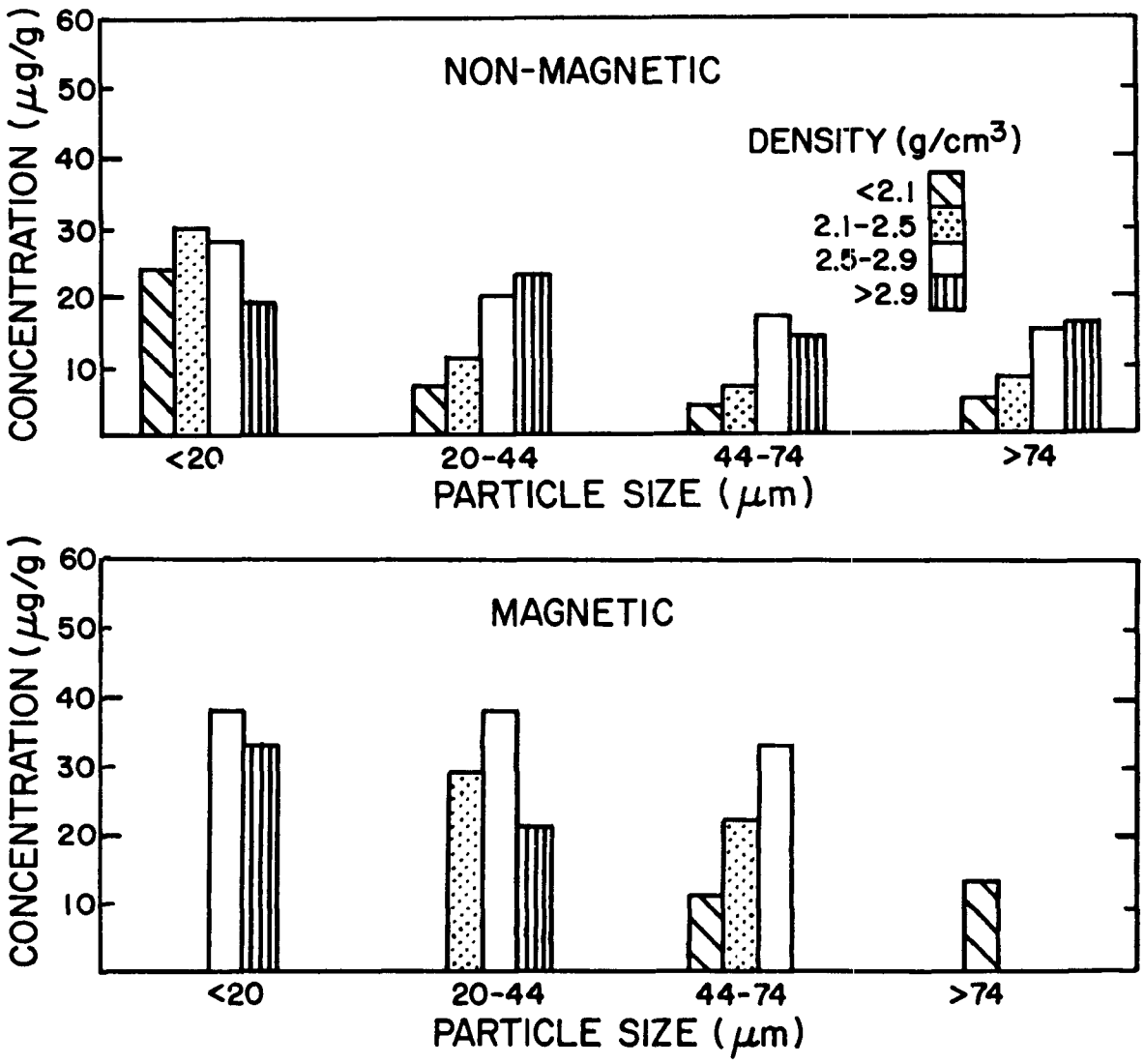

Figure 22. Concentration of antimony in non-magnetic and magnetic coal fly ash fractions as a function of particle size and density. (Data of Loh, 1975.)

only partially reflected in the elemental concentration data. It is noteworthy to point out that this fly ash sample was obtained from within the plant, so that the particles are relatively large compared with particles obtained from the stack. Any dependence of concentration on surface area is thus diminished. Kaakinen et al. (1975) also collected particles in bulk from within the plant and obtained linear correlations between the elemental concentrations and the specific surface area. When the effects of particle size, density and ferromagnetism are delineated, however, no simple correlation is found.

The dependence of the trace element concentrations on particle size, density, ferromagnetism, matrix elements and specific surface area has enabled the classification of three groups of trace elements:

Group I--those not expected to volatilize during coal combustion and showing either a preference (Sr, Co, Sc, Th, U) or no preference (Eu, Dy, Hf, Ta, Sm, La) for certain particle matrices. These elements are present in trace amounts in fly ash and evidently remain associated with the same matrix elements with which they are present in coal.

Group II--those expected to be volatilized during coal combustion and showing a preference for small particles and for certain particle matrices (Na, Cs, Ga, Sb).

Group III--those expected to be only partly volatilized during coal combustion and showing a preference for certain particle matrices. The elements Zn and Cr exhibit a preference for small particles and have a behavior similar to Group II. The elements Mn, Ba and As showed no significant preference for particle size and are postulated to be associated with the same matrix elements in fly ash and in coal. Arsenic has a distribution similar to Mn and Ba and is included in this group even though As is expected to almost completely volatilize during coal combustion.

It is apparent from the foregoing remarks that these results provide only a limited understanding of the distributional characteristics of the constituents. Consequently a second, more exhaustive, effort was undertaken in order to better examine the relationship between particle size and elemental concentration.

Dependence of elemental concentration on particle size

Fly ash analyses were carried out for twenty-five elements as a function of physical or equivalent aerodynamic particle diameter. Samples included both stack (airborne) and precipitator samples and reflected more narrow size fractions than those reported earlier in part V. The results are graphically presented in Figures 23 to 32 and are also summarized in Appendix B. Note that the precipitator ash was physically sized while the stack ash was sized aerodynamically. These two quantities are related by Equation 1. Note that separation of density or magnetic fractions was not carried out as previously. Fly ash particles larger than 74 μm exhibited no dependence of element concentration on particle size, so the concentrations shown for this fraction are averages over all larger fractions. The figures show that for

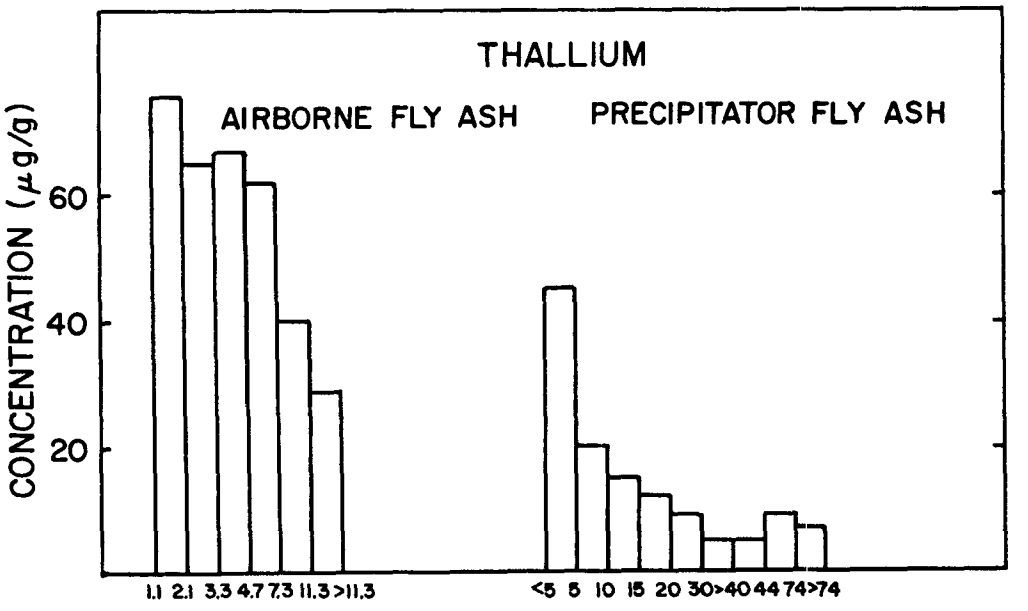

Figure 23. Concentration of thallium in coal fly ash fractions as a function of particle size. (Data of Davison et al., 1974.)

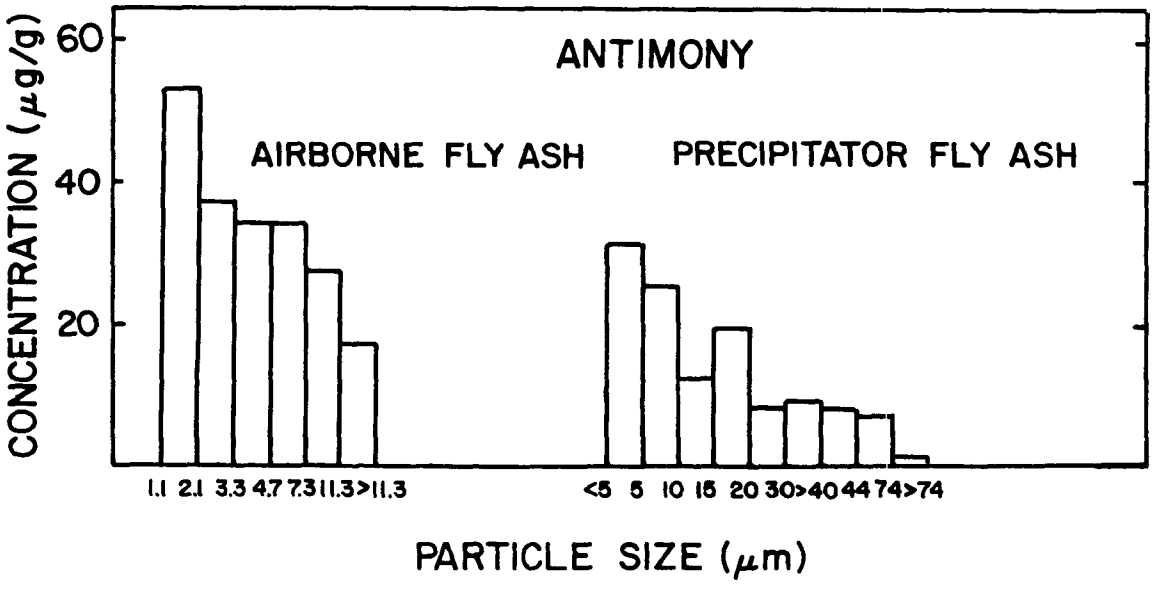

Figure 24. Concentration of antimony in coal fly ash fractions as a function of particle size. (Data of Davison et al., 1974.)

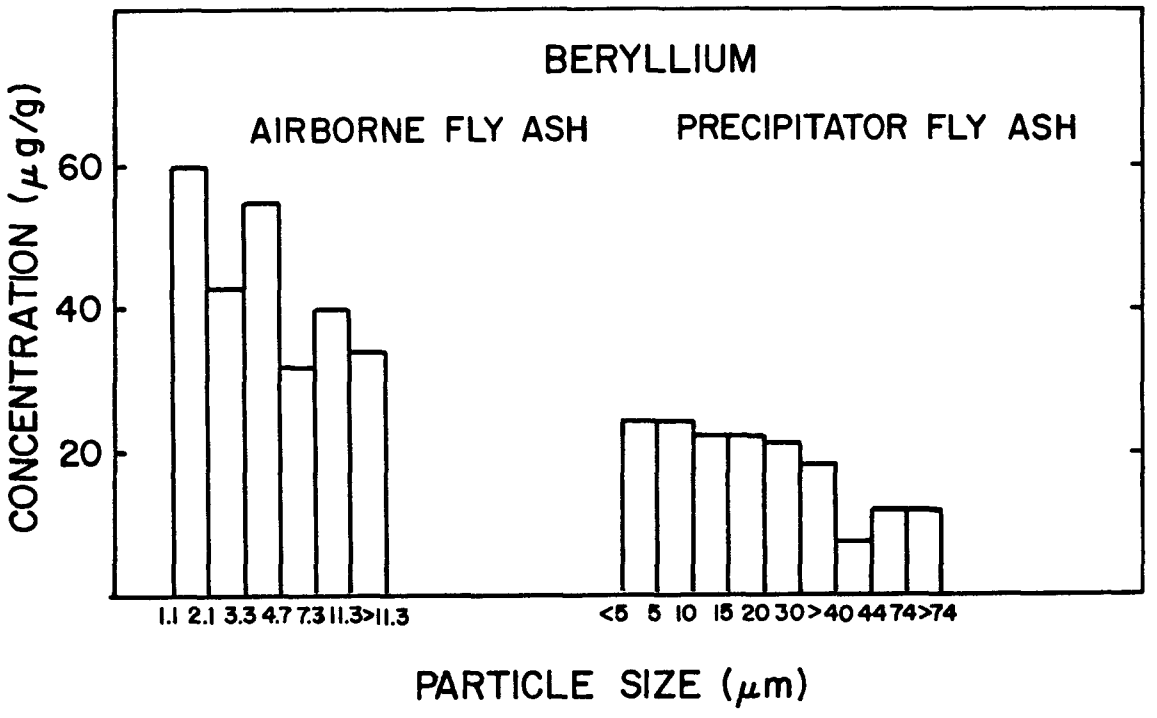

Figure 25. Concentration of beryllium in coal fly ash fractions as a function of particle size. (Data of Davison et al., 1974.)

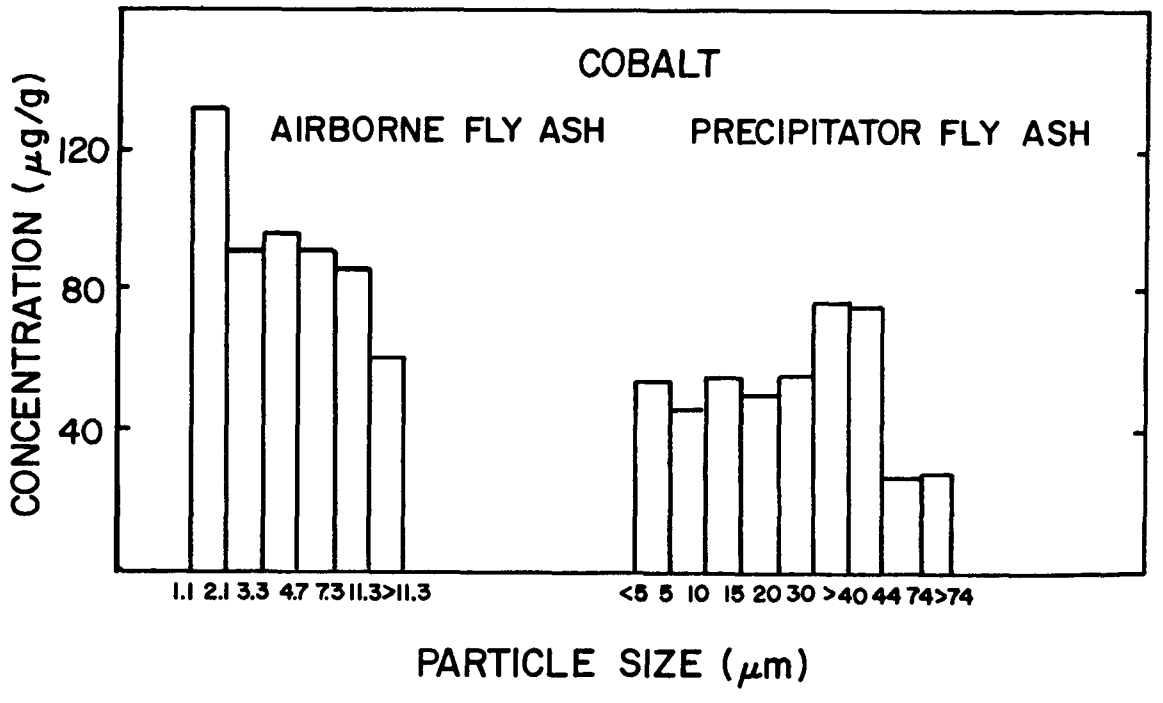

Figure 26. Concentration of cobalt in coal fly ash fractions as a function of particle size. (Data of Davison et al., 1974.)

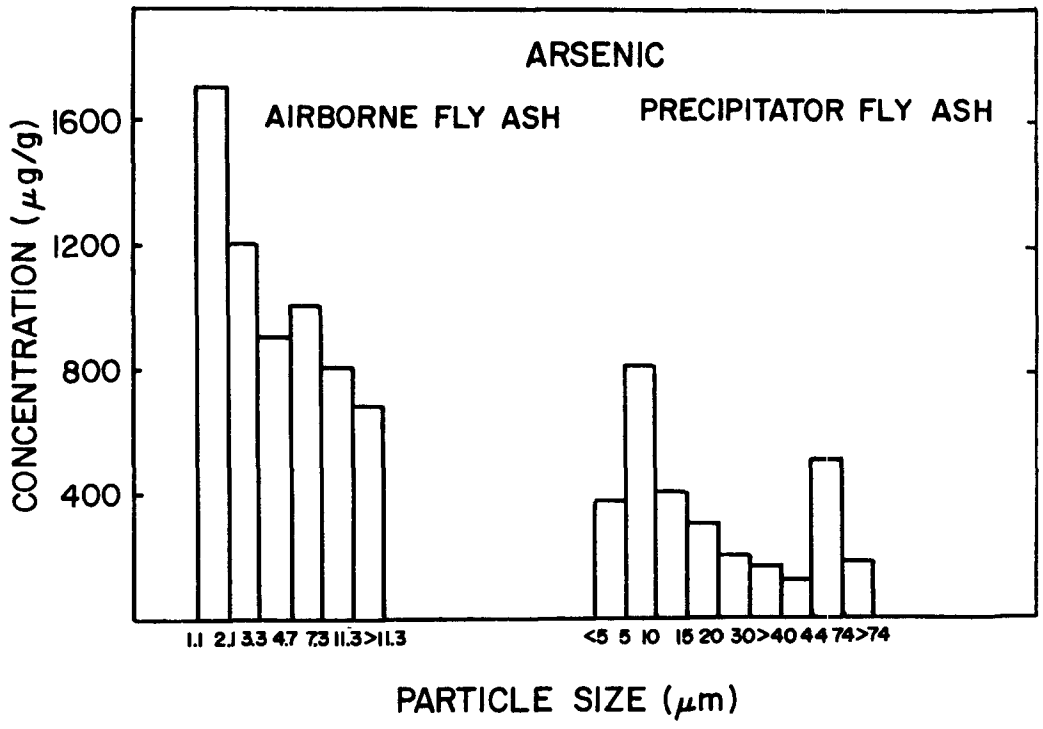

Figure 27. Concentration of arsenic in coal fly ash fractions as a function of particle size. (Data of Davison et al., 1974.)

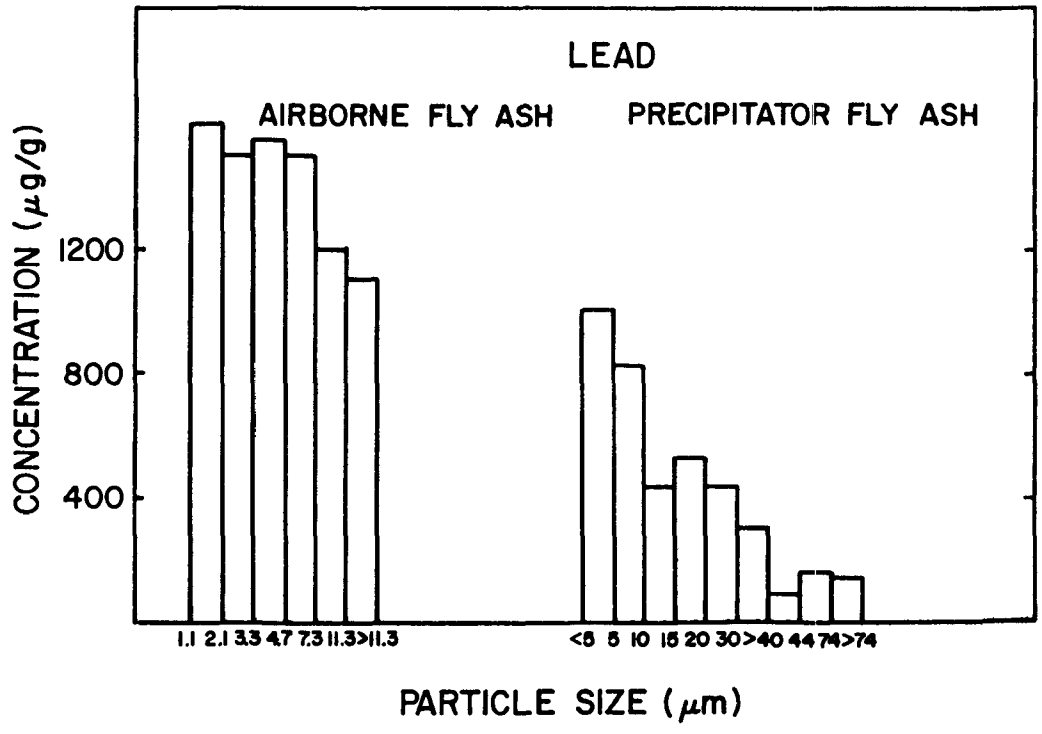

Figure 28. Concentration of lead in coal fly ash fractions as a function of particle size. (Data of Davison et al., 1974.)

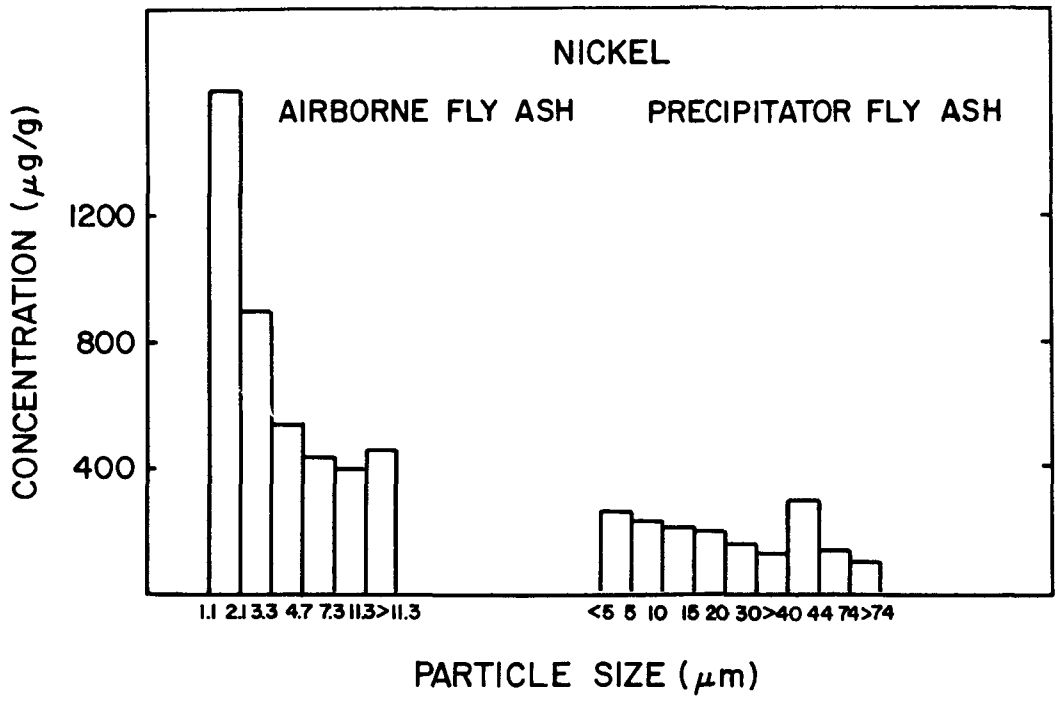

Figure 29. Concentration of nickel in coal fly ash fractions as a function of particle size. (Data of Davison et al., 1974.)

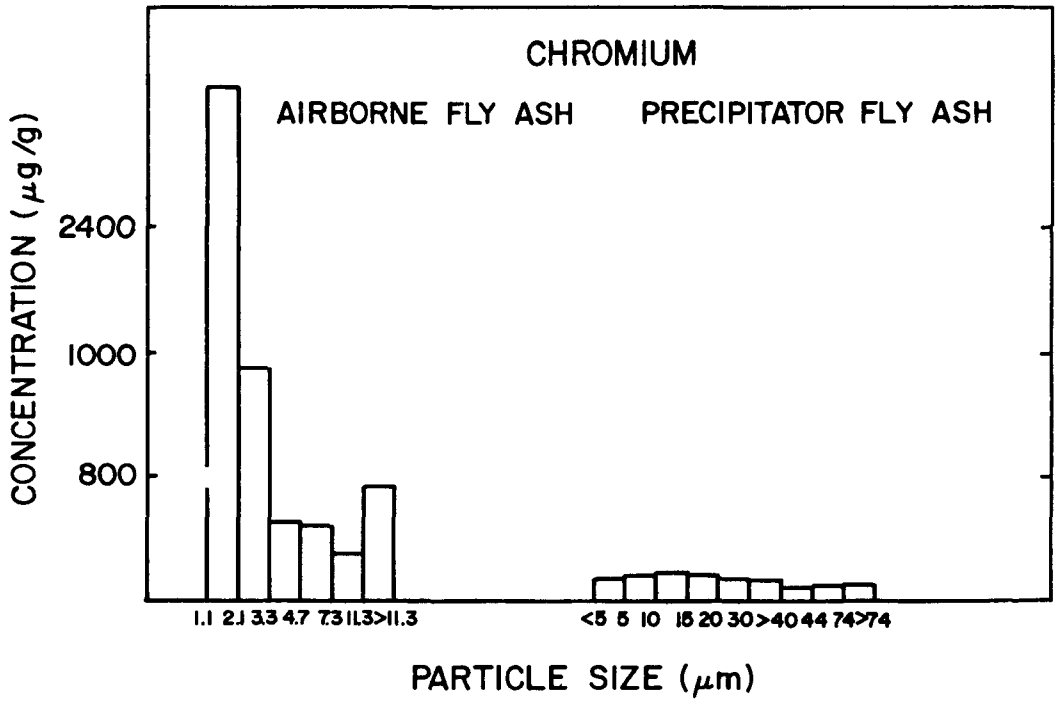

Figure 30. Concentration of chromium in coal fly ash fractions as a function of particle size. (Data of Davison et al., 1974.)

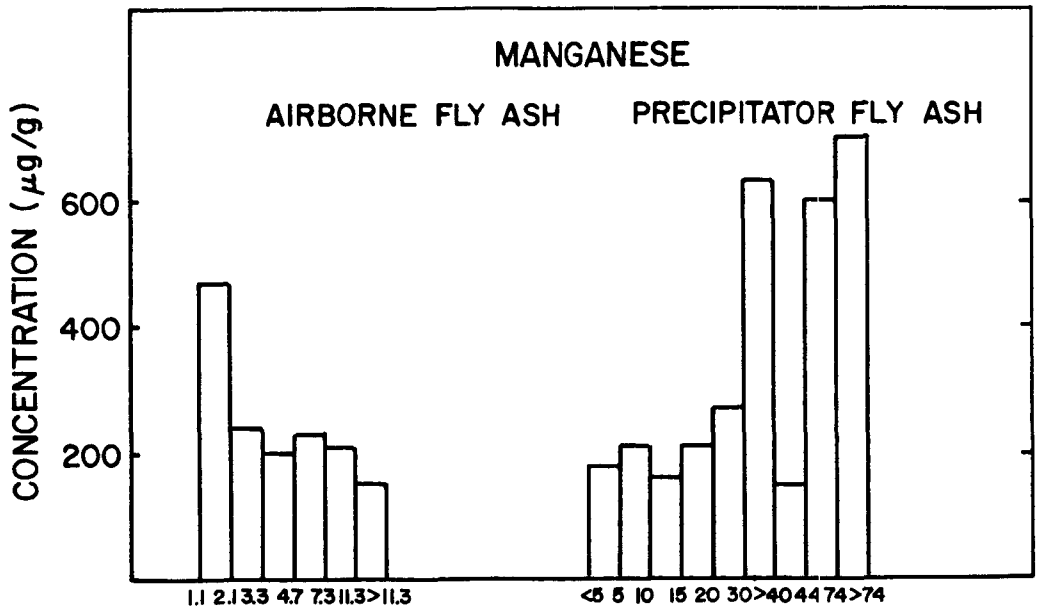

Figure 31. Concentration of manganese in coal fly ash fractions as a function of particle size. (Data of Davison et al., 1974.)

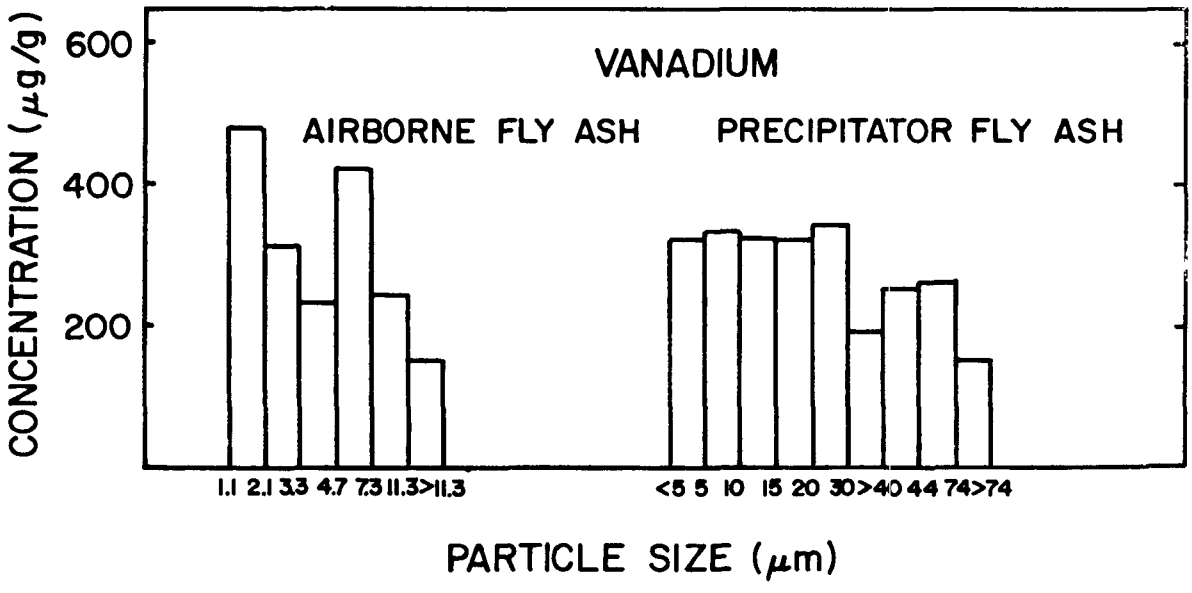

Figure 32. Concentration of vanadium in coal fly ash fractions as a function of particle size. (Data of Davison et al., 1974.)

this particular ash the elements As, Be, Co, Cr, Ni, Pb, Sb, and Tl are preferentially found in small particles. The trends for Mn and U are less clear but suggest that similar trends exist for the smallest particles.

A large number of investigators have reported that many trace elements show a preferential concentration in smaller particles. Lee and von Lehmden (1973) found an essentially similar dependence of element concentration on fly ash particle size for Cd, Pb, Mn and Cr. Toca (1973) found a similar trend for Pd and Cd and noted that 70% of the Cd present in flue gases was associated with particles <5 μm in diameter. Sparks (1973) reported that the elements Pb, Ba, Sr, Rb, As, and Zn in fly ash particles collected on a 0.4 μm filter following the last stage of a Brinks impactor were enriched on a weight for weight basis by at least an order of magnitude over those deposited on the last impactor stage.

Recently several reports in which concentration trends for a large number of elements were studied have appeared in the literature. The most comprehensive of these, in addition to the data just presented (Davison et al., 1974), are those of Block and Dams (1976), Klein et al. (1975), Cambell et al. (1978), Coles et al. (1979), and Smith et al. (1979). The results are generally consistent in classification of elements to Group I (no trends), Group II (increasing concentration with decreasing size) and Group III (intermediate behavior or concentration decreases with decreasing size). A comparison of the classification of different elements is given in Table 8.

The comparison of the classifications of the various elements given in Table 8 reveals several interesting facts. First, while most of the matrix elements consistently fall within Group I and many of the more volatile elements into Group II, many elements either exhibit intermediate behavior or else fall into different categories depending on the particular study. The discrepancies between results are probably a function of the many different coals, combustion conditions and collection and analysis systems utilized by the different workers.

In spite of the problems inherent in classifying the Group III elements, the result of this and the other studies on size dependence do support four significant points.

1. A coal fired power plant produces enrichment of certain elements in the smallest emitted particles.

2. The highest concentrations of these trace elements are found in particles which may deposit in the pulmonary region of the respiratory system.

3. Existing particle control devices are least effective for removing the particles bearing some of the most toxic elements.

4. Estimates of toxic element emissions based on analyses of undifferentiated fly ash collected from particle precipitators will be much lower than actual emissions.

TABLE 8. SUMMARY OF ELEMENTAL CONCENTRATION DEPENDENCE ON PARTICLE SIZE*

A. Elements showing clear inverse concentration-particle size dependence

As	Cl	Mo	Sb
Br	Ga	Nb§	Se
Cd	I¶	Pb	Tlϕ
Cu	In¶	S	Zn

B. Elements showing less well established inverse concentration particle size dependence

Ag¶	Cr	Uψ
Au¶	Mn	U
Beξ	Na	W
Cs	Ni	Zn§

C. Elements showing no concentration-particle size dependence

Al	Ce	Fe	Mg	Si	Ta	Yb
Ba	Co	Hf	Nd	Sm	Tb	
Bi†	Dy	K	Rb	Snϕ	Th	
Ca	Eu	La	Sc	Sr	Ti	

* Based on the data of Loh (1975); Davison et al. (1974); Coles et al. (1979); Klein et al. (1975); Cambell et al. (1978); and Block and Dams (1976). Elements listed reflect the classifications of a majority of the authors cited.

† Data of Klein et al. (1975) and Block and Dams (1976) only.

¶ Data of Block and Dams (1976) only.

§ Data of Cambell et al. (1978) only.

ϕ Data of Davison et al. (1974) only.

ξ Data of Davison et al. (1974) and Coles et al. (1979) only.

ψ Data of Coles et al. (1979) and Klein et al. (1975) only.

In fact, only a small fraction of the total fly ash mass has particle diameters less than 10 μm and by no means all of this is emitted to the atmosphere. However, the fraction emitted undoubtedly presents a greater potential health hazard per unit weight than that retained (see also the discussion of element solubilities below).

Explanations of Preferential Elemental Concentration on Small Particles

Several theories has been suggested to explain the preferential association of different metals with small particles. These are generally based on one of three general explanations; volatilization and subsequent condensation or adsorption of the particular element, geochemical fractionation, or the "bursting" of larger particles.

In support of the volatilization and adsorption/condensation hypothesis it is noteworthy that all the elements (except Nb) listed in Table 8A have boiling points comparable to or below the temperature of the coal combustion zone (1300-1600°C) (see Table 9). This is also true of Ba, Sr, and Rb as determined by Sparks (1973). This implies that metal compounds are reduced to the element before volatilization. However, while reduction in the combustion zone is certainly feasible, such reduction is not necessary to the basic hypothesis. It is suggested that these elements have access to the vapor phase as sulfides, halides, oxyhalides or even as carbonyls, whose highly transient formation during coal combustion has been postulated (Schroeder, 1971). Mercury, of course, undoubtedly volatilizes as the element and is predicted to exhibit a dependence of concentration on particle size if the proposed mechanism is valid.

A simple model can be constructed by considering a single particle in which an element, X, is uniformly deposited on the particle surface at a concentration C_s (μg/cm). In addition, X is assumed to be uniformly distributed throughout the particle with a concentration C_o (μg/g). The total concentration of X, C_X (μg/g), is then given by:

$$C_X = C_o + \frac{C_s A}{\rho V} \qquad (3)$$

where X = element, C_o = bulk concentration of X, C_s = surface concentration of X, C_X = total concentration of X, V = particle volume, A = particle surface area, and ρ = particle density. By summing over all fly ash particles and assuming spherical particles, the average concentration of X, $\bar{C}_X$, is given by

$$\bar{C}_X = \bar{C}_o + \frac{6\bar{C}_s}{\bar{\rho}} \cdot \frac{1}{D} \qquad (4)$$

where the bars denote average values and D the particle diameter.

TABLE 9. BOILING POINTS OF POSSIBLE INORGANIC SPECIES EVOLVED DURING COAL COMBUSTION

Species boiling or subliming < 1550°C	Species boiling or subliming > 1550°C
As, As_2O_5, As_2O_3, As_2S_3	Al, Al_2O_3
Ba	Be, BeO
Bi	Bi_2O_3
Ca	C
Cd, CdO, CdS	CaO
$Cr(CO)_6$, $CrCl_3$, CrS(1550)	Co, CoO, CoS
K	Cr, C, Cr_2O_3
Mg	Cu, CuO
$Ni(CO)_4$	Fe, Fe_2O_3, Fe_3O_4, FeO
Pb	MgO, MgS
Rb	Mn, MnO, MnO_2
S	Ni, NiO
Se, SeO_2, SeO_3	Si, SiO_2
Sb, Sb_2S_3, Sb_2O_3(1550)	Sn, SnO_2
SnS	Ti, TiO_2, TiO
Sr	U, UO_2
Zn, ZnS	
Tl, Tl_2O, Tl_2O_3	

In order to substitute the values in Figures 23-32 in Equation (4) it is necessary either to make the assumption that ρ is not a function of particle diameter, D, or to determine $\bar{\rho}$ for each size fraction. Appropriate values of D for each size fraction can be obtained by assuming

$$D = \frac{(ECD)_u + (ECD)_\ell}{2} \tag{5}$$

where $(ECD)_u$ and $(ECD)_\ell$ are the upper and lower 50%-effective cutoff diameters for each stage of the Andersen cascade impactor stack sampler. Equation (3) thus assumes a symmetrical distribution of the mass of X over the diameter range $(ECD)_u$ to $(ECD)_\ell$. Incorporating these assumptions allows construction of a plot of $\bar{C}_X$ versus D^{-1}, as depicted in Figure 33, from which it can be seen that the results are in at least qualitative agreement with the proposed model.

The thickness, ℓ, of the deposition layer can be estimated from the expression

$$\ell = \bar{C}_s/\bar{\rho}' \tag{6}$$

where $\bar{\rho}'$ is the density of the deposition layer, which was assumed to approximate 3 g/cm³. Values of $\bar{C}_s$, $\bar{C}_o$, and ℓ are presented in Table 10. These values, with the notable exception of those for sulfur, are considered reasonable for a thin surface-deposited layer. The 600Å layer thickness obtained for sulfur is considered too great to be accounted for by a simple adsorption process. Indeed, the high concentrations of S obtained for the 0.65-1.1 μm size fraction (Appendix C) can be accounted for only if sulfur is present as the element. This suggestion is at variance with the findings of Hulett (1973), who has shown, using electron spectroscopy, that S predominates as sulfate. We, therefore, consider that the sulfur values listed in Appendix C are all proportionately high due to lack of a fly ash standard having sulfur deposited on the surface of appropriately sized particles as required for X-ray fluorescence analysis.

If observed dependences of element concentration on particle size are, in fact, due to volatilization followed by adsorption or condensation as suggested, one would expect the same phenomenon to be exhibited by particles derived from all high-temperature solid-combustion operation. Data for combustion sources other than coal-burning power plants are not widely available to substantiate this suggestion. If correct, however, it suggests that many sources may preferentially emit small particles enriched in toxic elements or their compounds. The mass median diameters of such elements in the emitted particle distribution will thus be reduced as a direct result of preferential surface deposition. The extent of reduction can be determined by combining Equation (4) with the mass distribution function appropriate for

TABLE 10. ELEMENTAL SURFACE CONCENTRATIONS AND LAYER THICKNESSES CALCULATED* USING THE SURFACE DEPOSITION MODEL

Element	Sample pairs	C_s (μg/cm²)	C_o (μg/g)	Linear correlation coefficient	Estimated surface thickness (Å)
Pb	6	0.04	1000	0.73	1
Tl	6	0.003	40	0.80	0.1
Sb	6	0.003	20	0.93	0.1
Cd	6	0.002	10	0.99	0.7
Se	6	0.004	0.7	0.92	0.1
As	6	0.009	600	0.97	0.3
Zn	6	0.6	6000	0.60	20
Ni	6	0.1	100	0.98	4
Cr	6	0.3	-300	0.94	9
S	4	19	5 × 10	--	600

* Calculations were based on the airborne particle data in Appendix C assuming $\rho = 3$ g/cm³. The slope of the line in Figure 33 can be obtained from C_s by multiplying by 10^4.

a given particle source. In the case of a log-normal distribution this gives the following:

$$\frac{dM_X}{d(\ln D)} = \frac{1}{\sqrt{2\pi}\,\ln\sigma_g}\left\{\bar{C}_o \exp - \left[\frac{(\ln D/D_g)^2}{2(\ln \sigma_g)^2}\right] + \frac{6C_s}{\bar{\rho}} \exp\left[\frac{(\ln \sigma_g)^2}{2}\right] \exp - \left[\frac{(\ln D/D_g + \ln^2 \sigma_g)}{2\ln^2\sigma_g}\right]\right\} \quad (7)$$

where σ_g = geometric standard deviation, M_X = mass of X, D_g = mass median diameter of original distribution, C_o = bulk concentration of X, C_s = surface concentration of X, p = particle density, and D = particle diameter.

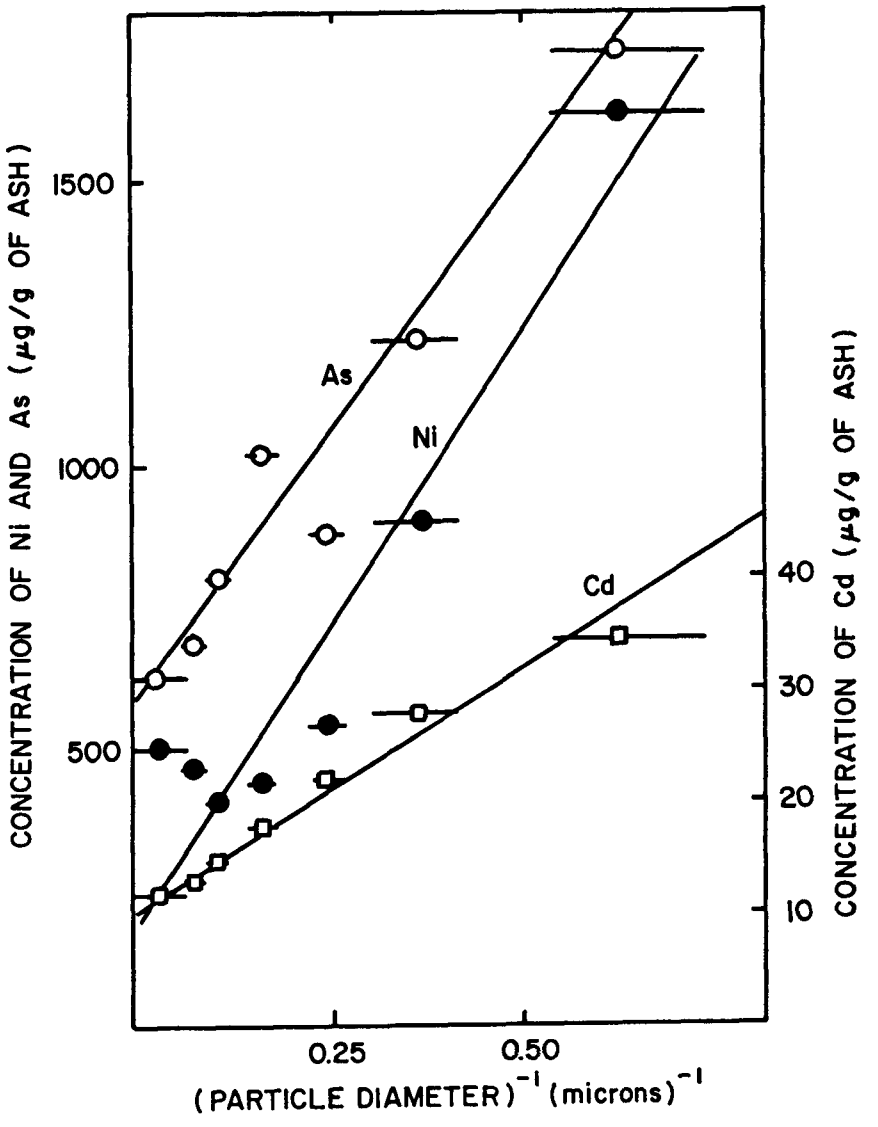

Figure 33. Dependence of As, Ni, and Cd concentrations in coal fly ash on particle size. (Reprinted by permission of D. F. S. Natusch and the American Association for the Advancement of Science from Natusch et al., 1974. Copyright American Association for the Advancement of Science 1974.)

Equation (7) does not provide a simple analytical expression for the mass median diameter $D_g(X)$ except when $\bar{C}_o = 0$, i.e., X is present only in the deposited layer. In this case, it can readily be shown (Butcher and Charlson, 1972) that

$$\ln D_g(X) = \ln D_g - \ln^2\sigma_g \tag{8}$$

Equations (7) and (8) demonstrate that the mass median diameter of a surface-deposited species, X, is considerably less than that of the median diameter based on total particulate mass.

Several authors (Block and Dams, 1975; Coles et al., 1979; Klein et al., 1975) have suggested that the preferential concentration of certain elements in small particles is a result of their lithophilic or chalcophilic properties. Lithophilic elements are those generally found associated with alumino-silicate materials, while chalcophiles are associated with sulfide-containing minerals. This classification of elements generally relies on the scheme proposed by Mason (1966), although slight differences exist with other reports (Krauskopf, 1972; Nicholls, 1968).

Most reports indicate that Al, Ba, Be, Ca, Cs, Hf, K, Mg, Mn, Na, Rb, Ta, Th, Ti, U, V, and the rare earths (Ce, Dy, Eu, La, Nd, Sm, Tb, and Yb) are classified as lithophiles. Similarly, As, Cd, Ga, Mo, Pb, Sb, Se, and Zn are chalcophiles. Elements that may be either lithophilic or chalcophilic in their behavior include Cr, Co, Cu, Fe, Ni, and W. In terms of small particle behavior, the lithophiles belong mainly to Group I, showing little preferential concentration on small particles. The Group II elements, which are much more easily volatized during combustion, are generally chalcophiles. Group III elements include, but are not limited to, those elements that may belong to both classes.

In general, this geochemical classification scheme is consistent with the volatilization-condensation theory suggested. The ultimate behavior of the different elements is still determined by the coal and combustion facility, but prior analysis of the coal based on its geochemistry may permit better predictions concerning which elements, if any, will be preferentially concentrated in small particles.

Recently, a third hypothesis concerning trace metal-small particle relationships was proposed (Smith et al., 1979). In this study it was found that concentrations of trace elements that increased with decreasing particle size in the range of 1 to 10 μm became independent of size below 1 μm. As as result, the authors suggested that gas expansion caused a "busting" of larger particles, with the resulting production of a large number of small particles. These small particles then coagulate into the 0.1-1.0 μm size particles. Condensation would occur concurrently with the busting and coagulation process. Data to support this hypothesis are largely circumstantial.

Elemental Enrichment in Coal Fly Ash

If the concentration of toxic trace metals in small particles is a widespread phenomenon, as has been suggested, then one would expect volatile elements present in urban aerosols to have significantly lower mass median diameters than nonvolatile elements. In fact, data obtained by the National Air Surveillance Network (NASN) have shown that the more easily volatilized elements Zn, Ni, Pb, Cd, and Ba have statistically lower mass median diameters than common nonvolatilizable (particle matrix) elements. In addition, a number of toxic elements, including Pb, Se, Sb, Cd, Ni, V, Sn, and Zn, in urban aerosols have been reported to have equivalent mass median diameters of the order of one micrometer or less, which is considerably less than those reported for common matrix elements such as Fe, Al, and Si, whose mass median diameters lie in the range of 2.5-7.0 micrometers (Rahn et al., 1971; Lee et al., 1972; Colovos et al., 1974). Ondov et al. (1979) also reported this to be true for particles emitted to the atmosphere from electrostatic precipitators and especially from scrubber systems or coal-fired power plants. Also, although not substantiated statistically, Se and Sb have been shown to have small mass median diameters in ambient aerosols (Gladney et al., 1973; Ondov et al., 1979). Lead, of course, is not expected to be typical, since it is derived mainly from a single source (the automobile) known to produce small particles.

The predominance of certain elements in small particles is also significant in determining the degree of enrichment of these elements in an urban aerosol, since the smallest particles have the longest atmospheric residence time. Indeed, Gordon and Zoller (1973) have shown enrichment factors of greater than ten times over natural crustal abundance for Tl, Cr, Ni, Cu, Zn, As, Cd, Sn, Pb, Se, S, Cl, and Br in the Boston aerosol and have established substantial correlations with enrichment patterns in coal fly ash, municipal incinerator fly ash, and residual fuel oil ash. In the present context, it is noteworthy that the majority of these elements could be volatilized during combustion.

A number of authors (Kaakinen et al., 1975; Gladney et al., 1976; Ondov et al., 1977) state that enrichment of toxic trace elements in coal fly ash may be quite significant. Some of the enrichment factors compared with the original coal samples are given in Table 11; these tend to exceed a factor of three enrichment.

Volatile Species in Coal Fly Ash

Although we have considered only trace elements present in particulate matter, the importance of vapor species, especially of selenium, arsenic, and mercury, should not be overlooked. Thermodynamic data (Hodgeman, 1963) indicate that, at 25°C, as much as 80 $\mu g/m^3$ of Se as SeO_2 and 70 $\mu g/m^3$ of As as As_2O_3 can exist as vapors. These levels are much greater than normally observed for Se and As in urban aerosols ($\leq$ 10 ng/m^3). It is possible, therefore, that additional amounts of these elements may be emitted as vapors. Consistent with this suggestion, Pillay and Thomas (1971) have reported that at least 50% of the Se present in urban air passes through a filter designed to collect all particles greater than 0.1 μm in diameter.

TABLE 11. ENRICHMENT FACTORS FOR IN-STACK TOTAL SUSPENDED PARTICULATE MATERIAL

Element	Gladney*	Kaakinen†	Ragaini and Ondov¶
As	6.8	3.1	7.3
Cr	1.1	NR§	2.0
Ga	1.2	NR	3.1
Pb	4.0	5.8	NR
Sb	4.7	3.2	6.7
Se	6.2	5.7	2.5
Zn	1.5	3.2	6.4

* Gladney et al. (1976).

† Kaakinen et al. (1975).

¶ Ragaini and Ondov (1977).

§ NR = Not reported.

Klein et al. (1975) and Andren et al. (1975) report that 20-32% of the selenium that passes through a coal-fired power plant does so as a non-particulate-associated vapor and that much of the selenium is present in the zero oxidation state. Klein et al. (1975) also suggest that, based on mass balance information, a minimum of 60% and probably about 90% of the mercury entering the coal stream is emitted as the vapor. Little information is presently available for arsenic, but its behavior would be expected to parallel that of Se and Hg.

INORGANIC CHEMICAL SPECIATION AND LEACHING CHARACTERISTICS

Chemical Compounds in Coal Fly Ash

Studies of fly ashes derived from the oxidative combustion of coal have defined, in part, the chemical forms of sulfur and carbon. In some cases the salts in which trace metals occur can be inferred.

Electron Spectroscopy for Chemical Analysis (ESCA) shows that sulfur is primarily present in the +6 oxidation state (Linton et al., 1977). Particulates derived from coal conversion processes that involve reducing conditions

also contain sulfur in the -2 oxidation state (Keyser et al., 1978). Neither result is unexpected. Time Resolved Solvent Leaching (TRSL) studies of coal fly ash, in which analyses of soluble anions are performed by means of ion chromatography, indicate that sulfate is the only sulfur-containing anion leached by water. It is probably, therefore, that the sulfur species present in the surface layer of coal fly ash is, at least predominantly and probably exclusively, in the form of sulfate. However, this must be tempered by the fact that most elemental sulfides are highly insoluble.

Some evidence is available regarding the cations associated with sulfate species in coal fly ash. Thus, X-ray powder diffraction analyses of some fly ashes indicate the presence of either anhydrite ($CaSO_4$) or gypsum ($CaSO_4 \cdot 2H_2O$). Fisher et al. (1976) also suggested crystalline anhydrite or gypsum was present on the surfaces of some ashes, based on ion microprobe analysis. The two $CaSO_4$ species are present most commonly in fly ashes derived from western U.S. coals, which contain especially high levels of calcium. The second form results, apparently, from exposure of the highly hygroscopic anhydrite to moisture. In a sense, therefore, the occurrence of gypsum is probably artifactual.

Quite strong indications have also been obtained for the existence of several trace metal sulfates in coal fly ash. Thus, both Fourier transform infrared Spectroscopy (FTIR) and Time Resolved Solvent Leaching (TRSL) provide evidence for the presence of Cd, Co, Cr, Mo, and Ni sulfates in coal fly ash. The alkali metals Ba, Cu, and Ca are also present, at least partly, as sulfates. Even stronger leaching evidence is available for the existence of Al and Fe as sulfates in the surface layer of fly ash (Natusch and Tompkins, 1978).

In the case of carbon, a number of alkali and alkaline earth carbonates have been quantified at trace levels. Part of the evidence comes from carbonate decomposition as fly ash is heated with a slowly increasing temperature ramp. Evolved CO_2 was monitored by plasma emission spectrometry using an atomic carbon wavelength. The temperature of decomposition and associated-CO_2 evolution was characteristic of the metal to which it is bound. In an additional experiment using the same emission detector, CO_2 was evolved by acidification of the fly ash with aqueous HCl. The total amounts of CO_2 released from each fly ash by thermal and aqueous methods were comparable.

The thermal evolution data alone does not allow unambiguous identification and quantitation of the carbonate compounds. However, combined with the acid evolution procedure, an accurate determination can be made. Thus, the analyses of the leachate obtained from treating a fly ash with the amount of acid just necessary to dissolve all the carbonate coupled with the leaching time enables identification of all of the metals that were present as carbonates. The leachates were analyzed by atomic spectrometry for Fe, Li, Na, K, Rb, Mg, Ca, Sr, and Ba. These results, when combined with the thermal CO_2 evolution data, defined concentrations or concentration limits on carbonate species (Table 12). Note that the existence of carbonates seems to be a general phenomenon, regardless of the source of the ash.

TABLE 12. UPPERLIMIT CONCENTRATIONS (ppm)* OF CARBONATE COMPOUNDS IN COAL FLY ASH. NUMBER IN PARENTHESES REPRESENTS PERCENT DEVIATION

Compound	Fly ash from indicated coal			
	Illinois #1	Illinois #2	New York	Montana
Li_2CO_3	≦220 (15)†	≦45.3 (14)	≦202 (26)	≦85.7 (1)
Na_2CO_3	759-1090¶ (15)	456 (19)	≦438 (26)	≦129 (8)
K_2CO_3	570¶ (12)	474 (19)	≦1680 (26)	≦332 (8)
Rb_2CO_3	≦0.32 (15)	--§	--§	--§
$FeCO_3$	2630§ (4)	438 (12)	819 (14)	517 (6)
$MgCO_3$	1910¶ (14)	≦1710 (14)	596§ (14)	1670-1770§ (1)
$CuCO_3$	2270¶ (14)	1770-3870 (14)	487 (27)	2000-2100¶ (1)
$SrCO_3$	1060-1520¶ (15)	797-1330 (8)	≦150 (26)	--§
$BaCO_3$	816¶ (12)	177 (19)	≦676 (26)	3300 (11)

* ppm of ash.

† Percent deviation.

¶ For the following sets of elements: Mg and Fe in "New York"; Mg and Cu in "Montana"; Mg, Cu, and Fe in "Illinois #1"; and Li, Na, and Sr in "Illinois #1. Contributions from the individual metals could not be resolved. The numbers listed are maximum values assuming no contribution from the others in the set.

§ No meaningful data.

In several cases the mass balance indicates more metal is leachable than can be accounted for by carbonates alone. Table 13 presents the percent of each metal that is bound in fly ash as the carbonate, as defined by the leaching procedure. Note that the procedure is not exhaustive; therefore, these percentages represent upper limits.

At present, there is no evidence to indicate whether the carbonate compounds are associated with the surfaces of coal fly ash. Nevertheless, since the flue gas in which the ash is entrained contains high concentrations of CO_2 and H_2O, a surface-preferred reaction is quite likely.

TABLE 13. CARBONATE SPECIES CONTRIBUTION TO LEACHABLE ELEMENTAL CONCENTRATIONS (%)

Element	Fly ash from indicated coal			
	Illinois #1	Illinois #2	New York	Montana
Li	0-100	0-100	0-100	0-100
Na	0.6-0.8¶ (16)†	100 (19)	0-100	0-100
K	7.8¶ (14)	100 (19)	0-100	0-100
Rb	0-100	--§	--§	--§
Fe	4.9¶ (30)	7.2 (19)	40.1§	4.3 (17)
Mg	3.0¶ (18)	0-100	91.4 (45)	1.6-1.7¶ (3)
Ca	0.8¶ (16)	1.7-3.8 (15)	4.0 (28)	0.7¶ (3)
Sr	9.3-13.3¶ (19)	--§	0-100	23.2-38.7 (9)
Ba	5.6¶ (12)	100	0-100	58.3 (14)

* ppm of ash.

† Percent deviation.

¶ For the following sets of elements: Mg and Fe in "New York"; Mg and Ca in "Montana"; Mg, Ca, and Fe in "Illinois #1"; and Li, Na, and Sr in "Illinois #1; contributions from the individual metals could not be resolved. The numbers listed are maximum values, assuming no contribution from the others in the set.

§ No meaningful data.

Present indications are that a large fraction of the elements present in fly ash are bound as sulfates and carbonates and that, while definitive evidence is lacking, these elements are present in the so-called surface layer. It must be recognized that the actual compounds may be mixed salts. For example, the existence of alkali iron tri-sulfates has been suggested by numerous authors (Covey et al., 1945; Nelson and Cain, 1960; Weintraub et al., 1961), and various combinations of Ca, Mg, and Fe occur in naturally occurring carbonate minerals. No evidence has been found for the presence of free H_2SO_4 in fly ash particles.

AQUEOUS LEACHING OF COAL FLY ASH

Introduction

The foregoing sections have concentrated on a description of research directed towards establishing the physical and chemical characteristics of coal fly ash. In order to obtain some assessment of the probably environmental impact of this material, however, it is necessary to obtain information about the characteristics and behavior of coal fly ash between its point of discharge into the environment and its adverse interaction with an environmental or biological system.

In this last regard, it is suggested that few, if any, pollutant species can have an adverse effect upon any biological organism unless that species is capable of entering into solution either in water or into one or more of the several types of body fluids that may be encountered. If one accepts this hypothesis, it follows that determination of the solubility of various pollutant species is of fundamental importance to an assessment of their capability for exerting a toxic effect.

It has been reported (Shannon and Fine, 1974; Theis and Wirth, 1977; James et al., 1977; Dreesen et al., 1977) that the bulk solubility of coal fly ash in water is very low and rarely exceeds 2-3 percent by weight. The low bulk solubility is clearly a result of both the glassy and crystalline matrix materials identified earlier, and one would expect elements that are either chemically or physically trapped within this matrix to exhibit low solubility. On the other hand, at least some of the material present in the surface layer is readily soluble in water (Linton et al., 1977). Indeed, it is now quite well established (Linton et al., 1977; Natusch, 1978a; Fisher et al., 1978) that most of the soluble fraction of fly ash is derived from this surface layer and is thus quite rich in trace elements.

A number of authors have concentrated on laboratory leaching (James et al., 1977; Shannon and Fine, 1974; Fisher et al, 1979; Theis and Wirth, 1977; Brimblecombe and Spedding, 1975; Cox et al., 1978; Eggett and Thorpe, 1978; Phung et al., 1979), but few studies exist of natural systems (Talbot et al., 1978). Unfortunately, there is considerable confusion involved in interpreting and understanding results obtained from different studies of fly ash solubility. Specifically, quite different results are obtained by workers using apparently similar laboratory leaching techniques and few are readily transferrable to field studies. However, the work of Dressen et al. (1977) is an exception. In this study, laboratory leaching of fly ash was related to effluent water measurements made at the same power plant. Their results showed that, among the elements found to be most extractable in the laboratory by either water (B, F, Mo, and Se) or acid (As, B, Cd, F, Mo, and Se) leaching, many were also elevated in the effluent water (As, B, F, Mo, and Se). In general, however, factors that control leachate composition under both laboratory and field conditions have not been well studied, nor has an attempt been made to standardize or compare different leaching techniques.

Some insight into leaching behavior can be obtained by recognizing that a soluble inorganic species, M_iA_i, associated with fly ash particles can dissociate into its component cations, M_i, and anions, A_i, in aqueous solution and that both dissolution and deposition (e.g., precipitation) processes can occur in competition with each other. Furthermore, cations and anions present in solution can interact so as to set up multiple equilibria, which may involve ion pairing, complexation, precipitation, or acid-base behavior (e.g., M_iA_j or M_jA_i). The result can be expressed simplistically by the following equations:

$$
\begin{array}{ccc}
 & P \sum_{i=1}^{n} M_iA_i & \\
 & k_{-1} \downarrow \uparrow k_1 & \\
P + \sum_{i=1}^{n} M_i & + & \sum_{i=1}^{n} A_i \\
+ & & + \\
\sum_{j=1}^{m} A_j & & \sum_{j=1}^{m} M_j \\
k_{-2} \uparrow \downarrow k_2 & & k_{-3} \uparrow \downarrow k_3 \\
\sum_{i=1}^{m} \sum_{j=1}^{n} M_iA_j & + & \sum_{i=1}^{m} \sum_{j=1}^{n} M_jA_i
\end{array}
\qquad (9)
$$

Here P represents the parent (host) particles and k_n, k_{-n}, are the rate constants for forward and reverse reactions, respectively. It is apparent from Equation (9) that, when leaching studies are conducted under batch conditions such that the amount of fly ash and solvent are maintained constant, an equilibrium will be established between particulate and solution species. Consequently, only a fraction of the potentially soluble material will enter solution, and some of this may be precipitated by other ionic reactions. On the other hand, if conditions are such that soluble material is continuously removed by providing fresh solvent or by providing a large solution sink in the form of complexing ligands or acids, then all potentially soluble material will ultimately be dissolved.

It is apparent from the equilibrium outlined in Equation 9 that any factor capable of altering the position of the general equilibria indicated will directly affect the composition of the leachate solution from a fly ash-solution contact. Furthermore, it is reasonable to suppose that many of these factors will also control the rate at which soluble species are leached from the fly ash mass. It has been the primary objective of the present work, therefore, to identify those parameters that are capable of influencing the position of equilibrium and thus of affecting leachate composition. Such factors have been shown to be the ratio of fly ash mass to solution volume, the temperature of the solution, the pH of the solution, the presence of complexing or precipitating agents capable of promoting or suppressing solution of individual species, the particle size of the fly ash, the origin of the fly ash, and, perhaps most important, the method by which the leaching solution and the fly ash are brought into, and maintained in, contact. A large body of data has been gathered with respect to establishing the influence of these factors on leachate composition. Specifically, emphasis has been placed on the following objectives:

1. The need to establish standard methods whereby leaching can be conducted in different laboratories and the same results reproducibly obtained.

2. Determination of the characteristics of leaching and the composition of leachates under conditions closely representing those likely to be encountered in real environmental situations.

3. Establishment of a predictive model capable of determining the composition of a given leachate under known field conditions.

In order to address these objectives, several types of leaching procedures were developed and the influence of the parameters listed above determined for each. The experimental methods, as well as the actual data, are presented in Appendices A and D, respectively. The fly ash used in these studies was obtained from the Corrette Plant in Billings, Montana, which uses a sub-bituminous coal from Colestrip, Montana.

Continuous Single-Pass Leaching

This method involves passing the leaching solution from a reservoir through a bed of coal fly ash and analyzing aliquots of the collected leachate as a function of time (volume). Emphasis is placed on maintaining the fly ash bed in the configuration of a flat disk to reduce the possibility of equilibrium being obtained between the fly ash and the solution actually present in the bed. For the same reason, a comparatively fast flow rate is employed. Details of the parameters actually employed in these studies are given in the several tables describing the results (see Appendix D).

It will be noted that in continuous single-pass leaching, fresh solution is continuously being brought into contact with the fly ash so that the equilibria indicated in Equation (9) are established at most only momentarily, with the result that there is a net transfer of material from the left- to the right-hand side of Equation (9). Consequently, all readily soluble material will be removed from the fly ash so that a so-called

"exhaustive" leaching process is achieved. Such a leaching process, when carried to its logical conclusion of extremely long time periods, is, of course, capable of completely dissolving all of the fly ash material away.

Table 14 gives the pH of the leachate emerging from the column as a function of leaching time (volume) through the column. Three different pH's were employed. The results establish quite clearly that the material leached from the coal fly ash contributes a net alkalinity to the leachate but that the ability to leach alkaline material into solution falls off quite rapidly with time (volume).

The anion concentrations in the column leachate increased with decreasing pH, as expected. Furthermore, changing the fly ash solution contact time showed that, for some species (e.g., sulfate), contact time can have a significant effect upon leaching solution composition. The data given here are, however, not sufficiently definitive to establish whether its effect results from partial establishment of equilibrium in the solution contained in the bed or simply from different rates of solubility. In the case of sulfate, one inclines marginally to the latter view.

Analysis of the changes in cationic concentrations indicate that

1. A number of elements, including cadmium, phosphorus, molybdenum, manganese, sodium, aluminum, calcium, barium, potassium, chromium, strontium, lead, and lithium, appear either to be present at higher concentrations near the external surface of the fly ash particles or are present in readily soluble form in fly ash. If high solubility is, in fact, the case, it is expected that most of the material is near the surface, as has been discussed.

2. In contrast, several elements (notably magnesium) seem either to achieve equilibrium rather slowly with the leaching solution or to be exposed as leaching proceeds. It is noteworthy that this behavior is observed under high, rather than low, pH conditions.

3. As a general rule, larger amounts of most of the trace elements listed are leached by more acidic leaching solutions. Since many of the compounds are likely to be oxides, this result is not unexpected.

Column leaching was also applied to different fly ash size fractions with distilled water. The data, however, proved to be inconclusive with respect to the dependence of leachate concentration on particle size. Thus, consideration of only two smaller size ranges (20-30 and 30-45 μm) indicates that the amount of material that can be leached increases with decreasing particle size, as would be expected if the hypothesis of volatilization followed by condensation of several trace metal species onto particle surfaces is valid. On the other hand, the data presented for the large (150-180 μm) sample would seem to refute this, and repeated experiments indicate that the results are generally valid.

Consideration of the morphologies of coal fly ash particles described in an earlier section and of the specific surface areas listed in Table 6

TABLE 14. CHANGES IN MEASURED pH RESULTING FROM COLUMN LEACHING OF A BULK WESTERN SUB-BITUMINOUS COAL FLY ASH WITH SOLUTIONS OF DIFFERENT pH

Leaching solution	Time (min)*-volume (ml)											
	0	15-45	60-180	120-360	180-540	360-1080	540-1620	720-2160	1440-4310	1800-5400	2160-6480	2880-8640
distilled H_2O	12.30	12.05	12.10	11.70	11.60	11.05	10.70	10.50	10.05	10.35	10.80	9.80
pH 3†	12.20	12.05	11.85	11.20	10.40	3.70	3.30	3.30	3.20	3.15	3.10	3.10
pH 1¶	1.15	1.00	1.00	1.00	1.00	1.00	1.00	1.00	1.00	1.00	1.00	1.00

* Flow rate = 3 ml/min.

† pH 3: 0.07 ml of conc. HNO_3 in 1000 ml H_2O.

¶ pH 1: ~50 ml of conc. HNO_3 in 5000 ml H_2; ~0.15 M HNO_3.

indicates that the large particles may have significantly different characteristics than the small, predominantly spherical particles. It is conceivable, therefore, that these characteristics may overshadow the size trends that would otherwise be expected.

Soxhlet Extraction

The use of conventional soxhlet extraction offers a useful method for the preparation of leachates under standard conditions. Since the process of soxhlet extraction washes the solid fly ash sample with fresh aliquots of solvent, it is possible, at least in principle, to quantitatively remove all soluble material and, as indicated for the case of continuous single-pass leaching in the previous section, to dissolve the fly ash completely if sufficient time is allowed to elapse. Since each aliquot is of comparatively small volume (on the order of 10 ml), the equilibrium (Equation 9) between solid and dissolved species may be established in many cases during the period a given aliquot is in contact with a fly ash. On the other hand, the overall soxhlet extraction process is an equilibrium situation in that the material in the solvent leaving the soxhlet will be in equilibrium with the batch solvent material below.

Two types of analytical measurement are of potential interest with respect to soxhlet extraction of coal fly ash. The first involves determination of the concentrations of individual species present in each aliquot drained from the region of the extraction thimble. Such measurements should be roughly, though not rigorously, comparable to the measurements made in continuous single-pass leaching described in the previous section. The second type of measurements involves determination of the concentrations of individual species present in the bottom flask of the soxhlet extractor, which accumulates all leached material. In the second case, however, it should be noted that, as the concentration of many ion-cation pairs (e.g., sulfate and barium) in solution increases, precipitation may soon result so that both soluble and colloidal material may be present in the bottom flask.

Soxhlet extraction has the advantage of being a simple, well-characterized procedure for the extraction or leaching of solid materials. It is, however, limited in use to constant boiling mixtures, so that, for most purposes, only pure liquids can be used for leaching. This may be a severely limiting factor in situations where leaching with acidic solutions or with solutions containing specific complexing agents may be desired. In addition, the temperature of the leaching liquid is generally only a few degrees below its boiling point, which hardly represents realistic environmental conditions. This problem can be partly overcome by performing soxhlet extraction under reduced pressure so as to lower the boiling point of the leaching liquid. In the case of water, it has not proven practical to operate below about 35°C because of difficulties encountered with "bumping" within the boiling flask. For this reason, we have developed a useful modification of the soxhlet extraction procedure whereby any constant boiling liquid can be presented to the material in the extraction thimble at a desired temperature close to ambient. The apparatus used for this purpose, the operation of which is fairly self-explanatory, is illustrated in Figure 34.

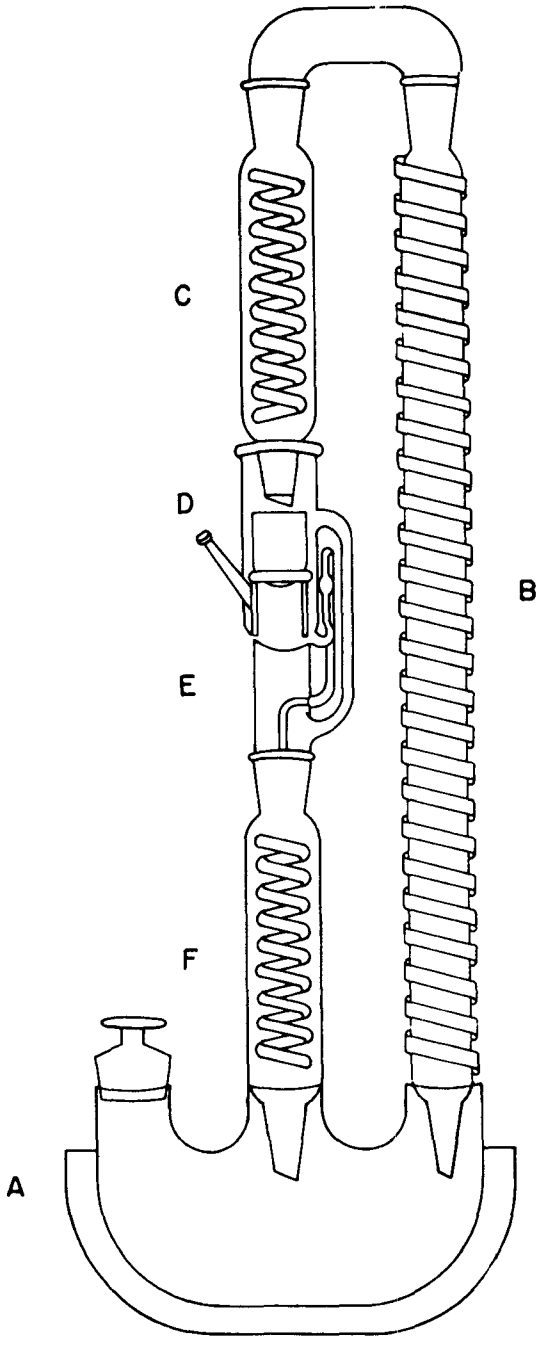

Figure 34. Apparatus for ambient temperature soxhlet leaching. A, bottom flask; B, heating tape; C, cooling condenser; D, extraction thimble; E, interval sampling region; F, condenser to isolate soxhlet.

Several samples of the bulk Corrette fly ash were subjected to soxhlet extraction at room temperature with the apparatus depicted in Figure 34. In all cases, 10 gm of coal fly ash were leached at 25°C, and selected aliquots of the leachate were sampled and analyzed for both cationic and anionic species as a function of time throughout the extraction. In addition, samples of the solution in the bottom flask of the extractor were also analyzed as a function of time and corrected for the dilution necessitated by removal of these aliquots from the bottom flask.

The results are noteworthy primarily because they illustrate great differences between the concentrations of material found in individual aliquots of leachate and those aliquots collected from the soxhlet bottom flask. Thus, concentrations measured in individual aliquots collected directly from the solution that has been in immediate contact with the soxhlet thimble give results generally similar to those obtained for continuous single-pass leaching, as would be expected. On the other hand, analyses of material collected from the bottom flask rather dramatically illustrate the operation of solubility equilibrium for several of the species present, e.g., iron and fluoride.

In general, however, the soxhlet extraction procedure provides no particular advantage over the previously described method of continuous single-pass leaching other than that of simplicity of unattended operation. It is expected that the equilibria attained in the bottom flask of a soxhlet extraction apparatus are likely to resemble those likely to operate in a real environmental system.

Batch Leaching with Sonic Agitation

This procedure involves sonic agitation of a suspension of the solid fly ash in solution. In contrast with the procedures described previously, this method maintains the ratio of fly ash mass to solution as a constant and thus achieves equilibrium between the solid and the leachate. The information obtained, therefore, is likely to be pertinent to situations (e.g., ponding of fly ash) in which a constant volume of fly ash and water are brought into contact. On the other hand, if a very small amount of fly ash is sonically agitated with a very large volume of water, it is possible to determine approximately the total amount of leachable material.

Not unexpectedly, sonic leaching results in the greatest variability in concentrations of almost every element. The multiple equilibriua previously discussed clearly have considerable effects on the solution concentrations. Changes in the amount of leaching solution did not result in a linear or even uniform response in terms of increased concentrations. This method lacked reproducibility as well, indicating that it is is a generally less desirable laboratory method for studying fly ash solubility.

SURFACE CHARACTERIZATION

The surface predominance of potentially toxic elements has been demonstrated recently in coal fly ash particles emitted to the atmosphere (Linton et al., 1976). Preliminary studies also indicate that elemental surface

predominance may be a general phenomenon occurring in airborne particles derived from high-temperature combustion operations (Linton et al., 1976; Linton et al., 1977).

These findings are of significance in part because they provide direct confirmation of previous predictions (Davison et al., 1974; Kaakinen et al., 1975) that surface predominance should occur. The phenomenon is attributed to the condensation of species previously volatilized in the high-temperature combustion zone of a particulate emission source (Davison et al., 1974; Kaakinen et al., 1975).

The existence of elemental surface predominance is also important in demonstrating that bulk analysis techniques, which give only average concentration values, provide little insight into the actual chemical nature of the particles. For example, results obtained solely on the basis of bulk analysis markedly underestimate the potential environmental impact of airborne particles derived from high-temperature combustion operations in that (1) surface regions of the particles have enhanced concentrations of elements, including some that are potentially toxic, and (2) the smallest particles will have much higher bulk (μg/g) concentrations of such elements because of larger surface area to volume ratios (Davison et al., 1974).

On the basis of the discussion in Section V, it is apparent that there is a need for analytical techniques capable of surface and in-depth elemental characterization of individual particles. Several approaches to obtain this analytical information comprise the subject matter of this section. Principal methods employed include the surface analytical techniques of secondary ion mass spectrometry (SIMS) and Auger electron spectrometry (AES) as practices for microanalysis, i.e., ion microprobe mass spectrometry and scanning Auger microscopy.

This section also illustrates the benefits of a multitechnique approach, not only by the application of several complementary surface microanalytical techniques but also by the use of solvent leaching in conjunction with both surface and bulk (spark source mass spectrometry) analyses. Specifically, the combination of leaching, bulk, and surface techniques demonstrates that the observed elemental surface predominance is not the consequence of artifacts, especially those that may result from the use of ion sputtering to obtain depth profiles. It also permits semi-quantitation of elemental concentrations in the surface region.

In the case of coal fly ash, the information obtained by this approach provides substantial insight into the physicochemical characteristics of fly ash surfaces and permits assessment of its potential environmental impact.

Ion microprobe depth profiles for 15 elements in fly ash are shown in Figures 35-40. These elements include all of the major and minor elements in fly ash (greater than 1% by weight), as well as six trace elements with concentrations below 1000 ppm, as determined by bulk analysis. Other elements of possible surface predominance and toxicity (Davison et al., 1974; Natusch et al., 1974) could not be characterized, including Co, As, Ni, Zn,

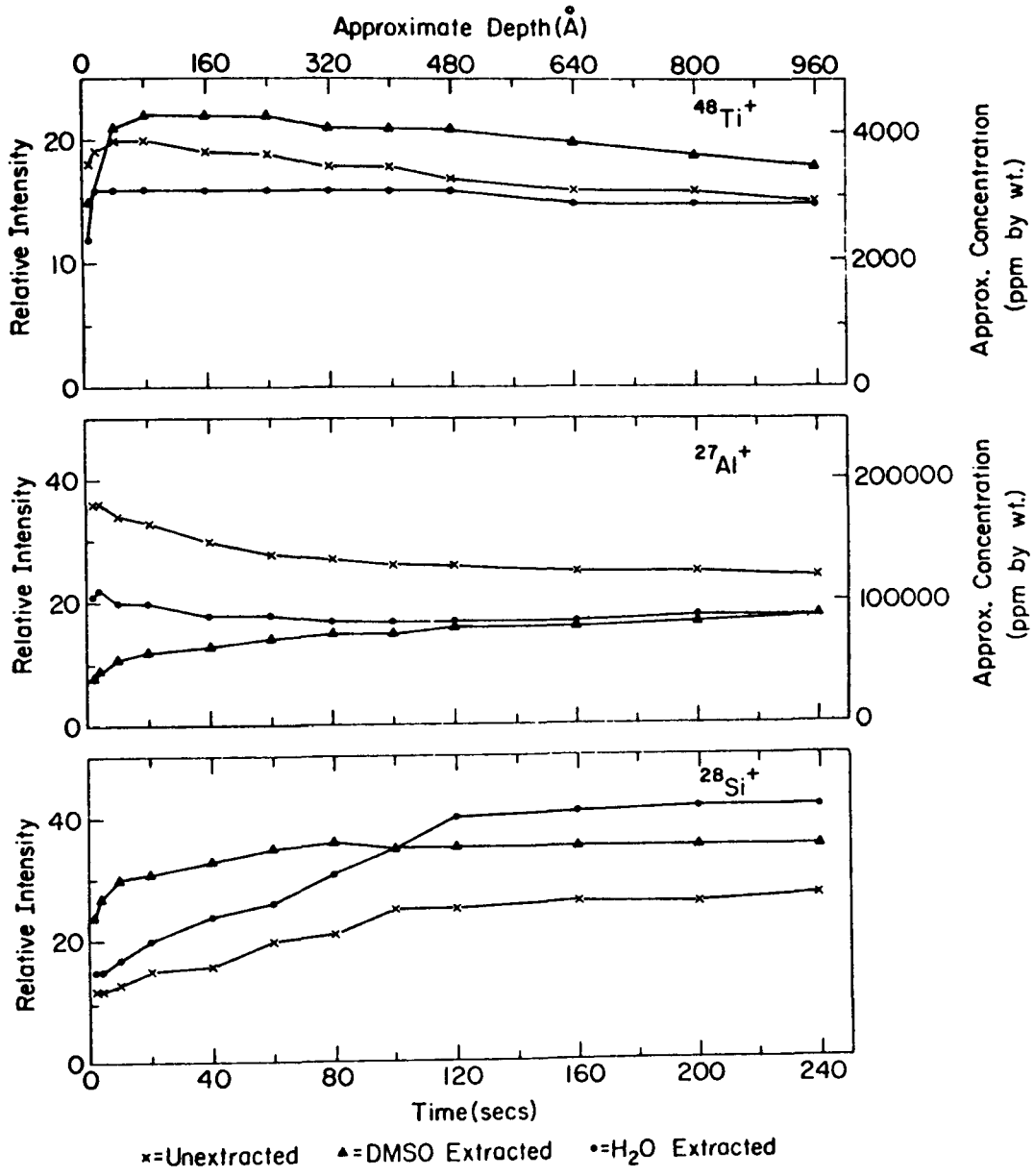

Figure 35. Ion microprobe depth profiles of the Group A elements (Ti, Al, Si) in unleached and leached fly ash. (Reprinted by permission of R. Linton and The American Chemical Society from Linton et al., 1977.)

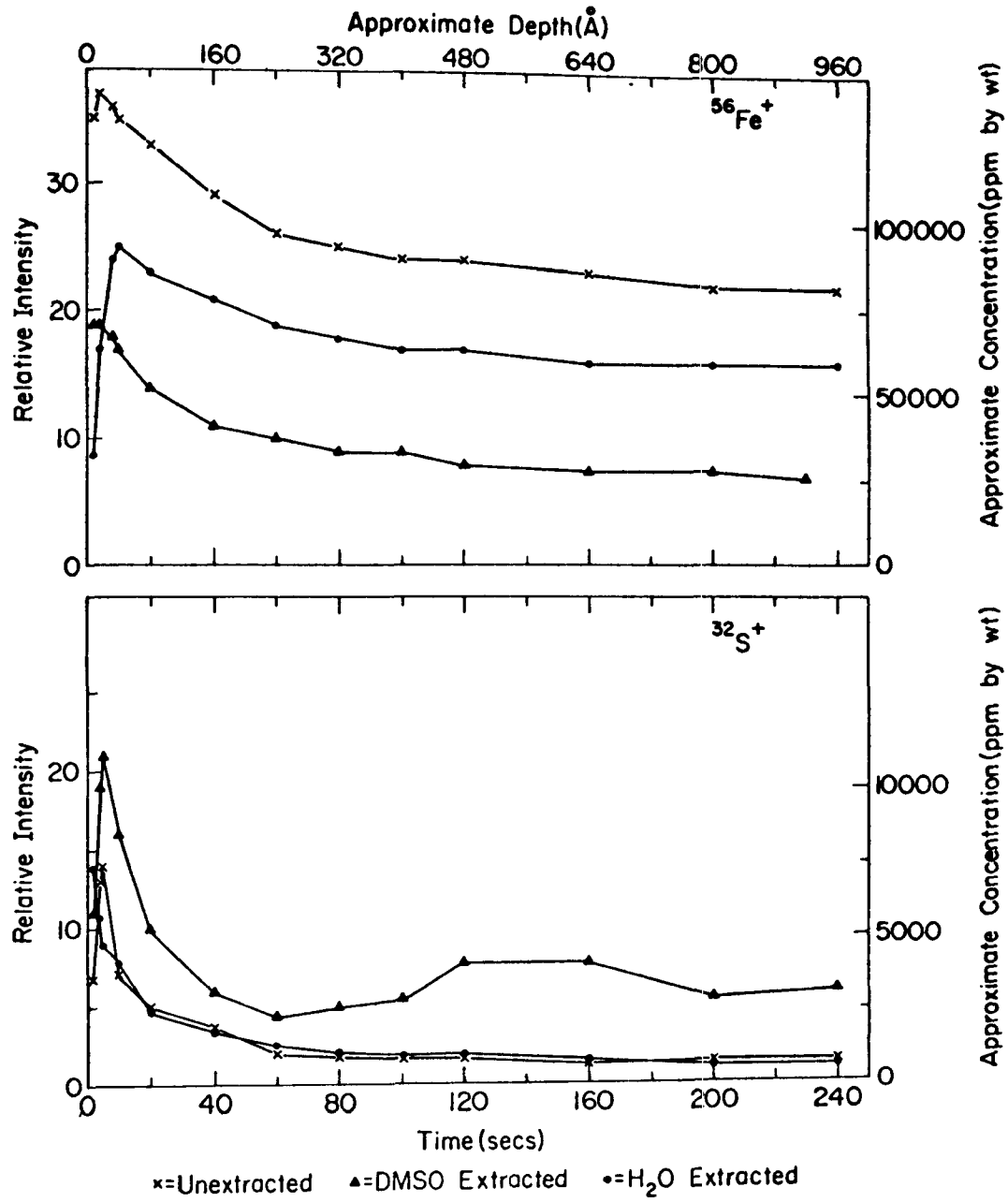

Figure 36. Ion microprobe depth profiles of the Group B elements (Fe, S) in unleached and leached fly ash. (Reprinted by permission of R. Linton and the American Chemical Society from Linton et al., 1977.)

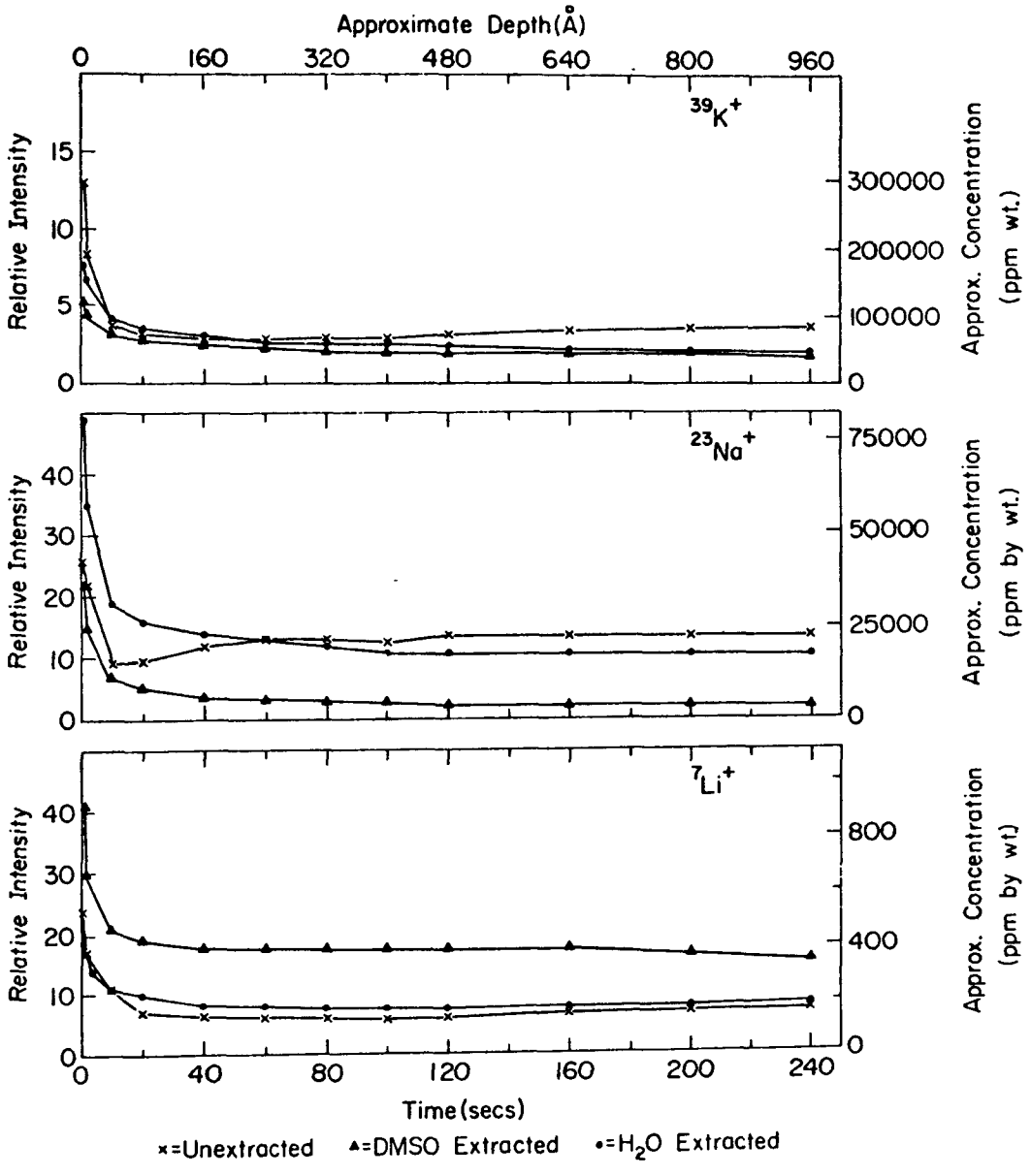

Figure 37. Ion microprobe depth profiles of the Group B elements (K, Na, Li) in unleached and leached fly ash. (Reprinted by permission of R. Linton and the American Chemical Society from Linton et al., 1977.)

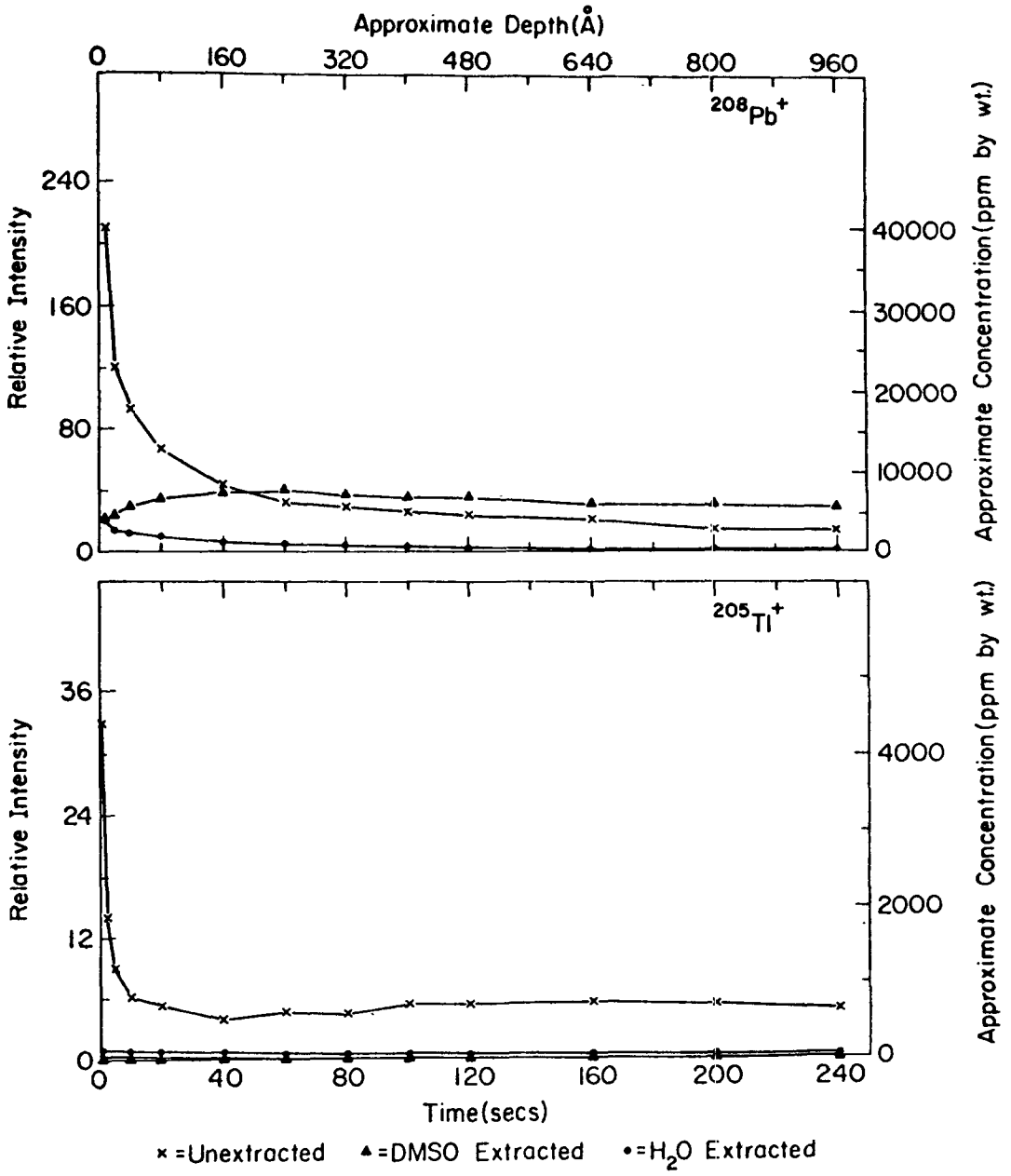

Figure 38. Ion microprobe depth profiles of the Group C elements (Pb, Tl) in unleached and leached fly ash. (Reprinted by permission of R. Linton and the American Chemical Society from Linton et al., 1977.)

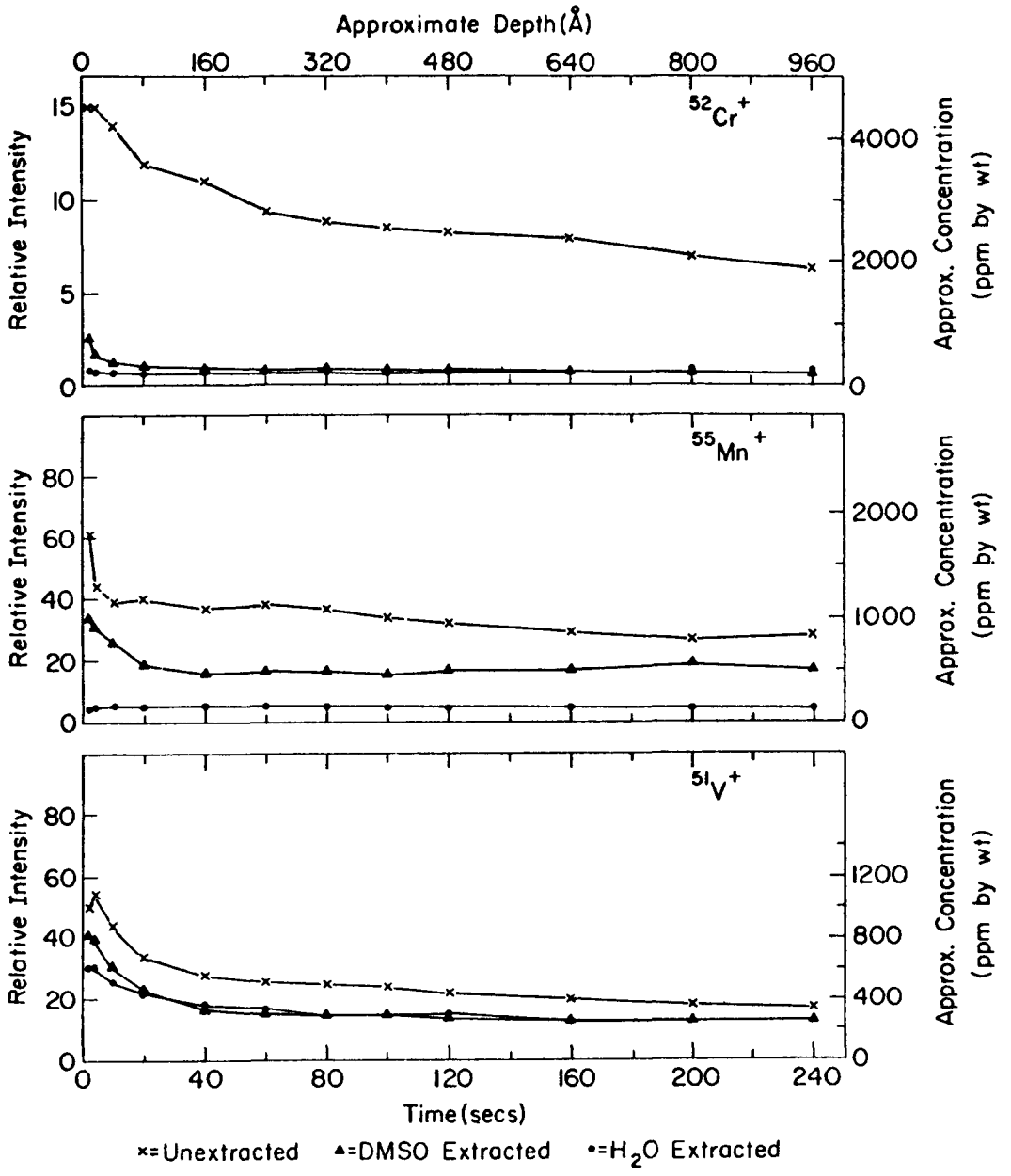

Figure 39. Ion microprobe depth profiles of the Group C elements (Cr, Mn, V) in unleached and leached fly ash. (Reprinted by permission of R. Linton and the American Chemical Society from Linton et al., 1977.)

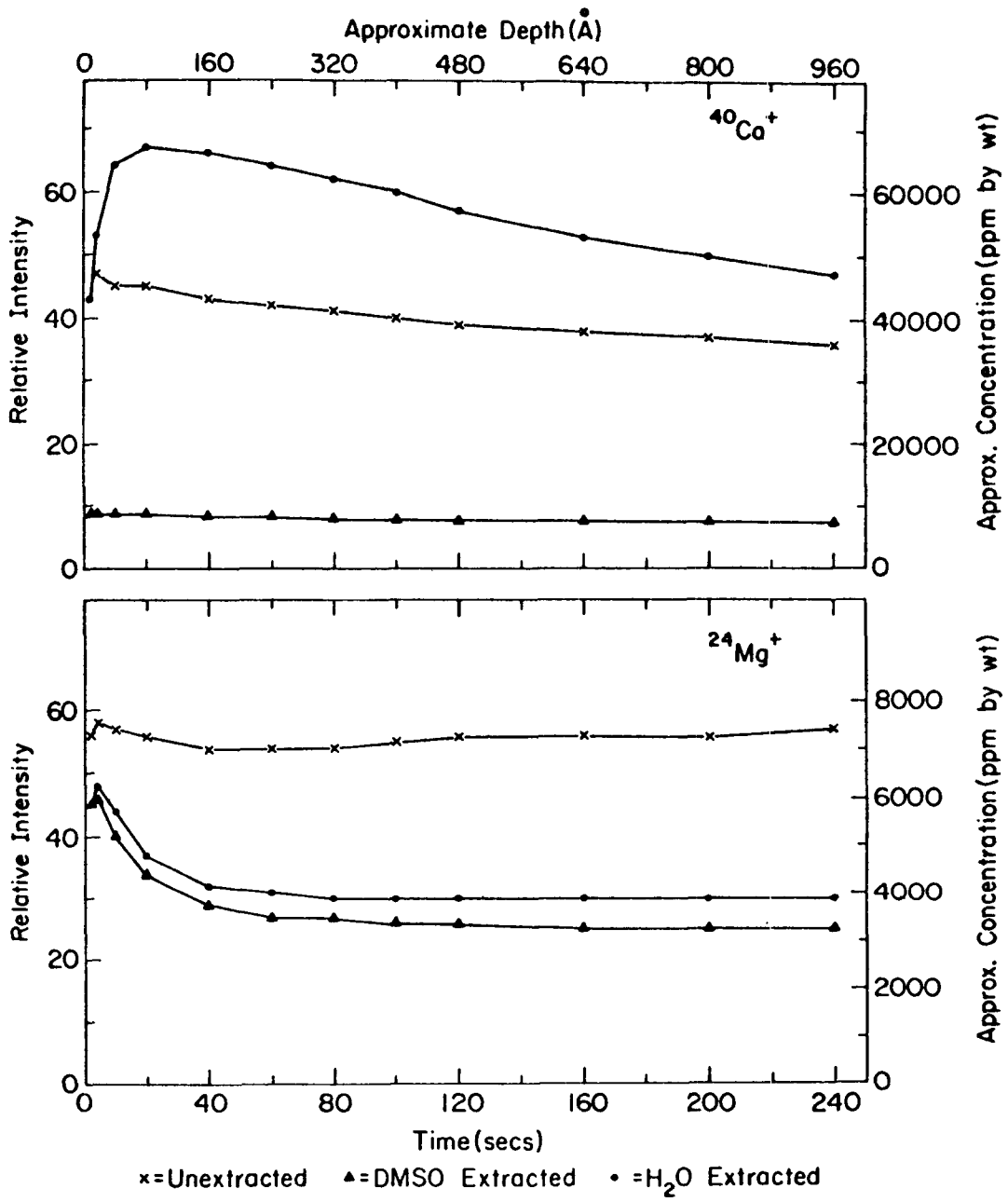

Figure 40. Ion microprobe depth profiles of the Group D elements (Ca, Mg) in unleached and leached fly ash. (Reprinted by permission of R. Linton and the American Chemical Society from Linton et al., 1977.)

Se, Cd, Hg, and Sb. The last elements were present at low bulk concentrations ranging from approximately 10 to 1000 ppm by weight. Secondary ion mass spectral interferences from species such as molecular ions, hydrocarbons, and isotopes of major elements were common in the fly ash mass spectra and generally required the use of high spectral resolution (Bakale, 1975; Williams and Evans, 1975), with an accompanying loss in sensitivity. The above eight elements were not of sufficient intensity to be characterized. Elemental identifications were made only when multi-isotopic species exhibited correct isotope ratios or when mono-isotopic species could be mass resolved from interferences and identified by mass difference measurements. Most of the elements listed above also have intrinsically poor detection limits, since they have relatively low positive secondary ion yields (Townsend et al., 1976).

Figures 35-40 indicate that the elements Fe, Na, Li, K, S, Pb, Tl, Mn, Cr, and V all show a surface predominance. However, it was necessary to obtain additional experimental confirmation that elemental surface predominance was not the consequence of analysis artifacts. This was accomplished by the use of the following: (1) complementary surface analytical techniques such as Auger Electron Spectrometry (to be discussed later) and (2) solvent leaching of the fly ash particles.

Semiquantitative values for bulk elemental leachabilities were obtained by ratioing the total mass of an element in a solution leachate to its total mass in the original fly ash sample as determined using spark source mass spectrometry (SSMS). Analytical precision for the solution or ash sample were about ±20%. The percent leached values (Table 15) were accurate to within about a factor of two of the true value. This can be attributed to the small variations in the sensitivity of the same element in different matrices (Ahearn, 1967). (That is, the sensitivity of an element in the leachate solution doped onto graphite differs somewhat from its sensitivity in the fly ash-graphite mixtures.)

High elemental leachability should, in part, reflect high surface accessibility. Results indicated that the extent of leachability (Table 15) did correlate with the extent of surface predominance (depth profiles of unextracted particles in Figs. 35-40). Specifically, the elements that the ion microprobe indicated were not surface predominant (e.g., Si, Mg, Ca, Ti) generally had the lowest leachabilities.

Of the instrumental methods used, the ion microprobe was the only one that detected trace-level elements, including Pb, Tl, Cr, Mn, and V. Solvent leaching was used to substantiate the surface predominance of these elements by comparison of their depth profiles before and after solvent leaching (Figs. 38 and 39). Normalized secondary ion intensities for a given element were reproducible to about a factor of two for different particles in either the leached or unleached samples. Following leaching, secondary ion intensities of Pb, Tl, Cr, and Mn near the surface were reduced by more than a factor of four (Figs. 38 and 39). Thus, the depletions in the surface region concentrations of these elements following leaching were indeed significant.

TABLE 15. ELEMENTAL CONCENTRATIONS IN COAL FLY ASH LEACHATES (DATA OF LINTON ET AL., 1977).

Element	Concentration (ppm by wt) in unleached particles	% Leached (wt%)	
		DMSO	H_2O
Ti	4,700	1.5	0.5
Al*	>6,600		
Si	120,000	0.1	0.3
Fe	92,000	0.7	5.8
S	7,100	27	36
K	39,000	0.2	6.0
Na*	>5,300	>5.2	
Li	200	17	14
Pb	620	3.4	0.4
Tl	30	25	11
Cr	380	2.4	4.5
Mn	310	7.1	35
V	380	1.5	3.9
Ca*	>12,000	>1.3	>5.8
Mg	12,000	0.6	2.7

* Could not be quantitated because of interferences, or analytical lines were too intense to fall within the working range for the internal standards.

The factor of two irreproducibility in the depth profiles was largely the result of variations in the chemical composition of individual particles. Because of this imprecision, solvent leaching cannot be considered to have a significant effect on the depth profiles of the other elements (Figs. 35-37). As was anticipated, depth profiles of elements (Al, Si, Ti, Ca, Mg) with negligible surface concentrations and only low to moderate leachability generally showed no significant change following leaching (Figs. 35 and 40). However, the highly leachable and surface-predominant elements (Na, K, Li, S, Fe) showed no significant reduction in peak secondary ion intensity after leaching (Figs. 36 and 37). There are several possible explanations for this. First, Na, K, Li, and S all diffuse to the surface during ion bombardment, accounting for at least some, if not most, of the surface predominance (Coburn, 1976; McCaughan and Kushner, 1974). Second, these elements (except for Li and S) are also present at high concentrations in less soluble forms as part of the bulk matrix composition of fly ash. Such high "interior" concentrations may obscure the effect of the surface leaching of Fe, K, and Na on the shape of depth profiles within the limits of reproducibility for different particles. These elements also may be present to some extent in soluble species near the particle surface. Thus, dissolution of such elements may be limited in part by solubility product considerations.

The results obtained by the ion microprobe and leaching studies were supplemented by the results of analyses using Auger Electron Spectrometry (AES). Depth resolutions are roughly comparable to those of the ion microprobe, and microfocusing of the primary electron beam permitted analysis of individual particles.

Because of basic limitations discussed in Appendix A, Auger electron spectrometry was used only to obtain qualitative elemental depth profiles of Al, Ca, Fe, K, Na, S, and Si contained in fly ash particles. For unleached particles, Auger depth profiles showed agreement with the ion microprobe results in that only K, Na, and S exhibited major surface enhancement. Examples of Auger elemental depth profiles are shown in Figure 41. The qualitative agreement between the Auger and ion microprobe data obtained using different surface sputtering conditions offers additional evidence that both techniques yield depth profiles that reflect the actual elemental composition of the surface region.

It is evident that the combination of solvent leaching with bulk multielemental analysis and with surface micro-analysis provides the information necessary to construct a composite picture of the physicochemical characteristics of the surface regions of fly ash particles. Based on the leachability and the extent of surface predominance, the elements studied can be categorized into four general groups (Table 16).

The Group A elements (Si and Al) are major constituents of the glassy fly ash particle matrix (Natusch et al., 1975). The refractory nature and low solubility expected for Al and Si coalesced as oxides in the fly ash matrix account for the lack of surface predominance and low leachabilities observed for these elements. Similar analytical results for Ti and its close association with complex silicates in the original coal (Ruch et al., 1974)

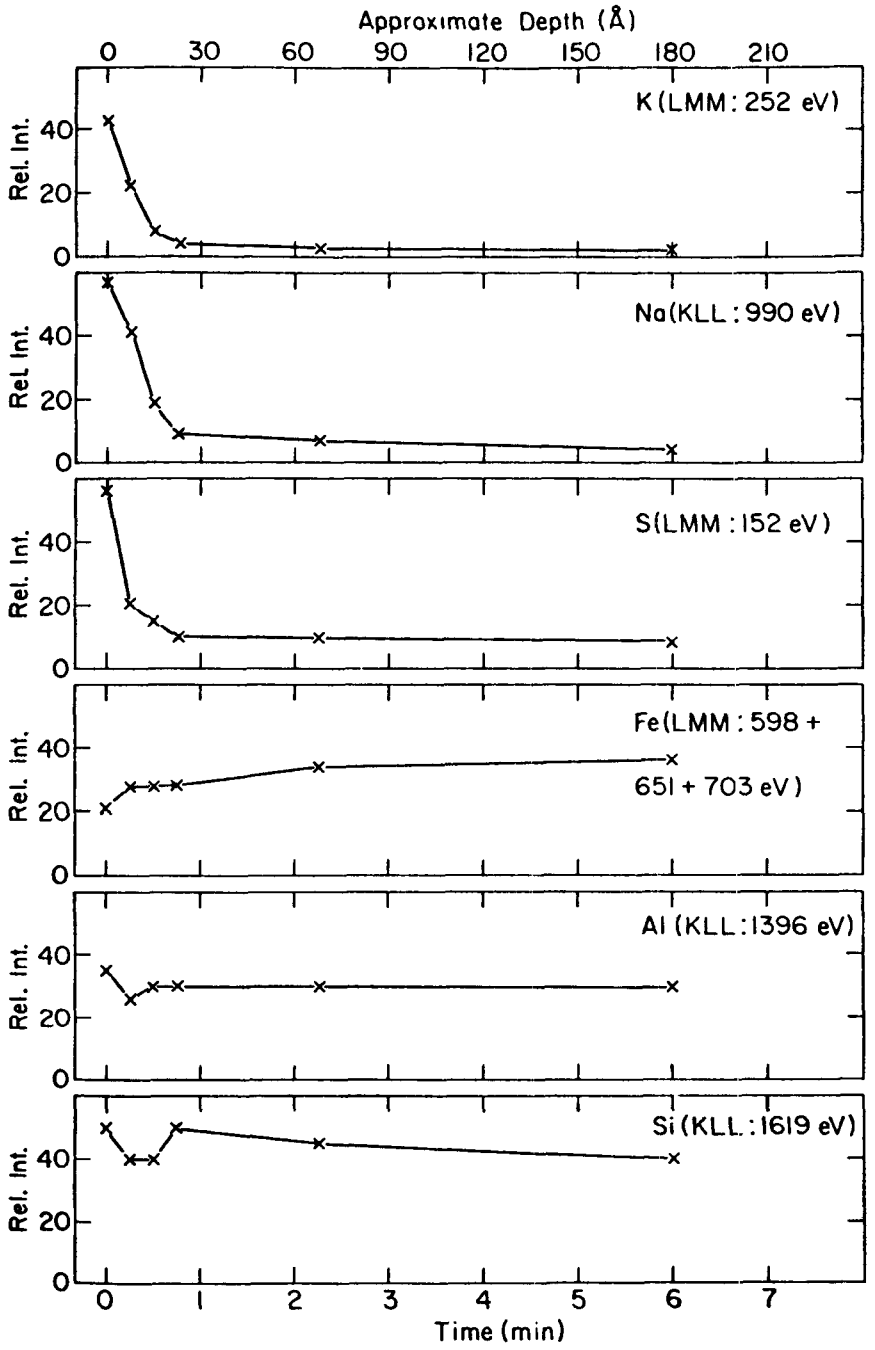

Figure 41. Auger Electron Spectrometry (AES) elemental depth profiles for unleached fly ash. (Reprinted by permission of R. Linton and the American Chemical Society from Linton et al., 1977.)

TABLE 16. SUMMARY OF ANALYTICAL RESULTS-SURFACE CHARACTERIZATION OF COAL FLY ASH

Group	Elements	Significant surface concentration observed?	Effect of leaching on concentrations in the immediate surface region	Leachability
A	Al, Ti, Si	No	Insignificant	Low
B	Fe, Na, Li K, S	Yes	Insignificant	Moderate to high
C	Pb, Tl, Mn Cr, V	Yes	Depletions observed following solvent leaching	Moderate to high Moderate to high
D	Mg, Ca	No	Generally not significant	Moderate

indicate that Ti is also incorporated as a minor component in the fused fly ash matrix.

The Group D elements (Ca, Mg) exhibit behavior similar to that of the Group A elements. The alkaline earths are often present largely as carbonates in coal and subsequently decompose to form oxides during combustion (Reid, 1971). The refractory nature of the alkaline earth oxides apparently explains their lack of surface predominance in fly ash. The oxides are potentially quite soluble, as are alkaline earth sulfates, which form by reaction with sulfur oxides in the flue gas (Ruch et al., 1974; Miguel, 1976; Fisher et al., 1976).

The surface predominance observed for the Group B and C elements (Table 16) apparently results from the volatilization of these species in the high-temperature combustion zone and their subsequent deposition on the surfaces of refractory particles as the temperature falls inside the stack (Linton et al., 1976; Davison et al., 1974). Most of these elements fall within either Group II (concentration dependent on particle size) or Group III (intermediate behavior, may or may not show a concentration dependence) as outlined in the section on trace elements. It should be noted, however, that the higher leachability of the Group B elements coupled with the relatively minor change in observed surface concentrations suggests that much of the leached material is not derived from the surface. The surface migration of Na, Li, K and S under ion bombardment may be responsible for the observed surface concentrations of these elements.

As has been discussed previously, certain trace metals, for example Hg and Se, are so volatile that a large percentage of their total emission from coal-burning power plants is in the vapor phase (Kaakinen et al., 1975; Klein et., 1975). Enrichments of elemental concentrations observed in fly ash relative to the residual slag or bottom ash are in excellent agreement with the results of the depth profiles. Specifically, elements which were not surface predominant (Groups A and D) have shown negligible concentration enhancements in fly ash relative to the slag (Klein et al., 1975). However, elements which exhibited significant surface predominance in this study (Groups B and C) also have been observed to show minor to major enrichments in fly ash relative to the slag (Klein et al., 1975). In summary, the results of the ion microprobe and AES depth profiles, the enrichment of elements in fly ash relative to the slag (Klein et al., 1975), and the inverse dependence of bulk elemental concentrations on particle size (Davison et al., 1974) strongly suggest that a volatilization-condensation process occurs for the Group B and C elements.

HEALTH EFFECTS

Possibly the greatest impact of high trace metal concentrations in smaller particles is in the area of health. This is the case since most of the small particle fractions' mass is concentrated in the size range 0.5 to 10.0 micrometers (μm) which is inhaled and deposited in the human respiratory system (Natusch and Wallace, 1974; Miller et al. 1979).

A number of workers (Morrow, 1964; Hatch and Gross, 1964; U.S. Dept. of H.E.W., 1969) have shown that inhaled airborne particles are deposited in different regions of the body depending on their aerodynamic size. From a toxicological standpoint, the smallest particles (less than 1 μm) which deposit in the pulmonary region of the respiratory tract are of greatest concern. This is because the efficiency of extraction of toxic species from particles deposited in the pulmonary region is high (60-80%) (Langham, 1960; Hatch and Gross, 1964; Patterson and Salvia, 1968; Dautreband, 1968; Schroeder, 1971), whereas the extraction efficiency from the larger particles which deposit in the nasopharyngeal and tracheo-bronchial regions and are removed to the pharynx by cilial action and swallowed is low (5-15%). Consequently, toxic species which predominate in submicrometer-sized particles will have their entry to the bloodstream enhanced over those which predominate in larger particles.

Potentially toxic elements including Pb, Tl, Cr, and Mn have been shown to have surface concentrations much higher than hitherto supposed on the basis of conventional bulk analytical data. For example, Pb and Tl were present at concentrations of only 620 and 30 ppm on the basis of bulk analysis (Table 16), but reached respective concentrations of 4% and 4500 ppm near the particle surfaces (Figure 35). In addition, the surface predominant region for such elements was highly leachable. The region of surface predominance is thus very likely to be accessible to the environment either by washout processes in the atmosphere or ground waters, or by solubilization in lung and digestive fluids of higher organisms.

PARTICULATE ASSOCIATED ORGANIC COMPOUNDS

Introduction

Particulate associated organic material emitted from fossil fueled power plants is known to contain both aliphatic and aromatic compounds (Committee on Biological Effects, 1972). To date, essentially all studies have been directed towards the latter class of compounds with special emphasis being given to polynuclear aromatic (PNA) species which include many well established carcinogens (Committee on Biological Effects, 1972; Searle, 1976). Even within this group, primary emphasis has been placed on hydrocarbons and little attention has been paid to heterocyclic compounds containing oxygen, nitrogen, or sulfur. Similarly, derivatives containing substituents such as carboxylic, nitro, sulfonic acid, or phenolic groups (if, indeed, they occur) have received little attention. At this time, only eighteen polycyclic organic compounds have been uniquely identified as being associated with fly ash emitted by fossil fuel power plants. These compounds are listed in Table 17 (Committee on Biological Effects, 1972; Hangebrauck et al., 1967). It should be noted that many more compounds have been tentatively identified but have not yet received full confirmation.

TABLE 17. POLYCYCLIC AROMATIC COMPOUNDS IDENTIFIED* IN EMITTED COAL FLY ASH

Fluorene¶	1-methylpyrene
Phenanthrene¶	Benzophenanthrene¶
Anthracene¶	Benzo[a]anthracene
9, 10-dimethylanthracene¶	Perylene
Fluoranthene¶	Benzo[a]pyrene¶
Triphenylene¶	Benzo[e]pyrene¶
Pyrene¶	Benzo[ghi]perylene
Chrysene¶	Anthanthrene
Benzofluorene	Coronene

* By gas chromatography or literature data (Committee on Biological Effects, 1972; Hangebrauck et al., 1967).

¶ Identity confirmed by GC/MS using reconstructed ion chromatograms.

A number of studies of particulate polycyclic organic matter (POM) emitted by fossil fuel power plants have concluded that total emissions are negligibly small compared with those from other sources (Committee on Biological Effects, 1972). A summary of reported emission factors for several coal combustion operations is presented in Table 18. These figures translate to a total annual emission of 500 tons of benzo[a]pyrene from all heat and power generating plants in the United States. The much higher emission factors associated with hand stoked furnaces are attributed to inefficient combustion. The latter observation is consistent with previous work (Diehl, et al., 1967) in which it was found that combustion conditions were of far more importance in determining POM emissions than was the source of fuel.

The detailed mechanism(s) of POM formation are not well understood; however, it is widely believed that POM is formed via a free radical mechanism (Badger, 1962). Formation occurs as the result of combustion of any carbonaceous material, is promoted by reducing conditions, and similar relative amounts of individual compounds are produced irrespective of the nature of the fuel (Committee on Biological Effects, 1972). Although the free radical mechanism suggests a vapor phase origin for POM there is a large body of data which attests to the fact that POM present in the atmosphere is almost invariably found in particulate form (Committee on Biologial Effects, 1972). It is apparent, therefore, that vapor-to-particle conversion takes place between the points of formation of POM in a combustion source and its determination in the atmosphere. It is the mechanism of this vapor-particle transformation and the subsequent oxidative transformation of particulate POM which constitute the subject of this section.

TABLE 18. POLYCYCLIC AROMATIC HYDROCARBON EMISSION FACTORS FOR COAL-FIRED FURNACES*

	POM emission factors (lb/ton coal × 10^4)		
Species	Pulverized firing	Chain grate stoker	Hand fired
Benzo[a]pyrene	0.2-0.52	0.3	3520
Pyrene	0.8-1.6	3.5	5260
Benzo[e]pyrene	0-2.1	1.1	880
Perylene	0-0.6	---	526
Fluoranthene	---	6.0	8800

* Committee on Biological Effects (1972) Data.

VAPOR-PARTICLE TRANSFORMATION

Introduction

A number of workers have reported the presence of vapor phase POM in combustion sources where elevated temperatures are encountered (U.S. Environmental Protection Agency, 1976a, 1976b, 1976c; Bertsch et al., 1974; Pupp et al., 1974; Hangebrauck, 1967). In other words, the saturation vapor pressure or dew point of POM must be attained for these processes to take place (Castellan, 1971). On the other hand, adsorption of POM vapor onto the surface of particulate material present in stack or exhaust gases can certainly take place and could account for the almost exclusive occurrence of particulate POM at ambient atmospheric temperatures. In order to investigate the possible operation of an adsorption mechanism we have conducted a study which involves theoretical modelling, field measurement, and laboratory simulation experiments. These are described briefly, together with the results, in the following sections.

Theoretical Model

The theoretical model is designed to consider the active adsorption of POM (primarily polynuclear aromatic hydrocarbons [PAH]) from the vapor phase onto the surface of particulate material (coal fly ash) as the two move down a nonuniform temperature gradient (the stack system). The treatment is, however, quite general and applies to any vapor species and any particulate adsorbant.

The basic assumption is that a given POM, P, present in the vapor phase, can adsorb onto the surface, S, of particulate material to provide an adsorbed entity, P·S, and that the reverse process can also take place. Thus,

$$P + S \underset{k_{-1}}{\overset{k_1}{\rightleftharpoons}} P \cdot S \qquad (10)$$

where k_1 and k_{-1} are the rate constants for adsorption and desorption, respectively. If one assumes, a priori, that k_1 and k_{-1} in Equation 10 represent first-order processes, then the rate of adsorption of P can be written

$$\frac{d[P \cdot S]}{dt} = k_1[P](1-\theta)A - k_{-1}[P \cdot S] \qquad (11)$$

In Equation 11, θ is the fraction of the total available adsorption sites which are occupied and A is the surface area of the particulate material.

The rate constant for desorption, k_{-1}, is given by

$$k_{-1} = \frac{kT}{h} \exp\left[-E_d/RT\right] \qquad (12)$$

where E_d is the activation energy for desorption, T is the absolute temperature, and k, h and R are Boltzmann's constant, Planck's constant, and the universal gas constant, respectively. The rate constant for adsorption, k_1, is

$$k_1 = c\left[\frac{RT}{2\pi M_a}\right]^{\frac{1}{2}} \exp\left[-E_a/RT\right] \qquad (13)$$

where c is the so-called "sticking coefficient" (the probability that the orientation of a molecule with the spherical particle surface will result in adsorption), M_a is the molecular weight of the adsorbate species, and E_a is the activation energy for adsorption. A number of assumptions are inherent in equations (12) and (13). These are presented briefly (Natusch and Tomkins, 1978) and discussed in detail in a forthcoming publication (Miguel, Schure, and Natusch, 1979).

In order to evaluate the rate and extent of adsorption as a function of temperature it is convenient to compute the mole fraction, X, of total POM adsorbed and the time ($t_{\frac{1}{2}}$) taken to achieve one half of the equilibrium adsorption at a given temperature. The equations used to evaluate the adsorption process are beyond the scope of this report; however, Figure 42 gives the temperature-dependent plots of X and T, assuming that the fractional surface coverage is dependent on temperature and the values of E_a and E_d (energy of desorption). The plots assume (1) that the adsorption process is zero order in its dependence on the fractional surface area, (2) that the available literature values for ρ and W_ρ, the density and mass per unit volume of the adsorbing particles, respectively, are reasonable, and (3) that d_m and d_s, the mass and surface median diameters of the particle size distribution, respectively, are also reasonable.

In the case of a log NORMAL distribution of particle sizes, d_m and d_s are related by

$$\ln d_s = \ln d_m - \ln^2\sigma \qquad (14)$$

where σ is the geometric standard deviation of the distribution (Butcher and Charlson, 1972).

Consideration of the data presented in Figure 42 shows that, over a wide range of conditions, POM present at combustion source temperatures (>150°C) is predicted to occur mainly in the vapor phase, whereas at the ambient temperatures following emission (<40°C), essentially quantitative adsorption is predicted. Variations from this general behavior are, however, different for individual compounds and different particle size distributions and mass loadings.

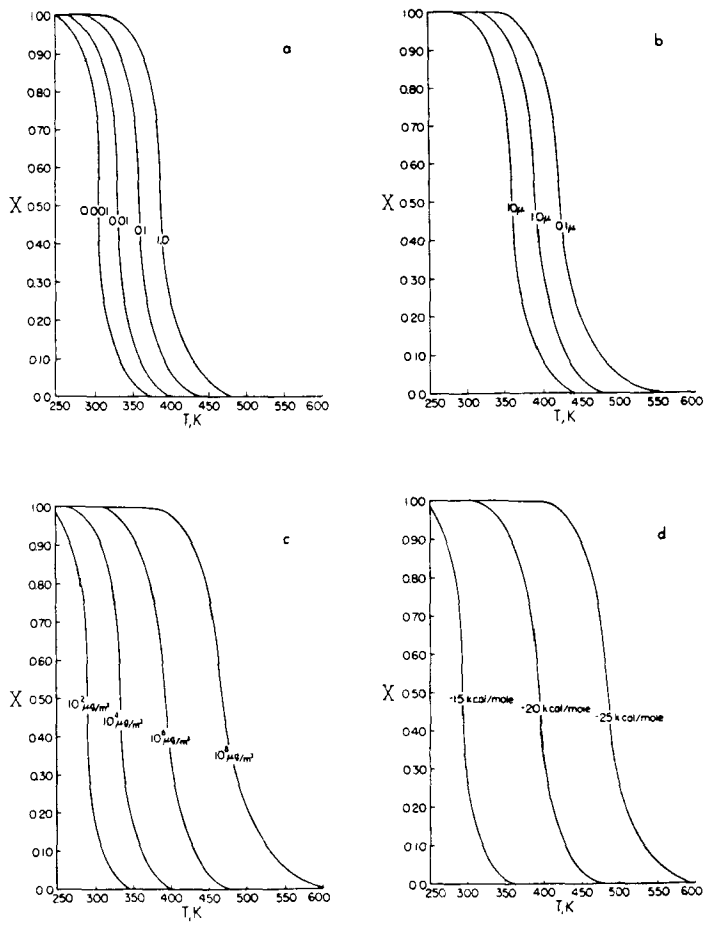

Figure 42. Dependence of mole fraction (X) of PAH adsorbed on temperature. (Reprinted by permission of D.F.S. Natusch and Raven Press from Natusch and Tomkins, 1978.)

Reference values: $c = 1$; $m_a = 3.360\ (10^{-22})$ g/molecule; $w_p = 10^6\ \mu g/m^3 = 10^{-6}\ g/cm^3$; $\rho = 3\ g/cm^3$; $d_m{}^3 d_s{}^2 = 10^{-4}$ cm; $E_a = -10$ kcal/mole; $E_d = -30$ kcal/mole; $\theta = \frac{1}{2}$.

(a) Variation of mole fraction of PAH adsorbed as a function of temperature and C = 0.001, 0.01, 0.1, 1.0.

(b) Variation of mole fraction of PAH adsorbed as a function of temperature and $d_m{}^3/d_s{}^2 = 0.1, 1.0, 10.0\ \mu m$.

(c) Variation of mole fraction of PAH adsorbed as a function of temperature and $w_p = 10^2, 10^4, 10^6, 10^8\ \mu g/m$.

(d) Variation of mole fraction of PAH adsorbed as a function of temperature and $E_a - E_d = -15, -20, -25$ kcal/mole; $E_a = -10$ kcal/mole.

The temperature dependencies shown in Figure 42 are generated with the assumption that adsorption equilibrium is achieved at all temperatures. This requires that the rate of attainment of equilibrium is fast compared with the rate of change of temperature experienced by a given vapor-particle combination. The rate of attainment of equilibrium is indicated in terms of the half-time for reaction in Figure 43. These data show that reaction times depend primarily on the activation energies of adsorption, E_a, and desorption, E_d, and that achievement of sub-second reaction times at both in-stack and ambient temperatures requires activation energy values to be at the lower end of the range investigated. Indeed, reduction of the activation energy for adsorption by only a few kcals results in achievement of equilibrium within a few seconds even at ambient temperatures.

While the foregoing brief discussion is far from rigorous or conclusive, it does validate the possibility of vapor-to-particle conversion of POM occurring via an adsorption mechanism. Further, it points out the very strong temperature dependence of such a process.

Field Measurements

In order to investigate the occurrence of vapor-to-particle conversion in a combustion source, measurements were made in the stack system and in the emitted plume of a small coal fired power plant. This plant was specially chosen because it was of obsolete design utilizing a chain grate stoker known to produce high POM emissions (Hangebrauck, et al., 1967); it possessed no particle control equipment, thereby facilitating collection of large amounts of particulate material; and it had a relatively short stack such that sample collection from the emitted plume was convenient.

Fly ash samples were collected during the same time periods both inside the stack (temp. ~290°C) and from the emitted plume (temp. ~5°C) using both cascade impaction and total collection on glass fiber filters. Collected material was extracted with benzene and analyzed for POM using gas chromatography (GC), gas chromatography/mass spectrometry (GC/MS), and fluorimetry. All necessary analytical precautions were taken and it was established by chemical and microscopic means that material collected from the plume was derived exclusively from the power plant.

The results of these analyses are presented in Table 19, which lists the individual compounds uniquely identified and provides a quantitative measure of the specific concentrations (μg/g) of several compounds associated with fly ash at the two sampling points. Preliminary identification was established using GC retention time data and in many cases was confirmed using either a single-ion mass chromatogram or a mass spectrum from a GC peak. Only crude vapor traps were employed during sample collection so no quantitative measure of vapor phase POM was obtained. Fluorescence measurements of condensation trap residues did, however, indicate that a considerable quantity of gaseous POM was present from in-stack sampling but none was in residues from plume sampling.

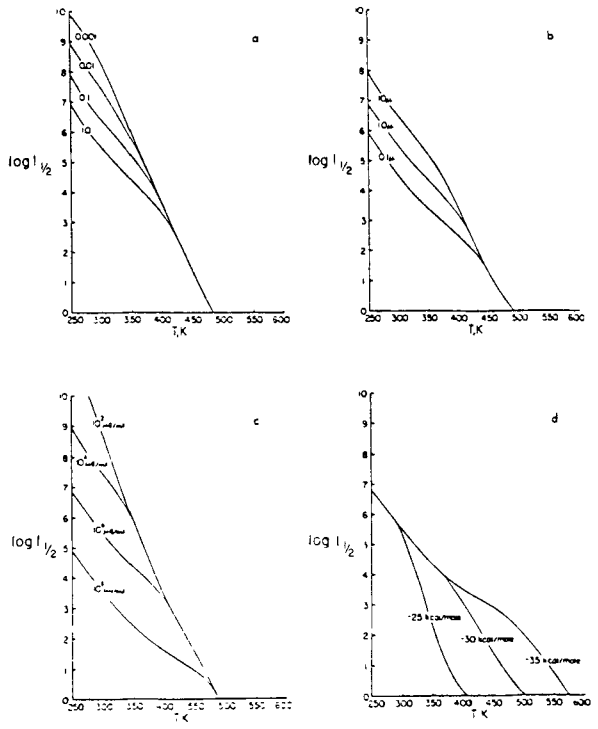

Figure 43. Dependence of half-time of adsorption on temperature. (Reprinted by permission of D.F.S. Natusch and Raven Press from Natusch and Tomkins, 1978.)

Reference values: $c = 1$; $m_a = 3.360\ (10^{-22})$ g/molec; $w_p = 10^6$ $\mu g/m^3 = 10^{-6}$ g/cm^3; $\rho = 3$ g/cm^3; $d_m{}^3/d_s{}^2 = 10^{-4}$ cm; $E_a = -10$ kcal/mole; $E_d = -30$ kcal/mole; $\theta = \frac{1}{2}$.

(a) Dependence of half-time for adsorption on temperature and $C = 0.001, 0.01, 0.1, 1.0$.

(b) Dependence of half-time for adsorption on temperature and $d_m{}^3/d_s{}^2 = 0.1, 1.0, 10.0$ μm.

(c) Dependence of half-time for adsorption on temperature and $w_p = 10^2, 10^4, 10^6, 10^8$ $\mu g/m^3$.

(d) Dependence of half-time for adsorption on temperature and $E_d = -25, -30, -35$ kcal/mole.

TABLE 19. MEASUREMENT OF POM EMITTED FROM A COAL-FIRED POWER PLANT STACK*

Compound	Inside stack (ng/g)	Outside stack (μg/g)
Fluorene	<1	0.5
Phenanthrene	<1	12
Fluoranthene	<1	17
Pyrene	<1	12
Benzofluorene	<1	2
1-methylpyrene	<1	0.6
Benzophenanthrene	<1	3
Benzo[a]pyrene	<1	5
Fluorescence/g total	3.6×10^{-3} units	370 units

* Data of Korfmacher et al. (1977).

These results establish quite firmly that, in this power plant, considerably more POM is associated with fly ash collected from the plume at a temperature of 5°C than with that collected from the same stream at a temperature of 190°C. This behavior is in exact accord with that predicted in Figure 42. Furthermore, since the two collection points were only ~100 ft. apart, quite rapid vapor-to-particle conversion is indicated. Unfortunately, while the full range of aerodynamic equivalent particle sizes accessible to Anderson-Stack and Hi Vol samplers was collected, this represented only a small range of specific surface area due to the considerable particle irregulatiry encountered. Nevertheless, correspondence between specific concentration of POM and specific surface area of fly ash fractions was noted. This further suggests the operation of a surface adsorption mechanism.

Laboratory Experiments

In an attempt to obtain direct measurements of the rate(s) and extent(s) of POM adsorption and to evaluate the quantities c, E_a, E_d (equations 12 and 13), a series of laboratory simulation experiments were set up. Fresh coal fly ash that had previously been shown to contain no detectable POM was fluidized in an expanded bed through which a stream of air containing pyrene

vapor was passed (Natusch and Miguel, 1975; Miguel et al., 1979). The objective was to expose all particles to the same constant concentration of pyrene for different times and to determine the specific concentrations of pyrene as a function of time at different temperatures.

The experiments showed that the uptake of pyrene was so rapid that a uniform vapor phase concentration could not be achieved. The amount of pyrene required to saturate the fly ash was, however, shown to increase significantly with decreasing temperature. Furthermore, attempts to remove adsorbed pyrene by heating in a stream of clean air were unsuccessful. (Miguel, 1976). While these experiments were essentially qualitative they do establish the facts that coal fly ash will strongly adsorb pyrene (and probably other POM) and that the saturation capacity is a strong inverse function of temperature.

Overall, therefore, the results of these studies point strongly towards the idea that POM, formed initially as vapor, is adsorbed onto co-entrained particulate material as the temperature falls, consistent with the curves in Figure 42. There is some doubt about the rate at which this process takes place, but the evidence is in favor of rapid (on the order of seconds) adsorption even at ambient temperatures, under most conditions encountered in or near combustion sources.

Ramifications of POM Transformation

The gas-to-particle transformation studies discussed above, while far from definitive, do point out several important considerations which should be borne in mind in assessing the environmental/health impact and methodology for the measurement and control of POM. These may be categorized as follows:

1. From the standpoint of the environmental and potential human health impact of POM, it is important to note that adsorption of vapor phase POM onto particulate matter should result in the predominance of POM on small particles, which provide the largest available surface area per unit mass. Thus, POM should be preferentially concentrated in particles whose aerodynamic size falls in the range which can remain airborne for several days and which is capable of being deposited in the pulmonary region of the human respiratory system when inhaled. (Davison et al., 1974; Natusch and Wallace, 1974). This prediction is in accord with the results of measurements of the atmospheric aerosol size distribution of POM (Natusch and Wallace, 1974).

2. If POM is capable of converting rapidly from vapor to particulate form, then the relative amounts of each would be expected to vary with the position (i.e. temperature and particle surface density) in a combustion system. Consequently, separate measurements of vapor and particulate POM concentrations will apply only to a specific point in a specific plant generated under specific conditions and cannot be extended to other power plants in general. Furthermore, the predictions of Figures 42 and 43 suggest that considerable vapor-to-particle conversion may actually occur within the sampling device--especially when it is maintained at a temperature that is different from that of the stream being

sampled. As a result, measurements of the particle size distribution of POM and of the particulate to vapor phase POM concentration ratio will not represent true quantities but will reflect sampling artifacts.

3. Of more practical importance, however, is the very clear need to collect both vapor and particulate POM in order to establish total POM emission factors. Current methodology for sampling emission sources does employ vapor collection devices; however, some doubt has been expressed concerning their collection efficiencies, (Jones et al., 1976) and it seems likely that present POM emission estimates may be low where measurements are made at elevated temperatures. Certainly emission estimates based on analyses of particulate material alone, when it is collected from within an emission source, are likely to be grossly in error (Natusch, 1978b).

4. The vapor-to-particle transformation behavior of POM has two important consequences in terms of emission control. First, the fraction of the total POM which is in the vapor phase during passage through particle control devices will not be collected. Secondly, the effect of adsorption is to move the aerodynamic equivalent mass median diameter of the adsorbed species to values which are significantly smaller than those of the substrate particle mass as described by equation (7) (Section V). Just as this enhances the ability of POM to penetrate the human respiratory system, it will also increase the difficulty of controlling POM emissions since small particles in the range of interest (0.1 to 5.0 μm aerodynamic diameter) are collected with reduced efficiency by most particle control devices (White, 1963).

5. One postive point which can be made is that collection of POM vapor by scrubbers may be quite efficient insofar as the low temperatures encountered in liquid systems may promote adsorption and at least partial collection of vapor species.

6. Finally, it is important to recognize that the processes descirbed herein, although presented in terms of a coal-fired power plant, should occur quite generally. They must, therefore, be taken into account when considering any combustion source.

Oxidative Transformation

Information about the fate of particulate PAH compounds released to the atmosphere is presently fragmentary and unclear. It is generally assumed, however, that photochemical oxidation processes play an important role (Committee on Biological Effects, 1972). There is ample evidence that most PAH's will undergo photo-oxidation in solution, as the pure solid, and when adsorbed onto certain solid substrates such as alumina (Committee on Biological Effects, 1972) and it has been inferred that similar processes take place when the compounds are adsorbed on airborne particulate material (Committee on Biological Effects, 1972; Falk et al., 1956; Mukai et al., 1968). Indeed, it has been suggested that the half-lives of such PAHs in the presence of sunlight may be "only hours or days" (Committee on Biological Effects, 1972). Contrary to this expectation, the present studies show that the rate and

extent of photodecomposition of PAHs may be decreased substantially by adsorption onto coal fly ash particles. Certain PAHs are, however, found to undergo rapid oxidation in the dark when adsorbed onto fly ash.

Studies were conducted using a model system in which individual PAHs were adsorbed onto the surface of fly ash collected from the electrostatic precipitators of several coal fired power plants. Known gas phase concentrations of individual PAHs were generated by a simple diffusion cell (Miguel, 1976; Miguel et al., 1979) and passed through an expanded bed of fly ash. Regulation of the bed temperature and the time of exposure provided a means of controlling the amount of a PAH adsorbed. All fly ash samples were size fractionated by sieving; the 44-74 μm physical size range was utilized. Exhaustive pre-extraction with several solvents (cyclohexane, benzene, methanol) showed that none of the fly ashes employed contained more than 50 mg/g of total PAH.

Sample irradiation was achieved using outdoor sunlight and several artificial light sources (150W Xenon arc lamp, 275W commercial sunlamp, 5-OT3/C1 General Electric "quartz line" lamps; all unfiltered). The fly ash was tumbled in a quartz container to provide equal exposure of all surfaces and radiant fluxes were estimated to be equal to or greater than that of midday summer sunlight (45°N lat.) over the wavelength range 300 to 800 nm. Portions of each fly ash sample were exhaustively extracted directly following exposure to gaseous PAH and then after irradiation or dark storage. Analyses for the original PAH and for degradation products were performed by high performance liquid chromatography (ultraviolet [UV] absorbance detection) and by UV absorption and fluorescence spectrometry. The extent of decomposition was determined both from the disappearance of the original PAH and from the appearance of its reaction products. (Reproducibility of multiple analyses was established to be ±8% relative standard deviation RSD). Experiments were conducted to determine the influence of PAH type and concentration, irradiation time, intensity, and wavelength distribution, dark stability, and the nature of the adsorbing substrate on the rate and extent of PAH decomposition.

Rather unexpectedly none of the PAHs irradiated following adsorption onto fly ash exhibited significant photodegradation (Table 20 and Figure 44). The data indicates (Figure 44) that the % change was not significantly different from zero at the 95% confidence level. Furthermore, no significant dependence on irradiation intensity nor amount of PAH adsorbed was observed. Under similar illumination conditions, however, extensive photodecomposition was observed for all PAHs irradiated in solution (Figure 44) and for both anthracene and benzo[a]pyrene adsorbed onto alumina from methanolic solution. Additional evidence for the apparent influence of adsorbent substrate on photodecomposition was obtained by adsorbing anthracene and benzo[a]pyrene vapors onto both fly ash and alumina, which were then coated on thin layer chromatographic plates and exposed to identical irradiation. In a typical experiment of this type benzo[a]pyrene present on the alumina surface underwent 50 per cent decomposition upon exposure for 80 minutes to an unfiltered 150W Xenon arc lamp. By contrast, only 15 per cent decomposition was observed for the benzo[a]pyrene adsorbed on fly ash and irradiated under identical conditions.

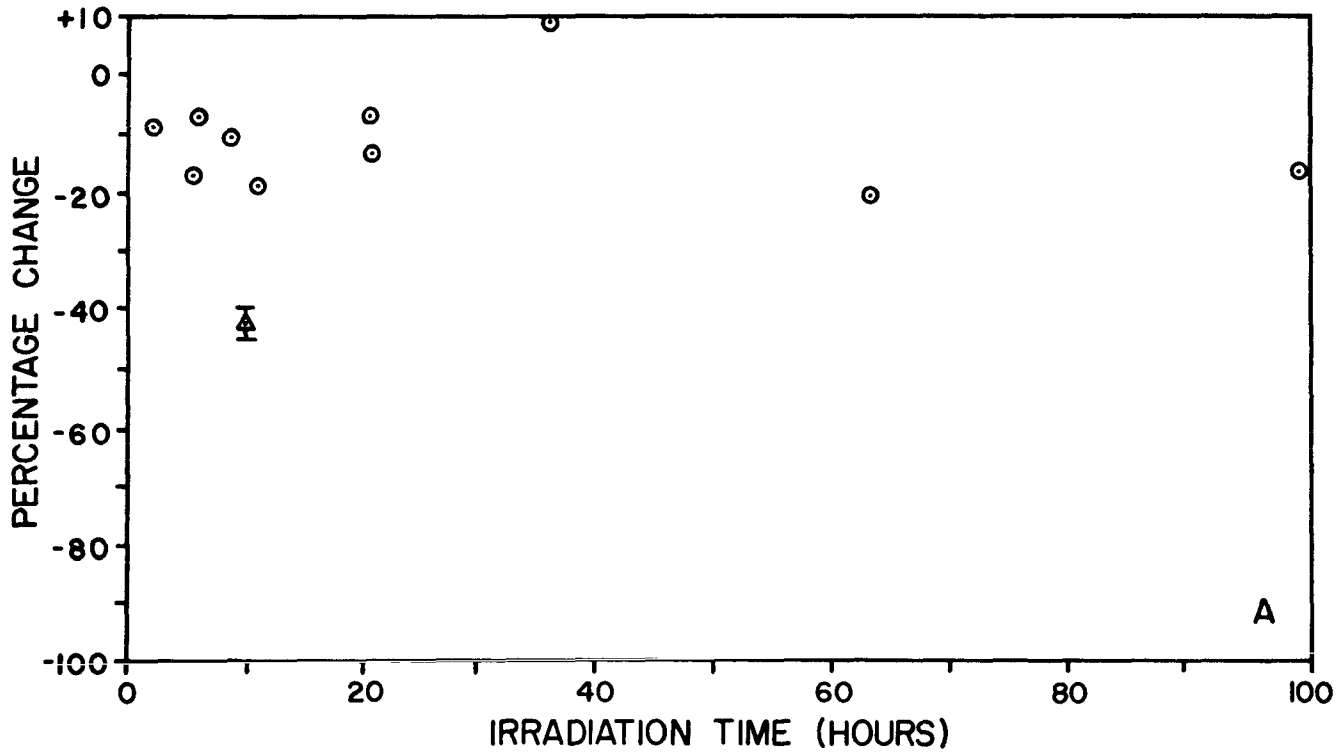

Figure 44. Percent conversion of irradiated benzo[a]pyrene compared to a non-irradiated sample as a function of time, o = adsorbed onto fly ash; Δ = solution. (Reprinted by permission of W. A. Korfmacher from Korfmacher, 1978.)

TABLE 20. DECOMPOSITION OF IRRADIATED POLYCYCLIC AROMATIC HYDROCARBONS ABSORBED ON COAL FLY ASH (KORFMACHER, 1978)

Compound	Irradiation time (hr)	Conc. PAH adsorbed (μg/g)	No. of Sampled	Average change (%)
Pyrene	5-126	67-291	19	-6.3 (±14.7)
Phenanthrene	2-113	129-186	5	+10 (±12.3)
Fluoranthene	2.5-18	49,115	2	-7.2 (±2.0)
Anthracene	3-24	300	3	-11 (±7.0)
Benzo[a]pyrene*	2.5-36.5	44-110	5	-8 (±8)
Benzo[a]pyrene¶	21-100	15-44	4	-14 (±7)

* Quartzline lamp.

¶ Xenon arc lamp.

While the extent of photodegradation of PAHs adsorbed on fly ash is apparently small, a number of the compounds studied (Table 21) were found to undergo quite extensive oxidation in the absence of light. In particular, different fly ashes were found to give different oxidation rates. In all cases, however, the major oxidation product was the same ketone or quinone as obtained from the photo-oxidation process. As illustrated in Figure 45 for fluorene, which oxidizes to 9-fluorenone, considerable conversion occurs during the actual PAH adsorption step but subsequent irradiation has no effect upon the rate or extent of further reaction. The extent of initial reaction, which occurs at the elevated adsorption temperature, varies from 7 to 90 percent decomposition depending on the type of fly ash used as the adsorbent substrate and was shown not to be due simply to passage of a PAH through the adsorption apparatus. It is apparent, therefore, that the nature of the adsorbent is an important factor in determining the rate of this dark reaction. This observation is borne out by the findings that nonphotochemical conversion does not occur for solid fluorene, for fluorene dissolved in methanol or cyclohexane, nor for fluorene adsorbed onto alumina, silica gel, Linde 13X molecular sieve, glass and Ambersorb XE-340 adsorbent resin. However, fluorene adsorbed onto activated carbon and graphite did decompose in a manner similar to that of fluorene adsorbed on coal fly ash.

Finally, it is noteworthy that all of the compounds that undergo spontaneous oxidation as a result of adsorption onto coal fly ash (Table 21)

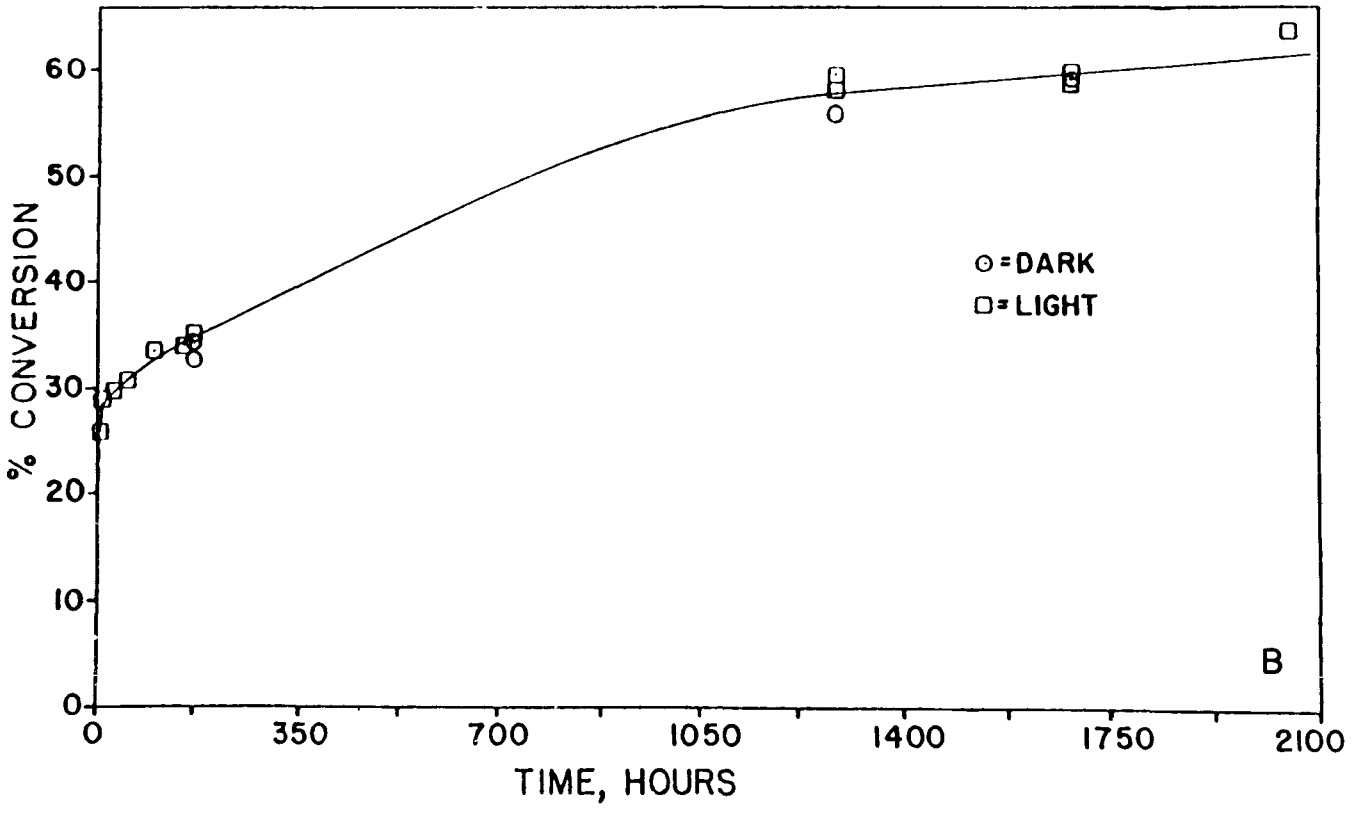

Figure 45. Percent conversion of fluorene adsorbed on coal fly ash as a function of time. (Reprinted by permission of W. A. Korfmacher from Korfmacher, 1978.)

TABLE 21. DECOMPOSITION OF NON-IRRADIATED POLYCYCLIC AROMATIC HYDROCARBONS ADSORBED ON COAL FLY ASH (KORFMACHER, 1978)

Compound	Change	Compound	Change
Acenaphtene	None	Fluorene	Decomposed
7,12-Dimethylbenz[a]anthracene	None	Benzo[b]fluorene	Decomposed
Carbazole	None	Benzo[a]fluorene	Decomposed
Acridine	None	9,10-Dimethylanthracene	Decomposed
Phenazine	None	9,10-Dihydroanthracene	Decomposed
Fluoranthene	None	4-Aza fluorene	Decomposed
Benzo[a]pyrene	None	Anthracene	Decomposed
Phenanthrene	None		

contain a benzylic carbon atom, indicating that this structure is especially susceptible to non-photochemical oxidative attack. Possible exceptions to this rule are afforded by anthracene and benzo[a]pyrene, which exhibit very slow non-photochemical oxidation when adsorbed onto fly ash.

It is apparent from the foregoing results that PAH adsorbed onto the surface of coal fly ash exhibits quite different chemical behavior from that of PAH adsorbed onto other solid substrates or present either as the pure solid or in solution. The net result is stabilization of PAH against photochemical oxidation, on the one hand, but promotion of spontaneous non-photochemical oxidation for a limited class of compounds, on the other. The reasons for this behavior are not clear. It is conceivable that the limited photochemical decompostion is the result of either efficient competive absorbence of radiation by the fly ash matrix (Wehry, 1971) or the PAH being largely present in pores, where light cannot penetrate. A more convincing suggestion, however, is that energetic adsorption, such as apparently occurs on fly ash, activated carbon, and graphite surfaces, effectively stabilizes PAHs against photo-oxidation, perhaps by molecular orbital rearrangment, which either increases the electronic excitation energy or decreases the lifetime of the excited state (Wehry, 1971). Any rapid photo-oxidation that did occur could then be due to a fraction of the PAH bonded not directly to the active surface but, rather, to another PAH molecule, or to a weakly adsorbing mineral impurity. The promotion of non-photochemical oxidation could, in turn, be due either to extensive molecular orbital rearrangement or simply to the ready availability of active oxygen on strongly adsorbing

surfaces (Lao et al., 1973). Not unexpectedly, the points of highest Bronsted acidity (e.g., position 9 in fluorene) are most susceptible to oxidative attack.

These findings are of considerable importance from an environmental standpoint because they show that:

1. The adsorption association of PAHs with coal fly ask stabilizes these compounds against photochemical degradation on the one hand, thereby preserving their potentially carcinogenic properties. On the other hand, however, a limited number of PAHs are quite rapidly converted to their corresponding ketones or quinones, whose toxic and carcinogenic potentials are largely unknown (Jones and Freudenthal, 1978; Searle, 1976). In this regard it is noteworthy that fluorenone is normally encountered at much higher levels in the atmosphere than is fluorene (Lao et al., 1973).

2. Based on the evidence presented here, one would not expect to find diurnal variations in the concentration of PAHs present in plumes emitted from coal-fired power plants. One would, however, expect to find significant differences between PAH transformation rates in plumes derived from different power plants because of the different surface characteristics of the fly ashes emitted.

3. If, in fact, all PAHs containing a benzylic carbon atom are susceptible to non-photochemical oxidation, as suggested here, then the probable oxidative behavior of a large number of PAHs can be predicted (Jones and Freudenthal, 1978; Korfmacher, 1978). For example, one would expect several strongly carcinogenic compounds such as dimethyl benz[a]anthracene and 3-methyl chloranthene (Committee on Biological Effects, 1972) to be rapidly oxidized and thus detoxified. Possible evidence for this prediction is afforded by the fact that neither of these compounds has been found in atmospheric particulate samples (Committee on Biological Effects, 1972; Lao et al., 1973).

In summary, then, the widespread belief that particulate association of PAHs will promote their photochemical conversion is not substantiated by experiment. Nevertheless, substantial non-photochemical conversion of PAHs adsorbed on coal fly ask can occur and may result in significant detoxication of several particulate PAHs.

Chemical Transformations

In addition to photochemical or non-photochemical oxidation, it is also possible for POM adsorbed onto particulate surfaces to react with other gases present in the atmosphere. Of special concern are those gases that often are present as the result of fossil fuel combustion or conversion processes, namely, NO, NO_2, SO_2, and SO_3. A report indicating that reactions between adsorbed POM and other atmospheric gases can produce compounds with increased or previously unobserved mutagenic activity (as indicated by the Ames test) has appeared in the literature (Pitts et al., 1978). In these studies, it was found that both benzo[a]pyrene (BaP) and perylene dispersed on glass

fiber filters reacted to form nitro derivatives when exposed to an atmosphere containing 1 ppm NO_2 and that the products were mutagenic (Pitts et al., 1978), even though one of the materials (perylene) did not previously exhibit such behavior.

We have studied the reactions of two PAHs adsorbed onto different substrates with a number of gases known to exist in the plumes of fossil fuel combustion and conversion sources in the laboratory and have found that both the gas and the particulate surface significantly affect the reactions observed.

Pyrene and benzo[a]pyrene (50-150 μg/g) were adsorbed onto the surfaces of several different particulate substrates (alumina, coal fly ash, and silica gel) using the same techniques that were previously described (Miguel, 1976; Miguel and Natusch, 1975; Miguel et al., 1979). Samples were then exposed to the individual gases NO, NO_2, SO_2, or SO_3 at room temperature for a period of 6 (NO) or 12 (NO_2, SO_2, SO_3) hours. Concentrations of approximately 100 ppm were used in all cases except that of SO_3, where precise quantification proved impossible because of experimental difficulties. Exposure was conducted both in the presence and in the absence of ultraviolet irradiation provided by a vitalite, quartzline lamp and natural daylight in order to observe whether the reactions might be photochemically induced. Following exposure the samples were Soxhlet extracted for 12 hours with benzene and the extract subjected to high-performance liquid chromatography using a Bondapak C18 reverse phase column and a water-methanol gradient elution program for the mobile phase. The chromatographic peaks were identified by high-resolution mass spectrometry following collection of fractions containing each separated compound. Electron Spectroscopy for Chemical Analysis (ESCA) was employed to examine particle surfaces both before and after exposure to the reactant gases.

In general, only two of the gases studied (NO_2 and SO_3) reacted with the two compounds used in this study. Neither NO nor SO_2 reacted significantly under the experimental conditions employed. None of the PAH-gas reactions was influenced by exposure to uv irradiation. Chromatograms of the extract resulting from the exposure of pyrene and benzo[a]pyrene (BaP) adsorbed on fly ash to NO_2 and SO_3 are shown in Figures 46 and 47, respectively, together with control chromatograms of extracted but unexposed material. Before gas exposure, only one major peak, the parent compound peak, A, is evident in both cases. Following exposure to NO_2, however, a second peak, labeled B in both figures, is observable. Mass spectrometric analyses indicate a mono-nitro derivative in both cases. The smaller peaks, labeled C-F in Figure 47, appear to be either a benzene impurity (peak C) or small amounts of oxidized BaP. Insufficient material was available to permit mass spectrometric identification of these smaller peaks.

The results of the PAH-SO_3 reactions were not as clear. Although several peaks (C-E in Figure 46 for pyrene and G-I in Figure 47 for benzo-[a]pyrene) were not present following SO_3 exposure, it was unclear whether these peaks were actually products of the reaction or were decomposition/oxidation products. It does appear that these substances are not simple substitution products analogous to the previously observed mono-nitro

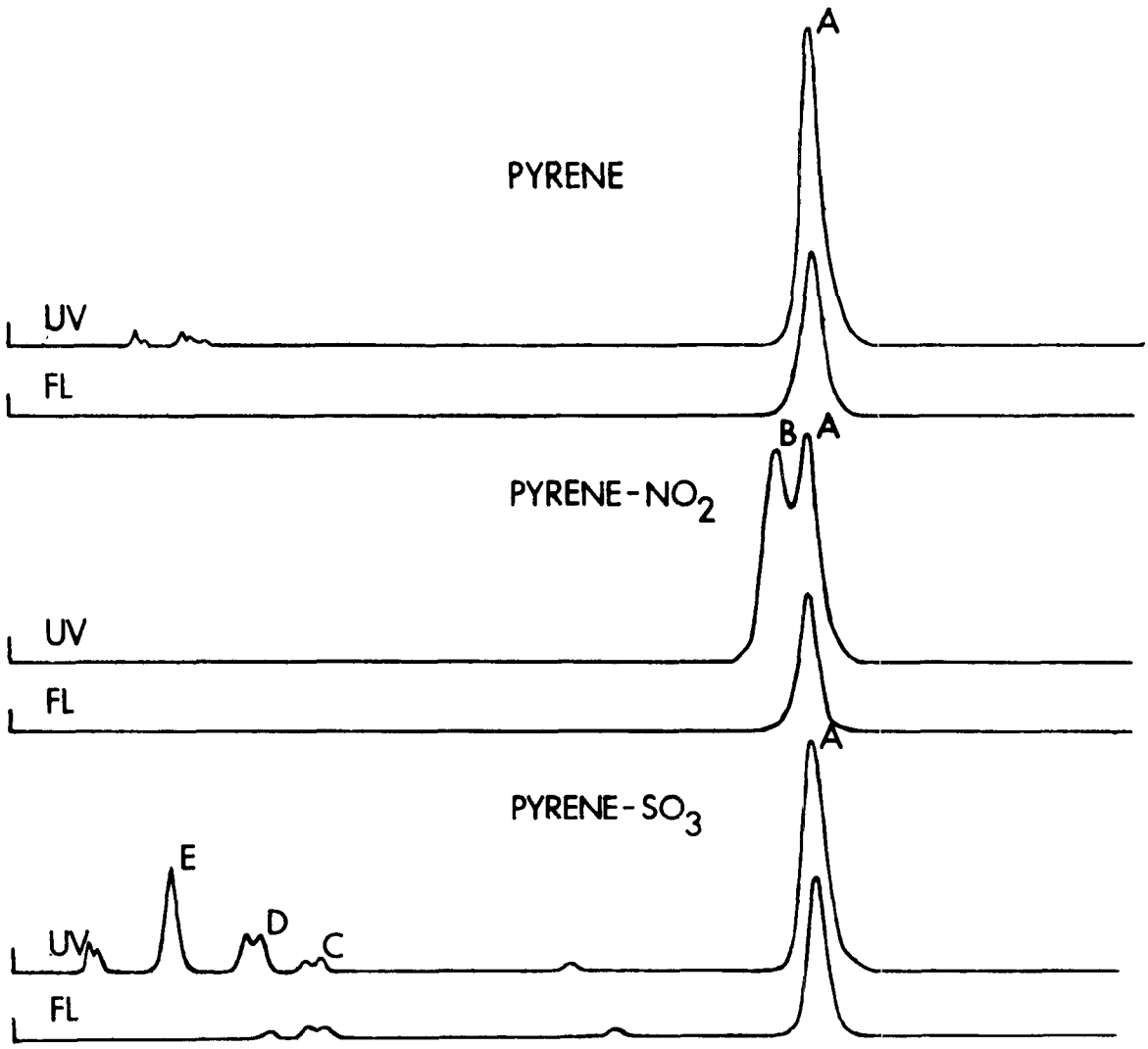

Figure 46. Chormatograms of extracts from pyrene adsorbed on coal fly ash before and after exposure to NO_2 and SO_3. Both uv and fluorescence traces are shown. For peak identification see text. (Reprinted by permission of D. F. S. Natusch.)

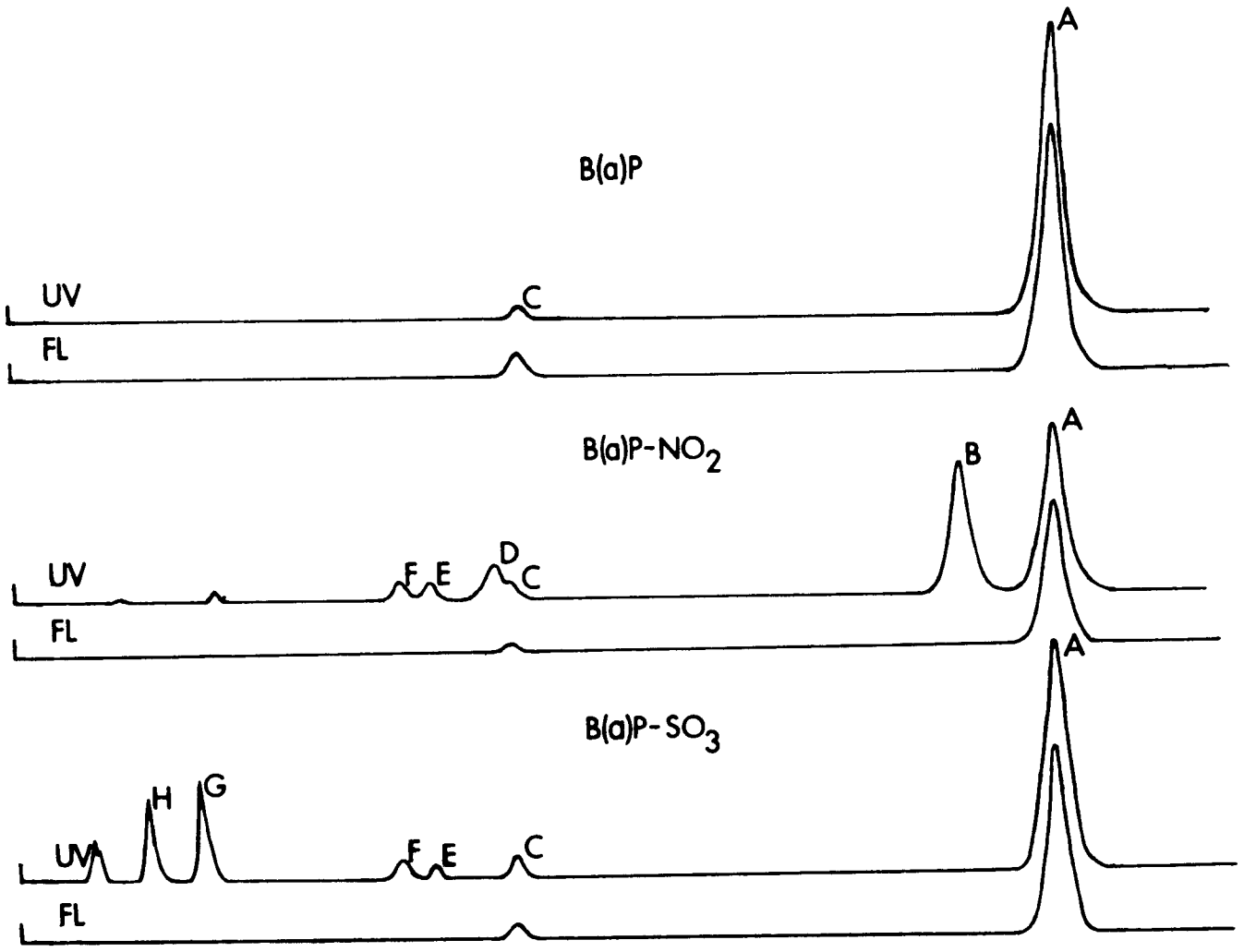

Figure 47. Chromatograms of extracts from benzo[a]pyrene adsorbed on coal fly ash before and after exposure to NO_2 and SO_3. Both uv and fluorescence traces are shown. For peak identification see text. (Reprinted by permission of D. F. S. Natusch.)

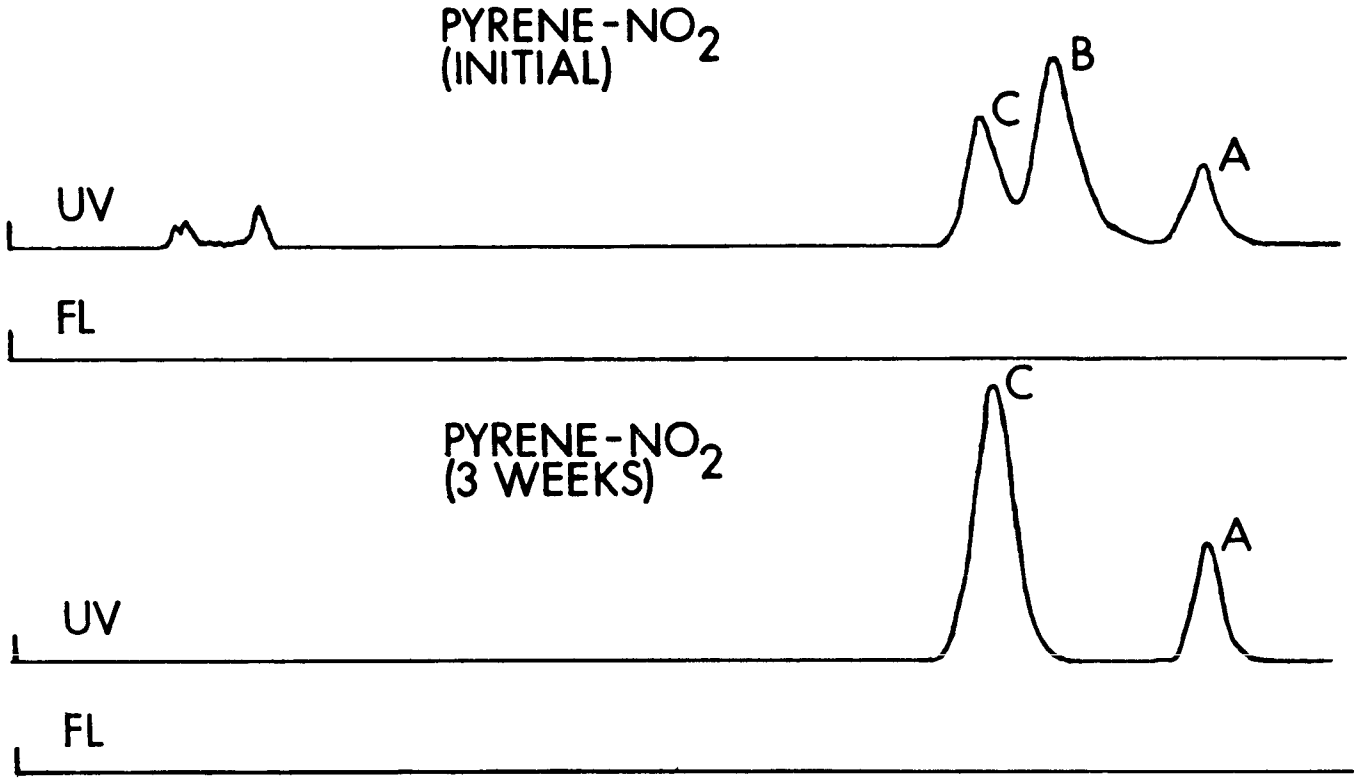

Figure 48. Chromatograms of extracts from pyrene adsorbed on silica gel exposed to NO_2, showing changes with aging. Both uv and fluorescence traces are shown. For peak identification see text. (Reprinted by permission of D. F. S. Natusch.)

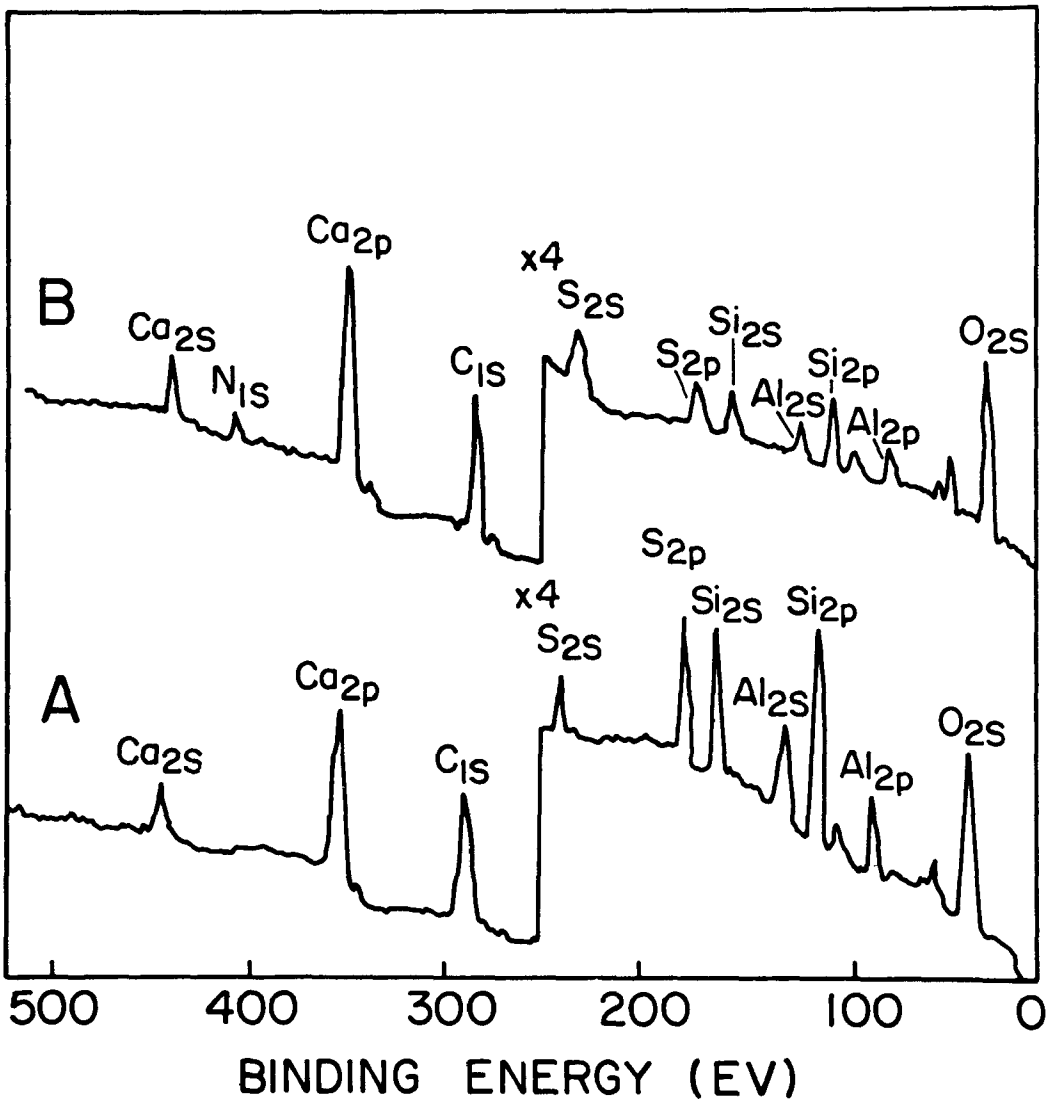

Figure 49. Low-resolution ESCA spectra of a (A) coal fly ash surface following pyrene adsorption and (B) the same coal fly ash surface following adsorption of pyrene and exposure to NO_2. (Reprinted by permission of D. F. S. Natusch.)

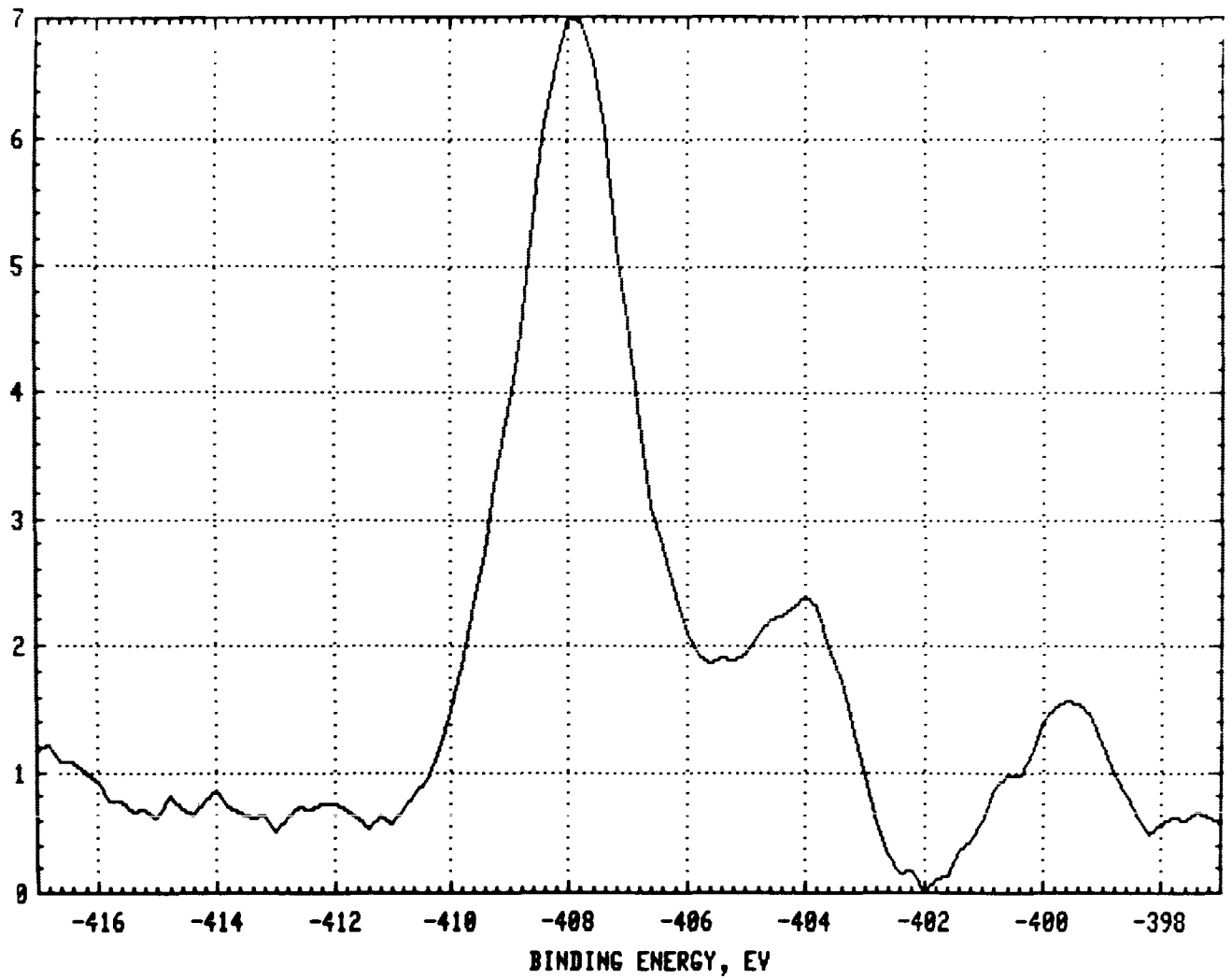

Figure 50. High-resolution ESCA spectrum of a coal fly ash surface following adsorption of pyrene and exposure to NO_2. (Reprinted by permission of D. F. S. Natusch.)

compounds. If reactions with SO_3 are occurring, it appears that the PAH itself must be decomposing.

The observed reactions appear to be highly surface dependent. Three different surfaces were investigated in this regard, viz. alumina, fly ash, and silica gel. Only the reactions of adsorbed pyrene and NO_2 were examined in these experiments. The results indicate that pyrene reacts similarly when adsorbed on alumina and fly ash but that the reactions on the silica gel surface are significantly different. Figure 48 shows the chromatogram of pyrene-silica gel extract obtained immediately after exposure to NO_2 and following aging for 3 weeks. Initially, three strong peaks are evident, none of which corresponds to pyrene. Peaks A and C have been identified as different dinitro pyrene products, and peak B appears to be the mono-nitro product previously observed in the fly ash and alumina systems. After 3 weeks, however, the mono-nitro pyrene has disappeared, but the two other products remain, and it appears that at least one of the dinitro products has increased by a comparable amount, suggesting that conversion, rather than decomposition, of the mono-nitro pyrene has occurred. Since the acidic surface of silica gel and existence of HNO_3 on the surface would be expected to promote nitration, it is probably that nitration is at least partly responsible for the reactions, as suggested by Pitts et al. (1978).

Further information concerning PAH-surface interactions were obtained from surface analytical studies using ESCA. A low-resolution scan of a fly ash surface after exposure to pyrene is shown in Figure 49A, and a scan following exposure of the same material to NO_2 is shown in Figure 49B. As can be seen in Figure 49, the principal difference between the two scans is the appearance of a nitrogen peak following NO_2 exposure. A high-resolution scan of the nitrogen region at liquid nitrogen temperature is presented in Figure 50. Three distinct regions are evident in this spectrum. The largest peak, at ~408 ev, corresponds to an inorganic nitrate (probably nitric acid), the peak at ~404 ev corresponds to that expected for an organic nitrate, and the peak at ~399 is probably that of a reduced nitrogen species, such as a nitrile, amino, or pyridino compound. Observation of the behavior of these three regions at both room temperature and 80°C shows a gradual depletion of the high binding energy nitrogen species and a slight increase in the reduced nitrogen species with increasing temperature.

These results suggest that nitric acid exists on the surface of the fly ash and are consistent with the idea that nitric acid is either a nitrating agent or a catalyst in these systems as in those studied by Pitts et al. (1978). No reduced nitrogen species were extracted or identified, but the formation of such species has been reported on soot by Chang and Novakov (1975). No useful information about PAH reaction products was obtained from examination of the high-resolution carbon and sulfur peaks.

The environmental implications of these results can be summarized as follows:

1. Particulate-associated PAH can undergo a variety of reactions when exposed to normal plume gases. Reactions appear to proceed most readily with NO_2 and SO_3, with NO and SO_2 being generally unreactive.

2. The extent of the reactions appears to be highly surface dependent. The nitration of PAH appears to be facilitated by the presence of inorganic nitrate on the surface.

3. The formation of new PAH species, at least in some instances, makes some PAHs carcinogenic where previously they displayed little such behavior. This increases the potential problem due to particulate-associated PAH.

SUMMARY

As this report has demonstrated, coal fly ash is a complex mixture of particles whose properties may vary considerably from source to source. However, there exist many similarities between these samples, and the report has attempted to stress them. Most important, it is the surface and the size of the fly ash that will be the primary factors in calculating the environmental impact. Thus, it is the smallest, most respirable particles that have the highest concentrations of inorganic and organic materials and that are most likely to present a health hazard. The accessibility of potentially toxic materials on or in coal fly ash to the environment and to man is not yet well understood but is an area that requires much future work.

REFERENCES

Ahearn, A. J. Spark Source Mass Spectrometric Analysis of Solids. In: Trace Characterization - Chemical and Physical, W. W. Meinke and B. F. Scribner, eds. Natl. Bur. Stand. (U.S.), Monogr. 100. 1967. pp. 347-376.

American Society for Testing Materials. X-ray Power Data File. 1970. 368 pp.

Ames, B. N., J. McCann, and E. Yamasaki. Methods for Detecting Carcinogens and Mutagens with the Salmonella/mammalian-microsome Mutagenicity Test. Mutat. Res., 31(6):347-363, 1975.

Anderson, C. A., H. J. Roden, and C. F. Robinson. Negative Ion Bombardment of Insulators to Alleviate Surface Charge-up. J. Appl. Phys., 40(8): 3419-3420, 1969.

Andren, A. W., D. H. Klein, and Y. Talmi. Selenium in Coal-Fired Steam Plant Emissions. Environ. Sci. Technol., 9(9):856-858, 1975.

Armstrong, J. T., and P. R. Buseck. Interaction between Natural and Anthropogenic Airborne Microparticles - An Electron Microprobe/SEM [Scanning Electron Microscope] Study. Abstracts of the First Chemical Congress of the North American Continent, Mexico City, Mexico, Nov. 30 - Dec. 5. Envir. Paper 48, 1975a.

Armstrong, J. T., and P. R. Buseck. Quantitative Chemical Analysis of Individual Micro Particles Using the Microprobe: Theoretical. Anal. Chem., 47:2178-2192, 1975b.

Badger, G. M. Mode of Formation of Carcinogens in Human Environment. In: Analysis of Carcinogenic Air Pollutants, E. Sawicki and K. Cassel, Jr., eds. Nat. Cancer Inst. Monogr. 9. U.S. Dept. of Health, Education and Welfare. 1962. pp. 1-16.

Bakale, D. K., B. N. Colby, and C. A. Evans, Jr. High Mass Resolution Ion Microprobe Mass Spectrometry of Complex Matrices. Anal. Chem., 47: 1532-1537, 1975.

Bertsch, W., R. C. Chang, and A. Zlatkis. The Determination of Organic Volatiles in Air Pollution Studies: Characterization of Profiles. J. Chromatogr. Sci., 12(4):175-182, 1974.

Bickelhaupt, R. E. Electrical Volume Conduction in Fly Ash. J. Air Poll. Control Assoc., 24:251-255, 1974.

Bickelhaupt, R. E. Surface Resistivity and the Chemical Composition of Fly Ash. J. Air Poll. Control Assoc., 25(2):150-152, 1975a.

Bickelhaupt, R. E. Volume Resistivity - Fly Ash Composition Relationship. Environ. Sci. Technol., 9(4):336-342, 1975b.

Block, C., and R. Dams. Study of Fly Ash Emissions During Combustion of Coal. Environ. Sci. Technol., 10:1011-1017, 1976.

Bolton, N. E., R. I. Van Hook, W. Fulkerson, W. S. Lyon, A. W. Andren, J. A. Carter, and J. F. Emery. Trace Element Measurements at the Coal-fired Allen Steam Plant. Progress Report June 1971 to January 1973, Oak Ridge National Laboratory, Oak Ridge, Tennessee, 1973.

Brecher, G., M. Schneiderman, and G. Z. Williams. Evaluation of Electronic Red Blood Cell Counter. Am. J. Clinical Pathology, 26:1439-1449, 1956. Chem. Abstr. 52:4943i.

Brimblecombe, P., and D. J. Spedding. The Dissolution of Iron from Ferric Oxide and Pulverized Fuel Ash. Atmos. Environ., 9:835-838, 1975.

Brindley, G. W., and M. J. Nakahira. The Kinetics of Dehydroxylation of Daolinite and Halloysite. J. Am. Ceram. Soc., 40:346-350, 1957.

Brown, J., N. J. Ray, and M. Ball. The Disposal of Pulverized Fuel Ash in Water Supply Catchment Area. Water Research, 10:1115-1121, 1976.

Bull, H. I., M. H. Hall, and W. E. Garner. Reaction Between Carbon and Oxygen at Low Pressures and Room Temperature. J. Chem. Soc., 837-847, 1931.

Butcher, S. S., and R. J. Charlson. An Introduction to Air Chemistry. Academic Press, New York, 1972. 241 pp.

Cabrera, J. G., and M. N. Gray. Specific Surface Pozzolanic Activity, and Composition of Pulverised-fuel Ash. Fuel, 52(3):213-219, 1973.

Cambell, J. A., J. C. Laul, K. K. Nielson, and R. D. Smith. Separation and Chemical Characterization of Finely Sized Fly-ash Particles. Anal. Chem., 50:1032-1040, 1978.

Cambell, J. A., R. D. Smith, L. E. Davis, and K. L. Smith. Characterization of Micron-size Fly Ash Particles by X-ray Photoelectron Spectroscopy (ESCA). Sci. Tot. Environ., 12(1):75-85, 1979.

Castellan, G. W. Physical Chemistry, Second Edition. Addison-Wesley Publishing Co., Reading, Mass., 1971. 866 pp.

Chang, C. C. Analytical Auger Electron Spectroscopy. In: Characterization of Solid Surfaces, P. F. Kane and G. B. Larrabee, eds. Plenum Press, New York, New York, 1974. pp. 509-575.

Chrisp, C. E., G. L. Fisher, and J. E. Lammert. Mutagenicity of Filtrates from Respirable Coal Fly Ash. Science, 199(4324):73-75, 1978.

Coburn, J. W. Sputtering in the Surface Analysis of Solids: A Discussion of Some Problems. J. Vac. Sci. Technol., 13(5):1037-1044, 1976.

Coles, D. G., R. C. Ragaini, J. M. Ondov, G. L. Fisher, D. Silberman, and B. A. Prentice. Chemical Studies of Stack Fly Ash from a Coal-fired Power Plant. Environ. Sci. Technol., 13:455-459, 1979.

Colovos, G., G. S. Wilson, and J. L. Moyers. Particle Size Determination of Trace Elements in Urban Air. Int. J. Environ. Anal. Chem., 3(3):239-252, 1974.

Committee on Biologic Effects of Atmospheric Pollutants: Particulate Polycyclic Organic Matter. National Academy of Sciences, Washington, D.C., 1972. 361 pp.

Corey, R. C., B. J. Cross, and W. T. Reid. External Corrosion of Furnace Wall Tubes - II. Significance of Sulphate Deposits and Sulphur Trioxide in Corrosion Mechanism. Trans. Am. Soc. Mech. Eng., 67: 289-302, 1945.

Cox, J. A., G. L. Lundquist, A. Przyjazny, and C. D. Schmulbach. Leaching of Boron from Coal Ash. Environ. Sci. Technol., 12:722-723, 1978.

Craig, N. L., A. B. Harker, and T. Novakov. Determination of the Chemical States of Sulfur in Ambient Pollution Aerosols by X-ray Photoelectron Spectroscopy. Atmos. Environ., 8(1):15-21, 1974.

Dalmon, J., and E. Raask. Resistivity of Particulate Coal Minerals. J. Inst. Fuel., 45(374):201-205, 1972.

Dalmon, J., and D. Tidy. Comparison of Chemical Additives as Aids to the Electrostatic Precipitation of Fly Ash. Atmos. Environ., 6:721-734, 1972.

Dautreband, L. Microaerosols. Academic Press, New York, 1962. 360 pp.

Davison, R. L., D. F. S. Natusch, J. R. Wallace, and C. A. Evans, Jr. Trace Metals in Fly Ash: Dependence of Concentration on Particle Size. Environ. Sci. Technol., 8:1107-1113, 1974.

Diehl, E. K., F. du Breuil, and R. A. Glenn. Polynuclear Hydrocarbon Emission from Coal-fired Installations. Trans. Am. Soc. Mech. Eng. J. Eng. for Power, 89:276-282, 1967.

Ditl, P., and R. W. Coughlin. Improving Efficiency of Electrostatic Precipitation by Physicochemical Modification of the Electrical Resistivity of Fly Ash. J. Am. Inst. Chem. Eng., 22(4):730-746, 1976.

Dreesen, D. R., E. S. Gladney, J. W. Owens, B. L. Perkins, C. L. Wienke, and L. E. Wangen. Comparison of Levels of Trace Elements Extracted from Fly Ash and Levels Found in Effluent Waters from a Coal-Fired Power Plant. Environ. Sci. Technol., 11:1017-1019, 1977.

Eggett, J. M., and T. M. Thorpe. Mobilization of Chromium from Fly Ash Particulates by Aqueous Systems Modeling Natural Waters. J. Environ. Sci. Health, A13(4):295-313, 1978.

Evans, C. A., Jr. Secondary Ion Mass Analysis: A Technique for Three-dimensional Characterization. Anal. Chem., 44(13):67A-80A, 1972.

Evans, C. A., Jr. Surface and Thin Film Compositional Analysis: Description and Comparison of Techniques. Anal. Chem., 47:818A-829A, 1975.

Falk, H. L., I. Markul, and P. Kotin. Aromatic Hydrocarbons. IV. Their Fate Following Emission into the Atmosphere and Experimental Exposure to Washed Air and Synthetic Fog. Am. Med. Assoc. Arch. Ind. Health, 13:13-17, 1956.

Farrar, H., IV. Relating the Mass Spectrum to the Solid Sample Composition. In: Trace Analysis by Mass Spectrometry, A. J. Ahearn, ed. Academic Press, New York, 1972. pp. 239-95.

Fisher, G. L. Personal Communication. Radiobiology Laboratory, University of California, Davis, California, 1978.

Fisher, G. L., D. P. Y. Chang, and M. Brummer. Fly Ash Collected from Electrostatic Precipitators: Microcrystalline Structures and the Mystery of the Spheres. Science, 192:553-555, 1976.

Fisher, G. L., B. A. Prentice, D. Silberman, J. M. Ondov, A. H. Biermann, R. C. Ragaini, and A. R. McFarland. Physical and Morphological Studies of Size Classified Coal Fly Ash. Environ. Sci. Technol., 12:447-451, 1978.

Fisher, G. L., D. Silberman, R. E. Heft, and J. M. Ondov. Filtration Studies with Neutron-activated Coal Fly Ash. Environ. Sci. Technol., 13:689-693, 1979.

Flesch, J. P., C. H. Norris, and A. E. Nugent, Jr. Calibrating Particulate Air Samplers with Monodisperse Aerosols: Application to the Anderson Cascade Impactor. Am. Ind. Hyg. Assoc. J., 28:507-516, 1967.

Gladney, E. S., G. E. Gordon, and W. H. Zoller. Abnormally Enriched Trace Elements in the Atmosphere. Seventh Annual Conference on Trace Substances in Environmental Health, University of Missouri, Columbia, Missouri, June, 1973.

Gladney, E. S., J. A. Small, G. E. Gordon, and W. H. Zoller. Composition and Size Distribution of a In-stack Particulate Material at a Coal-fired Power Plant. Atmos. Environ., 10:1071-1077, 1976.

Gladney, E. S., W. H. Zoller, A. G. Jones, and G. E. Gordon. Composition and Size Distribution of Atmospheric Particulate Matter in Boston Area. Environ. Sci. Technol., 8(6):551-557, 1974.

Gluskoter, H. J. Clay Minerals in Illinois Coals. J. Sed. Pet., 37:205-214, 1967.

Gooch, J. P., and S. Oglesby. A Theoretically Based Technique for Estimating the Size of Electrostatic Precipitators. Southern Research Institute Report to the Environmental Protection Agency, October, 1974. pp. 84-88.

Gordon, G. E. Study of the Emissions from Major Air Pollution Sources and their Atmospheric Interactions, First Year Progress Report, Nov. 1, 1972 to Oct. 31, 1973. University of Maryland, College Park, Maryland, 1973.

Gordon, G. E. Atmospheric Impact of Major Sources and Consumers of Energy. NSF-RANN Progress Report October 1974 to August 1975, University of Maryland, College Park, Maryland, 1975.

Gordon, G. E., and W. H. Zoller. Normalizations and Interpretation of Atmospheric Trace-element Concentration Patterns. Oak Ridge Trace Elements Conference, Oak Ridge, Tennessee, 1973.

Hangebrauck, R. P., D. J. Von Lehmden, and J. E. Meeker. Sources of Polynuclear Hydrocarbons in the Atmosphere. Public Health Service Publication 999-AP-33, U. S. Dept. of Health, Education and Welfare, 1967. 44 pp.

Hatch, T. F., and P. Gross. Pulmonary Deposition and Retention of Inhaled Aerosols. Academic Press, New York, 1964. 192 pp.

Heindrycks, R., and R. Dams. Continental, Marine, and Anthropogenic Contribution to the Inorganic Composition of the Aerosol of an Industrial Zone. J. Radioanal. Chem., 19(2):339-349, 1974.

Hodgeman, C. D. (ed.). Handbook of Chemistry and Physics, 44th Edition. The Chemical Rubber Publishing Co., Cleveland, Ohio, 1963. pp. 24-29.

Hopke, P. K. Chemistry Progress Report. Laboratory for Nuclear Science, Massachusetts Institute of Technology, Cambridge, Massachusetts, 1969.

Hulett, L. D. Personal Communication, 1973.

Hulett, L. D. Progress Report. Oak Ridge National Laboratories, Oak Ridge, Tennessee, 1973.

Hulett, L. D., and A. J. Weinberger. Some Etching Studies of the Microstructure and Composition of Large Aluminosilicate Particles in Fly Ash from Coal Burning Power Plants. Environ. Sci. Technol., Submitted, 1979.

James, W. D., M. Janghorbani, and T. Baxter. Leachability of Neutron Irradiated Fly Ash. Anal. Chem., 49:1994-1997, 1977.

Jones, H. R. Fine Dust and Particulates Removal. Pollution Control Review, No. 11. Noyes Data Corp., Park Ridge, New Jersey, 1972.

Jones, P. W., and R. I. Freudenthal (eds.). Carcinogenesis--A Comprehensive Survey, Vol. 3. Raven Press, New York, 1978. 512 pp.

Jones, P. W., R. D. Giammar, P. E. Strup, and T. B. Stanford. Efficient Collection of Polycyclic Organic Compounds from Combustion Effluents. Environ. Sci. Technol., 10(8):806-810, 1976.

Judikis, H. S., and S. Siegel. Particle-catalyzed Oxidation of Atmospheric Pollutants. Atmos. Environ., 7(6):619-631, 1973.

Kaakinen, J. W., R. M. Jorden, J. H. Lawasani, and R. E. West. Trace Element Behavior in Coal Fired Power Plants. Environ. Sci. Technol., 9:862-869, 1975.

Karolinska Institute. Proceedings of General Air Pollution and Human Health with Special Reference to Long-Term Effects Meeting, Stockholm, March 1977. Environ. Health Perspectives, 22:1-12, 1978.

Keyser, T. R., D. F. S. Natusch, C. A. Evans, Jr., and R. W. Linton. Characterizing the Surfaces of Environmental Particles. Environ. Sci. Technol., 12(7):768-773, 1978.

Klein, D. H., A. W. Andren, J. A. Carter, J. F. Emergy, C. Feldman, W. Fulkerson, W. S. Lyon, J. C. Ogle, Y. Talmi, R. I. Van Hook, and N. Bolton. Pathways of Thirty-seven Trace Elements Through Coal-fired Power Plant. Environ. Sci. Technol., 9:973-979, 1975.

Korfmacher, W. A. The Decomposition of Polycyclic Organic Matter Adsorbed on Coal Fly Ash. Ph.D. Thesis, University of Illinois, Urbana, Illinois, 1978. 272 pp.

Kotrappa, P., and M. E. Light. Design and Performance of the Lovelace Aerosol Particle Separator. Rev. Sci. Instrum., 43(8):1106-1112, 1972.

Krauskopf, K. B. Thermodynamics of Geochemistry, Chapter 3, In: Handbook of Geochemistry, Vol. I, K. H. Wedepehl, ed. Springer-Verlag, New York, 1972. pp. 37-76.

Kropp, L. I., I. N. Shmigol, G. S. Chekanov, S. Oglesby, Jr., and R. E. Bickelhaupt. J. Air Poll. Control Assoc., 29(6):665-669, 1979.

Lamb, R. E. The Chemical Characterization of Airborne Particles. Ph.D. Thesis, University of Illinois, Urbana, Illinois, 1975. 168 pp.

Langham, W. W. Radioisotope Absorption and Methods of Elimination: Relative Significance of Portals of Entry. In: Symposium on Radioisotopes in the Biosphere, R. S. Caldecott and L. A. Synder, eds. University of Minnesota Press, Minneapolis, Minnesota, 1960. pp. 489-513.

Lao, R. C., R. S. Thomas, H. Oja, and L. Debois. Application of a Gas Chromatograph - Mass Spectrometer-Data Processor Combination to the Analysis of the Polycyclic Aromatic Hydrocarbon Content of Airborne Pollutants. Anal. Chem., 45(6):908-915, 1973.

Lee, R. E., Jr., H. L. Crist, A. E. Riley, and K. E. MacLeod. Concentration and Size of Trace Metal Emissions from a Power Plant, a Steel Plant, and a Cotton Gin. Environ. Sci. Technol., 9:643-647, 1975.

Lee, R. E., Jr., S. S. Goransen, R. E. Enrione, and G. B. Morgan. National Air Surveillance Cascade Impactor Network. II. Size Distribution Measurements of Trace Metal Components. Environ. Sci. Technol., 6:1025-1030, 1972.

Lee, R. E., Jr., and D. J. Von Lehmden. Trace Metal Pollution in the Environment. J. Air Poll. Control Assoc., 23(10):853-857, 1973.

Linton, R. W., A. Loh, D. F. S. Natusch, C. A. Evans, Jr., and P. Williams. Surface Predominance of Trace Elements in Airborne Particles. Science, 191:852-854, 1976.

Linton, R. W., P. Williams, C. A. Evans, Jr., and D. F. S. Natusch. Unpublished Results, 1976.

Linton, R. W., P. Williams, C. A. Evans, Jr., and D. F. S. Natusch. Determination of the Surface Predominance of Toxic Elements in Airborne Particles by Ion Microprobe Mass Spectrometry and Auger Electron Spectrometry. Anal. Chem., 49:1514-1520, 1977.

Littlejohn, R. F., and J. D. Watt. The Distribution of Mineral Matter in Pulverized Fuel. In: The Mechanism of Corrosion by Fuel Impurities, H. R. Johnson and D. J. Littler, eds. Butterworths, London, 1963. pp. 102-112.

Lofroth, G. Mutagenicity Assay of Combustion Emissions. Chemosphere, 7(10):791-798, 1978.

Loh, A. Some Environmental Applications of Analytical Microscopy. Ph.D. Thesis, University of Illinois, Urbana, Illinois, 1975. 257 pp.

Lovering, J. F. Application of SIMS Microanalysis Techniques to Trace Element and Isotopic Studies in Geochemistry and Cosmochemistry. In: Secondary Ion Mass Spectrometry, K. F. J. Heinrich and D. E. Newburg, eds. Natl. Bur. Stand. (U.S.), Spec. Publ. 427, 1975. pp. 135-178.

Maney, J. P., J. L. Fasching, and P. K. Hopke. A Versitile and Comprehensive Analysis Code for Automated Reduction of Gamma Ray Spectral Data. Computers and Chemistry, 1:257-264, 1977.

Mason, B. Principles of Geochemistry, Third Edition. Wiley, New York, 1966. pp. 55-59. 329 pp.

Matthews, B. J., and R. F. Kemp. Development of Laser Instrumentation for Particle Measurement. TRW Report No. 14103-6003-R0-00, 1971.

Matusiewicz, H., and D. F. S. Natusch. To be submitted for publication.

McCaughan, D. V., and R. A. Kushner. Impurity-Movement Problems in Analysis Methods Using Particle Bombardment. In: Characterization of Solid Surfaces, P. R. Kane and G. B. Larrabee, eds. Plenum Press, New York, 1974. pp. 627-640.

McFarland, A. R., R. W. Bertch, G. L. Fisher, and B. A. Prentice. A Fractionator for Size-classification of Aerosolized Solid Particulate Matter. Environ. Sci. Technol., 11:781-784, 1977.

McHugh, J. A. Factors that Influence an Elemental Depth Concentration Profile. In: Secondary Ion Mass Spectrometry, K. F. J. Henrich and D. E. Newburg, eds. Natl. Bur. Stand. (U.S.), Spec. Publ. 427, 1975. pp. 179-189.

Miguel, A. H. Studies of Gas Solid Reactions of Environmental Significance: I. Pyrene Adsorption onto Fly Ash; II. Thiol Oxidation and Adsorption by Activated Charcoal. Ph.D. Thesis, University of Illinois, Urbana, Illinois, 1976. 136 pp.

Miguel, A. H., W. A. Korfmacher, E. L. Wehry, G. Mamantov, and D. F. S. Natusch. Apparatus for Vapor-phase Adsorption of Polycyclic Organic Matter onto Particulate Surfaces. Environ. Sci. Technol., 13(10): 1229-1232, 1979.

Miguel, A. H., M. R. Schure, and D. F. S. Natusch. Adsorption of Vapor Phase Polycyclic Organic Matter onto Fly Ash. Submitted to Anal. Chem., 1979.

Miller, F. J., D. E. Gardner, J. A. Graham, R. E. Lee, Jr., W. E. Wilson, and J. D. Bachman. Size Considerations for Establishing a Standard for Inhalable Particles. J. Air Poll. Control Assoc., 29(6):610-615, 1979.

Morabito, J. M. A Comparison of Auger Electron Spectoscopy (AES) and Secondary Ion Mass Spectrometry (SIMS). In: Secondary Ion Mass Spectrometry, K. F. J. Henrich and D. E. Newberg, eds. National Bur. Stand. (U.S.), Spec. Publ. 427, 1975. pp. 191-224.

Morey, G. W. The Properties of Glass, Second Edition. Reinhold, New York, 1954. 591 pp.

Morrow, P. E. Evaluation of Inhalation Hazards Based on the Respirable Dust Concept and the Philosophy and Application of Selective Sampling. Amer. Ind. Hyg. Assoc. J., 25:213-236, 1964.

Mukai, M., J. F. Thomas, and B. D. Tebbens. Fate of Airborne Benzo[a]pyrene. Environ. Sci. Technol., 2(1):33-39, 1968.

Muller, R. O. Spectrochemical Analysis by X-ray Fluorescence. Plenum Press, New York, 1972. pp. 72-86. 326 pp.

Natusch, D. F. S. Characterization of Fly Ash from Coal Combustion. Workshop Proceedings on Primary Sulfate Emissions from Combustion Sources, US EPA 600/9-78-020b, Vol. 2, 1978a. pp. 149-163.

Natusch, D. F. S. Potentially Carcinogenic Species Emitted from Fossil Fueled Power Plants. Environ. Health Perspectives, 22:79-90, 1978b.

Natusch, D. F. S., C. F. Bauer, H. Matusiewicz, C. A. Evans, J. Baker, A. Loh, R. W. Linton, and P. K. Hopke. Characterization of Trace Elements in Fly Ash. Proceedings of the International Conference on Heavy Metals in the Environment, Toronto, Vol. II, Part 2, 1975. pp. 535-575.

Natusch, D, F. S., and H. Matusiewicz. Unpublished results, 1976.

Natusch, D. F. S., and A. H. Miguel. A Diffusion Cell for the Preparation of Dilute Vapor Concentrations. Anal. Chem., 47:1705-1707, 1975.

Natusch, D. F. S., and M. R. Schure. Manuscript in preparation, 1979.

Natusch, D. F. S., and B. A. Tomkins. Theorectical Considerations of the Adsorption of PAH Vapor onto Fly Ash in a Coal Fired Power Plant. In: Carcinogenesis - A Comprehensive Survey, Vol. 3, Polynuclear Aromatic Hydrocarbons, P. W. Jones and R. I. Freudenthal, eds. Raven Press, New York, 1978. pp. 145-153.

Natusch, D. F. S., and J. R. Wallace. Urban Aerosol Toxicity: The Influence of Particle Size. Science, 186:695-699, 1974.

Natusch, D. F. S., J. R. Wallace, and C. A. Evans, Jr. Toxic Trace Elements: Preferential Concentration in Respirable Particles. Science, 183: 202-204, 1974.

Nelson, W., and C. Cain, Jr. Corrosion of Superheaters and Reheaters of Pulverised-Coal-Fired Boilers. Trans. Am. Soc. Mech. Eng. J. Eng. for Power, 82:194-204, 1960.

Nicholls, G. D. The Geochemistry of Coal Bearing Strata. In: Coal and Coal Bearing Strata, D. Merchison and P. Westoll, eds. American Elsevier, New York, 1968. pp. 269-307.

Novakov, T., S. G. Chang, and A. B. Harker. Sulfates as Pollution Particulates: Catalytic Formation on Carbon (Soot) Particles. Science 186: 259-261, 1974.

O'Gorman, J. V., and P. L. Walker, Jr. Mineral Matter Characteristics of some American Coals. Fuel, 50:135-151, 1971.

Olson, K. W., and R. K. Skogerboe. Identification of Soil Lead Compounds from Automotive Sources. Environ. Sci. Technol., 9:227-230, 1975.

Ondov, J. M., R. C. Ragaini, and A. H. Biermann. Comparison of Particulate Emissions from a Wet Scrubber and Electrostatic Precipitator at a Coal-fired Power Plant. Presented at American Chemical Society Meeting, Div. of Environmental Chemistry, San Francisco, August 29 - September 3, 1976.

Ondov, J. M., R. C. Ragaini, and A. H. Biermann. Elemental Emissions from a Coal-fired Power Plant. Comparison of a Venturi Wet Scrubber System with a Cold-side Electrostatic Precipitator. Environ. Sci. Technol., 13:598-606, 1979.

Ondov, J. M., R. C. Ragaini, R. E. Heft, G. L. Fisher, D. Silberman, and B. A. Prentice. Interlaboratory Comparison of Neutron Activation and Atomic Absorption Analyses of Size-classified Stack Fly Ash. Natl. Bur. of Stand. (U.S.) Special Publication 464. Proceedings of 9th IMR Symposium, Gaithersburg, Maryland, September 20-24, 1976, 1977.

Ondov, J. M., W. H. Zoller, I. Olmez, N. K. Aras, G. E. Gordon, L. A. Rancitelli, K. H. Able, R. H. Filby, K. R. Shah, and R. C. Ragaini. Elemental Concentrations in the National Bureau of Standards Environmental Coal and Fly Ash Standard Reference Materials. Anal. Chem., 47(7): 1102-1109, 1975.

Owens, E. B., and N. A. Giardino. Quantitative Mass Spectrometry of Solids. Anal. Chem., 35:1172-1178, 1963.

Patterson, C. C., and J. D. Salvia. Lead in the Modern Environment. How Much is Natural. Sci. and Citizen, 10:66-79, 1968.

Peuschel, R. F., C. C. Van Valin, and F. P. Parungo. Effect of Air Pollutants on Cloud Nucleation. Geophys., Res. Lett., 1(1):51-54, 1974.

Phung, H. T., L. J. Lund, A. L. Page, and G. R. Bradford. Trace Elements in Fly Ash and their Release in Water and Treated Soils. J. Environ. Qual., 8(2):171-175, 1979.

Pillay, K. K. S., and C. C. Thomas, Jr. Determination of the Trace Element Levels in Atmospheric Pollutants by Neutron Activation Analysis. J. Radioanal. Chem., 7(1):107-118, 1971.

Pitts, J. N., Jr., K. A. Van Cauwenberghe, D. Grosjean, J. P. Schmid, D. R. Fitz, W. L. Belser, Jr., G. B. Knudson, and P. M. Hynds. Atmospheric Reactions of Polycyclic Aromatic Hydrocarbons: Facile Formation of Mutagenic Nitro Derivatives. Science, 202:515-519, 1978.

Price, N. B., and G. R. Angell. Determination of Minor Elements in Rocks by Thin Film X-ray Fluorescence Techniques. Anal. Chem., 40(3): 660-663, 1968.

Pringle, W. J. S., and E. Bradburn. Mineral Matter in Coal. (II) Composition of the Carbonate Minerals. Fuel, 37:166-180, 1958.

Pupp, C., R. C. Lao, J. J. Murray, and R. F. Pottie. Equilibrium Vapour Concentrations of some Polycyclic Aromatic Hydrocarbons, As_4O_6 and SeO_2 and the Collection Efficiencies of these Air Pollutants. Atmos. Environ., 8(9):915-925, 1974.

Raabe, O. G. Aerosol Aerodynamic Size Conventions for Inertial Sampler Calibration. J. Air. Poll. Control Assoc., 26(9):856-860, 1976.

Raask, E. Cenospheres in Pulverized-fuel Ash. J. Inst. Fuel, 41:339-344, 1968.

Rahn, K. A., R. Dams, J. A. Robbins, and J. W. Winchester. Diurnal Variations of Aerosol Trace Element Concentrations as Determined by Nondestructive Neutron Activation Analyses. Atmos. Environ., 5:413-422, 1971.

Ranz, W. E., and J. B. Wong. Jet Impactors for Determining the Particle Size Distributions of Aerosols. Ind. Hyg. Occup. Med., 5:464-477, 1952.

Rao, C. P., and H. J. Gluskoter. Occurrence and Distribution of Minerals in Illinois Coals. Illinois State Geological Survey Circular No. 476, 1973. 56 pp.

Reid, W. T. External Corrosion and Deposits: Boilers and Gas Turbines. Elsevier, New York, 1971. 199 pp.

Ruch, R. R., H. J. Gluskoter, and N. F. Shimp. Occurrence and Distribution of Potentially Volatile Trace Elements in Coal. Illinois State Geological Survey Report No. 72, 1974.

Sarofim, A. F., J. B. Howard, and A. S. Padia. Physical Transformation of the Mineral Matter in Pulverized Coal Under Simulated Combustion Conditions. Combust. Sci. Technol., 16:187-204, 1977.

Schmidt, F. J., and J. L. Royer. Submicrogram Determination of Arsenic, Selenium, Antimony, and Bismuth by Atomic Absorption Utilizing Sodium Borohydride Reduction. Anal. Letters, 6(1):17-23, 1973.

Schroeder, H. A. Metals in the Environment. Environment, 13(8):18-32, 1971.

Searle, C. E. (ed.). Chemical Carcinogens. American Chemical Society, Monog. 173, 1976. 788 pp.

Shannon, D. G., and L. O. Fine. Cation Solubilities of Lignite Fly Ashes. Environ. Sci. Technol., 8(12):1026-1028, 1974.

Simons, D. S., J. E. Baker, and C. A. Evans, Jr. Evaluation of the Local Thermal Equilibrium Model for Quantitative Secondary Ion Mass Spectrometric Analysis. Anal. Chem., 48(9):1341-1348, 1976.

Simons, H. S., and J. W. Jeffery. An X-ray Study of Pulverised Fuel Ash. J. Appl. Chem., 10:328-336, 1960.

Smith, R. D., J. A. Cambell, and K. K. Nielson. Concentration Dependence upon Particle Size of Volatilized Elements in Fly Ash. Environ. Sci. Technol., 13(5):553-558, 1979.

Southern Research Institute. Survey of Information on Fine Particle Control. Electric Power Research Institute, Report No. 259, Palo Alto, California, 1975. 247 pp.

Sparks, C. J. Personal communication, 1973.

Stahley, S. Personal communication, 1976.

Steyermark, A. Quantitative Organic Microanalysis. Academic Press, New York, 1961. p. 222. 665 pp.

Strauss, W. Industrial Gas Cleaning, Second Edition. Pergamon Press, Elmsford, New York, 1975. 471 pp.

Talbot, R. W., M. A. Anderson, and A. W. Andren. Qualitative Model of Heterogeneous Equilibria in a Fly Ash Pond. Environ. Sci. Technol., 12:1056-1062, 1978.

Theis, T. L., and J. L. Wirth. Sorptive Behavior of Trace Metals on Fly Ash in Aqueous Systems. Environ. Sci. Technol., 11(12):1096-1100, 1977.

Theriault, G., T. Barry, and M. Thomas. Technique of Preparing Powder Samples for AES (Auger Electron Spectroscopy) and/or ESCA (Electron Spectroscopy for Chemical Analysis) Analysis. Anal. Chem., 47(8)1492-1493, 1975.

Toca, F. M. Lead and Cadmium Distribution in the Particulate Effluent from a Coal Fired Boiler. Ph.D. Dissertation, University of Iowa, July, 1972. See also Dissertation Abstracts International, 33:3156B (1973). 174 pp.

Townsend, P. D., J. C. Kelly, and N. E. W. Hartley. Ion Implantation, Sputtering and Their Applications. Academic Press, New York, 1976. pp. 125, 233. 344 pp.

Urone, P., and W. H. Schroeder. Sulfur Dioxide in the Atmosphere: A Wealth of Monitoring Data, but Few Reaction Rate Studies. Environ. Sci. Technol., 3:436-445, 1969.

U. S. Department of Health, Education, and Welfare. Air Quality Criteria for Particulate Matter. National Air Pollution Control Administration Publ. No. AP-49, Washington, D.C., 1969.

U. S. Environmental Protection Agency. Emissions from Residential and Small Commercial Stoker-Coal-Fired Boilers under Smokeless Operation. Publ. EPA-600/7-76-029. Office of Research and Development, Washington, D.C., 1976a. 78 pp.

U. S. Environmental Protection Agency. Environmental Assessment Sampling and Analysis: Phased Approach and Techniques for Level 1. Publ. EPA-600/2-77-115. Office of Research and Development, Washington, D.C., 1977. 34 pp.

U. S. Environmental Protection Agency. Field Testing: Trace Element and Organic Emissions from Industrial Boilers. Publ. EPA-600/2-76-086b. Office of Research and Development, Washington, D.C., 1976c. 146 pp.

U. S. Environmental Protection Agency. Preliminary Emissions Assessment of Conventional Stationary Combustion Systems; Volume I - Executive Summary. Publ. EPA-600/2-76-046a. Office of Research and Development, Washington, D.C., 1976b. 3 Volumes.

U. S. Government Printing Office. The Clean Air Act as Amended August 1977, Serial No. 95-11, Washington, D.C., 1977.

Von Lehmden, D. J., R. H. Jungers, and R. E. Lee, Jr. Determination of Trace Elements in Coal, Fly Ash, Fuel Oil, and Gasoline. Preliminary Comparison of Selected Analytical Techniques. Anal. Chem., 46(2):239-245, 1974.

Wallace, J. R. The Physical and Chemical Characterization of Airborne Particulate Matter. Ph.D. Thesis, University of Illinois, Urbana, Illinois, 1974. 162 pp.

Watt, J. D., and D. J. Thorne. The Composition and Pozzolanic Properties of Pulverised Fuel Ashes. J. Appl. Chem., 15:585-604, 1965.

Wehry, E. L. Analytical Problems in the Study of Photochemical Reactions. In: Analytical Photochemistry and Photochemical Analysis, J. M. Fitzgerald, ed. Marcel Dekker, New York, 1971. pp. 167-212.

Weintraub, W., S. Goldberg, and A. A. Orning. A Study of Sulfur Reactions in Furnace Deposits. Trans. Am. Soc. Mech. Eng. J. Eng. for Power, 83: 444-450, 1961.

White, H. J. Industrial Electrostatic Precipitation. Addison-Wesley, Reading, Massachusetts, 1963. 376 pp.

Williams, P., and C. A. Evans, Jr. High Resolution Secondary Ion Mass Spectrometry. In: Secondary Ion Mass Spectrometry, K. F. J. Heinrich and D. E. Newbury, eds. Natl. Bur. Stand. (U.S.), Spec. Publ. 427, 1975. pp. 63-68.

Williams, P., and C. A. Evans, Jr. A Simple Electronic Aperature for Rastered-beam Depth Profiles. Int. J. Mass Spectrom. Ion Phys., 22(3/4): 327-331, 1976.

Yeh, H. C., R. F. Phalen, and O. G. Raabe. Factors Influencing the Deposition of Inhaled Particles. Environ. Health Perspectives, 15:147-156, 1976.

APPENDICES

APPENDIX A

EXPERIMENTAL PROCEDURES AND INSTRUMENTAL TECHNIQUES

Sample Sources and Fractionation Procedures

A number of different fly ashes were studied. The sources included two coal-fired power plants burning midwestern bituminous coals, the Iowa/Illinois Gas and Electric Plant in Davenport, Iowa, and the Vermilion Plant near Danville, Illinois. The former utilized a chain grate stoker, while the other used a pulverized coal feed system.

Samples were collected in the stack systems at temperatures in the range of 200-300°C. Ash from the chain grate stoked plant was studied most extensively because it had generally higher trace element bulk concentrations, facilitating detection by the various analytical techniques. Large particles (45-180 μm physical diameter) were analyzed to facilitate both particle handling and the characterization of individual particles using surface microanalytical techniques. The trace element studies of the aerodynamically sized fly ash studied in the trace metal section came from the pulverized feed system. Samples for that study represented a) fly ash retained in the cyclone precipitation system and b) airborne fly ash collected in the ducting approximately 10 feet from the base of the stack. The western fly ash was collected from the electrostatic precipitators of the Corrette plant in Billings, Montana, which burns a Montana sub-bituminous coal.

Size separations were made in three different ways. Aerodynamic laboratory separations on the bulk ash were made using a Rollar particle size analyzer (American Instrument Co.). Physical separations were made by sieving with a sonic sifter (ATM Corp., Milwaukee, Wisconsin). Airborne fly ash samples were collected and size differentiated *in situ* using a stainless steel Andersen stack sampler which is designed to operate at the stack temperature (Andersen Samplers, Inc., Atlanta, Georgia).

Particle size calibrations were based on data supplied by the sampler manufacturers. These data are established in terms of equivalence to the aerodynamic diameter of spherical particles of unit density (Ranz and Wong, 1952; Flesch et al., 1967). The size distributions of particles collected on the third and fourth plates (4.6-7.1 μm and 3.0-4.6 μm) of the Andersen stack sampler were also examined using a Coulter counter (Coulter Electronics, Inc., Hialeah, Florida) in the timed analysis mode with a 100 μm aperture (Brecher et al., 1956). Milligram portions of the fly ash were dispersed in a 50% mixture of methanol in water and ultrasonically agitated for five minutes before adding the suspension to the counter. (Since the major constituents of the fly ash are aluminum, silicon and iron oxides, little, if

any, of the fly ash particles dissolves in this solution; hence, one would not expect any systematic error due to solvation effects.) Volume median diameters of 6.2 μm and 4.3 μm were obtained assuming a particle density of 2.5 g/cm^3 in order to convert physical diameters to aerodynamic diameters. These results indicate the relative validity of the aerodynamic diameters quoted. Physical diameters were confirmed by the use of a scanning electron microscope.

Morphology Studies

A JSM U-3 SEM (Jeol, Inc., Medford, Massachusetts) equipped with an ORTEC 7000 Series Si(Li) X-ray detector and an ORTEC Model 6200 Multi-channel Analyzer (Ortec, Inc., Oak Ridge, Tennessee) were used to study the morphology and elemental distribution of the matrix elements, respectively. The particles were deposited onto Cambridge type SEMS stubs (Structure Probe, Inc., Westchester, Pennsylvania) using one of the following supporting media:

1. Scotch double-sided adhesive tape (Minnesota Mining and Manufacturing Co., St. Paul, Minnesota).

2. Dag 154 (Acheson Colloids Co., Port Huron, Michigan), a suspension of colloidal graphite in alcohol.

3. Dotite Paint Type D-550 (Fujikura Kasei Co., Ltd., Japan), a suspension of silver powder in alcohol.

The particles are then made conducting by depositing on their surface a layer of carbon about 1,000Å thick under vacuum using a Denton DV-503 vacuum evaporator (Denton Vacuum, Inc., Cherry Hill, New Jersey). All X-ray analysis were carried out with the specimen stage tilted at a 30° angle towards the X-ray detector. This enabled X-rays to emerge from the sample at a high take-off angle and thus decreased topographical effects.

Elemental Analyses

The chemical analyses of the different samples were obtained through a variety of techniques. These techniques fall into two classes, viz., those that analyzed the fly ash directly as the solid (Instrumental Neutron Activation Analysis, X-ray Fluorescence, Spark Source Mass Spectrometry and DC Arc emission spectroscopy), and those that analyzed the sample in solution following wet digestion (Atomic Absorption). The former methods retain sample integrity but involve calibration uncertainties; the latter allow easy calibration but are susceptable to possible formation of analytically intractable compounds during digestion.

The matrix elements in the separated fly ash samples (Fe, Ti, Al, Si, Ca, K, S and Mg) were analyzed with wavelength dispersive X-ray fluorescence spectrometry. A vacuum path single crystal Phillips Norelco X-ray spectrometer (Phillips Electronic Instruments, Mount Vernon, New York) was used with a 1500 watt chromium X-ray tube as the source. A thallium acid phthalate (TLAP) wavelength analyzing crystal was used to disperse Si, Al and Mg X-rays, an ethylene diamine d-tartrate (EDDT) crystal for K, Ca and S X-rays,

and a lithium fluoride (LiF) crystal for Ge and Ti X-rays. Thin samples were used to approximate an infinitely thin film so that matrix effects can be neglected. To ensure the thinness of the samples, all samples of nominal particle diameter >4 μm were ground further so as to minimize surface sampling and inhomogeneity effects. The powders were suspended in propanol and dispersed ultrasonically before deposition by filtration onto 0.4 μm millipore membrane filters (Price and Angell, 1968). National Bureau of Standards Certified Fly Ash and Rock Samples were used as standards. K_α radiation was monitored for all elements and a vacuum radiation path maintained for all elements except Fe and Ti. A lithium fluoride crystal was employed for detecting Fe and Ti, EDDT was used for Al, Si, Ca, K and S and ADP was used for Mg. For this method, precisions of ±5% were achieved.

Trace elements in some of the separated fly ash fractions were determined by instrumental neutron activation analysis. The samples were irradiated for one hour in the Illinois Reactor Facility which had a neutron flux of 2×10^{12} neutrons-cm^{-2}-sec^{-1} in the irradiation region. The resultant γ-emissions were measured on a multichannel analyzer equipped with a Ge(Li) detector. National Bureau of Standards Certified Fly Ash and Rock Samples were run simultaneously for calibration. The resulting spectra were recorded on magnetic tape and analyzed with the "GAMANL" Program (Hopke, 1969).

An A.E.I. model MS-7 spark source mass spectrometer was used for the qualitative determination of all elements of atomic number greater than Li and for quantitative determination of Bi, Pb, Tl, Sb, Sn, As, Zn, Cu, Ni, Fe, V, Ca, K, and Si. One part of fly ash was mixed by weight with two parts of spectroscopic graphite for five minutes in a Wig-L-Bug and the mixture pressed into an electrode. Electrodes were manually positioned and sparked with a 25-μsec spark duration and a repetition rate of 300 sec^{-1} at 10^{-6} torr source pressure. Mass spectra were recorded photographically.

Internal standardization of the mass spectra was achieved by referencing line intensities both to the Pb in the sample and to 60 μg/gm of solution-doped Au. The Pb was determined independently by atomic absorption spectroscopy. The $^{197}Au^+$ ion was at least two orders of magnitude more intense than $^{181}Ta^{16}O^+$ from source contamination. Element concentrations were calculated from the expression (Farrar, 1972)

$$C_X = C_S \frac{I_X}{I_S} \cdot \left[\frac{M_X}{M_S}\right]^2 \frac{\Phi_S}{\Phi_X} \; k \qquad \text{(A-1)}$$

where I = peak intensity of ion beam, D = isotope abundance, M = mass of analyte, C = concentration of analyte, X = analyte, S = internal standard, k = sensitivity factor for a given element relative to the standard.

This expression assumes that the line width on the photographic plate is proportional to $M^{\frac{1}{2}}$ and emulsion sensitivity is proportional to $M^{-\frac{1}{2}}$ (Owens and Giardino, 1963). Values of k were determined by doping increasing amounts of Pb, Tl, Sb, Sn, As, and Ni into the graphite before forming a series of

electrodes with fly ash. For these elements values of k ranged from 1.0 to 1.8. For the remaining elements k was set equal to unity, an assumption usually valid within a factor of three (Farrar, 1972). Precisions of ±20% were achieved.

Carbon present as SiC, FeC, and free C was determined as CO_2 after combustion with O_2 on a V_2O_5 catalyst (Steyermark, 1961).

Sample digestion was achieved by heating 0.5 g of fly ash, 3.5 ml of 3:1 concentrated HCl/HNO_3 (aqua regia), 0.5 ml water, and 2.5 ml of an aqueous solution containing 48% HF for two hours at 110°C in a 25 ml teflon-lined Parr pressure bomb (Parr Instrument Co., Moline, Illinois). After cooling, 2.5 g of boric acid was added to neutralize the HF. The small amount of black, solid residue remaining was removed by centrifugation and was shown by spark source mass spectrometry to contain mainly Ca, F and Al in addition to carbon. At least 95% extraction of the elements of interest was achieved.

Atomic absorption analyses were performed by direct aspiration of dilutions of the original digest for Pb, Tl, Cd, As, Ni and Be. Air-acetylene flames were employed for all elements except Be, for which nitrous oxide-acetylene was used. A Jarrel Ash 8-10 dual beam, double monochromator instrument was employed. Background corrections were achieved by monitoring a non-absorbing wavelength within 40Å of the analytical wavelength. Se was determined by its atomic absorption after conversion to volatile H_2Se according to the method of Schmidt and Royer (1973). Standard addition calibrations were performed in all cases, and a precision of ±10% was achieved.

The elements Pb, Be, Cr, Mn, Co and Ni were determined by DC arc emission spectroscopy with a Baird-Atomic 3 meter spectrograph. Samples coarser than 325 mesh (Tyler series) were ground to pass through a 325-mesh sieve. One part by weight of fly ash was mixed with four parts of spectroscopic graphite for one minute in a Wig-L-Bug mechnical shaker (Spex Industries). Spex mix A-7 pure graphite standards doped with 49 elements were used for comparative standards. Approximately 50 mg of graphite diluted sample were burned to completion in a cup electrode operating with a 4 mm gap and 10 amp current. Element concentrations were obtained with a precision of ±30%.

Method Evaluation

All the techniques have their strengths and limitations in terms of the number of elements that can be analyzed, interferences, amount of sample required, sample handling procedures, etc. A detailed discussion of these factors is beyond the scope of this report. However, several comments are especially relevant to particulate analyses. Instrumental Neutron activation analysis (INAA) is probably the best overall technique. It is a non-destructive multielement technique with good precision and accuracy. However, a reactor, considerable analysis time, and skilled personnel are required. In addition, since not all elements can be analyzed by INAA, a supplemental technique is necessary.

Of the other techniques utilized, spark source mass spectrometry undoubtedly affords the greatest advantage for multielemental determination

of solid fly ash, although the analyses are extremely time consuming. In addition, interferences prevent the analysis of Te, Cd, Se, Co, Mn, Cr, and S and permit only a semiquantitative estimate for Be. D.C. arc emission spectroscopy exhibits no significant advantages over spark source mass spectroscopy other than detection of Co, Mn, Cr and Be and wider availability. The X-ray fluorescence method employed has the advantages of high speed and precision but is somewhat limited by calibration difficulties and matrix effects. The shallow penetration depths of soft X-rays from the lighter elements, such as sulfur and magnesium, necessitate high matrix identity between samples and standards and a very small particle size (Muller, 1972).

Atomic absorption spectrometry is considered the most accurate technique employed in this work. However, large amounts of sample are required if more than a few elements are determined. Also, great care must be taken to achieve good background corrections because of the large number of elements present. Atomic absorption spectrometry displayed no evidence of loss of sample integrity as a result of the fly ash digestion. One possible exception was Tl, for which analyses were consistently 3-5 times lower than those obtained by spark source mass spectrometry and anodic stripping voltammetry.

X-ray Powder Diffraction

Diffraction patterns were obtained with a Phillips Norelco X-ray Diffraction system (Phillips Electronic Instruments, Mt. Vernon, New York). The samples were ground to a particle size of less than 44 μm and a thin film of particles was placed in a monochromatric beam of copper K_α (8.05 keV) X-rays. The intensity of the diffracted X-rays was measured between 15°-60° 2θ angles with a proportional counter.

Surface Techniques

The variation of elemental concentrations as a function of depth for both leached and unleached fly ash particles was determined by ion microprobe mass spectrometry and Auger electron spectrometry combined with ion etching. The procedure for particle mounting involved placing large particles (45-180 μm) in a folded strip of indium foil and hand pressing to imbed them into the foil. This mounting technique has the advantages that indium is electrically conducting; presents few spectral interferences; is soft and malleable, allowing imbedding of particles without physical alteration; has a low vapor pressure for ultra-high vacuum compatibility; and is inexpensive (Theriault, et al., 1975).

An AEI Model IM-20 ion microprobe was used to obtain elemental depth profiles. Basic features of the instrumentation have been described previously (Bakale, et al., 1975). A 25-keV negative oxygen primary beam of 40 nA and 20-μm diameter was rastered rapidly over an area of 100 μm by 100 μm. The rastering procedure was important primarily because it enabled fairly uniform current densities to be maintained over the entire area of the particle being analyzed. Mass spectrometer resolving powers used ranged from 250 to 1800 (10% valley definition) as required to resolve molecular ion interferences. Depth profiles were acquired by two methods: (1) continuously monitoring the positive secondary ion intensity of one element vs.

time, using electrical detection, and (2) using photographic detection of the positive secondary ions as dispersed by the double-focusing Mattuch-Herzog analyzer. Results reported herein were obtained only by electrical detection, since the use of photographic detection was limited by a lack of sensitivity.

Elemental depth profiles were also obtained with a Physical Electronics Industries Model 545 Scanning Auger Microprobe. The indium foil containing the imbedded particles was mounted on the standard carrousel at 30° grazing incidence to a 5-keV, 50-μm primary electron beam. Elemental depth profiles were obtained by recording entire Auger spectra after incremental periods of sputtering with 2-keV Ar^+. Sputtering rate calibrations were achieved in an manner analagous to that used for the ion microprobe depth profiles.

On the basis of its inherently high sensitivity, good depth resolution, and ability to perform microanalysis of samples (including those which are insulators), ion microprobe mass spectrometry was a priori one of the most useful surface analytical techniques for the in-depth characterization of airborne particles. Specific analytical concerns or objectives involved using the ion microprobe to obtain elemental depth profiles of individual fly ash particles were the following: (1) to establish which elements of environmental interest could be characterized, (2) to analyze particles before and after solvent leaching to reduce concerns about possible sputtering artifacts, and (3) to use solvent leaching and bulk analysis to substantiate and to quantitate the ion microprobe results, i.e., to estimate surface constraints on the analysis such as limits to depth resolution or possible effects due to charging.

The major potential constraints on the depth resolution of the ion microprobe elemental depth profiles of fly ash (Figures 32-37) are variations in the sputtering rate over the area of the particle being analyzed (Townsend et al., 1976), crater edge effects (Evans, 1972; Williams and Evans, 1976), escape depths of secondary ions (McHugh, 1975), and cascade mixing of subsurface layers resulting from penetration of the primary ion beam into the sample (Morabito, 1975; Coburn, 1976).

In order to convert sputtering time to depth, sputtering rates for SiO_2 were measured under primary ion beam conditions identical to those used for the analysis of fly ash. The time required to sputter a 3000-Å SiO_2 layer on Si was determined by monitoring the Si intensity that corresponded to a sputtering rate of 4 Å (+0.5 Å) per second. Since fly ash is predominately a silicate material, the rates were considered comparable. The major limitation in applying this calibrated rate to fly ash was that the irregular surface of a fly ash particle may cause substantial variations in sputtering rate over the region sampled. That is, microtopographical features approaching grazing incidence with respect to the primary beam (e.g., the edges of a particle) will sputter faster (up to about a factor of 3) than those at normal incidence (Townsend et al., 1976). Therefore, the calibrated sputtering rate was considered a minimum rate for fly ash, with secondary ions actually being produced from a range of depths approximately 1-3 times greater than the calibrated depth. Thus, the remaining factors mentioned

above affecting depth resolution are considered insignificant relative to the effects of sputtering rate variation and would in any case tend to diminish and broaden, rather than enhance, surface peaks.

One of the most important analytical requirements was to establish that the observed elemental surface predominance was not the consequence of sputtering or analysis artifacts. Conventional methods to assure that variations in secondary ion intensities reflect relative differences in element concentrations are to (1) perform the profile under conditions that ensure a high oxygen concentration in the sample surface, (2) reference the profiled element intensity to a uniformly distributed element, and (3) apply quantitation procedures to the data (Morabito, 1975). All of these methods have been utilized and will be discussed as follows.

First, a high oxygen concentration in the sample surface was ensured by using an oxygen primary beam. Specifically, the purpose of using a negative oxygen primary beam was twofold: (1) oxygen promotes the production of stable, high-intensity yields of positive secondary ions (Lovering, 1975) and (2) a negative primary beam has been shown to maintain charge neutrality on insulating surfaces (Andersen et al., 1969). The absence of large variations in the secondary ion intensities of matrix elements (Al, Ti in Figure 32) beyond the intial rise in the first 100 Å did indicate that secondary ion yields are relatively constant over the greater part of the depth profile.

All secondary ion intensities (Figures 32-37) were referenced to Si in order to permit a direct comparison of depth profiles for different elements and to compare the same element in the leached vs. the unleached sample. Use of Si as the internal standard allowed compensation for variations in the amount of sample within the rastered area and for variable ion extraction efficiency. Silicon was considered the most appropriate element, since (1) it was homogenously distributed in all particles at depths greater than several hundred angstroms, (2) the Si profiles showed minor variations for different particles in the same sample, and (3) Si was negligibly leached by either DMSO or H_2O. The use of Si as an internal standard was also necessary in the quantitation procedures to be discussed.

With regard to methods for quantitation of surface region concentrations, it is well known that secondary ion yields are highly variable from element to element and exhibit strong matrix effects. For fly ash, the surface elemental composition apparently is very different from the interior, and standards suitable for surface analysis are not available. For the estimates of elemental concentrations shown in Figures 32-37, the essentially constant secondary ion intensities observed for all elements at depths greater than about 500 to 1000 Å were taken to approximate bulk concentration levels. As summarized below, this assumption was verified with calculated relative elemental sensitivity factors, the bulk concentration of Si in fly ash as an internal standard, and the results of bulk analysis with SSMS.

Our quantitation procedure was based upon the empirical observation that a simplified form of the Saha-Eggert equation can be used to reduce secondary ion yields to elemental concentrations (Simons et al., 1976):

$$\frac{N_i^+}{N_i^0} = \frac{AT^{3/2}w}{N_e} [\exp^{-1} i/kT] \qquad \text{(A-2)}$$

where N_i^+ and N_i^0 are the number densities of singly charged and neutral atoms of element i, A is a numerical constant, w is the ratio of ground state statistical weights of the ion and netural, I, is the first ionization potential and N_e (electron density) and T (temperature) are fitting parameters. An empirical relationship between the parameters N_e and T in the Saha-Eggert equation has also been established, giving an equation with only one dependent variable (T) (Simons et al., 1976). In the absence of several internal standards for the fly ash samples, sets of relative elemental sensitivity factors were calculated using the one-parameter equation for various values of the fitting parameter T. Relative atomic concentrations (C_i^{rel}) were then obtained from relative sensitivity factors and ion count rates corrected for isotopic abundance (I_i^+) according to the relation:

$$C_i^{rel} = I_i^+ \quad 1 + \left[\frac{N_i^+}{N_i^0} \quad -1\right] \qquad \text{(A-3)}$$

Absolute concentration values were established by assuming that the Si intensity measured at the end of each elemental profile resulted from 12% by weight Si [Spark Source Mass Spectrometry (SSMS) bulk value].

The bulk analysis values were used to guide the choice of the best value of T at which to calculate relative sensitivity factors as follows. All elements exhibited nearly constant secondary ion intensities at depths greater than 500 Å to 100 Å. In addition, the region of surface predominance can be shown to make a negligible contribution to the bulk concentration determined by SSMS for the large particles studied. Therefore, at a depth of 1000 Å, where comparisons to Si were made, the concentrations of surface predominant elements should approach their bulk analysis values. For the ten elements for which complete SSMS data were available (Pb, Tl, Cr, Mn, V, K, Li, Fe, Ti, Mg), a value of T of 12000°K satisfied these conditions best. In fact, for the fitting parameter chosen, all ten elements for all samples at the 1000 Å depth were within approximately a factor of 3 of the SSMS concentration. The only exceptions were Pb, Tl, and Cr in the unleached sample, for which elemental concentrations were more than 5 times above the bulk value. From a comparison of the secondary ion intensity at 1000 Å depth for the unleached sample and the maximum secondary ion intensity observed for the leached sample, it is apparent that sputtering to 1000 Å did not completely remove the surface predominant region for the elements Tl and Cr.

An alternative approach to the quantitation of surface region concentrations was to ratio the mass of a given element leached from the particles to the total mass removed from the particles during leaching. This procedure was deemed unsatisfactory for the following reasons: (1) it integrates the elemental concentration over the entire surface region that is leached, and (2) it is not known how uniformly, or to precisely what depth, the particles are leached.

Auger Electron Spectrometry--The application of Auger electron spectrometry (AES) for in-depth characterization was of interest, since Auger depth resolutions are roughly comparable to those obtainable with the ion microprobe, and microfocusing the primary electron beam also permits analysis of individual particles. Unfortunately, the application of AES was severely limited by electron beam charging effects (Chang, 1974) and the inability to detect elements at concentrations below about 0.1-1% atomic in the analytical volume.

The charging problem was the result of the insulating nature of fly ash. Charging effects are normally minimized by using grazing or glancing incidence to increase secondary electron emission coefficients. However, for irregular surfaces such as those of fly ash particles, grazing incidence cannot be readily maintained over the entire area being analyzed. The resultant charging caused occasional loss of particles during analysis, instabilities and/or shifts in the positions of Auger peaks (especially those having energies below a few hundred eV), and shifts in the position of the electron beam.

The solvent-leaching experiments were of minor value in substantiating the Auger results for two reasons: (1) the highly leachable, surface-predominant trace elements could not be detected and (2) the leached particles were more susceptible to charging. No pronounced changes in the Auger depth profiles were observed following leaching except for Na and K. The stronger surface enhancement shown by Na and K following leaching may have resulted from charge-induced migration of alkalies to the particle surface (McCaughan and Kushner, 1974). Leached particles were generally observed to be more susceptible to charging because of the apparent removal of a more conducting surface layer by solvent leaching.

Despite the limitations discussed, scanning Auger microscopy does have several advantages over the ion microprobe for particle characterization: (1) The initial surface spectrum is obtained without sputtering and thus is not subject to the effects of sputtering artifacts. (2) Multielement depth profiles of the same particle are more readily obtained. (The IM20 ion microprobe does not have rapid magnetic peak switching or multiple electrical detection capabilities.) (3) Spectral interferences may be less severe for a few elements. For example, sulfur was routinely determined by Auger, but the ion microprobe mass spectrometric analysis required high mass resolution.

Other Techniques (Scanning Electron Microscopy, Electron Spectroscopy) for Chemical Analysis--The major disadvantage of scanning electron microscope or electron microprobe methods for in-depth characterization is the lack of depth resolution; i.e., x-ray escape depths are on the order of a micron

relative to the 10-50 Å analytical escape depths for the ion microprobe or Auger techniques.

Qualitative differences between surface and interior composition can be discerned, however, by comparing X-ray spectra before and after the removal of material in the surface region by ion sputtering (Linton et al., 1976; Loh, 1975; Hulett, 1973). X-ray intensities can also be measured from the sputtered and unsputtered sides of the same particle (Linton et al., 1976; Loh, 1975). Experimental results using Ar^+ sputtering of fly ash were previously reported using scanning electron microscopy-energy dispersive x-ray spectrometry (SEM/EDS) (Linton et al., 1976; Loh, 1975). Results indicated enhanced surface region concentrations of Pb, Zn, K, Na, P, and S, with no detectable surface predominance of Ca, Si, Al, and Fe. Thus, the SEM/EDS technique is significant for providing a qualitative corroboration of the results obtained with the true surface microanalytical techniques for the mutually detectable elements.

Other possible approaches to the surface characterization of particles using the electron microprobe include the following: (1) varying the primary electron beam energy to produce a variation in the analysis depth (Armstrong and Buseck, 1975b) or (2) ratioing X-ray intensities of elements to matrix elements as a function of particle size (Linton et al., 1976; Peuschel et al., 1974). Both methods suffer from the poor depth resolutions obtainable with electron probe techniques. Using the first technique above also requires a very stable electron beam current and extensive X-ray quantitation methods, including corrections for particle shape (Armstrong and Buseck, 1975a; Armstrong and Buseck, 1975b). Elemental detection limits also increase at lower electron beam energies, thus limiting the extent to which beam energies may be reduced. The second approach assumes that the smaller the particle, the greater the relative surface area being sampled by the electron beam (Peuschel et al., 1974). However, this approach oversimplifies the mechanisms of X-ray production and really requires detailed corrections for the effects of particle shape on the emission of X-rays.

Electron spectroscopy for chemical analysis (ESCA) is another technique used for surface characterization of environmental particles (Craig et al., 1974; Gordon, 1975; Cambell et al., 1979). ESCA not only has depth resolution and detection limits generally comparable to those of AES, but also has advantages over AES for surface characterization in that (1) chemical information is more available, since ESCA chemical shifts are usually more readily related to oxidation states (Evans, 1975), and (2) charging of insulating particles is minimized, since X-rays, rather than electrons, serve as the source of ionization (Linton et al., 1976). However, ESCA is not favored over AES for in-depth characterization, because (1) chemical information is potentially lost, since destructive ion sputtering may alter the forms of the elements present (Evans, 1975), and (2) individual particles cannot be depth profiled, since ESCA microanalysis is not yet feasible Linton et al., 1976). Thus, heterogeneity and variations in sputtering rate within the field of particles being analyzed are major difficulties in obtaining meaningful ESCA depth profiles.

Leachate Analysis

Leaching studies were undertaken in two experinments. In the comparison tests of the different leaching methods, four techniques were used. These are described in the text in Section V.

The techniques used in the surface study leaching experiments were performed with Fisher reagent grade dimethyl sulfoxide (DMSO) and triply distilled water. DMSO was chosen after inorganic species were found in DMOS extracts during studies investigating the extraction of trace organics, while H_2O was employed to simulate leaching in the natural environment. Leaching with DMSO was carried out for 48 hrs in a Soxhlet extractor at a temperature of 40°C and a pressure of ~0.1 mm Hg. A DMSO blank was prepared by leaching an empty Soxhlet thimble in identical experimental conditions. Leaching with H_2O was performed by placing fly ash in a glass jar containing triply distilled water for a 12-hr period. The jar was also placed in a DISONtegrator Model 320 and sonicated for 1 hr in a water bath in order to maximize interaction of the solvent with fly ash surfaces. The leachate solution was then filtered twice through Whatman No. 41 filter paper, as was an H_2O solution serving as the blank. The aqueous leaching procedure was used primarily to indicate relative elemental leachabilities under the conditions employed, and thus it may not solubilize the entire avilable fraction of most elements (Natusch and Matusiewicz, 1976).

APPENDIX B

MATRIX ELEMENT DISTRIBUTION FOR A SIZE, MAGNETIC AND DENSITY FRACTIONATED FLY ASH

TABLE B-1. CONCENTRATION OF SILICON (WT %) IN FRACTIONATED FLY ASH

	Particle size (μm)	Density (g/cm³)			
		<2.1	2.1-2.5	2.5-2.9	>2.9
Non-magnetic	<20	26.43	23.97	18.90	--*
	20-44	22.93	23.17	19.73	18.37
	44-74	22.70	23.70	19.02	14.65
	>74	23.77	24.14	22.44	15.73
Magnetic	<20	--	--	9.99	10.51
	20-44	--	--	21.01	6.49
	44-74	22.82	21.93	17.78	12.25
	>74	--	22.28	21.69	11.56

* No meaningful data.

TABLE B-2. CONCENTRATION OF ALUMINUM (WT %) IN FRACTIONATED FLY ASH

	Particle size (μm)	Density (g/cm³)			
		<2.1	2.1-2.5	2.5-2.9	>2.9
Non-magnetic	<20	13.37	15.15	10.38	--*
	20-44	18.03	13.12	10.66	11.06
	44-74	15.47	13.04	10.88	8.78
	>74	14.35	14.86	11.04	8.14
Magnetic	<20	--	--	6.04	5.98
	20-44	--	--	10.11	3.94
	44-74	13.65	11.54	9.95	7.48
	>74	--	12.20	12.26	6.19

* No meaningful data.

TABLE B-3. CONCENTRATION OF IRON (WT %) IN FRACTIONATED FLY ASH

	Particle size (μm)	Density (g/cm³)			
		<2.1	2.1-2.5	2.5-2.9	>2.9
Non-magnetic	<20	5.34	3.32	18.40	--*
	20-44	5.56	8.01	9.74	14.38
	44-74	8.08	8.77	11.43	18.25
	>74	8.12	6.68	12.00	19.72
Magnetic	<20	--	--	41.75	41.36
	20-44	--	--	14.80	41.31
	44-74	11.44	14.46	20.51	35.22
	>74	--	13.67	13.46	38.61

* No meaningful data.

TABLE B-4. CONCENTRATION OF POTASSIUM (WT %) IN FRACTIONATED FLY ASH

	Particle size (μm)	Density (g/cm³)			
		<2.1	2.1-2.5	2.5-2.9	>2.9
Non-magnetic	<20	2.69	2.34	2.22	1.73
	20-44	2.63	2.28	1.33	1.09
	44-74	1.89	1.63	1.05	0.45
	>74	1.79	1.48	1.06	0.13
Magnetic	<20	--*	--	0.76	0.70
	20-44	--	1.92	1.48	0.73
	44-74	1.78	1.60	1.27	0.85
	>74	1.37	1.62	1.49	0.83

* No meaningful data.

TABLE B-5. CONCENTRATION OF SODIUM (μg/g) IN FRACTIONATED FLY ASH

	Particle size (μm)	Density (g/cm³)			
		<2.1	2.1-2.5	2.5-2.9	>2.9
Non-magnetic	<20	3621	2903	2500	3492
	20-44	2494	3011	1709	1473
	44-74	1984	2447	1443	738
	>74	2249	2940	1574	1275
Magnetic	<20	--*	--	1059	881
	20-44	--	2554	1860	883
	44-74	1869	1952	1618	--
	>74	1761	--	--	--

* No meaningful data.

TABLE B-6. CONCENTRATION OF CALCIUM (WT %) IN FRACTIONATED FLY ASH

	Particle size (μm)	Density (g/cm^3)			
		<2.1	2.1-2.5	2.5-2.9	>2.9
Non-magnetic	<20	10.0	5.0	6.0	3.0
	20-44	6.0	5.3	4.6	7.0
	44-74	3.2	4.0	4.1	8.3
	>74	3.3	3.4	4.4	5.2
Magnetic	<20	--*	--	6.0	5.0
	20-44	--	10.0	9.0	6.0
	44-74	11.0	11.0	12.0	10.0
	>74	6.0	7.0	14.0	7.0

* No meaningful data.

TABLE B-7. CONCENTRATION OF SULFUR (WT %) IN FRACTIONATED FLY ASH

	Particle size (μm)	Density (g/cm^3)			
		<2.1	2.1-2.5	2.5-2.9	>2.9
Non-magnetic	<20	0.24	0.40	0.22	--*
	20-44	0.11	0.48	0.82	0.43
	44-74	0.21	0.37	1.26	1.02
	>74	0.31	0.12	0.48	0.71
Magnetic	<20	--*	--	0.16	0.19
	20-44	--	--	0.45	0.09
	44-74	0.10	0.21	0.34	0.28
	>74	--	0.43	0.20	0.14

* No meaningful data.

TABLE B-8. CONCENTRATION OF TITANIUM (WT %) IN FRACTIONATED FLY ASH

	Particle size (μm)	Density (g/cm^3)			
		<2.1	2.1-2.5	2.5-2.9	>2.9
Non-magnetic	<20	0.80	0.50	2.39	--*
	20-44	0.97	1.08	1.10	1.34
	44-74	1.19	3.92	0.88	1.13
	>74	0.94	0.65	0.77	0.73
Magnetic	<20	--*	--	0.70	0.72
	20-44	--	--	1.12	0.55
	44-74	0.94	1.10	0.94	0.68
	>74	--	0.79	0.69	0.55

* No meaningful data.

APPENDIX C

TRACE ELEMENT DISTRIBUTIONS FOR A SIZE DENSITY AND MAGNETICALLY FRACTIONATED COAL FLY ASH

TABLE C-1. CONCENTRATION OF MAGNESIUM (WT %) IN FRACTIONATED FLY ASH

	Particle size (μm)	Density (g/cm^3)			
		<2.1	2.1-2.5	2.5-2.9	>2.9
Non-magnetic	<20	0.77	0.97	0.71	--*
	20-44	0.80	0.83	0.79	1.21
	44-74	0.87	1.22	1.21	0.99
	>74	1.10	0.90	1.19	0.80
Magnetic	<20	--	--	0.48	0.49
	20-44	--	--	0.86	0.28
	44-74	0.93	0.92	0.84	0.62
	>74	--	0.87	0.84	0.36

* No meaningful data.

TABLE C-2. CONCENTRATION OF MANGANESE (μg/g) IN FRACTIONATED FLY ASH

	Particle size (μm)	Density (g/cm³)			
		<2.1	2.1-2.5	2.5-2.9	>2.9
Non-magnetic	<20	608	643	648	504
	20-44	313	729	1083	1570
	44-74	280	546	1101	2399
	>74	288	615	916	1596
Magnetic	<20	--	--	722	611
	20-44	--	904	899	543
	44-74	401	493	749	--
	>74	477	--	--	--

* No meaningful data.

TABLE C-3. CONCENTRATION OF ARSENIC (μg/g) IN FRACTIONATED FLY ASH

	Particle size (μm)	Density (g/cm³)			
		<2.1	2.1-2.5	2.5-2.9	>2.9
Non-magnetic	<20	46	90	86	74
	20-44	12	77	133	164
	44-74	19	42	129	126
	>74	30	49	93	156
Magnetic	<20	--	--	70	63
	20-44	--	79	111	40
	44-74	--	59	97	48
	>74	41	54	80	62

* No meaningful data.

TABLE C-4. CONCENTRATION OF BARIUM (μg/g) IN FRACTIONATED FLY ASH

	Particle size (μm)	Density (g/cm^3)			
		<2.1	2.1-2.5	2.5-2.9	>2.9
Non-magnetic	<20	216	209	287	522
	20-44	309	390	714	3143
	44-74	409	364	559	7432
	>74	448	492	500	1070
Magnetic	<20	--	--	300	240
	20-44	--	373	525	269
	44-74	535	366	609	168
	>74	574	161	249	91

* No meaningful data.

TABLE C-5. CONCENTRATION OF STRONTIUM (μg/g) IN FRACTIONATED FLY ASH

	Particle size (μm)	Density (g/cm^3)			
		<2.1	2.1-2.5	2.5-2.9	>2.9
Non-magnetic	<20	<75	192	180	214
	20-44	120	261	377	363
	44-74	210	139	329	274
	>74	248	237	148	222
Magnetic	<20	--	--	118	91
	20-44	--	129	182	85
	44-74	198	164	101	75
	>74	251	180	44	136

* No meaningful data.

TABLE C-6. CONCENTRATION OF CESIUM (μg/g) IN FRACTIONATED FLY ASH

	Particle size (μm)	Density (g/cm^3)			
		<2.1	2.1-2.5	2.5-2.9	>2.9
Non-magnetic	<20	--*	--	--	--
	20-44	--	0.31	--	0.14
	44-74	0.33	0.27	0.23	0.07
	>74	0.29	0.20	0.19	0.14
Magnetic	<20	--	--	--	2.00
	20-44	--	5.70	3.50	1.50
	44-74	5.60	4.40	3.50	--
	>74	--	--	--	--

* No meaningful data.

TABLE C-7. CONCENTRATION OF RUBIDIUM (μg/g) IN FRACTIONATED FLY ASH

	Particle size (μm)	Density (g/cm³)			
		<2.1	2.1-2.5	2.5-2.9	>2.9
Non-magnetic	<20	--*	--	--	--
	20-44	--	92	--	40
	44-74	87	102	69	32
	>74	83	<146	78	18
Magnetic	<20	--	--	<55	<49
	20-44	--	<137	<76	<44
	44-74	<100	<55	<155	--
	>74	--	--	--	--

* No meaningful data.

TABLE C-8. CONCENTRATION OF ZINC (μg/g) IN FRACTIONATED FLY ASH

	Particle size (μm)	Density (g/cm³)			
		<2.1	2.1-2.5	2.5-2.9	>2.9
Non-magnetic	<20	--*	--	--	--
	20-44	--	48	--	69
	44-74	42	39	64	203
	>74	37	40	93	327
Magnetic	<20	--	--	1100	1100
	20-44	--	460	480	500
	44-74	110	350	480	--
	>74	--	--	--	--

* No meaningful data.

TABLE C-9. CONCENTRATION OF CHROMIUM (μg/g) IN FRACTIONATED FLY ASH

	Particle size (μm)	Density (g/cm³)			
		<2.1	2.1-2.5	2.5-2.9	>2.9
Non-magnetic	<20	--*	--	--	--
	20-44	--	10.7	--	10.0
	44-74	6.0	6.1	6.2	8.9
Magnetic	<20	--	--	312	300
	20-44	--	214	200	214
	44-74	211	189	216	--
	>74	--	--	--	--

* No meaningful data.

TABLE C-10. CONCENTRATION OF COBALT (μg/g) IN FRACTIONATED FLY ASH

	Particle size (μm)	Density (g/cm^3)			
		<2.1	2.1-2.5	2.5-2.9	>2.9
Non-magnetic	<20	--*	--	--	--
	20-44	--	10.2	--	13.5
	44-74	7.0	8.7	11.0	12.3
	>74	7.8	8.6	15.7	14.8
Magnetic	<20	--	--	119	113
	20-44	--	41	52	84
	44-74	48	45	57	--
	>74	--	--	--	--

* No meaningful data.

TABLE C-11. CONCENTRATION OF EUROPIUM (μg/g) IN FRACTIONATED FLY ASH

	Particle size (μm)	Density (g/cm^3)			
		<2.1	2.1-2.5	2.5-2.9	>2.9
Non-magnetic	<20	1.9	2.3	2.1	1.7
	20-44	1.4	1.7	1.4	1.9
	44-74	1.0	1.0	1.4	3.3
	>74	1.0	1.2	0.9	2.0
Magnetic	<20	--	--	1.4	1,2
	20-44	--	2.2	2.0	1.5
	44-74	1.4	1.5	1.6	0.7
	>74	1.3	1.0	0.8	0.6

* No meaningful data.

TABLE C-12. CONCENTRATION OF SCANDIUM (μg/g) IN FRACTIONATED FLY ASH

	Particle size (μm)	Density (g/cm^3)			
		<2.1	2.1-2.5	2.5-2.9	>2.9
Non-magnetic	<20	--*	--	--	--
	20-44	--	11.0	--	10.4
	44-74	7.8	8.5	9.3	10.7
	>74	6.8	5.8	10.1	9.5
Magnetic	<20	--	--	40	38
	20-44	--	49	54	38
	44-74	47	41	47	--
	>74	--	--	--	--

* No meaningful data.

TABLE C-13. CONCENTRATION OF THORIUM (μg/g) IN FRACTIONATED FLY ASH

	Particle size (μm)	Density (g/cm^3)			
		<2.1	2.1-2.5	2.5-2.9	>2.9
Non-magnetic	<20	--*	--	--	--
	20-44	--	5	--	5
	44-74	16	16	13	12
	>74	14	9	17	12
Magnetic	<20	--	--	17	15
	20-44	--	23	23	15
	44-74	22	18	--	--
	>74	--	--	--	--

* No meaningful data.

TABLE C-14. CONCENTRATION OF URANIUM (μg/g) IN FRACTIONATED FLY ASH

	Particle size (μm)	Density (g/cm^3)			
		<2.1	2.1-2.5	2.5-2.9	>2.9
Non-magnetic	<20	15	15	15	12
	20-44	13	16	17	28
	44-74	9	9	16	15
	>74	6	13	15	17
Magnetic	<20	--*	--	7	6
	20-44	--	5	7	6
	44-74	6	6	7	8
	>74	12	9	10	9

* No meaningful data.

TABLE C-15. CONCENTRATION OF DSYPROSIUM (μg/g) IN FRACTIONATED FLY ASH

	Particle size (μm)	Density (g/cm^3)			
		<2.1	2.1-2.5	2.5-2.9	>2.9
Non-magnetic	<20	9	10	9	7
	20-44	7	37	17	14
	44-74	9	9	12	11
	>74	8	9	12	10
Magnetic	<20	--*	--	12	10
	20-44	--	15	17	10
	44-74	14	13	13	7
	>74	5	7	7	6

* No meaningful data.

TABLE C-16. CONCENTRATION OF HAFNIUM (μg/g) IN FRACTIONATED FLY ASH

	Particle size (μm)	Density (g/cm³)			
		<2.1	2.1-2.5	2.5-2.9	>2.9
Non-magnetic	<20	--*	--	--	--
	20-44	--	5.0	6.0	9.9
	44-74	4.5	4.1	3.8	11.1
	>74	4.6	2.0	4.9	3.2
Magnetic	<20	--*	--	4.0	3.9
	20-44	--	8.5	6.7	4.2
	44-74	6.2	6.4	12.9	--
	>74	--	--	--	--

* No meaningful data.

TABLE C-17. CONCENTRATION OF TANTALUM (μg/g) IN FRACTIONATED FLY ASH

	Particle size (μm)	Density (g/cm^3)			
		<2.1	2.1-2.5	2.5-2.9	>2.9
Non-magnetic	<20	--*	--	--	--
	20-44	--	0.7	--	0.8
	44-74	0.5	0.6	0.7	0.7
	>74	0.7	0.4	0.8	0.6
Magnetic	<20	--*	--	--	0.5
	20-44	--	1.0	0.8	0.7
	44-74	1.4	0.9	1.0	--
	>74	--	--	--	--

* No meaningful data.

TABLE C-18. CONCENTRATION OF SAMARIUM (μg/g) IN FRACTIONATED FLY ASH

	Particle size (μm)	Density (g/cm³)			
		<2.1	2.1-2.5	2.5-2.9	>2.9
Non-magnetic	<20	9.1	12.1	13.0	8.7
	20-44	8.5	10.4	9.8	13.4
	44-74	6.4	6.5	8.0	9.1
	>74	6.4	7.0	8.3	8.9
Magnetic	<20	--*	--	7.5	6.3
	20-44	--	9.8	10.0	6.7
	44-74	8.6	7.9	--	--
	>74	6.4	--	--	--

* No meaningful data.

TABLE C-19. CONCENTRATION OF LANTHANUM (μg/g) IN FRACTIONATED FLY ASH

	Particle size (μm)	Density (g/cm^3)			
		<2.1	2.1-2.5	2.5-2.9	>2.9
Non-magnetic	<20	51	53	51	41
	20-44	51	53	42	55
	44-74	41	36	33	34
	>74	39	35	34	34
Magnetic	<20	--*	--	25	22
	20-44	--	41	40	24
	44-74	43	39	36	21
	>74	39	25	27	20

* No meaningful data.

TABLE C-20. CONCENTRATION OF GALLIUM (μg/g) IN FRACTIONATED FLY ASH

	Particle size (μm)	Density (g/cm³)			
		<2.1	2.1-2.5	2.5-2.9	>2.9
Non-magnetic	<20	90	93	70	55
	20-44	30	22	22	24
	44-74	8	13	21	20
	>74	11	17	29	28
Magnetic	<20	--*	--	58	50
	20-44	--	29	34	30
	44-74	14	23	31	46
	>74	23	24	48	11

* No meaningful data.

TABLE C-21. CONCENTRATION OF ANTIMONY (μg/g) IN FRACTIONATED FLY ASH

	Particle size (μm)	Density (g/cm^3)			
		<2.1	2.1-2.5	2.5-2.9	>2.9
Non-magnetic	<20	24	30	28	19
	20-44	7	11	20	23
	44-74	4	7	17	14
	>74	5	8	15	16
Magnetic	<20	--*	--	38	33
	20-44	--	29	38	21
	44-74	11	22	33	--
	>74	13	--	--	--

* No meaningful data.

TABLE C-22. DEPENDENCE OF ELEMENTAL CONCENTRATIONS ON PARTICLE SIZE FOR SIZE-FRACTIONATED COAL FLY ASH

Particle diameter (μm)	Pb	Ti	Sb	Cd	Se	As	Ni	Cr	Zn	S (wt %)	Mass fraction (%)
	(μg/g)										
A. Precipitator fly ash											
Sieved fractions											
>74	140	7	1.5	<10	<12	180	100	100	500	--	66.30
44-74	160	9	7	<10	<20	500	140	90	411	1.3	22.89
Aerodynamically sized fractions											
>40	90	5	8	<10	<15	120	300	70	730	<0.01	2.50
30-40	300	5	9	<10	<15	160	130	140	570	0.01	3.54
20-30	430	9	6	<10	<15	200	160	150	480	--	3.25
15-20	520	12	19	<10	<30	300	200	170	720	--	0.80
10-15	430	15	12	<10	<30	400	210	170	770	4.4	0.31
5-10	820	20	25	<10	<50	800	230	160	1100	7.8	0.33
<5	980	45	31	<10	<50	370	260	130	1400	--	0.08
B. Airborne fly ash											
>11.3	1100	29	17	13	13	680	460	740	8100	8.3	
7.3-11.3	1200	40	27	15	11	800	400	290	9000	--	
4.7-7.3	1500	62	34	18	16	1000	440	460	6600	7.9	
3.3-4.7	1550	67	34	22	16	900	540	470	3800	--	
2.1-3.3	1500	65	37	26	19	1200	900	1500	15000	25.0	
1.1-2.1	1600	76	53	35	59	1700	1600	3300	13000	--	
0.65-1.1	--	--	--	--	--	--	--	--	--	48.8	

TABLE C-23. DEPENDENCE OF ELEMENTAL CONCENTRATIONS ON PARTICLE SIZE FOR SIZE-FRACTIONATED COAL FLY ASH

Particle diameter (μm)	Fe (wt %)	Mn (μg/g)	V (μg/g)	Si (wt %)	Mg (wt %)	C (wt %)	Be (μg/g)	Al (wt %)
A. Precipitator fly ash								
Sieved fractions								
>74	--	700	150	--	--	--	12	--
44-74	18	600	260	18	0.39	11	12	9.4
Aerodynamically sized fractions								
>40	50	150	250	3.0	0.02	0.12	7.5	1.3
30-40	18	630	190	14	0.31	0.21	18	6.9
20-30	--	270	340	--	--	0.63	21	--
15-20	--	210	320	--	--	2.5	22	--
10-15	6.6	160	320	19	0.16	6.6	22	9.8
5-10	8.6	210	330	26	0.39	5.5	24	13
<5	--	180	320	--	--	--	24	--
B. Airborne fly ash								
>11.3	13	150	150	34	0.89	0.66	34	19.7
7.3-11.3	--	210	240	--	--	0.70	40	--
4.7-7.3	12	230	420	27	0.95	0.62	32	16.2
3.3-4.7	--	200	230	--	--	0.57	55	--
2.05-3.3	17	240	310	35	1.4	0.81	43	21.0
1.06-2.06	--	470	480	--	--	0.61	60	--
0.65-1.06	15	--	--	23	0.19	--	--	9.8

TABLE C-24. DEPENDENCE OF ELEMENTAL CONCENTRATIONS ON PARTICLE SIZE FOR SIZE-FRACTIONATED COAL FLY ASH

Particle diameter (μm)	Bi	Sn	Cu	Co	Ti	Ca	K
	(μg/g)				(wt %)		
A. Precipitator fly ash							
Sieved fractions							
>74	<2	<2	120	28	--	--	--
44-74	<2	<2	260	27	0.61	5.4	1.2
Aerodynamically sized fractions							
>40	<2	<2	220	75	0.01	2.5	2.54
30-40	<2	<2	120	76	0.64	6.3	6.26
20-30	<2	<2	160	55	--	--	--
15-20	<2	<2	220	50	--	4.5	4.46
10-15	<2	<2	220	55	0.66	4.0	4.04
5-10	<2	<2	390	46	1.09	--	--
<5	<2	<2	490	54	--	--	--
B. Airborne fly ash							
>11.3	<1.7	7	270	60	1.12	4.9	4.9
7.3-11.3	<3.5	11	390	85	--	--	--
4.7-7.3	<4.0	18	380	90	0.92	4.2	4.2
3.3-4.7	<4.8	19	--	95	--	--	--
2.06-3.3	<4.5	16	330	90	1.59	5.0	5.0
1.06-2.06	<4.4	18	300	130	--	--	
0.65-1.06	--	--	--	--	1.08	2.6	2.6

APPENDIX D

RESULTS OF DIFFERENT COAL FLY ASH LEACHING EXPERIMENTS

TABLE D-1. ANION CONCENTRATIONS RESULTING FROM COLUMN LEACHING AT 3 ML/MIN OF BULK CORRETTE FLY ASH WITH SOLUTIONS OF DIFFERENT pH

Anions*	Time (min)											
	0	15	60	120	180	360	540	720	1440	1800	2160	2880
						pH 7†						
F^-	3.7	1.4	0.25	0.15	0.11	0.08	0.07	0.06	0.04	0.03	0.02	0.01
Cl^-	4.3	0.4	0.11	0.09	0.05	0.03	0.02	0.01	0.01	<0.01	<0.01	<0.01
CO_3^{2-}	700	320	200	160	<100	<100	<100	<100	<100	<100	<100	<100
NO_3^-	45.	15.	8.5	5.8	3.2	3.0	2.6	2.4	2.0	1.2	0.83	0.42
SO_4^{2-}	750	24.	23.	22.	16.	8.4	5.6	3.9	2.8	2.0	1.3	0.8
						pH 3†						
F^-	2.6	0.80	0.70	0.62	0.50	0.48	0.40	0.30	0.21	0.13	0.05	0.02
Cl^-	3.3	1.5	1.4	0.86	0.48	0.24	0.22	0.20	0.13	0.07	0.04	0.01
SO_4^{2-}	860	31.	24.	23.	20.	10.	7.2	6.3	5.5	3.2	2.1	1.0
						pH 1†						
F^-	3.1	1.6	1.2	0.96	0.62	0.38	0.30	0.22	0.18	0.14	0.11	0.06
Cl^-	4.0	1.9	1.8	1.3	0.73	0.43	0.31	0.19	0.10	0.08	0.05	0.02
SO_4^{2-}	1000	44.	26.	25.	19.	16.	12.	9.9	6.3	4.1	1.9	1.1
						pH 7¶						
F^-	3.1	1.0	0.23	0.40	0.29	0.14	0.10	0.06	0.05	0.03	0 01	0.01
Cl^-	3.6	0 80	0.57	0.46	0.23	0.15	0.11	0.08	0.06	0.05	0.03	0.01
CO_3^{2-}	730	170	<100	<100	<100	<100	<100	<100	<100	<100	<100	<100
NO_3^-	36.	9.3	4.9	3.2	2.0	0.86	0.57	0.29	0.11	0.06	0.04	0.02
SO_4^{2-}	320	20.	18.	11.	9.3	5.9	3.2	1.8	0.70	0.60	0.40	0.20

* Concentrations expressed as μg of anion extracted per gram of fly ash.

† 6 mm fly ash column height.

¶ 5 mm fly ash column height.

TABLE D-2. ELEMENTAL CONCENTRATIONS RESULTING FROM COLUMN LEACHING AT 3 ML/MIN OF BULK CORRETTE FLY ASH WITH A pH 7 SOLUTION

	Time (min)											
Element*	0	15	60	120	180	360	540	720	1440	1800	2160	2880
B	19.	16.	3.4	2.5	1.8	0.66	0.10	0.02	<0.02	<0.02	<0.02	<0.02
Cd	12.	12.	8.5	8.5	7.6	7.9	7.2	5.2	2.4	1.1	1.1	1.1
Be	0.19	0.07	0.07	0.04	0.03	0.02	0.01	<0.01	<0.01	<0.01	<0.01	<0.01
Mg	<0.07	<0.07	<0.07	<0.07	1.8	1.2	0.78	0.50	0.21	0.07	<0.07	<0.07
P	49.	41.	53.	46.	59.	62.	41.	36.	30.	28.	33.	10.
Si	42.	33.	27.	26.	15.	12.	12.	5.0	4.4	4.1	4.0	3.7
Mo†	2.2	1.5	0.75	0.28	0.08	0.07	<0.01	<0.01	<0.01	<0.01	<0.01	<0.01
Mn†	2.9	1.7	1.0	1.3	0.75	0.47	0.30	0.11	0.09	0.04	0.01	<0.01
Ni†	<0.01	<0.01	<0.01	<0.01	<0.01	<0.01	<0.01	<0.01	<0.01	<0.01	<0.01	<0.01
Na	45.	36.	29.	16.	13.	10.	5.7	2.3	2.1	1.0	0.34	0.12
Cu	<0.01	<0.01	<0.01	<0.01	<0.01	<0.01	<0.01	<0.01	<0.01	<0.01	<0.01	<0.01
Al†	44.	42.	41.	31.	26.	22.	14.	10.	9.0	7.2	7.0	6.9
Ca	2800	1200	870	740	290	160	35.	13.	1.1	<1.0	<1.0	<1.0
Ba†	22.	27.	13.	9.0	6.0	5.3	2.9	0.56	0.11	<0.05	<0.05	<0.05
K	47.	55.	58.	55.	39.	29.	28.	21.	15.	11.	11.	9.1
Cr†	3.0	2.1	2.0	1.6	1.6	0.81	0.63	0.23	0.06	<0.01	<0.01	<0.01
Sr†	50.	18.	5.8	3.0	2.8	1.6	0.37	0.30	0.16	0.04	<0.01	<0.01
Pb†	4.6	2.1	0.08	0.69	0.67	0.31	0.15	<0.01	<0.01	<0.01	<0.01	<0.01
Li¶	1.2	0.10	0.04	0.03	0.02	0.02	0.02	0.01	0.01	0.01	0.01	0.01
Fe§	0.01	<0.01	<0.01	0.03	0.10	0.12	0.10	0.09	0.07	0.06	0.05	0.04
Zn§	0.07	0.25	0.04	0.03	0.02	0.02	0.01	0.01	0.06	<0.01	<0.01	<0.01
pH	12.2	12.1	11.9	11.2	10.4	3.7	3.3	3.3	3.2	3.2	3.1	3.1

* Concentrations expressed as μg of element extracted per gram of fly ash.

† Calcium stray light corrections applied.

¶ Flame emission.

§ Atomic absorption.

TABLE D-3. ELEMENTAL CONCENTRATIONS AND pH CHANGES RESULTING FROM COLUMN LEACHING AT 3 ML/MIN OF BULK CORRETTE FLY ASH WITH A pH 3 SOLUTION

	Time (min)											
Element*	0	15	60	120	180	360	540	720	1440	1800	2160	2880
B	52.	14.	0.22	<0.02	<0.02	<0.02	<0.02	<0.02	<0.02	<0.02	<0.02	<0.02
Cd	45.	65.	48.	35.	21.	2.0	0.03	<0.03	<0.03	<0.03	<0.03	<0.03
Be	1.2	0.96	0.70	0.40	0.28	0.06	<0.01	<0.01	<0.01	<0.01	<0.01	<0.01
Mg	150	330	160	100	76.	54.	38.	24.	17.	10.	3.2	0.98
P	205	250	230	120	41.	15.	12.	8.3	12	7.1	4.2	4.0
Si	345	375	260	190	105	61.	48.	20.	5.1	5.1	4.0	<0.10
Mo†	8.1	6.1	0.67	<0.01	<0.01	<0.01	<0.01	<0.01	<0.01	<0.01	<0.01	<0.01
Mn†	15.	13.	12.	7.0	3.5	0.10	<0.01	<0.01	<0.01	<0.01	<0.01	<0.01
Ni†	<0.01	<0.01	<0.01	<0.01	<0.01	<0.01	<0.01	<0.01	<0.01	<0.01	<0.01	<0.01
Na	77.	160	66.	41.	17.	8.3	1.2	0.24	0.09	<0.05	<0.05	<0.05
Cu	<0.01	<0.01	<0.01	<0.01	<0.01	<0.01	<0.01	<0.01	<0.01	<0.01	<0.01	<0.01
Al†	480	380	330	210	110	95.	61.	38.	10.	4.0	1.0	0.03
Ca	11,800	5400	820	815	430	190	180	150	135	72	31	8.0
Ba†	36.	63	38.	16.	8.2	6.4	0.54	0.11	<0.05	<0.05	<0.05	<0.05
K	285	400	300	190	84.	67.	33.	22.	1.0	<0.05	<0.05	<0.05
Cr†	8.4	5.4	4.0	1.1	0.91	<0.01	<0.01	<0.01	<0.01	<0.01	<0.01	<0.01
Sr†	110	45.	16.	12.	6.6	4.0	3.8	3.8	1.5	0.41	<0.01	<0.01
Pb†	4.8	4.6	0.33	0.01	<0.01	<0.01	<0.01	<0.01	<0.01	<0.01	<0.01	<0.01
Li¶	0.77	0.21	0.16	0.14	0.13	0.10	0.08	0.07	0.05	0.03	0.02	0.02
Fe§	31.	34.	20.	14.	11.	6.4	4.8	3.1	1.4	0.73	0.43	0.33
Zn§	0.14	0.27	0.12	0.09	0.04	0.03	0.02	0.01	1.7	0.01	0.01	0.01

* Concentrations expressed as μg of element extracted per gram of fly ash.

† Calcium stray light corrections applied.

¶ Flame emission.

§ Atomic absorption.

TABLE D-4. ELEMENTAL CONCENTRATIONS RESULTING FROM COLUMN LEACHING AT 3 ML/MIN OF BULK CORRETTE FLY ASH WITH A pH 1 SOLUTION

Element*	Time (min)											
	0	15	60	120	180	360	540	720	1440	1800	2160	2880
B	9.5	9.1	2.0	0.89	0.81	0.68	0.28	0.10	0.04	<0.02	<0.02	<0.02
Cd	1.5	0.87	0.85	0.54	0.44	0.39	0.38	0.29	0.30	0.25	0.24	0.26
Be	<0.01	<0.01	<0.01	<0.01	<0.01	<0.01	<0.01	<0.01	<0.01	0.01	0.04	0.03
Mg	<0.07	<0.07	0.03	0.23	0.40	0.47	0.50	0.52	0.58	0.60	0.70	0.70
P	14.	3.2	3.6	2.7	1.8	5.0	2.1	1.9	6.0	1.1	7.1	0.99
Si	13.	42.	20.	18.	4.2	1.9	2.2	1.9	0.84	0.69	3.0	4.0
Mo†	4.1	0.22	0.01	<0.01	<0.01	<0.01	<0.01	<0.01	<0.01	<0.01	<0.01	<0.01
Mn†	0.36	0.03	0.08	0.11	0.04	0.35	0.03	0.08	0.25	0.05	0.27	0.06
Ni†	<0.01	<0.01	<0.01	<0.01	<0.01	<0.01	<0.01	<0.01	<0.01	<0.01	<0.01	<0.01
Na	37.	11.	6.8	5.4	5.0	2.5	2.0	0.98	0.50	0.44	0.32	0.11
Cu	<0.01	<0.01	<0.01	<0.01	<0.01	<0.01	<0.01	<0.01	<0.01	<0.01	<0.01	<0.01
Al†	18.	52.	25.	11.	8.8	8.7	6.0	3.7	2.8	1.2	1.1	1.2
Ca	1800	560	260	170	70.	3.5	<1.0	<1.0	<1.0	<1.0	<1.0	<1.0
Ba†	5.5	13	7.4	6.5	2.8	0.84	0.50	0.49	0.42	0.37	0.12	0.09
K	75.	54.	37	26.	22.	16.	12.	13.	18.	14.	11.	12.
Cr†	3.0	0.73	0.72	0.52	0.49	0.31	0.22	0.11	0.07	0.07	<0.01	<0.01
Sr†	26	12.	4.0	2.1	1.3	0.09	<0.01	<0.01	<0.01	<0.01	<0.01	<0.01
Pb†	9.5	2.5	2.0	1.7	0.83	0.39	0.26	0.22	0.11	0.05	<0.01	<0.01
Li¶	1.38	0.08	0.03	0.03	0.02	0.01	0.01	0.01	0.01	0.01	0.01	0.01
Zn§	<0.01	<0.01	<0.01	<0.01	<0.01	<0.01	<0.01	<0.01	<0.01	<0.01	0.15	0.38

* Concentrations expressed as μg of element extracted per gram of fly ash.

† Calcium stray light corrections applied.

¶ Flame emission.

§ Atomic absorption.

TABLE D-5. ANION CONCENTRATIONS* RESULTING FROM COLUMN LEACHING AT 3 ML/MIN OF DIFFERENT SIZE FRACTIONS OF CORETTE FLY ASH WITH A pH 7 SOLUTION

	Time (min)								
	150-180 μm								
Anions	0	15	60	120	180	360	540	720	1440
F^-	3.2	0.95	0.60	0.25	0.11	0.09	0.07	0.05	<0.01
Cl^-	5.6	0.50	0.36	0.20	0.07	0.05	<0.01	<0.01	<0.01
SO_4^{2-}	930	44.	18.	18.	14.	13.	12.	9.8	7.9
	45-74 μm								
F^-	1.8	0.55	0.17	0.15	0.11	0.06	0.05	<0.01	<0.01
Cl^-	1.9	0.15	0.10	0.09	0.05	<0.01	<0.01	<0.01	<0.01
CO_3^{2-}	300	220	175	<100	<100	<100	<100	<100	<100
SO_4^{2-}	560	21	4.8	2.8	1.9	1.0	0.80	0.60	0.50
	20-30 μm								
F^-	1.8	0.31	0.10	0.05	<0.01	<0.01	<0.01	<0.01	<0.01
Cl^-	0.85	0.15	0.09	0.02	<0.01	<0.01	<0.01	<0.01	<0.01
CO_3^{2-}	280	200	155	<100	<100	<100	<100	<100	<100
SO_4^{2-}	540	28.	10.	6.5	5.1	4.9	3.8	1.9	1.1

* Concentrations expressed as μg of anion extracted per gram of fly ash.

TABLE D-6. ELEMENTAL CONCENTRATIONS* RESULTING FROM COLUMN LEACHING AT 3 ML/MIN OF THE 20-30 μm SIZE FRACTION OF CORRETTE FLY ASH WITH A pH 7 SOLUTION

	Time (min)								
Element	0	15	60	120	180	360	540	720	1440
B	30.	20.	6.2	1.2	0.81	0.23	0.09	0.02	<0.02
Cd	<0.03	0.44	0.60	0.74	0.79	0.91	0.99	0.97	0.32
Be	<0.01	<0.01	<0.01	<0.01	<0.01	<0.01	<0.01	<0.01	<0.01
Mg	0.57	0.61	0.77	0.70	0.62	0.51	0.47	0.21	0.31
P	1.9	<0.10	3.77	<0.10	2.0	1.0	<0.10	<0.10	<0.10
Si	8.0	6.8	6.7	3.5	2.0	1.1	1.0	1.0	1.0
Mo†	1.3	0.43	0.27	0.08	0.01	<0.01	<0.01	<0.01	<0.01
Mn†	<0.01	<0.01	<0.01	<0.01	<0.01	<0.01	<0.01	<0.01	<0.01
Ni†	<0.01	<0.01	<0.01	<0.01	<0.01	<0.01	<0.01	<0.01	<0.01
Na	65.	2.0	1.9	<0.05	<0.05	<0.05	<0.05	<0.05	<0.05
Cu	<0.05	<0.01	<0.01	<0.01	<0.01	<0.01	0.01	<0.01	<0.01
Al†	37.	29.	19.	13.	10.	7.2	6.8	5.8	4.1
Ca	1400	480	220	120	77.	30.	12.	10.	8.1
Ba†	14	12	6.2	2.3	1.2	1.1	0.83	0.64	0.21
K	140	51	6.4	3.4	1.6	0.78	0.28	0.09	0.13
Cr†	0.40	0.20	0.15	<0.01	<0.01	<0.01	<0.01	<0.01	<0.01
Sr†	42.	25.	10.	4.0	2.0	1.1	0.48	0.27	0.18
Pb†	1.3	0.35	0.25	<0.01	<0.01	<0.01	<0.01	<0.01	<0.01

* Concentrations expressed as μg of element extracted per gram of fly ash.

† Calcium stray light corrections applied.

TABLE D-7. ELEMENTAL CONCENTRATIONS* RESULTING FROM COLUMN LEACHING AT 3 ML/MIN OF THE 45-74 μm SIZE FRACTION OF CORRETTE FLY ASH WITH A pH 7 SOLUTION

	Time (min)								
Element	0	15	60	120	180	360	540	720	1440
B	19.	18.	4.1	1.1	0.68	0.28	0.03	<0.02	<0.02
Cd	<0.03	<0.03	0.13	0.27	0.32	0.48	0.52	0.50	0.49
Be	<0.01	<0.01	<0.01	<0.01	<0.01	<0.01	<0.01	<0.01	<0.01
Mg	<0.07	<0.07	<0.07	<0.07	<0.07	<0.07	<0.07	<0.07	<0.07
P	1.1	<0.10	0.21	5.3	3.0	<0.10	2.0	<0.10	<0.10
Si	12.	7.0	2.3	2.2	2.0	1.9	1.2	1.3	1.2
Mo†	1.1	0.59	0.28	0.24	0.11	0.08	<0.01	<0.01	<0.01
Mn†	<0.01	0.37	1.4	<0.01	<0.01	<0.01	<0.01	<0.01	<0.01
Ni†	<0.01	<0.01	<0.01	<0.01	<0.01	<0.01	<0.01	<0.01	<0.01
Na	23.	7.1	1.6	1.5	1.0	0.92	0.63	0.21	0.20
Cu	<0.01	<0.01	<0.01	<0.01	<0.01	<0.01	<0.01	<0.01	<0.01
Al†	9.8	4.7	4.2	4.1	4.0	4.0	2.2	2.0	1.3
Ca	2400	1100	350	190	110	39.	21.	17.	13.
Ba†	9.7	18.	6.5	2.8	1.2	0.88	0.24	0.25	0.21
K	280	120	18.	7.3	4.8	0.57	0.28	0.29	0.30
Cr†	0.26	0.20	0.14	0.12	0.07	0.03	<0.01	<0.01	<0.01
Sr†	51.	24.	6.9	3.1	2.2	2.0	1.5	1.2	1.0
Pb†	1.4	0.49	0.31	0.21	0.02	<0.01	<0.01	<0.01	<0.01

* Concentrations expressed as μg of element extracted per gram of fly ash.

† Calcium stray light corrections applied.

TABLE D-8. METAL CONCENTRATIONS* RESULTING FROM COLUMN LEACHING AT 3 ML/MIN OF THE 45-74 μm SIZE FRACTION OF CORRETTE FLY ASH WITH A pH 7 SOLUTION

	Time (min)								
Element	0	15	60	120	180	360	540	720	1440
B	23.	16.	4.9	1.9	0.5	0.2	0.08	<0.02	<0.02
Cd	<0.03	<0.03	<0.03	<0.03	<0.03	<0.03	<0.03	<0.03	<0.03
Be	<0.01	<0.01	<0.01	<0.01	<0.01	<0.01	<0.01	<0.01	<0.01
Mg	<0.07	<0.07	<0.07	<0.07	<0.07	<0.07	<0.07	<0.07	<0.07
P	<0.10	<0.10	<0.10	<0.10	<0.10	<0.10	<0.10	<0.10	<0.10
Si	18.	31.	40.	41.	46.	38.	37.	40.	47.
Mo†	1.2	0.7	0.59	0.13	<0.01	<0.01	<0.01	<0.01	<0.01
Mn†	0.29	0.42	1.2	0.22	<0.01	<0.01	<0.01	<0.01	<0.01
Ni†	<0.01	<0.01	<0.01	<0.01	<0.01	<0.01	<0.01	<0.01	<0.01
Na	11.	7.7	5.4	3.0	1.0	0.51	<0.05	<0.05	<0.05
Cu	<0.01	<0.01	<0.01	<0.01	<0.01	<0.01	<0.01	<0.01	<0.01
Al†	0.86	3.0	7.0	14.	15.	16.	17.	17.	17.
Ca	4200	2700	1800	550	280	120	78.	45.	29.
Ba†	14.	32.	8.5	2.2	1.0	0.78	0.56	0.11	0.08
K	190	50.	44.	29.	4.9	3.1	2.1	1.8	1.1
Cr†	0.17	0.08	0.06	0.03	<0.01	<0.01	<0.01	<0.01	<0.01
Sr†	53.	22.	8.3	4.0	2.9	2.0	1.4	1.3	1.1
Pb†	1.4	0.67	0.35	<0.01	<0.01	<0.01	<0.01	<0.01	<0.01

* Concentrations expressed as μg of element extracted per gram of fly ash.

† Calcium stray light corrections applied.

TABLE D-9. ANION CONCENTRATIONS* RESULTING FROM MODIFIED SOXHLET LEACHING OF BULK CORRETTE FLY ASH WITH A pH 7 SOLUTION

	Anion							
	F^-		Cl^-		NO_3^-		SO_4^{2-}	
Time (min)	S.E.†	B.F.¶	S.E.	B.F.	S.E.	B.F.	S.E.	B.F.
1st cycle	1.3	15	1.8	33	<0.01	<0.01	103	760
15	1.0	12	1.5	26	<0.01	<0.01	70	600
60	0.37	6.8	0.73	12	<0.01	<0.01	6.6	240
120	0.29	7.6	0.55	12	<0.01	0.40	2.4	310
180	0.18	8.4	0.22	16	<0.01	2.0	0.88	300
360	0.17	9.6	0.30	15	<0.01	4.8	0.51	340
540	0.13	11.	0.15	16	<0.01	11.	0.42	340
720	0.11	11.	0.10	16	<0.01	12.	0.29	330
900	0.14	12.	0.04	19	<0.01	14.	0.23	350
1080	0.10	13.	<0.01	21	<0.01	15.	0.22	350
1260	0.09	13.	<0.01	21	0.01	16	0.20	340
1440	0.07	14.	<0.01	23	0.03	16.	0.18	340
1800	0.13	16.	<0.01	24	0.06	18.	0.35	380
2160	0.07	16.	<0.01	22	0.07	18.	0.20	370
2880	0.06	17.	<0.01	23	0.07	17.	0.20	350

* Concentration expressed as μg of anion extracted per gram of fly ash.

† Soxhlet extractor (interval).

¶ Bottom flask (cumulative).

TABLE D-10. ELEMENTAL CONCENTRATIONS* RESULTING FROM MODIFIED SOXHLET LEACHING OF BULK CORRETTE FLY ASH WITH A pH 7 SOLUTION. CONCENTRATION (INTERVAL) IN EXTRACTOR

	Element										
Time (min)	Li†	Na	K	Be	Mg	Ca	Sr¶	Ba¶	Cr¶	Mo¶	Mn¶
1st cycle	13.	3.4	1.8	<0.01	1.0	150	11.	3.6	0.03	0.39	<0.01
15	6.0	0.57	0.16	<0.01	1.0	110	7.4	1.9	<0.01	0.07	<0.01
60	3.6	0.21	0.05	<0.01	0.66	79.	6.7	1.3	0.02	0.01	<0.01
120	3.1	0.20	0.04	<0.01	0.63	65.	5.6	1.3	0.06	<0.01	<0.01
180	3.2	0.15	0.07	<0.01	0.20	54.	3.8	1.3	0.04	<0.01	<0.01
360	2.8	0.16	0.08	<0.01	0.12	40.	1.8	1.3	0.07	<0.01	<0.01
540	2.5	0.10	0.05	<0.01	0.70	31.	0.80	1.2	0.40	<0.01	<0.01
720	2.5	0.07	0.10	<0.01	0.70	22.	0.70	1.2	0.09	<0.01	<0.01
900	2.3	0.05	0.58	<0.01	0.91	18.	0.40	1.1	0.07	<0.01	<0.01
1080	2.1	0.22	1.0	<0.01	0.89	16.	0.20	0.95	0.05	<0.01	<0.01
1260	2.0	0.30	2.0	<0.01	1.0	16.	0.10	0.90	0.04	<0.01	<0.01
1440	1.9	0.50	2.9	<0.01	1.5	16.	<0.01	0.96	0.07	<0.01	<0.01
1800	1.9	0.88	3.8	<0.01	1.9	16.	<0.01	0.70	1.1	<0.01	<0.01
2160	1.8	4.8	4.3	<0.01	2.4	15.	<0.01	0.64	0.02	<0.01	<0.01
2880	1.8	4.5	4.6	<0.01	2.2	15.	<0.01	0.68	0.07	<0.01	<0.01

TABLE D-10. (Continued).

Time (min)	Element									
	Fe§	Ni¶	Cu	Zn§	Cd	B	Al¶	Si	Pb	P
1st cycle	0.62	<0.01	0.14	0.36	0.15	2.8	4.8	<0.10	0.58	2.1
15	0.51	0.08	0.16	0.42	0.16	1.7	3.0	0.60	0.11	1.9
60	0.47	0.12	0.17	0.60	0.21	1.2	2.0	2.1	0.01	2.2
120	0.30	0.28	0.36	0.51	0.42	0.21	1.3	5.9	0.02	4.0
180	0.31	0.28	0.37	0.33	0.42	<0.02	0.88	7.5	<0.01	3.7
360	0.25	0.29	0.31	0.26	0.39	0.12	0.44	7.7	0.15	3.5
540	0.20	0.51	0.40	0.64	0.50	0.33	0.48	12.	0.28	4.9
720	0.26	0.42	0.36	0.26	0.41	0.32	0.44	12.	<0.01	2.4
900	0.31	0.46	0.40	0.30	0.52	0.36	0.21	13.	0.02	1.7
1080	0.35	0.54	0.37	0.31	0.56	0.49	0.11	13.	0.04	1.5
1260	0.25	0.58	0.39	0.32	0.60	0.46	0.18	15.	0.12	1.8
1440	0.31	0.59	0.40	0.33	0.59	0.51	<0.03	16.	0.23	1.5
1800	0.33	0.70	0.37	0.26	0.66	0.46	<0.03	17.	0.35	1.7
2160	0.47	0.62	0.35	0.84	0.57	0.35	<0.03	17	<0.01	2.3
2880	0.31	0.55	0.24	0.42	0.55	0.29	<0.03	15.	0.22	1.5

* Concentrations expressed as μg of element extracted per gram of fly ash.

† Flame emission.

¶ Calcium stray light corrections applied.

§ Atomic absorption.

TABLE D-11. ELEMENTAL CONCENTRATIONS* RESULTING FROM MODIFIED SOXHLET LEACHING OF BULK CORRETTE FLY ASH WITH A pH 7 SOLUTION. CONCENTRATION (CUMULATIVE) IN BOTTOM FLASK

	Element										
Time (min)	Li†	Na	K	Be	Mg	Ca	Sr¶	Ba¶	Cr¶	Mo¶	Mn¶
1st cycle	24.	<0.05	62.	<0.01	1.2	600	16.	2.3	0.34	0.29	0.5
15	25.	13.	69.	<0.01	2.3	1000	33.	4.2	0.97	0.57	1.0
60	29.	55.	86.	<0.01	5.6	1600	75.	7.4	1.5	0.97	1.7
120	33.	<0.05	250	<0.01	1.8	1900	120	9.0	4.0	3.0	3.6
180	35.	<0.05	250	<0.01	<0.07	2100	160	10.	5.8	10.	10.
360	40.	140	470	<0.01	<0.07	3000	240	22.	7.7	10.	9.8
540	45.	100	660	<0.01	<0.07	3100	290	50.	12.	17.	18.
720	50.	34.	700	<0.01	<0.07	3400	350	100	7.6	10.	13.
900	52.	50.	760	<0.01	<0.07	3500	390	160	6.4	7.6	11.
1080	56	69.	800	<0.01	<0.07	3800	420	220	6.5	7.5	12.
1260	57.	76.	830	<0.01	<0.07	3900	440	270	6.6	7.6	14.
1440	58	<0.05	1700	<0.01	1.6	3700	450	270	11.	10.	19.
1800	63.	<0.05	1700	<0.01	16.	3800	470	210	14.	12.	26.
2160	64.	<0.05	1800	<0.01	18.	3800	480	190	16.	9.2	28.
2880	67.	<0.05	1900	<0.01	16.	3600	480	210	16.	9.6	26.

TABLE D-11 (continued).

Time (min)	Element								
	Fe§	Ni¶	Cu	Zn§	Cd	B	Al¶	Si	Pb
1st cycle	2.6	<0.01	<0.01	3.8	1.0	6.9	18.	30.	<0.01
15	2.1	0.06	<0.01	3.6	1.0	20.	35.	120	<0.01
60	1.3	0.34	<0.01	3.7	1.1	42.	59.	220	0.3
120	2.3	1.1	0.13	3.5	2.9	51.	68.	340	<0.01
180	2.6	1.7	0.79	3.3	4.5	74	91.	290	6.9
360	2.8	2.5	1.5	2.9	6.5	100	93.	140	7.7
540	2.7	3.4	<0.01	4.4	6.4	130	50.	50.	12.
720	2.9	<0.01	<0.01	5.0	9.0	170	54	<0.1	<0.01
900	3.0	1.4	<0.01	4.1	9.8	180	64.	<0.1	7.0
1080	3.2	1.9	0.20	3.9	10.	200	73.	<0.1	8.0
1260	3.4	2.0	0.60	3.3	10.	210	83.	<0.1	8.2
1440	4.0	19.	<0.01	2.8	26.	130	64.	<0.1	38.
1800	4.0	15.	4.0	5.3	18.	140	86.	<0.1	36.
2160	5.3	15.	5.6	4.0	21.	150	98.	<0.1	56.
2880	6.6	17.	4.0	3.4	18.	160	115.	<0.1	64.

* Concentrations expressed as μg of element extracted per gram of fly ash.

† Flame emission.

¶ Calcium stray light corrections applied.

§ Atomic absorption.

TABLE D-12. ELEMENTAL CONCENTRATIONS* RESULTING FROM MODIFIED SOXHLET LEACHING OF BULK CORRETTE FLY ASH AND $CaSO_4$. CONCENTRATION (CUMULATIVE) IN BOTTOM FLASK

	Element									
Time (min)	Na	K	Be	Mg	Ca	Sr†	Ba†	Cr†	Mo†	Mn
1st cycle	10.	7.3	<0.01	0.46	1000	6.6	1.1	0.1	<0.01	<0.01
15	42.	6.3	<0.01	<0.07	1700	11.	2.1	0.29	<0.01	<0.01
60	110	14.	<0.01	1.3	2700	24.	4.5	0.9	<0.01	<0.01
120	74.	81.	<0.01	0.66	3300	34.	5.9	2.8	0.9	<0.01
180	74.	98.	<0.01	<0.07	3800	42.	7.7	2.6	0.66	0.53
360	160	96.	<0.01	1.3	5900	70.	14.	4.6	1.3	<0.01
540	92.	190	<0.01	1.0	7800	98.	90.	6.8	2.0	1.2
720	110	200	<0.01	4.8	9300	120	25.	7.6	2.2	0.6
900	120	180	<0.01	7.0	--	140	30.	8.0	2.2	0.6
1080										
1260	130	160	<0.01	12.	--	170	34.	11.	3.0	<0.01
1440	<0.05	440	<0.01	5.2	15000	190	32.	19.	7.2	0.80
1800	<0.05	440	<0.01	11.	18000	220	20.	22.	7.6	<0.01
2160	56.	450	<0.01	12.	20000	240	100	26.	10.	<0.01
2880	12.	390	<0.01	18.	17000	96.	9.6	31.	13.	<0.01

TABLE D-12 (continued).

Time (min)	Element					
	Ni†	Cu	Cd	B	Al†	Si
1st cycle	0.40	<0.01	0.1	<0.02	1.9	<0.10
15	0.46	<0.01	0.3	<0.02	7.6	<0.10
60	0.86	<0.01	0.8	<0.02	28.	9.2
120	2.5	<0.01	1.1	<0.02	44.	<0.10
180	2.5	<0.01	2.9	<0.02	66.	2.6
360	3.8	<0.01	2.1	<0.02	130	69.
540	5.4	<0.01	7.4	<0.02	170	62.
720	5.0	<0.01	7.2	<0.02	220	82.
900	5.8	<0.01	9.4	<0.02	270	110
1080						
1260	6.4	<0.01	8.4	<0.02	340	50.
1440	12.	0.80	28.	<0.02	320	<0.10
1800	13.	<0.01	23.	<0.02	360	<0.10
2160	16.	0.80	27.	<0.02	400	<0.10
2880	17.	10.	22.	<0.02	460	<0.10

* Concentrations expressed as μg of element extracted per gram of fly ash.

† Flame emission.

¶ Calcium stray light corrections applied.

§ Atomic absorption.

TABLE D-13. ELEMENTAL CONCENTRATIONS* RESULTING FROM CONTINUOUS RECYCLE (SOXHLET) LEACHING OF BULK CORRETTE FLY ASH AS A FUNCTION OF DILUTION

	Dilution (ml/g)									
Element	5	10	25	50	75	100	200	600	1000	10000
Li	4.6	10.	5.9	6.2	5.9	7.2	8.1	7.8	10.	31.
Na	52.	76.	19.	12.	13.	<0.05	<0.05	<0.05	<0.05	<0.05
K	9.5	8.6	1.3	<0.05	<0.05	<0.05	<0.05	<0.05	<0.05	<0.05
Mg	<0.07	2.7	<0.07	0.30	1.8	0.60	0.80	180	500	1900
Ca	2400	6200	8500	5600	7000	11000	25000	13000	22000	170000
Sr	150	210	320	280	310	380	490	480	600	2900
Ba	320	510	550	320	370	470	670	410	560	3800
Fe	0.05	0.20	0.15	0.11	0.16	0.15	0.78	1.7	2.3	13.
Zn	0.09	0.10	0.23	0.08	0.01	0.05	2.4	0.38	2.0	11.
Cu	0.04	0.09	0.06	0.24	0.10	0.52	0.42	0.15	1.0	2.0
Cd	<0.03	<0.03	<0.03	<0.03	<0.03	<0.03	<0.03	0.04	0.05	0.57
Cr	<0.01	<0.01	0.13	0.22	0.24	0.84	2.5	4.1	4.6	7.0
Mn	0.01	0.03	0.02	0.02	0.02	0.06	0.14	0.90	1.3	7.0
Pb	0.02	0.02	0.21	0.02	<0.01	0.15	6.2	0.37	1.0	7.5
Ni	<0.01	<0.01	0.06	<0.01	0.01	0.01	0.05	0.10	<0.01	3.0
pH	12.7	12.5	12.2	11.3	10.8	11.5	11.5	8.5	8.5	8.2

* Concentrations expressed as μg of element extracted per gram of fly ash.

TABLE D-14. ELEMENTAL CONCENTRATIONS* RESULTING FROM CONTINUOUS RECYCLE (SOXHLET) LEACHING OF BULK CORRETTE FLY ASH

Element	Time (min)						
	5	15	60	180	360	720	1440
Li	0.19	0.78	1.9	1.9	1.1	0.56	0.50
Na	<0.05	5.3	17.	12.	6.6	<0.05	6.9
K	--	--	1.6	--	0.6	--	3.1
Mg	1.4	0.60	0.70	0.80	1.4	1.5	1.5
Ca	190	500	1100	2200	2800	3900	4700
Sr	1.6	14.	47.	74.	69.	86.	73.
Ba	3.1	12.	41.	91.	170	450	720
Fe	0.34	0.09	0.11	0.07	0.08	0.07	0.09
Zn	0.24	0.21	0.40	0.54	0.59	0.89	1.0
Cu	0.02	0.02	0.02	0.02	0.05	0.06	0.07
Cd	<0.03	<0.03	<0.03	<0.03	<0.03	<0.03	<0.03
Cr	0.01	0.02	0.01	0.08	0.06	0.06	0.06
Mn	0.06	0.02	0.02	0.01	<0.01	<0.01	<0.01
pH	9.2	10.0	10.8	11.0	11.1	11.0	11.8

* Concentrations expressed as μg of element extracted per gram of fly ash.

TABLE D-15. ELEMENTAL CONCENTRATIONS* RESULTING FROM CONTINUOUS AND INTERMITTENT RECYCLE (SOXHLET) LEACHING OF BULK CORRETTE FLY ASH FOR 24-HOUR AND 7-DAY TIME PERIODS

	Quantity			
	Continuous		Intermittent	
Element	24 hr	7 days	24 hr	7 days
Li	6.2		7.0	
Na	16		48	
K	--		--	
Mg	1.1		7.9	
Ca	5600	12000	15000	12000
Sr	280	550	370	500
Ba	270	720	1500	520
Fe	0.05		0.85	
Zn	1.2		3.9	
Cu	0.09		0.28	
Cd	<0.03		0.04	
Cr	0.26		0.28	
Mn	<0.01		0.10	
pH	11.9	12.0	--	--
Specific conductivity (μmhos/cm)	5900	3200		6600
Alkalinity (mg/liter $CaCO_3$)	1000	690		1400
Hardness (mg/liter $CaCO_3$)	1100	780		1500
SO_4^{2-} (μg/ml)	<0.01	<0.01		--
F^- (μg/ml)	0.33	0.24		--

* Concentrations expressed as μg of element extracted per gram of fly ash.

TABLE D-16. ELEMENTAL CONCENTRATIONS* RESULTING FROM 24-HOUR CONTINUOUS RECYCLE (SOXHLET) LEACHING OF BULK CORRETTE FLY ASH AS A FUNCTION OF PARTICLE SIZE

	Particle diameter (μm)					
Element	>180	150-180	74-150	45-74	30-45	20-30
Li	1.3	2.2	5.3	6.8	11.	13.
Na	1.9	2.2	23.	59.	67.	82.
Mg	5.8	1.9	2.7	10.	14.	12.
Ca	46000	46000	48000	13000	11000	6600
Sr	240	290	370	380	420	430
Ba	1400	1900	3200	1500	680	600
Fe	0.77	0.99	0.70	1.1	0.89	2.5
Zn	1.5	8.3	1.6	5.3	0.85	1.4
Cu	0.77	0.98	0.64	0.16	0.15	0.16
Cd	0.05	0.05	0.05	0.04	0.03	0.04
Cr	0.74	0.63	0.87	0.36	0.60	0.73
Mn	0.09	0.01	0.02	0.02	0.04	0.02

* Concentrations expressed as μg of element extracted per gram of fly ash.

TABLE D-17. ELEMENTAL CONCENTRATIONS* RESULTING FROM 24-HOUR CONTINUOUS RECYCLE (SOXHLET) LEACHING AS A FUNCTION OF TEMPERATURE

Element	Temperature 25°C	65°C
Li	7.0	12.
Na	48.	140
K	5.3	91.
Mg	7.9	8.8
Ca	15000	25000
Sr	370	610
Ba	1500	2000
Fe	0.85	1.4
Zn	3.9	2.1
Cu	0.28	0.43
Cd	0.04	0.04
Cr	0.28	1.5
Mn	0.10	0.08

* Concentrations expressed as μg of element leached per gram of fly ash.

TABLE D-18. ANION CONCENTRATIONS* RESULTING FROM A 3-HOUR SONIC EXTRACTION OF BULK CORRETTE FLY ASH AS A FUNCTION OF DILUTION

	Dilution (ml/g)											
Anion	5	10	25	40	50	75	100	200	400	600	1000	10000
F^-	8.1	17.	34.	47.	46.	53.	63.	110	92.	150	150	700
Cl^-	8.8	10.	16.	18.	15.	22.	28.	150	96.	320	300	3000
NO_3^-	4.7	6.3	12.	15.	19.	50.	76.	76.	150	290	660	7600
SO_4^{2-}	450	650	880	1300	1400	1400	1200	5300	6100	7500	8500	10000
pH	12.7	12.6	12.5	12.5	12.4	12.3	12.3	12.1	11.8	11.7	11.5	10.4

* Concentration expressed as μg of anion extracted per gram of fly ash.

TABLE D-19. ELEMENTAL CONCENTRATIONS* RESULTING FROM A 3-HOUR SONIC EXTRACTION OF BULK CORRETTE FLY ASH AS A FUNCTION OF DILUTION

Element	Dilution (ml/g)											
	5	10	25	40	50	75	100	200	400	600	1000	10000
B	90.	90.	95.	160	160	160	160	440	640	770	850	7600
Cd	<0.03	0.06	0.12	0.31	0.33	0.30	0.35	0.39	0.46	0.51	0.93	2.8
Be	0.04	0.09	0.50	0.51	1.3	2.9	3.2	6.7	10.	14.	20.	62.
Mg	<0.07	<0.07	<0.07	<0.07	<0.07	<0.07	<0.07	20.	27.	160	180	5100
P	20.	100	200	210	440	590	420	300	130	110	140	1100
Si	6.5	19.	72.	87.	100	180	240	500	1800	2900	3100	15000
Mo†	3.0	3 1	4.0	5.0	6.6	12.	17.	47.	72.	120	150	780
Mn†	0.05	0.09	0.10	0.11	0.15	0.32	0.98	2.1	4.2	6.1	7.8	18.
Ni†	<0.01	0.09	0.11	0.12	0.19	0.39	0.99	1.2	1.4	2.1	4.3	11
Na	100	110	58.	18.	15.	10.	4.3	<0.05	<0.05	<0.05	<0.05	<0.05
Cu	0.03	0.08	0.17	0.22	0.31	0.52	0.88	1.3	1.5	2.0	2.1	5.2
Al†	6.8	14.	61.	265	500	600	730	3700	5100	7000	8600	15000
Ca	4800	9600	17000	20000	21000	25000	30000	44000	53000	60000	66000	765000
Ba†	26	27	210	320	310	370	530	530	570	680	880	12000
K	19.	17.	11.	10.	3.8	<0.05	<0.05	<0.05	<0.05	<0.05	<0.05	<0.05
Cr†	0.01	0.03	0.08	0.14	0.19	1.0	2.2	3.8	4.2	6.1	8.2	11.
Sr†	160	200	220	220	310	390	470	580	690	880.	1070	6800
Pb†	0.31	1.8	3.0	4.9	4.3	5.0	5.1	7.0	8.1	7.1	6.1	12.
Li¶	2.3	2.5	2.8	3.5	3.3	3.8	4.4	4.8	5.5	6.0	8.6	36.
Fe§	0.11	0.31	0.53	0.85	0.63	1.6	2.8	4.2	4.1	5.0	8.4	16.
Zn§	0.07	0.06	0.09	0.10	0.15	0.56	0.65	0.38	0.75	1.1	1.5	28.

* Concentrations expressed as μg of element extracted per gram of fly ash.

† Calcium stray light corrections applied.

¶ Flame emission.

§ Atomic absorption.

TABLE D-20. ELEMENTAL CONCENTRATIONS* RESULTING FROM A 3-HOUR SONIC EXTRACTION OF BULK CORRETTE FLY ASH WITH WATER AND WITH EDTA SOLUTION

Element	H_2O	0.1 M EDTA
Al†	260	3,500
B	160	340
Ba†	320	1,400
Ca	20,000	53,000
Cd	0.31	2.0
Cr†	0.14	2.6
Cu	0.22	11.
K	10.	130
Mg	<0.07	2,900
Mn†	0.11	210
Mo†	5.0	15.
Na	18.	
Ni†	0.12	0.10
Pb†	4.9	18.
Si	87.	5,600
Sr†	220	310
Li¶	3.5	7.0
Fe§	0.85	440
Zn§	0.10	1.9

* Concentrations expressed as μg of element extracted per gram of fly ash.

† Calcium stray light correction applied.

¶ Flame emission.

§ Atomic absorption.

TABLE D-21. ELEMENTAL AND ANIONIC CONCENTRATIONS* RESULTING FROM 3-HOUR SONIC EXTRACTIONS OF DIFFERENT COAL FLY ASHES

Anion or Element	Corrette	North Dakota	Niagara Mohawk	Will County	Corrette (EDTA)
pH	12.5	11.9	9.0	11.5	4.8
F^-	47.	94.	8.0	12.	
Cl^-	18.	18.	12.	190	
CO_3^{2-}	7600	15000	<150	26000	
NO_3^-	15.	10.	8.0	6.2	
SO_4^{2-}	1300	26000	4400	41000	
B	160	760	44.	110	340
Cd	0.31	0.13	0.48	0.05	2.1
Be	<0.01	<0.01	<0.01	<0.01	<0.01
Mg	<0.07	<0.07	54.	<0.07	2900
Si	87.	75.	29.	54.	5600
Mo†	5.0	19.	12.	21.	15.
Mn†	0.11	0.13	0.06	0.20	210
Ni†	0.12	0.2	0.18	0.19	0.10
Na	18.	6700	350	21000	
Cu	0.22	0.34	0.36	0.48	11.
Al†	260	65.	5.2	130	3500
Ca	20000	14000	1600	9100	53000
Ba†	320	19.	0.82	47.	1450
K	10.	2000	400	460	130
Cr†	0.14	0.47	0.35	0.46	2.6
Sr†	220	310	9.9	350	310
Pb†	4.9	7.8	1.2	7.9	18.
Li¶	3.5	5.0	36.	2.0	7.0
Fe§	0.85	0.40	0.35	2.0	440
Zn§	0.10	0.80	0.45	0.42	1.9

* Concentrations expressed as μg of element or anion extracted per gram of fly ash.

† Calcium stray light correction applied.

¶ Flame Emission.

§ Atomic absorption.

APPENDIX E

FLY ASH REPORT GLOSSARY

AES	Auger electron spectrometry
ESCA	Electron spectroscopy for chemical analysis
FTIR	Fourier transform infrared
GC	Gas chromatorgaphy
GC/MS	Gas chromatography/mass spectrometry
INAA	Instrumental Neutron Activation Analysis
MMED	Mass Median Equivalent Diameter
NBS	National Bureau of Standards
PAH	polynuclear aromatic hydrocarbon
POM	polycyclic organic matter
RSD	Relative Standard Deviation
SEM	Scanning electron microscopy
SEM/EDS	Scanning electron microscopy with energy dispersive X-ray spectrometry
SIMS	Secondary Ion Mass Spectrometry
SRM	Standard reference material
SSMS	Spark source mass spectrometry
μg	microgram (10^{-6} g)
μm	micrometer (10^{-6} meter)
uv	ultraviolet
VMD	volume mean diameter
XRF	X-Ray Fluorescence

TECHNICAL REPORT DATA
(Please read Instructions on the reverse before completing)

1. REPORT NO. EPA 600/3-80-093	2.	3. RECIPIENT'S ACCESSION NO.
4. TITLE AND SUBTITLE Environmental Effects of Western Coal Combustion: Part IV - Chemical and Physical Characteristics of Coal Fly Ash		5. REPORT DATE
		6. PERFORMING ORGANIZATION CODE
7. AUTHOR(S) David F. S. Natusch and David R. Taylor		8. PERFORMING ORGANIZATION REPORT NO.
9. PERFORMING ORGANIZATION NAME AND ADDRESS Department of Chemistry, Colorado State University, Fort Collins, Colorado 80523		10. PROGRAM ELEMENT NO. 1NE625, EHE625
		11. CONTRACT/GRANT NO. R803950
12. SPONSORING AGENCY NAME AND ADDRESS U.S. Environmental Protection Agency, Environmental Research Laboratory-Duluth, 6201 Congdon Boulevard, Duluth, Minnesota 55804		13. TYPE OF REPORT AND PERIOD COVERED Final
		14. SPONSORING AGENCY CODE EPA-600/03
15. SUPPLEMENTARY NOTES		

16. ABSTRACT

Coal fly ashes from different sources were extensively studied. Fly ash consists of as many as 12 different particle types, made up mainly of Si, Al, Ca, K, Na, and Fe. Many potentially volatile trace elements (As, Se, Ga, In, Pb, Cd) are always preferentially associated with more respirable particles. Many other minor and trace elements may also show an inverse particle size dependence, depending on the coal fly ash. Elements showing no dependence include Al, Ba, Ca, Co, Fe, K, Mg, Rb, Sc, Si, Sr, Ta, Ti, and the rare earths. Many of the more volatile and potentially hazardous trace elements are surface associated. Most potentially hazardous inorganic species in fly ash can be leached into aqueous solution but are unlikely to give rise to solution concentrations of great concern. The physical and chemical characteristics and behavior of polycyclic organic matter (POM) associated with coal fly ash was also studied. Theoretical models show that adsorption of POM on coal fly ash will occur in seconds in a typical emission stream and that the process is highly temperature dependent. Surface-adsorbed POM is highly reactive to some nitrogen and sulfur oxides at levels expected to be found in power plant plumes. It was found that some POM adsorbed on fly ash are stabilized against photochemical decomposition, while other compounds decompose readily upon adsorption. Although fly ash emitted to the atmosphere contains much more POM than precipitator ash, there is an insufficient amount to make a discernible impact on any terrestrial aquatic system.

17. KEY WORDS AND DOCUMENT ANALYSIS

a. DESCRIPTORS	b. IDENTIFIERS/OPEN ENDED TERMS	c. COSATI Field/Group
Fly ash Particulates Trace metals	Energy development Coal combustion Air emissions	10/B

18. DISTRIBUTION STATEMENT RELEASE TO PUBLIC	19. SECURITY CLASS *(This Report)* UNCLASSIFIED	21. NO. OF PAGES 215
	20. SECURITY CLASS *(This page)* UNCLASSIFIED	22. PRICE

EPA Form 2220-1 (Rev. 4-77) PREVIOUS EDITION IS OBSOLETE

US GOVERNMENT PRINTING OFFICE 1981-757-064/0197